INTRODUCTION AND SUMMARY OF WORKING GROUP C: PART I

J.S.T. NG

Stanford Linear Accelerator Center
P.O. Box 4349, MS 26, Stanford, California, 94309, USA
E-mail: jng@SLAC.Stanford.edu

This working group is divided into two parts: the first concerning aspects of astrophysics of interest is summarised here; summary of the second part concerning physics under intense electromagnetic fields is give elsewhere.

1 Introduction

This year the QABP Workshop has expanded to include subjects from the astrophysics discipline. Although at first sight it has not much to do with beam physics, the two disciplines do share some common themes: the investigation of high energy and high intensity phenomenon. As can been from the contributions to this Workshop, much progress has been made in the theoretical understanding and observational study of energetic astrophysical events. These observations, however, have been limited to physical processes taking place in an un-controlled environment. The purpose of this Working Group is study the possibility of using high energy and high intensity particle and photon beams to study astrophysical phenomenon in a laboratory setting.

2 High energy and high intensity phenomenon

2.1 Relativistic Jets in Microquasars

Quasars are extremely bright objects that lie in the centers of remote galaxies. They have much higher luminosities compared to ordinary galaxies, but they extend over a size smaller than our Solar system. Highly collimated jets have been observed to emanate from the nuclei of these objects at relativistic speeds which extend over a distance of millions of light years. It is believed that quasars are powered by central black holes with several million solar masses.

Recently, relativistic jets have also been observed in stellar-mass binary systems in our own Milky Way [1]. These systems are termed microquasars, because they mimic many of the phenomena observed in quasars on scales millions of times smaller. It is believed that they are powered by spinning black

holes with up to 10 solar masses. The proximity of microquasars eliminates some of the uncertainties in the interpretation of the nature of relativistic jets associated with quasars due their extreme distances. The study of microquasars could lead to a better understanding of relativistic jets observed elsewhere in the Universe.

In his talk, Felix Mirabel discussed the major progress in the understanding of accretion/ejection phenomenology based on multi-wavelength observations of two-sided relativistic jets in microquasars. He also reviewed open questions and future perspectives for this new field of research.

2.2 Gamma-ray Bursts and Ultra-high energy cosmic rays

Gamma-ray bursts (GRBs) are short, intense bursts of low energy photons (up to 1 MeV). GRBs at cosmological distances release approximately 10^{51} to 10^{53} ergs in a few seconds, making them the most luminous objects (electromagnetically) in the Universe [2]. Much progress in GRB observations has been made since its accidental discovery in the late sixties using the BATSE detector on the Gamma-Ray Observatory and, more recently, the BeppoSAX satellite. However, the origin of GRB's is still not understood.

In his talk, Livio Scarsi discussed recent results from BeppoSAX, including the discovery in the X-ray after-glow of GRBs and the observed shift in iron spectral lines. Because GRBs are such energetic events, it is likely that they are associated with the production of ultra-high energy cosmic ray particles. Proposal for a new satellite observatory, EUSO (Extreme Universe Space Observatory), is also presented in this talk. The EUSO will observe, from above, the fluorescence light in showers produced by $> 10^{19}$ eV particles in the Earth's atmosphere. It promises to open up a new window to the high energy neutrino universe.

2.3 Black holes - a theoretical model and observation

In addition to the two talks on observations, there was a presentation of theoretical models that might help explain some properties of the jets and gamma-ray bursts.

In his talk, Remo Ruffini presented recent progress towards a model of the black hole that he and his collaborators proposed sometime ago [3]. In this model, a region outside the horizon of a black hole with super critical field, the "dyadosphere" is postulated. The vacuum polarization process creates a dense shell of e^+e^- pairs. The ensuing relativistic Coulomb expansion can extract up to 50% of the mass-energy of the black hole. This burst of electromagnetic energy will interact with surrounding baryonic matter; and the associated

emission could be the source of Gamma-ray bursts. It is also suggested that the continuing dissipation of electromagnetic energy could contribute to the acceleration of cosmic rays or the propulsion of jets.

3 The Unruh effect - black hole physics in the laboratory?

Following Hawking's discovery that black holes can emit radiation with a blackbody spectrum at a temperature $kT_H = \hbar g/2\pi c$, it was realized that the Minkowski vacuum may correspond to a thermal bath of elementary particles at temperature $kT_D = \hbar a/2\pi c$ as measured by uniformly accelerated observers with proper acceleration a. Unruh proposed that an accelerated system (such as an electron) can interact with such a non-trivial vacuum to produce radiation of elementary particles observable in the laboratory frame [4].

Because of its connection to Hawking radiation, the study of Unruh radiation is of fundamental importance. In his talk, Pisin Chen presented his recent proposal to detect such radiation by violently accelerating electrons using peta-watt lasers [5]. Detailed theoretical calculations of the signal and Larmor background levels for this experimental setup was presented by Aleksandr Yashin. Investigations into the feasibility of such an experiment were presented by Johnny Ng. Although the signal-to-background level turned out to be favorable, the total flux is extremely small and difficult to detect with current technology.

The Unruh effect has been discussed by many authors for over more than 20 years. But, for various theoretical reasons, the existence of this radiation is still being debated. B.-L. Hu argued in his talk that there is no radiation in this case, when the detector (the accelerated observed) has reached a steady state. The case of transient or non-uniform accelerated motion, in which there is emitted radiation, was discussed in the talk of Philip Johnson.

Although the simple connection between acceleration and temperature is strictly true only for linearly accelerated systems, it is also interesting to look at circularly accelerated systems such as an electron in a storage ring. In this case, the electron's spin degree of freedom can be used as a probe of the Unruh effect. In particular, could the fact that the equilibrium spin polarization is lower than the predicted 100% be due to heating by the interaction with a thermal bath? These are other issues were addressed in Jon Leinaas' talk.

Acknowledgments

We would like to thank the organizers for making this workshop an intellectually stimulating experience, and the working group participants for their

contributions. This work is supported in part by the U.S. Department of Energy under Contract No. DE-AC03-76SF00515.

References

1. I.F. Mirabel and L.F. Rodriguez, Ann. Rev. Astron. Astrophys. **37**, 409 (1999).
2. For a review see T. Piran, Phys. Rept. **333**, 529 (2000).
3. R. Ruffini *et al*, Astron.& Astrop. **359**, 885 (2000).
4. For a review see H.C. Rosu, Gravitation & Cosmology **7**, 1 (2001).
5. P. Chen and T. Tajima, Phys. Rev. Lett. **83**, 256 (1999).

IS THERE EMITTED RADIATION IN UNRUH EFFECT?

B. L. HU
Department of Physics, University of Maryland, College Park, MD 20742, USA
Email: hub@physics.umd.edu

ALPAN RAVAL
Keck Graduate Institute, 535 Watson Drive, Claremont, CA 91711, USA
Email: raval@tki.org

The thermal radiance felt by a uniformly accelerated detector/oscillator/atom– the Unruh effect [1] – is often mistaken to be some emitted radiation detectable by an observer/probe/sensor. Here we show by an explicit calculation of the energy momentum tensor of a quantum scalar field that, at least in 1+1 dimension, while a polarization cloud is found to exist around the particle trajectory, *there is no emitted radiation from a uniformly accelerated oscillator in equilibrium conditions.* Under *nonequilibrium* conditions which can prevail for non-uniformly accelerated trajectories or before the atom or oscillator reaches equilibrium, there is conceivably radiation emitted, but that is not what Unruh effect entails.

1 Introduction

The title question has realistic significance in light of recent experimental proposals on the detection of 'Unruh *radiation' emitted* by linear uniformly accelerated charges[2]. Earlier findings of ours [3,4] and others had already addressed this issue, with the results that, at least in 1+1 dimension model calculations, *there is no emitted radiation from a linear uniformly accelerated oscillator in a steady state*, even though there exists a polarization cloud around it. There could be radiation emitted in nonequilibrium conditions, which arise for non-uniformly accelerated atoms (for an example of finite time acceleration, see[5]), or during initial transient time for a uniformly accelerated atom, when its internal states have not yet reached equilibrium through interaction with the field. For a review of earlier work on accelerated detectors, see e.g.,[6]. For a discussion of nonequilibrium processes beyond the Unruh effect, see[7,8].

After Unruh and Wald's[9] explication of what a Minkowski observer sees, Grove[10]questioned whether an accelerated detector actually emits radiated energy. Raine, Sciama and Grove[11](RSG) analyzed what an inertial observer placed in the forward light cone of the accelerating detector would measure, and concluded that the detector does not radiate. Unruh[12], in an independent calculation, basically concurred with the findings of RSG but he also showed the existence of extra terms in the two-point function of the field

which could contribute to the excitation of a detector placed in the forward light cone. Massar, Parentani and Brout[13] (MPB) pointed out that the missing terms in RSG constitute a polarization cloud around the accelerating detector. Further discussion were conducted by Hinterleitner[14], Audretsch, Müller and Holzmann[15] Massar and Parentani[13].

Both RSG and RHA treated particle- field interaction as a quantum dissipative system. RSG attributed the lack of radiation from the accelerated detector to the existence of a fluctuation-dissipation relation (FDR) governing its dynamics[a]. Using the open system concept RHA constructed the influence functional and derived a set of coupled stochastic equations for a system of n-detectors in arbitrary (yet prescribed) states of motion in a quantum field. One subcase they studied related to Unruh effect was the influence of an accelerated detector on a probe (which is not allowed to causally influence the accelerated detector itself) via the quantum field. They found that most of the terms in the correlations of the stochastic force acting on the probe cancel each other, owing to the existence of a correlation-propagation relation, related to the fluctuation-dissipation relation for the accelerated detector[b]. The remaining terms, which contribute to the excitation of the probe, are shown to represent correlations of the free field across the future horizon of the accelerating detector.

Here, we will use the simpler Heisenberg operator method to calculate the two point function and the energy momentum tensor of a massless quantum scalar field in a $1+1$ - dimensional Minkowski spacetime minimally coupled to an accelerated particle with internal oscillator coordinates. Our analysis (based on Chapter 2 of Alpan Raval's thesis[3]) is more general than that of MPB in that the two-point function is calculated for the two points lying in arbitrary regions of Minkowski space, and not restricted to lie to the left of the accelerated oscillator trajectory. We show where the extra terms in the two point function are which were ignored in the RSG analysis. More relevant to answering the title question, we show that at least in two dimensions the energy momentum tensor vanishes everywhere except on the horizon. This

[a] There is a common misconception that a FDR can be used to explain the cancellation of radiation reaction by vacuum fluctuations, not realizing that the former is classical in nature while the latter is a quantum entity. The FDR in our work exists at the quantum stochastic level and relates the quantum dissipation in a particle's trajectory [8] or an atom's internal degrees of freedom [4] to the vacuum fluctuations in a field. It does not involve radiation reaction, which vanishes for a uniformly accelerated charge because of special conditions existing for the classical acceleration fields [7].

[b] Such a relation can be equivalently viewed as a construction of the free field two-point function for each point on either trajectory from the two-point function along the uniformly accelerated trajectory alone.

means that beyond the initial transient, there is no net flux of radiation emitted from the uniformly accelerated oscillator.

2 Correlations and Stress Energy of Quantum Field

2.1 Minimal coupling particle- field model

As in RHA, we consider the scalar electrodynamic or "minimal" coupling of oscillators to a scalar field in 1+1 dimensions. This coupling provides a positive definite Hamiltonian, and is of interest because it resembles the actual coupling of charged particles to an electromagnetic field. We assume that the field and the detector are initially decoupled from each other, and that the field is initially in the Minkowski vacuum state.

The complete action of the minimally coupled field - particle system is

$$S = \tfrac{1}{2}\int d\tau \left\{ (\tfrac{dQ}{d\tau})^2 - \Omega_0^2 Q^2 \right\} + e\int d\tau \tfrac{dQ}{d\tau}\phi(x(\tau),t(\tau)) \\ + \tfrac{1}{2}\int dx \int dt \left\{ (\tfrac{\partial\phi}{\partial t})^2 - (\tfrac{\partial\phi}{\partial x})^2 \right\}. \quad (1)$$

where Ω_0 is the bare frequency of the oscillator and e its coupling constant to the field. Under uniform acceleration, the particle trajectory parametrized by the proper time τ is

$$x(\tau) = a^{-1}\cosh a\tau; \quad t(\tau) = a^{-1}\sinh a\tau. \quad (2)$$

Variation of the action leads to the following equations of motion:

$$\frac{d^2Q}{d\tau^2} + \Omega_0^2 Q = -e\tfrac{d\phi}{d\tau}(x(\tau),t(\tau)) \quad (3)$$

$$\frac{\partial^2\phi}{\partial t^2} - \frac{\partial^2\phi}{\partial x^2} = e\int d\tau \tfrac{dQ}{d\tau}\delta(x-x(\tau))\delta(t-t(\tau)). \quad (4)$$

Because the action is a quadratic functional of the field and oscillator variables, these are also the Heisenberg operator equations of motion for the system. We shall thus view the above equations as operator equations from now on.

The field equations are solved by introducing the retarded Green function of a massless scalar field in $1+1$ dimensions:

$$\phi(x,t) = \phi_0(x,t) + e\int_{-\infty}^{\infty} d\tau \frac{dQ}{d\tau} G_{ret}(x,t;x(\tau),t(\tau)) \quad (5)$$

where ϕ_0 is a solution to the homogenous field equations corresponding to $Q=0$. We will find it convenient to introduce the null coordinates $u = t-x$ and $v = t+x$. Correspondingly, we also find it convenient to define the regions F, P, R and L of Minkowski space as (R is called the Rindler wedge)

$$F: u>0, v>0 \quad P: u<0, v<0$$
$$R: u<0, v>0 \quad L: u>0, v<0. \tag{6}$$

In terms of the (u, v) coordinates, the retarded Green function for a massless scalar field in $1+1$ dimensions takes the form:

$$\begin{aligned} G_{ret}(x,t;x(\tau),t(\tau)) &= \tfrac{1}{2}\theta(t-t(\tau)-x+x(\tau))\theta(t-t(\tau)+x-x(\tau)) \\ &= \tfrac{1}{2}\theta(u+a^{-1}e^{-a\tau})\theta(v-a^{-1}e^{a\tau}). \end{aligned} \tag{7}$$

With this substitution, an integration by parts in Eq. (5) yields:

$$\begin{aligned} \phi(x,t) = \phi_0(x,t) + \tfrac{e}{2}\big[&\theta(-u)\theta(-\lambda)Q(-a^{-1}ln(\mid au \mid)) \\ &+ \theta(v)\theta(\lambda)Q(a^{-1}ln(\mid av \mid))\big] \end{aligned} \tag{8}$$

where we have also defined $\lambda = 1 + a^2uv$. The oscillator trajectory satisfies $\lambda = 0$. The quantities $-a^{-1}ln(\mid au \mid)$ and $a^{-1}ln(\mid av \mid)$ are just the retarded times of the point (x, t), according to whether it lies to the right or the left of the accelerated trajectory, respectively. These two cases are distinguished by the appearance of the step functions with argument $\mp\lambda$. The step functions in u and v distinguish the cases when the point lies anywhere in the past light cone or anywhere in the forward light cone of the accelerated particle (these two conditions are simultaneously satisfied only in the Rindler wedge). With this in mind, we see that the first term linear in the coupling constant contributes only for points to the right of the oscillator trajectory, whereas the second term contributes only for points to the left of the oscillator trajectory and within the forward light cone of the oscillator. In particular, as expected, there is no correction to the field operator in the region $L \cup P$, which cannot be causally influenced by the accelerated trajectory.

Along the accelerated trajectory, the solution for ϕ reduces to

$$\phi(x(\tau),t(\tau)) = \phi_0(x(\tau),t(\tau)) + \frac{e}{2}Q(\tau). \tag{9}$$

Putting this back to the equation of motion for Q, (3), we obtain:

$$\frac{d^2Q}{d\tau^2} + \frac{e^2}{2}\frac{dQ}{d\tau} + \Omega_0^2 Q = -e\frac{d\phi_0}{d\tau}(x(\tau),t(\tau)). \tag{10}$$

The term linear in the proper velocity of the oscillator degree of freedom arises from the oscillator - field interaction and corresponds to dissipation of a quantum origin in the oscillator.

2.2 Equation of motion for the detector

The above equation of motion is easily solved. If the oscillator field interaction has always been switched on, the oscillator has reached a steady state at any finite time. We can then ignore transient terms in the solution for Q and obtain:

$$Q(\tau) = -\frac{e}{\Omega}\int_{-\infty}^{\tau} d\tau' \sin\Omega(\tau-\tau')e^{-\gamma(\tau-\tau')}\frac{d\phi_0}{d\tau'}(x(\tau'),t(\tau')) \qquad (11)$$

where we have defined the dissipation constant $\gamma = \frac{e^2}{4}$, and the frequency $\Omega = \sqrt{\Omega_0^2 - \gamma^2}$. We may also solve equation (10) in frequency space. Ignoring transients as before, we obtain

$$\tilde{Q}(\omega) \equiv \frac{1}{2\pi}\int_{-\infty}^{\infty} d\tau e^{-i\omega\tau}Q(\tau) = \chi_\omega \tilde{J}(\omega) \qquad (12)$$

where

$$\tilde{J}(\omega) = -\frac{e}{2\pi}\int_{-\infty}^{\infty} d\tau e^{-i\omega\tau}\phi_0(x(\tau),t(\tau)) \qquad (13)$$

and χ_ω is the impedance function of the oscillator, given by

$$\chi_\omega = i\omega(-\omega^2 + \Omega_0^2 + 2i\omega\gamma)^{-1}. \qquad (14)$$

It satisfies the identity

$$\chi_\omega + \chi_\omega^* = 4\gamma \mid \chi_\omega \mid^2 \qquad (15)$$

which has the form of a fluctuation- dissipation relation. We now expand ϕ_0 in Minkowski normal modes:

$$\phi_0(t,x) = \phi_0^{(+)} + \phi_0^{(-)} = \int_{-\infty}^{\infty} \frac{d^2k}{\sqrt{(2\pi)^2 2\omega_k}}\mathbf{a_k}e^{i(kx-\omega_k t)} + h.c. \qquad (16)$$

where $h.c.$ denotes Hermitian conjugate and $\phi_0^{(-)}$ is the Hermitian conjugate of $\phi_0^{(+)}$. The operators $\mathbf{a_k}$ annihilate the Minkowski vacuum. Based on this separation of the field into positive and negative frequency parts, we obtain the corresponding separation of the oscillator degree of freedom:

$$Q(\tau) = Q^{(+)}(\tau) + Q^{(-)}(\tau) \qquad (17)$$

where

$$Q^{(+)}(\tau) = -\frac{e}{\Omega}\int_{-\infty}^{\tau} d\tau' \sin\Omega(\tau-\tau')e^{-\gamma(\tau-\tau')}\frac{d\phi_0}{d\tau'}^{(+)}(x(\tau'),t(\tau')) \qquad (18)$$

and $Q^{(-)}$ is the Hermitian conjugate of $Q^{(+)}$.

On the accelerated trajectory, Eq. (16) gives

$$\phi_0^{(+)}(x(\tau),t(\tau)) = \int_{-\infty}^{\infty} \frac{d^2k}{\sqrt{(2\pi)^2 2\omega_k}} \mathbf{a_k} [e^{\frac{ik}{a}e^{-a\tau}}\theta(k) + e^{\frac{ik}{a}e^{a\tau}}\theta(-k)]. \quad (19)$$

Introducing the Fourier transforms of $e^{\frac{ik}{a}e^{-a\tau}}$ and $e^{\frac{ik}{a}e^{a\tau}}$, we get

$$\begin{aligned}\phi_0^{(+)}(x(\tau),t(\tau)) &= \tfrac{1}{2\pi a}\int_{-\infty}^{\infty} \tfrac{d^2k}{\sqrt{(2\pi)^2 2\omega_k}} \mathbf{a_k} \int_{-\infty}^{\infty} d\omega e^{-i\omega\tau} e^{\frac{\pi\omega}{2a}} \times \\ &\left[\Gamma(-\tfrac{i\omega}{a}) \mid \tfrac{k}{a} \mid^{\frac{i\omega}{a}} \theta(k) + \Gamma(\tfrac{i\omega}{a}) \mid \tfrac{k}{a} \mid^{-\frac{i\omega}{a}} \theta(-k)\right]. \quad (20)\end{aligned}$$

Differentiating with respect to τ and substituting in the equation for $Q^{(+)}(\tau)$, (18), we obtain, after carrying out the integration over τ, an expression of $Q^{(+)}(\tau)$. Then we can substitute it back into the equation for the field operator (8) and get

$$\begin{aligned}\phi_{int}^{(+)}(x,t) &= -\tfrac{\gamma}{\pi a}\int_{-\infty}^{\infty} \tfrac{d^2k}{\sqrt{(2\pi)^2 2\omega_k}} \mathbf{a_k} \int_{-\infty}^{\infty} d\omega e^{\frac{\pi\omega}{2a}} \chi_\omega^* \\ &\times \left[\Gamma(-\tfrac{i\omega}{a}) \mid \tfrac{k}{a} \mid^{\frac{i\omega}{a}} \theta(k) + \Gamma(\tfrac{i\omega}{a}) \mid \tfrac{k}{a} \mid^{-\frac{i\omega}{a}} \theta(-k)\right] \\ &\times \left[\mid au \mid^{\frac{i\omega}{a}} \theta(-u)\theta(-\lambda) + \mid av \mid^{-\frac{i\omega}{a}} \theta(v)\theta(\lambda)\right] \quad (21)\end{aligned}$$

where $\phi_{int}^{(+)}(x,t) = \phi(x,t) - \phi_0^{(+)}(x,t)$ accounts for the interaction of the quantum field with the oscillator.

2.3 Two point function of the field

In order to evaluate the two-point function $\langle\phi(x,t)\phi(x',t')\rangle$ in the Minkowski vacuum, we first recognize that it is equal to $\langle\phi^{(+)}(x,t)\phi^{(-)}(x',t')\rangle$. This is because only operator products of the form $\mathbf{a_k}\mathbf{a_k}^\dagger$ contribute when taking the expectation value in the Minkowski vacuum. Denoting $\langle\phi(x,t)\phi(x',t')\rangle$ by $G(x,t;x',t')$ and $\langle\phi_0(x,t)\phi_0(x',t')\rangle$ by $G_f(x,t;x',t')$, we obtain

$$\begin{aligned}G(x,t;x',t') - G_f(x,t;x',t') &= \langle\phi_0^{(+)}(x,t)\phi_{int}^{(-)}(x',t')\rangle \\ &+\langle\phi_{int}^{(+)}(x,t)\phi_0^{(-)}(x',t')\rangle + \langle\phi_{int}^{(+)}(x,t)\phi_{int}^{(-)}(x',t')\rangle. \quad (22)\end{aligned}$$

Using the expression for $\phi_0^{(+)}(x,t)$ and $\phi_{int}^{(-)}(x',t')$ we obtain

$$\begin{aligned}&G(x,t;x',t') - G_f(x,t;x',t' = -\frac{\gamma}{2\pi}\int_{-\infty}^{\infty}\frac{d\omega}{\omega}(1-e^{-\frac{2\pi\omega}{a}})^{-1}\times \\ &\left[\mid \tfrac{au}{au'} \mid^{\frac{i\omega}{a}} \theta(-u)\theta(-u')\left\{\chi_\omega^*\theta(-\lambda) + \chi_\omega\theta(-\lambda') - 4\gamma \mid \chi_\omega \mid^2 \theta(-\lambda)\theta(-\lambda')\right\}\right. \\ &+ \left. \mid \tfrac{av}{av'} \mid^{-\frac{i\omega}{a}} \theta(v)\theta(v')\left\{\chi_\omega^*\theta(\lambda) + \chi_\omega\theta(\lambda') - 4\gamma \mid \chi_\omega \mid^2 \theta(\lambda)\theta(\lambda')\right\}\right.\end{aligned}$$

$$+ \quad \mid a^2uv' \mid^{\frac{i\omega}{a}} \theta(-u)\theta(v')\left\{\chi^*_\omega\theta(-\lambda)+\chi_\omega\theta(\lambda')-4\gamma \mid \chi_\omega \mid^2 \theta(-\lambda)\theta(\lambda')\right\}$$
$$+ \mid a^2u'v \mid^{-\frac{i\omega}{a}} \theta(-u')\theta(v)\left\{\chi^*_\omega\theta(\lambda)+\chi_\omega\theta(-\lambda')-4\gamma \mid \chi_\omega \mid^2 \theta(\lambda)\theta(-\lambda')\right\}\Big]$$
$$-\frac{\gamma}{4\pi}\int_{-\infty}^{\infty}\frac{d\omega}{\omega}(\sinh\tfrac{\pi\omega}{a})^{-1}\times$$
$$[\quad \mid \tfrac{au}{au'} \mid^{\frac{i\omega}{a}} \{\chi^*_\omega\theta(-u)\theta(-\lambda)\theta(u')+\chi_\omega\theta(-u')\theta(-\lambda')\theta(u)\}$$
$$+ \quad \mid \tfrac{av}{av'} \mid^{-\frac{i\omega}{a}} \{\chi^*_\omega\theta(v)\theta(\lambda)\theta(-v')+\chi_\omega\theta(v')\theta(\lambda')\theta(-v)\}$$
$$+ \quad \mid a^2uv' \mid^{\frac{i\omega}{a}} \{\chi^*_\omega\theta(-u)\theta(-\lambda)\theta(-v')+\chi_\omega\theta(v')\theta(\lambda')\theta(u)\}$$
$$+ \quad \mid a^2u'v \mid^{-\frac{i\omega}{a}} \{\chi^*_\omega\theta(u')\theta(\lambda)\theta(v)+\chi_\omega\theta(-u')\theta(-\lambda')\theta(-v)\}]. \qquad (23)$$

The role of the relation (15) in the cancellation of various terms in the first half of the above expression is thus made explicit. Different terms will vanish depending on which region of Minkowski space each of the two points is in, and according to whether these points are to the left or the right of the accelerated trajectory.

The above result can also be obtained via a different quantization procedure. Instead of expanding the field in Minkowski modes, as above, we can use Unruh modes which are linear combinations of Rindler modes and positive frequency with respect to Minkowski time (see, for example[16]). These modes are easier to handle in the manipulations involved. However, they have the disadvantage of being defined differently in each region (F, P, R and L). Although the Rindler modes are defined only in R and L, the Unruh modes, as linear combinations of Rindler modes, can be analytically extended to the entire spacetime. One then computes the two point function in a desired region by expanding the field in a complete set of Unruh modes as defined by analytic extension to that region. Of course, one always needs the mode decomposition in R, because the field operator at an arbitrary point depends both on the free field operator at that point as well as on the accelerated trajectory, which lies in R (see equations (8) and (18)). This procedure will not be repeated here, as it leads to the same result.

2.4 Energy Momentum Tensor

Let us first consider the coincidence limit of the two point function. In that case all terms involving u and u' or v and v' vanish as a consequence of the relation (15). The remaining terms can be simplified to give:

$$\langle\varphi^2(x,t)\rangle - \langle\varphi_0^2(x,t)\rangle = -\frac{\gamma}{2\pi}q(v)\int_{-\infty}^{\infty}\frac{d\omega}{\omega}(1-e^{-\frac{2\pi\omega}{a}})^{-1}\times$$
$$[\mid a^2uv \mid^{\frac{i\omega}{a}} \{\chi^*_\omega\theta(-u)\theta(-\lambda)+\chi_\omega\theta(\lambda)(\theta(u)e^{-\frac{\pi\omega}{a}}+\theta(-u))\}$$

$$+ \mid a^2uv \mid^{-\frac{i\omega}{a}} \{\chi_\omega \theta(-u)\theta(-\lambda) + \chi^*_\omega \theta(\lambda)(\theta(u)e^{-\frac{\pi\omega}{a}} + \theta(-u))\}]. \quad (24)$$

This corresponds to a static polarization cloud confined to the region $F \cup R$, i.e. $v > 0$. It is static because it is a function of $uv = t^2 - x^2$ in each region. Thus it is constant along any accelerated world line in particular. In F, the curves $t^2 - x^2 = constant$ are spacelike curves and therefore do not correspond to world-lines of physical particles. Therefore any physical detector in F will respond to the field in a non-trivial, time-dependent way.

However, it is simple to show that the renormalized energy-momentum tensor of the field vanishes everywhere except at the past null horizon $v = 0$ of the accelerated trajectory, and on the accelerated trajectory itself. The energy-momentum tensor is renormalized by subtracting out the free field contribution. It is thus given by

$$\begin{aligned} T_{uu} &= \lim_{u' \to u, v' \to v} \partial_u \partial_{u'} (G(x,t;x',t') - G_f(x,t;x',t')) \\ T_{vv} &= \lim_{u' \to u, v' \to v} \partial_v \partial_{v'} (G(x,t;x',t') - G_f(x,t;x',t')) \\ T_{uv} &= 0. \end{aligned} \quad (25)$$

Going back to the expression (23) for the two-point function, we find, in $P \cup L$ (i.e. $v, v' < 0$), that $G(x,t;x',t') - G_f(x,t;x',t') = 0$. Thus the renormalized energy momentum tensor trivially vanishes there. In the region $F \cup R$, and to the left of the trajectory, $\lambda, \lambda' > 0$, we have

$$\begin{aligned} G(x,t;x',t') - G_f(x,t;x't') &= -\tfrac{\gamma}{2\pi} \textstyle\int_{-\infty}^{\infty} \frac{d\omega}{\omega} \left(1 - e^{-\frac{2\pi\omega}{a}}\right)^{-1} \\ &\times [\left|a^2uv'\right|^{\frac{i\omega}{a}} \chi_\omega \left(\theta(-u) + \theta(u)\, e^{-\frac{\pi\omega}{a}}\right) \\ &+ \left|a^2u'v\right|^{-\frac{i\omega}{a}} \chi^*_\omega \left(\theta(-u') + \theta(u')\, e^{-\frac{\pi\omega}{a}}\right)]. \end{aligned} \quad (26)$$

The terms involving u, u' and v, v' all vanish as a consequence of (15). The remaining cross-terms do not contribute to the energy-momentum tensor, as can be checked by straightforward differentiation.

Similarly, to the right of the trajectory, $(\lambda, \lambda' < 0)$, we obtain

$$\begin{aligned} \langle \phi(x,t)\phi(x',t') \rangle - \langle \phi_0(x,t)\phi_0(x',t') \rangle &= -\tfrac{\gamma}{2\pi} \textstyle\int_{-\infty}^{\infty} \frac{d\omega}{\omega} (1 - e^{-\frac{2\pi\omega}{a}})^{-1} \\ &\times \left|a^2uv'\right|^{\frac{i\omega}{a}} \chi^*_\omega + \left|a^2u'v\right|^{-\frac{i\omega}{a}} \chi_\omega]. \end{aligned} \quad (27)$$

The energy-momentum tensor vanishes here as well, in a similar fashion.

If we therefore consider a world-tube formed by two accelerated world-lines with $\lambda > 0$ and $\lambda < 0$ in the Rindler wedge, then this tube encloses the accelerated trajectory $\lambda = 0$. Also the energy-momentum tensor vanishes everywhere on the boundary of the tube. Hence there is no flux of energy-momentum, or radiation from the oscillator at $\lambda = 0$.

The cross-terms in u, v' and u', v which appear in the above expressions are missing in RSG. Although we have found that they do not contribute to the energy-momentum tensor, they do signal the presence of a polarization cloud around the oscillator. These results support those of Unruh[12]and MPB[13]. However, the above analysis has the advantage of clearly displaying the role of the "fluctuation-dissipation relation" (15) in the cancellation of terms which would naively be expected to contribute to the energy-momentum. Also, we have here computed an expression for the two-point function which is valid over the entire spacetime. This is a generalization of previous work.

Calculation is underway in four dimensional spacetime, which is certainly more physical. In this case[17] we expect to see the ordinary classical radiation of the Larmor type from a uniformly accelerated charge, but the question of interest to us is whether in 4D there is emitted radiation. If there were it should manifest in the content of the energy momentum tensor and, being of quantum nature, discernible from the classical radiation. This would further clarify any existing confusion on the nature of Unruh radiation.

Acknowledgments

We thank Pisin Chen for his invitation to this interesting workshop and Stefania Petracca for her warm hospitality. This research is supported in part by NSF grant PHY98-00967.

Notes added in Proof:

Additional earlier work addressing the title question[18] were kindly brought to the attention of the authors by G. E. Matsas after this paper was submitted to the editor.

References

1. W. G. Unruh, Phys. Rev. **D14**, 3251 (1976)
2. Pisin Chen, "Event Horizon" This volume.
3. A. Raval, Ph. D. Thesis, University of Maryland, College Park, 1996
4. A. Raval, B. L. Hu and J. Anglin, Phys. Rev. **D 53**, 7003 (1996).
5. A. Raval, B. L. Hu and D. Koks, Phys. Rev. **D 55**, 4795 (1997).
6. S. Takagi, Prog. Theor. Phys. Suppl. 88, 1 (1986). V. L. Ginzburg and V. P. Frolov, Sov. Phys. Usp. 30, 1073 (1988)

7. B. L. Hu and P. R. Johnson, "Beyond Unruh Effect: Nonequilibrium Dynamics of Quantum Charged Particles". This Volume.
8. P. R. Johnson and B. L. Hu, "Worldline Influence Functional Derivation of Lorentz- Dirac- Langevin Equation from QED". This volume.
9. W. G. Unruh and R. M. Wald, Phys. Rev. D29, 1047 (1984)
10. P. G. Grove, Class. Quan. Grav. **3**, 801 (1986)
11. D. J. Raine, D. W. Sciama, and P. G. Grove, Proc. Roy. Soc. Lond. **A435**, 205 (1991).
12. W. G. Unruh, Phys. Rev. **D 46**, 3271 (1992).
13. S. Massar, R. Parentani and R. Brout, Class. Quantum Grav. 10, 385 (1993). S. Massar, R. Parentani, Phys. Rev. **D54**, 7426, 7444 (1996)
14. F. Hinterleitner, Ann. Phys. **226**, 165 (1993).
15. J. Audretsch and R. Müller, Phys. Rev. D49, 4056 (1994). J. Audretsch, R. Müller and M. Holzmann, Phys. Lett. A (1995) gr-qc/9503012
16. N. Birrell and P. W. C. Davies, *Quantum Fields in Curved Spaces* (Cambridge University Press, Cambridge, 1982)
17. M. L. Tseng, A. Raval and B. L. Hu, in preparation (2000)
18. George E.A. Matsas, Phys.Lett. B380, 24 (1996); A. Higuchi, G.E.A. Matsas, D. Sudarsky, Phys.Rev.D45, 3308; 46, 3450 (1992)

PROBING TOWARD THE SOLID STATE PLASMA ACCELERATOR FRONTIER USING CHANNELING RADIATION MEASUREMENTS AT THE FERMILAB A0 PHOTOINJECTOR

R. A. CARRIGAN, JR.,

*Fermi National Accelerator Laboratory, Batavia, Illinois 60510, USA**

J. FREUDENBERGER, S. FRITZLER, H. GENZ, A. RICHTER, A. USHAKOV, AND A. ZILGES

*Institut für Kernphysik, Technische Universität Darmstadt, Schlossgartenstrasse 9, D-64289 Darmstadt, Germany***

J. P. F. SELLSCHOP

Schonland Centre, University of the Witwatersrand, 2050 Johannesburg, South Africa

Plasmas offer the possibility of high acceleration gradients. An intriguing suggestion is to use the higher plasma densities possible in solids to get extremely high gradients. Although solid state plasmas might produce high gradients they would pose daunting problems. Crystal channeling has been suggested as one mechanism to address these challenges. There is no experimental or theoretical guidance on channeling in intense electron and laser beams. A high density plasma in a crystal lattice could quench the channeling process. An experiment is being carried out at the Fermilab A0 Photo-Injector Test Facility to observe electron channeling radiation at high bunch charges. An electron beam with up to 8 nC per electron bunch has been used to investigate the electron-crystal interaction. No evidence has been found of significant quenching of channeling at charge densities several orders of magnitude larger than in earlier experiments.

1 Introduction

Recently there has been interesting progress in studies of plasma acceleration in gasses [1]. This has been due in part to the development of terawatt laser technology [2] a decade ago. Gas plasmas have already delivered gradients in the 1 GV/cm range [3], one to two thousand times higher than RF cavities. Since accelerating gradients are approximately $\sqrt{n}$ V/cm, where n is the plasma density, plasmas in solids can potentially deliver gradients 100 times higher than gas plasmas. For example, for $n_e = 10^{22}/cm^3$, the gradient would be 100 GV/cm.

At the plasma densities required for acceleration there are severe material limitations. This has led to speculation about utilizing channeling [4] as an adjunct to solid state plasma acceleration [5]. Channeling could mitigate the problems and

perhaps also introduce focusing to prevent beam blow-up from multiple scattering. At the intensities needed for solid state accelerators there will be significant channeling problems since the crystal lattice will be severely disturbed or vaporized. As the bunch intensity rises energy loss and plasma generation with the concomitant rise in crystal disorder will cause degradation in channeling [6] so that channeling might be quenched.

If channeling is to be considered for solid state acceleration more information is needed on the character and limitations of channeling under extreme conditions. Although existing channeling theory can serve as a guide, no channeling studies have been done under the non-equilibrium conditions that couple intense electron or laser energy into a crystal. Understanding of the behavior of solids under the conditions required for acceleration is in its early stages [7]. These processes are complicated but have been investigated in connection with terawatt laser technology and pellet fusion.

A systematic study of channeling with increasing bunch charge was carried out at Darmstadt [8] using the Darmstadt superconducting linac. A planar channeling experiment has also been done at relatively high bunch charge at Stanford on the Stanford Mark III accelerator [9]. Both groups investigated channeling radiation from electron beams in the 5-30 MeV energy region. The experiments were some orders of magnitudes away from the plasma acceleration regime.

The new Fermilab A0 Photo-Injector [10] produces a bunch intensity high enough to approach the plasma acceleration regime more closely. The accelerator typically operates with kinetic energy of 16.5 MeV. An experiment is now being carried out at the photo-injector to observe channeling radiation in this regime. Channeling radiation is studied as a function of electron bunch intensity to investigate whether it quenches as the bunch intensity is increased. If crystal disorder reaches the stage where channeling is quenched or extinguished the channeling radiation signal will diminish or disappear. A later stage of the experiment may attempt solid-state plasma acceleration although the available beam intensities are still far from those required for interesting acceleration.

2 The Experiment

Channeling radiation is straightforward to observe. Particles moving along a crystal plane or axis oscillate about the plane and radiate in the same way synchrotron radiation is produced in an undulator. The electron beam is deflected by a magnet after it passes through the crystal. The undeflected channeling radiation is detected by an x-ray detector. In the relativistic regime the "line energy" of the radiation [11] goes as $p^{3/2}$ where p is the electron momentum. At A0 the channeling x-ray energies are in the 10-200 keV range. Channeling x-rays are separated from other sources such as bremsstrahlung by scanning the crystal through the characteristic channeling angular distribution that has a width related to the Lindhard critical angle. The expected channeling radiation x-ray yield per electron for Si is on the order of 10^{-4}.

At A0 there are characteristically $5*10^{10}$ electrons in a bunch so that there are of order $5*10^{6}$ channeling x-rays per bunch. These are concentrated in a cone that has an angular half width of $1/\gamma$ or 30 milliradians. In a pico-second long pulse 10^{5} photons will strike a 125 mm^2 detector 1.47 m downstream of the crystal.

Conventional single x-ray detectors do not work in the extremely high x-ray flux environment of the A0 photo-injector. Instead two other x-ray detector systems have been used. One employed an absorption-based, energy-resolved x-ray detector (AberX) using a Ross filter system [12] and a lens-coupled scintillating screen-CCD system. This detector was developed by Freudenberger [13] to study its feasibility for mammography. The Ross filter technique takes advantage of the K-edge absorption of x-rays by thin metallic foils. A result has been obtained with that detector [14]. The second approach employs x-ray detectors made with Calcium Tungstate scintillation films monitored by photomultipliers (AberX-lite) and a Ross filter wheel. The experiment reported here using the second approach is continuing.

The A0 photo-injector normalized rms beam emittance with 6 nC/bunch is $\varepsilon_n = 12$ mm·mrad for typical conditions [15]. This is in line with simulations using the program HOMDYN [16]. The beam spot size at the crystal is typically 0.5 mm (σ) so that the corresponding angular divergence is 0.7 milliradians. This is somewhat smaller than the axial channeling critical angle which is about 3 mrad for the Si <100> axis at A0 energies. The bunch length for a 5 nC bunch measured using a streak camera is typically $\sigma_t = 7$ ps.

Figure 1 shows a schematic of the Fermilab channeling radiation experiment. This apparatus consists of a crystal mounted in a remotely controlled goniometer, a spectrometer magnet to deflect the electron beam, and an x-ray detector system. Beam current is measured with an integrating current transformer (ICT) and a Faraday cup. The 20 μm thick, 25 mm diameter Si crystal was obtained from Virginia Semiconductor. The goniometer has two angular degrees of freedom, Θ_x and Θ_y. The goniometer design has been dictated by the requirements of the photo-injector dust-free, very high vacuum system.

The AberX-lite detector system has been calibrated in two separate ways. In one, the detector system was placed in a monoenergetic x-ray beam at the Argonne Advanced Photon Source with variable energy. The x-ray flux was measured by a calibrated ion chamber. The detector calibration extended over the 12-92 keV region. This gave the absolute response of the detector as a function of energy and the calibration of the Ross absorber system. The detector response was consistent with the foil thickness and the expected light yield of Calcium Tungstate.

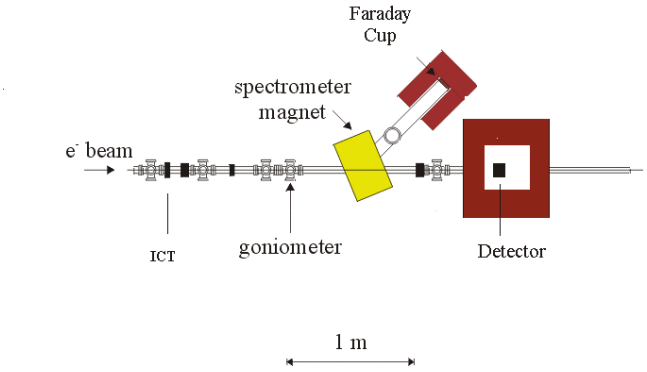

Figure 1. A0 channeling radiation apparatus.

In the second method the calibration is determined by integrating the x-ray yield over the bremsstrahlung spectrum and the channeling radiation spectrum determined from the 6.7 MeV Si <111> data of Genz et al. [17] extrapolated to 16.9 MeV and the 16.9 MeV diamond <100> data from Klein et al. [18] The response of the photomultiplier system can be determined from the bremsstrahlung yield. That in turn can be used to obtain the total number of channeling x-rays per electron. For this preliminary presentation the results from the two calibrations have been averaged and error bars shown that span the two methods. The Argonne light source calibration gives a lower response. Investigation of the differences between the calibrations is continuing.

Signal information from the Calcium Tungstate was collected using a digital oscilloscope. The scope integrated over the $CaWO_4$ pulse, collected data from the integrating current transformer (ICT in Figure 1) and normalized the ICT signal to get the charge. The scintillation light time distribution for the $CaWO_4$ has two time components; a short one with a time constant of 1.5 microseconds and a stronger one with 7.5 microsecond decay. The time structure of the A0 Photoinjector bunch train consists of a series of laser-driven pulses, each several pico-seconds long separated by one microsecond intervals. There is a background of dark current pulses coming at the 1.3 GHz frequency of the RF. Typically the amplitude of a dark current pulse is 10^{-4}-10^{-5} of the amplitude of a laser-driven pulse. The relative amplitudes of the two sets of pulses can be controlled by changing the amplitude of

the RF on the photo-injector RF gun and the laser pulse intensity. Since the principal aim of the experiment is to observe the channeling signal as a function of

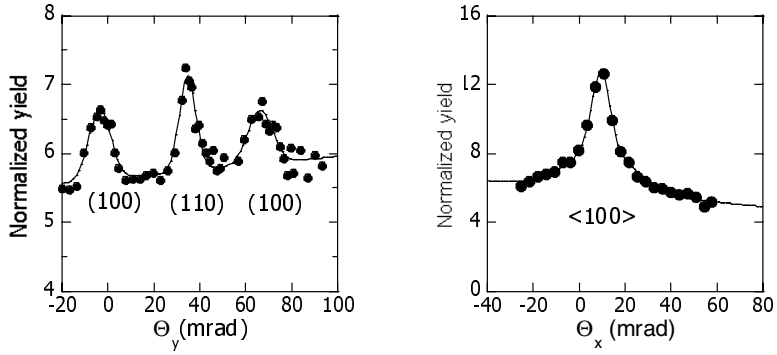

Figure 2. Planar and axial scans.

bunch charge it is desirable to operate over as wide a range of bunch charges as possible. This is done in two ways-by changing the laser intensity and by measuring the dark current yields. For the laser case care is taken to suppress the dark current and then subtract the residual by measuring the dark current just before the laser pulse and with no laser pulse. Typically measurements are made on the first laser pulse in a train and averaged over 10 cycles (A0 currently operates at 1 Hz).

3 Analysis

Data is taken by first scanning the crystal through Θ_x and Θ_y to find a plane, an axis, or a random orientation of the crystal. The "no crystal" background is typically 17% of the yield on axis. Even a small electron or x-ray halo is multiplied significantly because the crystal holder is more than 100 times the thickness of the crystal. Most of the random background is due to bremsstrahlung in the crystal. Figure 2 shows typical scans through several planes and the <100> axis. In the axial scan the crystal moves from the axis along a (110) plane because these planes are oriented in the horizontal and vertical directions. The peak is fitted with two co-located gaussians to account for the tilted planar portion. The 3.9 mrad width (σ) of the axial scan curve is consistent with the axial critical angle convoluted with the beam divergence and resolution due to other effects. The planar widths are slightly larger than expected. The ratio of the widths of the (100) and the (110) planes is consistent with

the fact that the 45 degree planes are scanned diagonally. The ratio of planar height to axial height is consistent with theory and the results of earlier experiments.

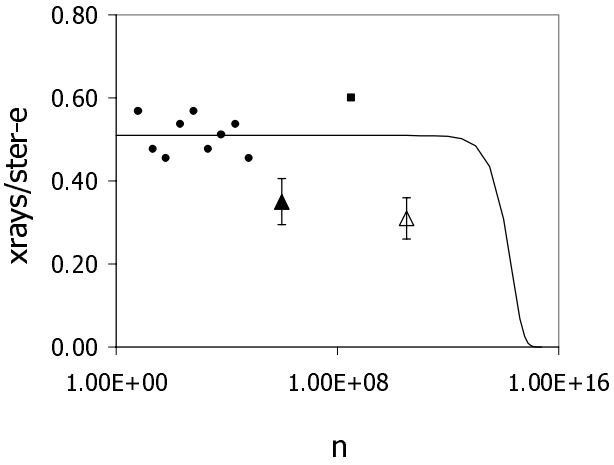

Figure 3. Channeling radiation yield as a function of bunch charge.

Figure 3 shows the x-ray yield per electron·steradian at A0 and for the earlier experiments as a function of electrons/bunch (n). The A0 results are represented by a laser driven axial channeling case with a bunch charge of 5 nC (open triangle) and a dark current measurement with a bunch charge of $1.5*10^{-4}$ nC (solid triangle). The dots are Darmstadt data taken at 5.4 MeV for diamond <110>. The yield has been scaled by $\gamma^{5/2}$ to account for the yield energy dependence. This has been further multiplied by a factor of 8.62 to give the total x-ray yield rather than a 10% band. The square is a Stanford Si (110) planar point [19] taken at 30 MeV and scaled to 16.9 MeV. The spectrum was integrated over all the x-rays and multiplied by 3.3 to account for the relative planar to axial yield. This assumption may overestimate the expected yield. It should be noted that both the Darmstadt and Stanford extrapolations introduce significant uncertainties by comparing different elements, orientations, and energies. The solid line is a schematic illustration of how the channeling radiation yield might quench with increasing bunch charge.

The A0 channeling radiation yield by itself is essentially flat over 4-5 decades while the combined Darmstadt-A0 set is flat to within 25% over ten decades. No evidence has been found of significant quenching of channeling at charge densities several orders of magnitude larger than in earlier experiments. This data is

preliminary. More data is being gathered and the relationship between the two calibrations is still under investigation.

This experiment has reached bunch charges of up to 8 nC in a beam spot with a sigma of 0.5 mm^2 and a pulse length of $\sigma = 7$ ps. This corresponds to a current on the order of 1000 A and a current density of 10^5 A/cm^2. The effective power density at A0 is typically $4*10^{11}$ W/cm^3. Achieving a 1 GeV/cm gradient could require power densities in the range of 10^{19}-10^{21} W/cm^3 so that the experiment is still a factor of 10^7-10^{10} away from where significant channeling acceleration could happen.

4 Outlook

4.1 Solid State Plasma Acceleration

Several approaches to solid state plasma acceleration have been discussed. One, particle wake field acceleration, uses a particle beam as a plasma driver. A laser beam can also be used to drive a plasma. Another approach is to use a side injected laser to avoid problems with pump depletion and particle dephasing [20]. Pump depletion is particularly troubling for the high plasma densities in solids. Approaches using laser beams are limited by the optical absorption depth for materials like Si and Ge as well as surface reflection.

As noted above, the A0 experiment is still far from the regime where significant solid state acceleration might occur. At A0 bunch compression can be used to reduce the bunch length to about 1 ps and the spot size might be reduced by a factor of two so that it may be possible to go one order of magnitude further. A major problem for studying solid state acceleration is the bunch length. Getting into the plasma regime requires bunch lengths of O(10 fs). An approach to higher bunch charge densities is to go to a higher energy accelerator such as SLAC. There one might obtain beams with transverse sizes on the order of 5 μm and bunch lengths of 50 fs [21]. This would increase the power densities by 10^5 over the A0 result and approach much closer to the solid state plasma regime. Another approach would be to use a fairly modest electron beam coupled with extremely intense laser illumination.

Although the experiment is still far from the plasma regime in both current and pulse length, an initial search for plasma acceleration at A0 could be performed by assuming the beam itself would generate a plasma. The putative wake field could affect the tail end of the bunch so that it gained or lost energy. This could be observed by using the spectrometer magnet to look for a changing shape of the momentum distribution after the spectrometer with higher bunch intensities and with the crystal aligned for channeling or a random direction. The rms multiple scattering angle for the crystal produces a projected multiple scattering angle of 12

mrad. This is equivalent to a momentum resolution of 0.6 MeV/c. A plasma density of about 10^{17} e/cm^3 would give a gradient of 0.3 GV/cm to give an equivalent energy gain in the 20 μm crystal. This could be achieved with a side coupled laser with an intensity of $3*10^{15}$ W/cm^2. The A0 laser can reach 10^8-10^9 watts/cm^2 for a 1.8 ps pulse. Thus at present it is not possible to reach into the acceleration regime at A0 with the existing A0 laser.

4.2 Other Applications

Channeling radiation may be able to provide sub-picosecond x-ray fluxes that are higher than some other approaches now under development [22]. Sub-picosecond x-ray processes are interesting because they can probe lattice vibration phenomena over a single oscillation. Existing synchrotron light sources are several orders of magnitude away from this possibility. Potential study topics include lattice vibration measurements, time-resolved chemistry, and 3-D motion of atoms. These types of experiments could not be done with the present pulse length at A0, which is currently longer than 1 ps.

5 Acknowledgements

The help of H. Edwards, R. Noble, J. Santucci (Fermilab), D. Haeffner, P. Lee, A. Mashayekhi, A. McPherson (Argonne), W. Hartung (Michigan State), J. Carneiro (Paris Sud-Orsay), M. Fitch (Rochester), and N. Barov (UCLA) is gratefully acknowledged.

*Operated by Universities Research Association, Inc. under contract No. DE-AC02-76CHO3000 with the United States Department of Energy
**Supported by BMBF contract number 06DA915I and by the DFG GK410

References

1. C. Clayton, , p. 13 and K. Nakajima, et al., p. 83 in **Advanced Accelerator Concepts**, eds. S. Chattopadhyay, J. McCullough, and P. Dahl, AIP Press C398, New York (1997).
2. See, for example, **Advanced Accelerator Concepts**, eds. S. Chattopadhyay, J. McCullough, and P. Dahl, AIP Press C398, New York (1997).
3. T. Katsouleas, p. 175 in **Advanced Accelerator Concepts**, eds. S. Chattopadhyay, J. McCullough, and P. Dahl (Lake Tahoe) AIP Press-CP398, New York (1997).

4. For recent summaries of channeling see H. Andersen, R. Carrigan, and E. Uggerhoj, Nucl. Instr. and Meth. **Channeling and other crystal effects at relativistic energy**, **B119** (1996) and R. A. Carrigan, Jr., p. 495 in **Handbook of Accelerator Physics and Engineering**, eds. A. Chao and M. Tigner, World Scientific, Singapore (1999).
5. P. Chen and R. J. Noble , p. 517 in **Relativistic Channeling**, eds. R. A. Carrigan, Jr. and J. A. Ellison (Plenum, 1987). P. Chen and R. Noble, p. 273 in **Advanced Accelerator Concepts**, eds. S. Chattopadhyay, J. McCullough, and P. Dahl, AIP Press C398, New York (1997).
6. R. A. Carrigan, Jr., p. 146 in **Advanced Accelerator Concepts**, eds. S. Chattopadhyay, J. McCullough, and P. Dahl (Lake Tahoe) AIP Press-CP398, New York (1997).
7. J. Davis, R. Clark, and J. Giuliani, Laser and Particle Beams, **13**, 3 (1995).
8. W. Lotz, et al., NIM **B48**, 256 (1990).
9. C. K. Cary, et al., Nucl. Instr. and Meth. **B51**, 458 (1990).
10. J.-P. Carneiro, et al., proceedings of the 1999 Particle Accelerator Conference, New York (1999).
11. H. Genz, et al., Phys. Rev. **B53**, 8922 (1996).
12. See, for example, P.A. Ross, Phys. Rev. 28, 425 (1926), I. V. Khutoretsky, Rev. Sci. Instrum. **66**, 773 (1995).
13. J. Freudenberger-Darmstadt thesis, "Roentgenstrahlung unter 180° bei Elektronenenergien von 30 bis 87 MeV am S-DALINAC, Aufbau eines Detektors fur Digitale Mammographie and Rontgenblitze sowie Test einer Rontgenlinse", Dissertation D17, Technische Universität Darmstadt (1999)-unpublished.
14. S. Fritzler, "Untersuchung von Channeling-strahlung bei Hohen Ladungsdichten am Photo-injector des Fermi National Accelerator Laboratory", Diploma Thesis, Technische Universität Darmstadt (2000)-unpublished and J. Freudenberger et al.-to be published.
15. J.-P. Carneiro, et al., submitted to FEL 99 and J.-P. Carneiro, "Etude experimentale du photo-injector de Fermilab", dissertation-Universite de Paris-Sud, Orsay (in preparation).
16. M. Ferrario et al., Particle Accelerators **52**, 1 (1996).
17. H. Genz, et al., App. Phys. Lett. **57**, 2956 (1990).
18. R. K. Klein, et al., Phys. Rev **B31**, **68** (1985).
19. C. K. Cary, et al., Phys. Rev. **B42**, 7 (1990).
20. T. Katsouleas, J. M. Dawson, D. Sultana, and Y. T. Yan, IEEE Transactions on Nuclear Science, Vol. NS-32 (1985).
21. P. Chen-private communication.
22. R. A. Carrigan, Jr. and M. Kh. Khokonov, p. 516 in Quantum Aspects of Beam Physics, ed. P. Chen, World Scientific, Singapore (1999).

INTEGRAL CHARACTERISTICS OF BREMSSTRAHLUNG AND PAIR PHOTOPRODUCTION IN A MEDIUM

V. N. BAIER AND V. M. KATKOV
Budker Institute of Nuclear Physics, Novosibirsk, 630090, Russia
E-mail: baier@inp.nsk.su

The bremsstrahlung of an electron and e^-e^+-pair creation by a photon in a medium is considered in high-energy region, where influence of the multiple scattering on the processes (the Landau-Pomeranchuk-Migdal (LPM) effect) becomes essential. The integral characteristics: the radiation length and the total probability of radiation and pair photoproduction are analyzed under influence of the LPM effect.

1 Introduction

When a charged particle is moving in a medium it scatters on atoms. With probability $\sim \alpha$ this scattering is accompanied by a radiation. At high energy the radiation process occurs over a rather long distance, known as the *formation length* l_c:

$$l_c = \frac{l_0}{1+\gamma^2\vartheta_c^2}, \quad l_0 = \frac{2\varepsilon\varepsilon'}{m^2\omega}, \tag{1}$$

where ω is the energy of emitted photon, $\varepsilon(m)$ is the energy (the mass) of a particle, $\gamma = \varepsilon/m$ is the Lorenz factor, $\varepsilon' = \varepsilon - \omega$, ϑ_c is the characteristic angle of photon emission, the system $\hbar = c = 1$ is used.

Landau and Pomeranchuk were the first who showed that if the formation length of bremsstrahlung becomes comparable to the distance over which the multiple scattering becomes important (when the mean angle of multiple scattering is of the order of the characteristic angle of photon emission $\sim 1/\gamma$), the bremsstrahlung will be suppressed [1]. Migdal [2] developed the quantitative theory of this phenomenon.

New activity with the theory of the LPM effect (see [3], [4], [5]) is connected with a very successful series of experiments performed at SLAC recently (see [6], [7]). In these experiments the cross section of the bremsstrahlung of soft photons with energy from 200 keV to 500 MeV from electrons with energy 8 GeV and 25 GeV is measured with an accuracy of the order of a few percent. Both LPM and dielectric suppression are observed and investigated. These experiments were the challenge for the theory since in all the mentioned papers calculations are performed to logarithmic accuracy which is not enough for description of the new experiment. The contribution of the Coulomb cor-

rections (at least for heavy elements) is larger than experimental errors and these corrections should be taken into account.

We developed the new approach to the theory of the Landau-Pomeranchuk-Migdal (LPM) effect [8] basing on the quasiclassical operator approach [9]. In this paper the cross section of the bremsstrahlung process in the photon energies region where the influence of the LPM is very strong was calculated with a term $\propto 1/L$, where L is characteristic logarithm of the problem, and with the Coulomb corrections taken into account. In the photon energy region, where the LPM effect is "turned off", the obtained cross section gives the exact Bethe-Maximon cross section (within power accuracy) with the Coulomb corrections. This important feature was absent in the previous calculations. Some important features of the LPM effect were considered also in [10], [11], [12], [13].

The crossing process for the bremsstrahlung is the pair creation by a photon. The created particles undergo here the multiple scattering. It should be emphasized that for the bremsstrahlung the formation length (1) increases strongly if $\omega \ll \varepsilon$. Just because of this the LPM effect was investigated at SLAC at a relatively low energy. For the pair creation by a photon with energy ω the formation length $l_p = \dfrac{2\varepsilon(\omega-\varepsilon)}{m^2\omega}$ attains maximum at $\varepsilon = \omega/2$ and this maximum is $l_{p,max} = (\omega/2m)\lambda_c$. Because of this even for heavy elements the effect of multiple scattering becomes noticeable at photon energies $\omega \geq$ 10 TeV. Starting from these energies one has to take into account the influence of a medium on the pair creation and on the bremsstrahlung hard part of the spectrum in electromagnetic showers being created by the cosmic ray particles of the ultrahigh energies. These effects can be quite significant in the electromagnetic calorimeters operating in the detectors on the colliders in TeV range.

In the present paper the radiation length is calculated under influence of the LPM effect. The total probability of photon radiation and the integral probability of the pair creation are considered also.

2 Influence of the multiple scattering on the bremsstrahlung

2.1 Bremsstrahlung spectrum at high energy

The spectral radiation intensity obtained in [8] (see Eq.(2.39)) has the form

$$dI = \omega dW = \frac{\alpha m^2 x dx}{2\pi(1-x)} \mathrm{Im}\ \left[\Phi(\nu) - \frac{1}{2L_c}F(\nu)\right], \quad x = \frac{\omega}{\varepsilon}, \tag{2}$$

where

$$\Phi(\nu) = \int_0^\infty dz e^{-it}\left[r_1\left(\frac{1}{\sinh z} - \frac{1}{z}\right) - i\nu r_2\left(\frac{1}{\sinh^2 z} - \frac{1}{z^2}\right)\right]$$
$$= r_1\left(\ln p - \psi\left(p + \frac{1}{2}\right)\right) + r_2\left(\psi(p) - \ln p + \frac{1}{2p}\right),$$
$$F(\nu) = \int_0^\infty \frac{dz e^{-it}}{\sinh^2 z}\left[r_1 f_1(z) - 2ir_2 f_2(z)\right],$$
$$f_1(z) = \left(\ln \varrho_c^2 + \ln\frac{\nu}{i} - \ln\sinh z - C\right) g(z) - 2\cosh z G(z),$$
$$f_2(z) = \frac{\nu}{\sinh z}\left(f_1(z) - \frac{g(z)}{2}\right), \quad g(z) = z\cosh z - \sinh z,$$
$$G(z) = \int_0^z (1 - y\coth y)dy$$
$$= z - \frac{z^2}{2} - \frac{\pi^2}{12} - z\ln\left(1 - e^{-2z}\right) + \frac{1}{2}\mathrm{Li}_2\left(e^{-2z}\right),$$
$$t = \frac{z}{\nu}, \quad r_1 = x^2, \quad r_2 = 1 + (1-x)^2, \quad t = t_1 + t_2,\ z = \nu t. \tag{3}$$

here $\alpha = 1/137,\ z = \nu t,\ p = i/(2\nu),\ \psi(x)$ is the logarithmic derivative of the gamma function, $\mathrm{Li}_2(x)$ is the Euler dilogarithm. Use of found form of Φ and the last representation of function $G(z)$ simplifies the numerical calculation. The term with $\Phi(\nu)$ in (2) describes the intensity in logarithmic approximation, the term with $F(\nu)$ is the first correction. The parameters in these formulas are

$$\nu^2 = i\nu_0^2, \quad \nu_0^2 = |\nu|^2 \simeq \nu_1^2\left(1 + \frac{\ln\nu_1}{L_1}\vartheta(\nu_1 - 1)\right), \quad \nu_1^2 = \frac{\varepsilon}{\varepsilon_e}\frac{1-x}{x},$$
$$\varepsilon_e = m\left(8\pi Z^2\alpha^2 n_a \lambda_c^3 L_1\right)^{-1},\ L_c \simeq L_1\left(1 + \frac{\ln\nu_1}{L_1}\vartheta(\nu_1 - 1)\right),\ L_1 = \ln\frac{a_{s2}^2}{\lambda_c^2},$$
$$\frac{a_{s2}}{\lambda_c} = 183 Z^{-1/3} e^{-f}, \quad f = f(Z\alpha) = (Z\alpha)^2\sum_{k=1}^{\infty}\frac{1}{k(k^2 + (Z\alpha)^2)}, \tag{4}$$

here Z is the charge of the nucleus, n_a is the number density of atoms in the medium, $\lambda_c = 1/m$ is the electron Compton wavelength. The LPM effect manifests itself when

$$\nu_1(x_c) = 1, \quad x_c = \frac{\varepsilon}{\varepsilon_e + \varepsilon}. \tag{5}$$

In the case $\varepsilon \ll \varepsilon_e$ in the hard part of spectrum ($1 \geq x \gg x_c$) the parameter $\nu_1^2 \simeq x_c/x \ll 1$ and the contribution into the integral (3) give the

region $z \ll 1$.

$$\text{Im } \Phi(\nu) \simeq r_1 \frac{\nu_1^2}{6} + r_2 \frac{\nu_1^2}{3}, \quad -\text{Im } F(\nu) = -\frac{1}{9}(r_2 - r_1)\nu_1^2(1 + O(\nu_1^4)). \tag{6}$$

Substituting into (2) we have

$$\frac{dI}{dx} = \frac{2Z^2\alpha^3 n_a \varepsilon}{3m^2}\left[r_1\left(L_1 - \frac{1}{3}\right) + 2r_2\left(L_1 + \frac{1}{6}\right)\right] \tag{7}$$

This is the Bethe-Maximon intensity spectrum (with the Coulomb corrections) in case of complete screening (if one neglects the contribution of atomic electrons) written down within power accuracy (omitted terms are of the order of powers of $1/\gamma$), see e.g. Eq.(18.30) in [14]. So, to obtain it in the limit considered one has to take into account the both terms in brackets in (2).

At very strong multiple scattering $\nu_0 \gg 1$ or $\varepsilon \gg \varepsilon_e$ one can omit e^{-it} in the integrand of function $F_(\nu)$ (3). Integrating over z we obtain

$$-\text{Im } F(\nu) = \frac{\pi}{4}(r_1 - r_2) + \frac{\nu_0}{\sqrt{2}}\left(\ln 2 - C + \frac{\pi}{4}\right) r_2, \tag{8}$$

where we take into account the next terms of the decomposition in the term $\propto r_2$. Under the same conditions ($\nu_0 \gg 1$) the function Im $\Phi(\nu)$ is

$$\text{Im } \Phi(\nu) = \frac{\pi}{4}(r_1 - r_2) + \frac{\nu_0}{\sqrt{2}} r_2. \tag{9}$$

Thus, at $\nu_0 \gg 1$ the relative contribution of the first correction $\dfrac{dW^1}{d\omega}$ is defined by

$$r = \frac{dW^1}{dW^c} = \frac{1}{2L_c}\left(\ln 2 - C + \frac{\pi}{4}\right) \simeq \frac{0.451}{L_c}. \tag{10}$$

In the case $\varepsilon \geq \varepsilon_e$ the intensity spectrum differs from the Bethe-Maximon one at $x \sim 1$ also. When $\varepsilon \gg \varepsilon_e$ we find in the interval not very close to the end of the spectrum ($x = 1$):

$$\frac{dI}{dx} \simeq \frac{2\sqrt{2}Z^2\alpha^3 n_a \varepsilon}{m^2}\sqrt{\frac{\varepsilon_e x}{\varepsilon(1-x)}}\left(1 + \frac{1}{4L_1}\ln\frac{\varepsilon(1-x)}{\varepsilon_e x}\right)\left[x^2\right.$$
$$\left.+2(1-x)\left(1 - \frac{\pi}{2\sqrt{2}}\sqrt{\frac{\varepsilon_e x}{\varepsilon(1-x)}}\right)\right], \quad \varepsilon(1-x) \gg \varepsilon_e x. \tag{11}$$

Now we turn to the integral characteristics of radiation. The total intensity of radiation in the logarithmic approximation can be presented as (see (2))

$$\frac{I}{\varepsilon}L^0_{rad} = 2\frac{\varepsilon_e}{\varepsilon}\mathrm{Im}\left[\int_0^1 \frac{dx}{g}\sqrt{\frac{x}{1-x}}(2(1-x)+x^2)\right.$$
$$\left.+\int_0^1 \frac{x^3dx}{1-x}\left(\psi(p+1)-\psi\left(p+\frac{1}{2}\right)\right)+2\int_0^1 xdx\left(\psi\left(p+1\right)-\ln p\right)\right], \quad (12)$$

where

$$p=\frac{g\eta}{2},\quad \eta=\sqrt{\frac{x}{1-x}},\quad g=\exp\left(i\frac{\pi}{4}\right)\sqrt{\frac{L_1}{L_c}\frac{\varepsilon_e}{\epsilon}},$$

L^0_{rad} is the radiation length in the logarithmic approximation. The relative energy losses of electron per unit time in terms of the Bethe-Maximon radiation length L^0_{rad}: $\dfrac{I}{\varepsilon}L^0_{rad}$ in gold is given in Fig.1 (curve 1), it reduces by 10% (15% and 25%) at $\varepsilon \simeq 700$ GeV ($\varepsilon \simeq 1.4$ TeV and $\varepsilon \simeq 3.8$ TeV) respectively, and it cuts in half at $\omega \simeq 26$ TeV. This increase of effective radiation length can be important in electromagnetic calorimeters operating in detectors on colliders in TeV range. The contribution of the correction terms r (see (10)) is $r \simeq 0.451/L_c$.

In Eqs.(7) and (11) we can use the main terms of decomposition only.

The main term in (7) gives after the integration over x the standard expression for the radiation length L_{rad} without influence of multiple scattering.

$$\frac{I}{\varepsilon}=\frac{\alpha m^2}{4\pi\varepsilon_e}\left(1+\frac{1}{9L_1}-\frac{4\pi}{15}\frac{\varepsilon}{\varepsilon_e}\right)\simeq L^{-1}_{rad}\left(1-\frac{4\pi}{15}\frac{\varepsilon}{\varepsilon_e}\right),$$
$$\frac{1}{L_{rad}}=\frac{2Z^2\alpha^3 n_a L_1}{m^2}\left(1+\frac{1}{9L_1}\right)=\frac{1}{L^0_{rad}}\left(1+\frac{1}{9L_1}\right) \quad (13)$$

The integration over x of the main term in (11) gives (terms $\propto\sqrt{\varepsilon_e/\varepsilon}$ in the square brackets are neglected)

$$I_0\simeq\frac{9\pi Z^2\alpha^3 n_a\sqrt{\varepsilon\varepsilon_e}}{4\sqrt{2}m^2}L_1\left[1+\frac{1}{4L_1}\left(\ln\frac{\varepsilon}{\varepsilon_e}-\frac{46}{27}\right)+r_0\right], \quad (14)$$

where $r_0=\left(\ln 2-C+\pi/4\right)/2L_1$. The corrections (without terms $\propto 1/L_1$) to (14) are calculated in Appendix B of [13](see Eq.(B.11)). The complete result is

$$\frac{I}{\varepsilon L_{rad}}\simeq\frac{5}{2}\sqrt{\frac{\varepsilon_e}{\varepsilon}}\left[1-2.37\sqrt{\frac{\varepsilon_e}{\varepsilon}}-4.57\frac{\varepsilon_e}{\varepsilon}+\frac{1}{4L_1}\left(\ln\frac{\varepsilon}{\varepsilon_e}-0.3455\right)\right] \quad (15)$$

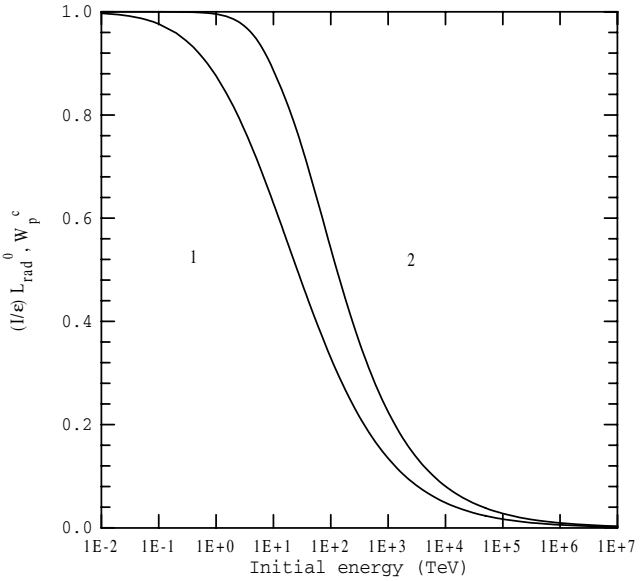

Figure 1. The relative energy losses of electron per unit time in terms of the Bethe-Maximon radiation length L^0_{rad}: $\frac{I}{\varepsilon}L^0_{rad}$ in gold Eq.(12) vs the initial energy of electron (curve 1) and the total pair creation probability per unit time W^c_p (see Eq.(22))in terms of the Bethe-Maximon total probability of pair creation W^{BH}_{p0} in gold vs the initial energy of photon (curve 2).

Although the coefficients in the last expression are rather large at two first terms of the decomposition over $\sqrt{\varepsilon_e/\varepsilon}$ this formula has the accuracy of the order of 10% at $\varepsilon \sim 10\varepsilon_e$.

The integral probability of radiation in terms of the Bethe-Maximon radiation length can be obtained from Eq.(12) dividing the integrand in all integrals by x. It is given in Fig.2. It should be mentioned that the standard Bethe-Maximon integral probability doesn't exist at all (the integral over ω has the logarithmic divergence at $\omega \to 0$). Due to the LPM effect the soft part of the spectrum is damped and integral over ω exists.

The integral probability of radiation for $\varepsilon \ll \varepsilon_e$ was calculated in [11]:

$$W = \frac{4}{3L^0_{rad}}\left(\ln\frac{\varepsilon_e}{\varepsilon} + C_2\right),$$

$$C_2 = 2C - \frac{5}{8} + 12\int_0^\infty \ln z \left(\frac{1}{z^3} - \frac{\cosh z}{\sinh^3 z}\right) dz \simeq 1.96 \tag{16}$$

In the case $\varepsilon \gg \varepsilon_e$ we can calculate the integral probability of radiation starting with Eq.(11). Conserving the main term, dividing it by $x\varepsilon$ and integrating over x we find

$$W_0 = \frac{11\pi Z^2\alpha^3 n_a}{2\sqrt{2}m^2}\sqrt{\frac{\varepsilon_e}{\varepsilon}}L_1\left[1 + \frac{1}{4L_1}\left(\ln\frac{\varepsilon}{\varepsilon_e} + \frac{8}{11}\right) + r_0\right] \tag{17}$$

The correction terms to Eq.(16) are calculated in Appendix B of [13](see Eq.(B.13)). Substituting them we have

$$W = \frac{11\pi Z^2\alpha^3 n_a}{2\sqrt{2}m^2}\sqrt{\frac{\varepsilon_e}{\varepsilon}}L_1\left[1 - 1.23\sqrt{\frac{\varepsilon_e}{\varepsilon}} + 1.65\frac{\varepsilon_e}{\varepsilon} + \frac{1}{4L_1}\left(\ln\frac{\varepsilon}{\varepsilon_e} + 2.53\right)\right]. \tag{18}$$

Ratio of the main terms of Eqs.(15) and (18) gives the mean energy of radiated photon

$$\bar{\omega} = \frac{9}{22}\varepsilon \simeq 0.409\varepsilon. \tag{19}$$

3 Influence of multiple scattering on pair creation process

The probability of the pair creation by a photon can be obtained from the probability of the bremsstrahlung with help of the substitution law:

$$\omega^2 d\omega \to \varepsilon^2 d\varepsilon, \quad \omega \to -\omega, \quad \varepsilon \to -\varepsilon, \tag{20}$$

where ω is the initial photon energy, ε is the energy of the created electron. Making this substitution in Eq.(2) we obtain the spectral distribution of the pair creation probability (over the energy of the electron)

$$\begin{aligned}
&\frac{dW_p^c}{d\varepsilon} = \frac{\alpha m^2}{2\pi\varepsilon\varepsilon'}\mathrm{Im}\ \left[\Phi_p(\nu) - \frac{1}{L_c}F_p(\nu)\right],\\
&\Phi_p(\nu) = \nu\int_0^\infty dt e^{-it}\left[s_1\left(\frac{1}{\sinh z} - \frac{1}{z}\right) - i\nu s_2\left(\frac{1}{\sinh^2 z} - \frac{1}{z^2}\right)\right]\\
&= s_1\left(\ln p - \psi\left(p + \frac{1}{2}\right)\right) + s_2\left(\psi(p) - \ln p + \frac{1}{2p}\right),\\
&F_p(\nu) = \int_0^\infty \frac{dz e^{-it}}{\sinh^2 z}\left[s_1 f_1(z) - 2is_2 f_2(z)\right],\\
&s_1 = 1, \quad s_2 = \frac{\varepsilon^2 + \varepsilon'^2}{\omega^2}, \quad \varepsilon' = \omega - \varepsilon.
\end{aligned} \tag{21}$$

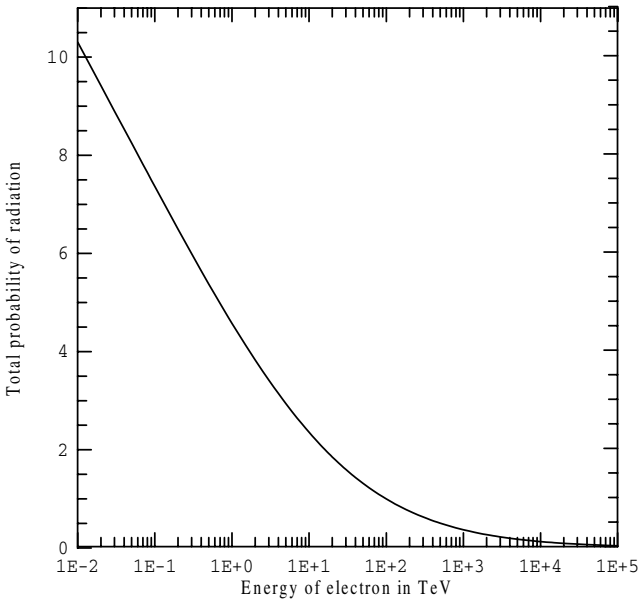

Figure 2. The total probability of photon emission W_0 in terms of the Bethe-Maximon radiation length L^0_{rad} in gold vs the initial energy electron .

All entering functions are defined in (3).

The total probability of pair creation in the logarithmic approximation can be presented as (see (21))

$$\frac{W_p^c}{W_{p0}^{BH}} = \frac{9}{14}\frac{\omega_e}{\omega}\mathrm{Im}\int_0^1 \frac{dy}{y(1-y)}\left[\left(\ln p - \psi\left(p+\frac{1}{2}\right)\right)\right.$$
$$\left. + \left(1-2y+2y^2\right)\left(\psi\left(p\right) - \ln p + \frac{1}{2p}\right)\right], \quad p = \frac{bs}{4}, \tag{22}$$

where

$$s = \frac{1}{\sqrt{y(1-y)}}, \quad b = \exp\left(i\frac{\pi}{4}\right)\sqrt{\frac{L_1}{L_c}\frac{\omega_e}{\omega}}, \quad \omega_e = m\left(2\pi Z^2\alpha^2 n_a \lambda_c^3 L_1\right)^{-1},$$

here W_{p0}^{BH} is the Bethe-Maximon probability of pair photoproduction in the logarithmic approximation. Note that ω_e is four times larger than ε_e, in gold $\omega_e = 10.5$ TeV. This is just the value of photon energy starting with the

LPM effect becomes essential for the pair creation process in heavy elements. The total probability of pair creation W_p^c in gold is given in Fig.1 (curve 2),it reduced by 10% at $\omega \simeq 9$ TeV and it cuts in half at $\omega \simeq 130$ TeV.

4 Conclusion

In this paper we considered the influence of multiple scattering on the bremsstrahlung process at any energy including the high-energy region ($\varepsilon \geq \varepsilon_e$), where all the spectrum of radiation is distorted. In this region the total intensity of radiation diminishes and respectively the radiation length increases. The cross section of e^-e^+ pair creation by a photon changes essentially if the photon energy $\omega \geq \omega_e = 4\varepsilon_e$, see Eq.(4).

If we restrict to the main terms of the decomposition Eq.(15) in asymptotic region $\varepsilon \gg \varepsilon_e$, then the intensity of radiation and the corresponding radiation length can be written as

$$I \simeq \frac{9}{16}\sqrt{\frac{\pi}{2}} Z\alpha^2 \left(\varepsilon n_a \ln\left(9\pi Z^2\alpha^2 \varepsilon n_a a_{s2}^4\right)\right)^{1/2}, \quad L_{rad} = \frac{\varepsilon}{I(\varepsilon)}. \tag{23}$$

The integral cross section of radiation follows from the integral probability of radiation (18)

$$\sigma = \frac{W}{n_a} \simeq \frac{11}{8}\sqrt{\frac{\pi}{2}} \frac{Z\alpha^2}{\sqrt{\varepsilon n_a}} \left(\ln\left(100\pi Z^2\alpha^2 \varepsilon n_a a_{s2}^4\right)\right)^{1/2}. \tag{24}$$

We have from for the total probability of pair creation by a photon at $\omega \gg \omega_e$ and the corresponding cross section

$$W_p \simeq \frac{3}{4}\sqrt{\frac{\pi}{2}} Z\alpha^2 \left(\frac{n_a}{\omega} \ln\left(2\pi Z^2\alpha^2 \omega n_a a_{s2}^4\right)\right)^{1/2}, \quad \sigma_p = \frac{W_p}{n_a} \tag{25}$$

The Eqs.(23)-(25) don't depend on the electron mass and the cross sections of bremsstrahlung and pair creation diminish with energy and density n_a growth.

In this paper we considered the case of an infinitely thick target where the formation length is much shorter than the thickness of a target. Because of this we neglected the boundary effects. These effects were considered in detail in [8],[10], they can give quite essential contribution in the soft part of spectrum depending on the target thickness. We neglected also by effects of the polarization of a medium. They were considered in detail in [8]. The relative contribution of polarization of a medium into probability of pair creation is discussed in [15]

$$\frac{\omega_0^2 \varepsilon\varepsilon'}{\omega^2 m^2} \leq \frac{\omega_0^2}{m^2} < 10^{-7} \ll 1, \quad \omega_0^2 = \frac{4\pi e^2 n_e}{m}, \tag{26}$$

where n_e is the number density of electron in the medium, ω_0 is the plasma frequency. The contribution of polarization of a medium into the total energy losses in thick target is of the order ω_0/m. The polarization of a medium affects at the soft part of the spectrum only at $\omega \leq \omega_p = \gamma\omega_0$ ($x \leq \omega_p/\varepsilon = \omega_0/m$). Even for heavy elements $\omega_0/m \sim 2 \cdot 10^{-4}$. This contribution was analyzed in [8].

Acknowledgments

. This work was supported in part by the Russian Fund of Basic Research under Grant 00-02-18007.

References

1. L. D. Landau and I. Ya. Pomeranchuk, *Dokl.Akad.Nauk SSSR* **92**, 535, 735, (1953). See *The Collected Paper of L. D. Landau* (Pergamon Press, New York 1965) for an English translation.
2. A. B. Migdal, *Phys. Rev.* **103**, 1811, (1956).
3. R.Blancenbeckler and S. D. Drell, *Phys.Rev.* D **53**, 6265, (1996).
4. R. Baier, Yu. L. Dokshitzer, A. H. Mueller, S. Peigne, and D. Schiff, Nucl. Phys. B **478**, 577, (1996).
5. B. G. Zakharov, *Pis'ma v ZhETF* **63**, 906, (1996).
6. P. L. Anthony, R. Becker-Szendy, P. E. Bosted, *et al*, *Phys.Rev.* D **56**, 1373, (1997).
7. S. Klein, *Rev. Mod. Phys.* **71**, 1501, (1999).
8. V. N. Baier and V. M. Katkov, *Phys.Rev.* D **57**, 3146, (1998).
9. V.N.Baier, V.M.Katkov and V.M.Strakhovenko, *Electromagnetic Processes at High Energies in Oriented Single Crystals* (World Scientific, Singapore, 1998).
10. V. N. Baier and V. M. Katkov, in *Quantum Aspects of Beam Physics*, ed. P Chen, (World Scientific, Singapore, 1998), p.525.
11. V. N. Baier and V. M. Katkov, *Phys.Rev.* D **59**, 056003, (1999).
12. V. N. Baier and V. M. Katkov, *Phys.Rev.* D **60**, 076001, (1999).
13. V. N. Baier and V. M. Katkov, *Phys.Rev.* D **62**, 036008, (2000).
14. V. N. Baier, V. M. Katkov, and V. S. Fadin, *Radiation from Relativistic Electrons* (in Russian), (Atomizdat, Moscou, 1973).
15. V. N. Baier and V. M. Katkov, *Phys.Lett.* A **252**, 263 (1999).

THE COULOMB CORRECTIONS TO THE E^+E^- PAIR PRODUCTION IN ULTRARELATIVISTIC HEAVY-ION COLLISIONS

R.N. LEE

Budker Institute of Nuclear Physics, 630090 Novosibirsk, Russia

We manifest the origin of the wrong conclusion made by several groups of authors on the absence of Coulomb corrections(CC) to the cross section of the e^+e^- pair production in ultrarelativistic heavy-ion collisions. The source of the mistake is connected with an incorrect passage to the limit in the expression for the cross section. When this error is eliminated, the CC do not vanish and agree with the results obtained within the Weizsäcker-Williams approximation.

The investigation of the process of e^+e^- pair production in ultrarelativistic heavy-ion collisions is one of the by-product purposes of such projects as RHIC and LHC. This circumstance explains the increased theoretical interest to this process in last two years. Extremely high energies of nuclei give one a hope, that the calculation of the cross section of this process can be done analytically. Recently there was a set of publications[1−3] in which the cross section of the process was calculated exactly in the parameters $\alpha Z_{A,B}$ ($Z_{A,B}$ being the charge numbers of the nuclei A and B, α is the fine-structure constant). In these papers the nuclei were treated as sources of the external field, moving with the speed, close to that of light (light-fronts approach), and the amplitude was calculated at a fixed impact parameter of the nuclei. After that the cross section was obtained by the integration over the impact parameter. As a result, the conclusion was made that the exact cross section coincides with that calculated in the lowest order perturbation theory with respect to $\alpha Z_{A,B}$ (Born cross section). On the other hand, in the Weizsäcker-Williams approximation with respect to one of the nuclei, the cross section of the process is proportional to the well-known cross section of the e^+e^- pair production by a photon in a Coulomb field[4] and, therefore, contains the CC. This obvious circumstance was noted by Ivanov *et al.*[5], who calculated the CC in the process under discussion. Though the existence of the CC is out of doubt, the source of the disagreement between the results was not revealed so far.This report is based on the results of the paper by R.N. Lee and A.I. Milstein[6], where the solution of this puzzle was presented.

Let the ultrarelativistic nuclei A and B move in the positive and negative directions of the z axis, respectively. Then the expression for the cross section

of the e^+e^- pair production, obtained in light-fronts approach[1–3], reads

$$d\sigma = \frac{m^2 d^3p d^3q}{(2\pi)^6 \varepsilon_p \varepsilon_q} \int \frac{d^2k}{(2\pi)^2} |F_B(\mathbf{k})|^2 |F_A(\mathbf{q}_\perp + \mathbf{p}_\perp - \mathbf{k})|^2 |\mathcal{M}(\mathbf{k})|^2 \ , \quad (1)$$

$$\mathcal{M}(\mathbf{k}) = \overline{u}(p) \frac{\boldsymbol{\alpha}\ (\mathbf{k} - \mathbf{p}_\perp) + \gamma_0 m}{-p_+ q_- - (\mathbf{k} - \mathbf{p}_\perp)^2 - m^2 + i\epsilon} \gamma_- u(-q) +$$

$$+ \overline{u}(p) \frac{-\boldsymbol{\alpha}\ (\mathbf{k} - \mathbf{q}_\perp) + \gamma_0 m}{-p_- q_+ - (\mathbf{k} - \mathbf{q}_\perp)^2 - m^2 + i\epsilon} \gamma_+ u(-q) \ .$$

Here $\mathbf{p}$ and ε_p ($\mathbf{q}$ and ε_q) are the momentum and energy of the electron (positron), $u(p)$ and $u(-q)$ are positive- and negative-energy Dirac spinors, $\boldsymbol{\alpha} = \gamma^0 \boldsymbol{\gamma}$, $\gamma_\pm = \gamma^0 \pm \gamma^z$, γ^μ are the Dirac matrices, $p_\pm = \varepsilon_p \pm p^z$, $q_\pm = \varepsilon_q \pm q^z$, m is the electron mass, $\mathbf{k}$ is a two-dimensional vector lying in the xy plane, and the function $F(\boldsymbol{\Delta})$ is proportional to the electron eikonal scattering amplitude in the potential $V(\mathbf{r})$ of the corresponding nucleus:

$$F(\boldsymbol{\Delta}) = \int d^2\rho \exp[-i\boldsymbol{\rho}\boldsymbol{\Delta}] \left\{\exp[-i\chi(\boldsymbol{\rho})] - 1\right\} \ , \quad (2)$$

$$\chi(\boldsymbol{\rho}) = \int_{-\infty}^{\infty} dz V(z, \boldsymbol{\rho}) \ .$$

For the potential $V(\mathbf{r}) = V_c(r) = -Z\alpha/r$, the integral in $\chi(\boldsymbol{\rho})$ becomes divergent and requires a regularization. This regularization can be made by using the potential $V(\mathbf{r}) = -Z\alpha \exp(-r/a)/r$. Performing the integration in (2), and taking the limit $a \to \infty$ at fixed $\boldsymbol{\Delta} \neq 0$, one obtains (up to the constant phase depending on a):

$$F(\boldsymbol{\Delta}) = \mathcal{F}(\boldsymbol{\Delta}) \equiv i\pi Z\alpha \frac{\Gamma(1 - iZ\alpha)}{\Gamma(1 + iZ\alpha)} \left(\frac{4}{\Delta^2}\right)^{1 - iZ\alpha} \ . \quad (3)$$

Actually, to obtain this result one can use any regularization of the phase $\chi(\boldsymbol{\rho})$ for which $\chi(\boldsymbol{\rho}) \to 0$ at $\rho \to \infty$. Since $|\mathcal{F}(\boldsymbol{\Delta})|^2 = (4\pi Z\alpha/\Delta^2)^2 \propto Z^2$, then the substitution (3) into (1) would lead to the wrong conclusion [1–3] that the exact cross section coincides with the Born result. Let us show that, in order to obtain the CC in (1), it is necessary first to take the integral over $\mathbf{k}$ using the functions $F(\boldsymbol{\Delta})$ with the regularized phase and then remove the regularization.

Consider the integral

$$G = \int \frac{d^2k}{(2\pi)^2} k^2 \left(|F(\mathbf{k})|^2 - |F^0(\mathbf{k})|^2\right) \ , \quad (4)$$

where $F^0(\mathbf{\Delta}) = -i\int d\boldsymbol{\rho}\exp(-i\mathbf{\Delta}\boldsymbol{\rho})\chi(\boldsymbol{\rho})$ is the first term of the expansion of $F(\mathbf{\Delta})$ with respect to the potential. For $F = \mathcal{F}$ and, correspondingly, $F^0 = \mathcal{F}^0 \equiv 4i\pi Z\alpha/\Delta^2$, the integrand in (4) vanishes. Let us show that the integral G is not equal to zero for the regularized F and is independent of the regularization method, if $V(\mathbf{r}) \to -Z\alpha/r$ at $r \to 0$ (when $\chi(\boldsymbol{\rho}) \to 2Z\alpha\ln(\rho) + const$ at $\boldsymbol{\rho} \to 0$).

Integrating by parts over $\boldsymbol{\rho}$, one can easily prove that

$$F(\mathbf{k}) = -\frac{1}{k^2}\int d\boldsymbol{\rho}\,\exp[-i\mathbf{k}\boldsymbol{\rho}](\mathbf{k}\nabla\chi(\boldsymbol{\rho}))\exp(-i\chi(\boldsymbol{\rho}))\ , \tag{5}$$

The function $F^0(\mathbf{k})$ can be obtained from (5) by omitting the exponent in the integrand. Substituting (5) into (4), we obtain

$$G = \int\frac{d\mathbf{k}}{(2\pi)^2}\int\int d\boldsymbol{\rho}_1\,d\boldsymbol{\rho}_2\,\exp[-i\mathbf{k}(\boldsymbol{\rho}_1-\boldsymbol{\rho}_2)]\times \\ \times\frac{(\mathbf{k}\nabla\chi(\boldsymbol{\rho}_1))(\mathbf{k}\nabla\chi(\boldsymbol{\rho}_2))}{k^2}\left\{\exp[-i\chi(\boldsymbol{\rho}_1)+i\chi(\boldsymbol{\rho}_2)]-1\right\}\ . \tag{6}$$

If one changes naively the order of integration over $\mathbf{k}$ and $\boldsymbol{\rho}_{1,2}$ and takes the integral over $\mathbf{k}$, then,due to the δ-function appeared, the integration over $\boldsymbol{\rho}$ results in zero. To demonstrate that the change of the integration order in (6) is invalid, we restrict the region of integration over $\mathbf{k}$ by the condition $k < Q$. After that one can change the order of integration in (6). Integrating over the angles of $\mathbf{k}$ and then over k, we obtain

$$G = \int\int\frac{d\boldsymbol{\rho}_1\,d\boldsymbol{\rho}_2}{2\pi\rho^2}(\nabla\chi(\boldsymbol{\rho}_1))_i(\nabla\chi(\boldsymbol{\rho}_2))_j\left\{\exp[-i\chi(\boldsymbol{\rho}_1)+i\chi(\boldsymbol{\rho}_2)]-1\right\} \\ \left[[1-J_0(Q\rho)]\left(\delta_{i\,j}-2\frac{\rho_i\rho_j}{\rho^2}\right)+Q\rho J_1(Q\rho)\frac{\rho_i\rho_j}{\rho^2}\right]\ , \tag{7}$$

where $\boldsymbol{\rho} = \boldsymbol{\rho}_1 - \boldsymbol{\rho}_2$. Substituting $\rho_{1,2} \to \rho_{1,2}/Q$, and taking the limit $Q \to \infty$ with the use of the asymptotics of χ, we find

$$G = 4(Z\alpha)^2\int\int\frac{d\boldsymbol{\rho}_1\,d\boldsymbol{\rho}_2}{2\pi\rho^2\rho_1^2\rho_2^2}\left\{\left(\frac{\rho_2}{\rho_1}\right)^{2iZ\alpha}-1\right\}\times \\ \times\left[[1-J_0(\rho)]\left(\boldsymbol{\rho}_1\boldsymbol{\rho}_2-2\frac{(\boldsymbol{\rho}_1\boldsymbol{\rho})(\boldsymbol{\rho}_2\boldsymbol{\rho})}{\rho^2}\right)+\rho J_1(\rho)\frac{(\boldsymbol{\rho}_1\boldsymbol{\rho})(\boldsymbol{\rho}_2\boldsymbol{\rho})}{\rho^2}\right]\ . \tag{8}$$

Integrating the term $\propto [1-J_0(\rho)]$ in square brackets by parts over the angle between $\boldsymbol{\rho}_1$ and $\boldsymbol{\rho}_2$ and using the relation

$$\int_0^{2\pi}d\phi\cos\,\phi\frac{J_1(\sqrt{\rho_1^2+\rho_1^2-2\rho_1\rho_2\cos\,\phi})}{(\sqrt{\rho_1^2+\rho_1^2-2\rho_1\rho_2\cos\,\phi})} = \tag{9}$$

$$= \frac{2\pi}{\rho_1^2 - \rho_2^2} \rho_2 J_0(\rho_2) J_1(\rho_1) - \rho_1 J_0(\rho_1) J_1(\rho_2) \, ,$$

we obtain

$$G = 8\pi (Z\alpha)^2 \int\limits_0^\infty \int\limits_0^\infty \frac{d\rho_1 \, d\rho_2}{\rho_1^2 - \rho_2^2} \left\{ \left(\frac{\rho_2}{\rho_1} \right)^{2iZ\alpha} - 1 \right\} \times$$
$$\times \left[\rho_2 J_0(\rho_2) J_1(\rho_1) - \rho_1 J_0(\rho_1) J_1(\rho_2) \right] \, . \qquad (10)$$

Making the change of variables $\rho_{1,2} = r \exp(\pm t/4)$, and integrating over r, we obtain the non-zero result for the quantity G:

$$G = 8\pi (Z\alpha)^2 \int\limits_0^\infty dt \frac{\cos(Z\alpha t) - 1}{\exp(t) - 1} = \qquad (11)$$
$$= -8\pi (Z\alpha)^2 [\mathrm{Re}\psi(1 + iZ\alpha) + C] = -8\pi (Z\alpha)^2 f(Z\alpha) \, ,$$

where C is the Euler constant, $\psi(x) = d \ln \Gamma(x)/dx$. Thus, we come to the remarkable statement: although the main contribution to the integral in (4) comes from the region of small k, where $|F(\mathbf{k})|$ differs from $|\mathcal{F}(\mathbf{k})| = 4\pi Z\alpha/k^2$ and depends on the regularization parameters (the radius of screening), nevertheless, the integral G itself is a universal function of $Z\alpha$. Note that the approximate formula for the integral (4) was found by Moliere[7] at the investigation of multiple scattering.

Now it is clear, how to derive the CC starting from the expression (1). Let us calculate the CC related to the nucleus B (the contribution of the higher order perturbation theory with respect to the parameter $Z_B\alpha$). For this purpose one should replace in (1) the functions $|F_B|^2$ and $|F_A|^2$ with $|F_B|^2 - |F_B^0|^2$ and $|\mathcal{F}_A^0|^2$, respectively, keeping the regularization in the functions F_B and F_B^0. The main contribution to the integral is given by the region of small $\mathbf{k}$. Therefore, we can neglect $\mathbf{k}$ in the argument of $\mathcal{F}_A^0$ and expand the matrix element $\mathcal{M}$ at small $\mathbf{k}$:

$$\mathcal{M}(\mathbf{k}) \approx \mathbf{k}\mathbf{L} \, , \qquad (12)$$
$$\mathbf{L} = \overline{u}(p) \left\{ \frac{\boldsymbol{\alpha} \, (\gamma_-/p_+ - \gamma_+/q_+)}{(p_- + q_-)} + \frac{2\gamma_- (\mathbf{p}_\perp/p_+ - \mathbf{q}_\perp/q_+)}{(p_- + q_-)^2} \right\} u(-q) \, .$$

Using (11) and (12), and performing the summation over electron and positron polarizations, we obtain the following expression for the CC related to the nucleus B:

$$d\sigma_B^c = \frac{2G_B d^3p \, d^3q}{(2\pi)^6 \varepsilon_p \varepsilon_q} \frac{|\mathcal{F}_A^0(\mathbf{p}_\perp + \mathbf{q}_\perp)|^2}{[p_+ q_+ (p_- + q_-)]^2} \Big\{ p_+ q_+ (\mathbf{p}_\perp + \mathbf{q}_\perp)^2 - \qquad (13)$$

$$-\frac{2(\mathbf{p}_\perp q_+ q_- + \mathbf{q}_\perp p_+ p_-)^2}{(p_- + q_-)^2}\Big\} .$$

Here G_B denotes the function G in (11) at $Z = Z_B$. The CC related to the nucleus A can be obtained from (13) by the substitution $Z_A \leftrightarrow Z_B$ and the replacement of indices $- \leftrightarrow +$.

It is necessary to note the following circumstance. Actually, in the expansion over $Z_A\alpha$ and $Z_B\alpha$ of the differential cross section $d\sigma/d\mathbf{p}d\mathbf{q}$ in (1) , only the lowest (Born) term is correct. As for the higher order terms in (1) (CC), they give the correct result only after the integration over the directions of the positron (electron) momentum. This is due to the fact that the asymptotic form of the wave functions used[1−3] corresponds to the problem of scattering, but not to the problem of pair production. If one calculates the cross section integrated over the direction of $\mathbf{q}$, then, due to the completeness relation, it is possible to replace the set of functions containing in asymptotics the converging spherical wave with the set of functions containing the diverging spherical wave. Thus, (13) should be integrated over the angles of $\mathbf{q}$ or $\mathbf{p}$. The same trick was made at the recalculation of the bremsstrahlung cross section integrated over the photon momentum from the cross section of pair photoproduction integrated over the positron momentum[8]. It explains why the CC (13) are given by the region of small $\mathbf{k}$, while at the calculation of the CC using the wave functions with the correct asymptotic behavior the main contribution would come from the region $k \sim m$. The same situation occurs at the calculation of bremsstrahlung and pair photoproduction cross sections, where the CC come from different regions of momentum transfers.

Let us calculate within the logarithmic accuracy the CC to the cross section $d\sigma/d\varepsilon_p d\varepsilon_q$ at $\varepsilon_{p,q} \gg m$. At the integration over the transverse momenta the main contribution comes from the region $\Delta = |\mathbf{p}_\perp + \mathbf{q}_\perp| \ll p_\perp, q_\perp \sim m$. The integral over Δ requires regularization at $\Delta \to 0$. It is obvious that the lower limit of integration over Δ coincides with that in the Weizsäcker-Williams method. In the rest frame of the nucleus B it has the form $\Delta_{min} = (\varepsilon_p^0 + \varepsilon_q^0)/\tilde{\gamma}$, where $\varepsilon_{p,q}^0$ are the energies of the electron and positron, $\tilde{\gamma}$ is the Lorentz factor of the nucleus A in this frame. In the laboratory frame, where the nuclei A and B have the Lorentz factors γ_A and γ_B, respectively, one has $\Delta_{min} = (p_+ + q_+)/\gamma_A$. Using this cutoff, we obtain

$$d\sigma_B^c = -\frac{4}{\pi m^2}(Z_A\alpha)^2(Z_B\alpha)^2 f(Z_B\alpha)\frac{d\varepsilon_p d\varepsilon_q}{(\varepsilon_p + \varepsilon_q)^2} \times \qquad (14)$$
$$\times \left(1 - \frac{4\varepsilon_p\varepsilon_q}{3(\varepsilon_p + \varepsilon_q)^2}\right)\left[\ln\frac{m^2}{\Delta_{1min}^2} + \ln\frac{m^2}{\Delta_{2min}^2}\right] .$$

The sum of logarithms in this formula corresponds to the contributions of

two kinematic regions: p^z, $q^z > 0$ and p^z, $q^z < 0$. In the first case $\Delta_{1min} = (\varepsilon_p + \varepsilon_q)/\gamma_A$, and the corresponding term in (14) is valid at $m \ll \varepsilon_{p,q} \ll m\gamma_A$. In the second case $\Delta_{2min} = m^2/(\varepsilon_p + \varepsilon_q)\gamma_A$, and the corresponding term is valid at $m \ll \varepsilon_{p,q} \ll m\gamma_B$. Performing the integration over $\varepsilon_{p,q}$ in the regions indicated, one has

$$\sigma_B^c = -\frac{28}{9\pi m^2}(Z_A\alpha)^2(Z_B\alpha)^2 f(Z_B\alpha)\ln^2(\gamma_A\gamma_B)\ . \tag{15}$$

The formulas (14) and (15) can be easily obtained in the Weizsäcker-Williams approximation using the well-known result for the exact in $Z\alpha$ pair photoproduction cross section in the field of a nucleus[5,9]. It also follows from the Weizsäcker-Williams method that the contribution of the terms, containing the higher orders of Z_A and Z_B simultaneously, can be neglected within our accuracy.

In the light-fronts approach[1−3] the amplitude of e^+e^- pair production was obtained at fixed impact parameter between the nuclei.In this amlitude there is no need to keep any regularization. The CC are obtained by subtracting from the exact matrix element squared the Born term. After that subtraction the integral over the impact parameter $\mathbf{b}$ converges in contrast with the case of Born term, for which it logarithmically diverges at large b. Let us show, that, due to the convergence, this integral gives the correct CC.

The CC related to the nucleus B have the form

$$d\sigma_B^c = \frac{m^2 d^3p\, d^3q}{(2\pi)^6\varepsilon_p\varepsilon_q}\int d^2b \iint \frac{d^2k_1}{(2\pi)^2}\frac{d^2k_2}{(2\pi)^2}\exp[i(\mathbf{k}_1-\mathbf{k}_2)\mathbf{b}]\mathcal{M}(\mathbf{k}_1)\mathcal{M}^*(\mathbf{k}_2)\times$$
$$\times\left[\mathcal{F}_B(\mathbf{k}_1)\mathcal{F}_B^*(\mathbf{k}_2) - \mathcal{F}_B^0(\mathbf{k}_1)\mathcal{F}_B^{0*}(\mathbf{k}_2)\right]\mathcal{F}_A^0(\mathbf{q}_\perp + \mathbf{p}_\perp - \mathbf{k}_1)\mathcal{F}_A^{0*}(\mathbf{q}_\perp + \mathbf{p}_\perp - \mathbf{k}_2). \tag{16}$$

Again, changing the order of integration would lead to zero result. Indeed, taking the integral over $\mathbf{b}$ first, we get the factor $\delta(\mathbf{k}_1 - \mathbf{k}_2)$ in the integrand, and, therefore, the integral over $\mathbf{k}_1$ vanishes due to the relation $|\mathcal{F}_B|^2 = |\mathcal{F}_B^0|^2$. Let us demonstrate that, similar to the case of the integral (4) calculation, the change of the integration order in (16) is incorrect, and the result (13) also follows from (16). For this purpose, we restrict the region of integration over $\mathbf{b}$ by the condition $b < R$. After that it is possible to change the order of integration and take the integral over $\mathbf{b}$. Then the main contribution to the integral over $\mathbf{k}_{1,2}$ comes from the region $k_{1,2} \le 1/R$. Since we are going to take the limit $R \to \infty$, we can replace $\mathcal{M}(\mathbf{k}_{1,2})$ with $\mathbf{k}_{1,2}\mathbf{L}$ and neglect $\mathbf{k}_{1,2}$ in $\mathcal{F}_A^0(\mathbf{q}_\perp + \mathbf{p}_\perp - \mathbf{k}_{1,2})$. Then, we have

$$d\sigma_B^c = \frac{m^2 d^3p d^3q}{(2\pi)^6\varepsilon_p\varepsilon_q}|\mathcal{F}_A^0(\mathbf{q}_\perp + \mathbf{p}_\perp)|^2\frac{|\mathbf{L}|^2}{2}\tilde{G}_B\ , \tag{17}$$

$$\tilde{G}_B = 8\pi(Z_B\alpha)^2 \int\int_0^\infty \frac{dk_1 dk_2}{k_1^2 - k_2^2} \left\{ \left(\frac{k_1}{k_2}\right)^{2iZ_B\alpha} - 1 \right\} \times$$
$$\times \left[k_2 R J_0(k_2 R) J_1(k_1 R) - k_1 R J_0(k_1 R) J_1(k_2 R)\right] \ .$$

Comparing the expression for the function $\tilde{G}_B$ with (10), we see that $\tilde{G}_B = G_B$. After the summation over the electron and positron polarizations the formula (17) comes into (13). Note that the expression (13) can be obtained directly from (16) by taking the integral over $\mathbf{k}_{1,2}$ in the region $k_{1,2} < k_0 \ll |\mathbf{p}_\perp + \mathbf{q}_\perp|$ and then integrating over b in the infinite limits.

Thus, the light-fronts approach[1−3] can be used for the calculation of the CC to the e^+e^- pair production cross section integrated over the direction of the positron (electron) momentum. Its careful application leads to the correct result.

References

1. B. Segev, J.C. Wells, Phys. Rev. A **57**, 1849 (1998); physics/9805013.
2. A.J. Baltz, L. McLerran, Phys. Rev. C **58**, 1679 (1998).
3. U. Eichmann, J. Reinhardt, S. Schramm, and W. Greiner, Phys.Rev. A **59**, 1223 (1999);
4. H. Bethe, L.C. Maximon, Phys. Rev. **93**, 768 (1954); H. Davies, H. Bethe, L.C. Maximon, Phys. Rev. **93**, 788 (1954).
5. D.Yu. Ivanov, A. Schiller, V.G. Serbo, Phys. Lett. B **454**, 155 (1999)
6. R.N Lee, A.I. Milstein, Phys.Rev. A **61**, 032103 (2000)
7. G. Molière, Z. Naturforsch. **2a**, 133 (1947).
8. V.B. Berestetskii, E.M. Lifshitz, L.B. Pitaevskii, Quantum Electrodynamics,
   98 (Nauka, Moscow, 1989).
9. D.Yu. Ivanov, E.A. Kuraev, A. Schiller, V.G. Serbo, Phys. Lett. B **442**, 453 (1998).

SPIN DEPOLARIZATION DUE TO BEAM-BEAM INTERACTION IN NLC

KATHLEEN A. THOMPSON
Stanford Linear Accelerator Center
Stanford University, Stanford, CA 94309
E-mail: kthom@SLAC.Stanford.edu

Calculations of spin depolarization effects due to the beam-beam interaction are presented for several NLC designs. The depolarization comes from both classical (Bargmann-Michel-Telegdi precession) and quantum (Sokolov-Ternov spin-flip) effects. It is anticipated that some physics experiments at future colliders will require a knowledge of the polarization to better than 0.5% precision. We compare the results of CAIN simulations with the analytic estimates of Yokoya and Chen for head-on collisions.[1] We also study the effects of transverse offsets and beamstrahlung-induced energy spread.

1 Introduction

In this note we give simulation and analytic results for the depolarization due to the beam-beam interaction in NLC nominal designs and some high-luminosity variations. Such depolarization effects are negligibly small in the SLC. However for precision tests of the Standard Model in NLC, it will be necessary to know the beam polarization to within a few tenths of a percent, which is comparable to the amount of luminosity-averaged depolarization due to the beam-beam interaction in NLC. Furthermore, the beam disruption is higher in NLC than in SLC, which makes it more difficult to obtain accurate measurements of the final polarization using a Compton polarimeter in the extraction line; hence accurate calculations of the beam-beam depolarization are needed.

We will compare analytic estimates[1] of the depolarization with the results of the beam-beam simulation program CAIN.[2] At present, CAIN is the only beam-beam simulation program that calculates beam-beam depolarization effects.

The strength of the beam-beam interaction may be characterized by

$$\Upsilon \equiv \frac{e\hbar}{m^3c^4}\sqrt{|F_{\mu\nu}p^\nu|^2} = \gamma\frac{E+B}{F_c} \quad , \tag{1}$$

where $p^\nu = (E, \overrightarrow{p})$ is the 4-momentum of the incoming electrons or positrons, m is the electron mass, $\gamma \equiv E/mc^2$ is the Lorentz factor, $F_{\mu\nu}$ is the energy-momentum tensor of the electromagnetic field produced by the oncoming beam, and $F_c \equiv m^2c^3/\hbar e \approx 4.4\times10^{13}$ Gauss is the Schwinger critical field. Sometimes

the parameter ξ is used instead:

$$\xi \equiv \frac{u_c}{m\gamma} \quad . \tag{2}$$

Here u_c is the critical energy of the classical synchrotron radiation spectrum. Υ and ξ are relativistic invariants and are related by $\Upsilon = \frac{3}{2}\xi$. For small disruption and gaussian beams, the effective value of Υ is given by[3]

$$\Upsilon_{eff} = \frac{5Nr_e^2\gamma}{6\alpha\sigma_z(\sigma_x + \sigma_y)} \quad , \tag{3}$$

where N is the number of particles per bunch, r_e is the classical electron radius, α is the fine-structure constant, $\sigma_{x,y}$ are the transverse bunch sizes, and σ_z is the bunch length.

2 Analytic estimates for beam-beam depolarization

There are two significant mechanisms of beam-beam depolarization. One, the BMT effect, arises from the classical precession of the longitudinally-polarized electrons in the beam-beam field, in accordance with the Bargmann-Michel-Telegdi equation. The other, Sokolov-Ternov spin-flip (ST effect), tends to polarize electrons along the magnetic field (e^+ parallel, e^- anti-parallel) and thus degrades the longitudinal polarization since the magnetic field is perpendicular to the longitudinal axis. Analytic estimates for both these effects have been previously derived by Yokoya and Chen.[1]

Following Yokoya and Chen (YC), the final outgoing depolarization will be denoted by angle brackets, i.e. $< \Delta P >$, and the luminosity-weighted depolarization by square brackets, i.e. $[\Delta P]$. According to YC, $< \Delta P >$ and $[\Delta P]$ are related by

$$[\Delta P] \approx 0.273 < \Delta P > \quad . \tag{4}$$

This is valid for both the BMT and ST contributions provided that the horizontal disruption $D_x << 1$.

YC's estimate of the depolarization due to the BMT effect is

$$< \Delta P_{BMT} > \approx \frac{3}{50\pi^2} n_{cl}^2 \left[\frac{a(\Upsilon_{eff})}{a(0)}\right]^2 \approx 0.0061 n_{cl}^2 \left[\frac{a(\Upsilon_{eff})}{a(0)}\right]^2 \quad . \tag{5}$$

The factor in square brackets was calculated by V.Baier[4] (see the CAIN manual[2]) and n_{cl} is the average number of synchrotron photons emitted per electron according to classical synchrotron radiation theory, which is given in YC as:

$$n_{cl} = \frac{5\sqrt{\pi}}{2\sqrt{3}}(\sqrt{2} - 1)\frac{\alpha r_e N}{\sqrt{\sigma_x \sigma_y}} f(R) \quad , \tag{6}$$

where $R = \sigma_x/\sigma_y$ and $f(R) \equiv \frac{2\sqrt{R}}{1+R}$.

YC's estimate of the depolarization due to the ST effect is

$$< \Delta P_{ST} > \approx 2U_f(\xi_{eff})n_{cl} = 2\frac{U_f(\xi_{eff})}{U_0(\xi_{eff})}n_\gamma \quad , \tag{7}$$

which is always less than $0.04n_\gamma$. $U_f(\xi)$ and $U_0(\xi)$ may be expressed in terms of modified Bessel functions; formulas for and plots of these functions are given by YC.[1] Note that the actual number of synchrotron photons emitted per electron is given by $n_\gamma = U_0(\xi)n_{cl}$.

3 Basic parameters for six baseline designs and variations

We give some luminosity-related parameters for the basic NLC designs[5] near 0.5, 1.0, and 1.5 TeV center of mass energy in Tables 1, 2, and 3. The quantities $\mathcal{L}_D$ and $\mathcal{L}_D$ are the luminosity per bunch (in units m^{-2}), with and without the pinch enhancement due to disruption. The quantity L_D is the luminosity (in units $\mathrm{cm}^{-2}\mathrm{sec}^{-1}$) taking into account the repetition rate and number of bunches per train.

Parameters for some alternative designs that are also under consideration for NLC are given in Table 4. These are designs which have equal beta functions in the horizontal and vertical directions, and thus the beams are less flat. This leads to significantly higher disruption and beamstrahlung, as well as higher depolarization.

4 Polarization Results

In Table 5 we give the final outgoing depolarization for the nominal NLC designs. For comparison we show the results from the analytic formulas discussed above, as well as the results from CAIN simulations. The ST depolarization in CAIN simulations can only be done if BMT depolarization is also turned on, so the simulation result quoted for ST alone, $< \Delta P_{ST} >$, is simply the difference $< \Delta P_{tot} > - < \Delta P_{BMT} >$, where $< \Delta P_{BMT} >$ is the result with only BMT turned on, and $< \Delta P_{tot} >$ is the result with both BMT and ST turned on. In Table 6 we give the luminosity-weighted outgoing depolarization for the nominal NLC designs, again including the results from both the analytic formulas and CAIN simulations. The analytic results are somewhat higher than the simulation results for the BMT case; it is expected that the analytic BMT result may be an overestimate since it does not take account of the fact that the polarization vector will oscillate back and forth across the longitudinal axis when the disruption is high. Apart from this, the agreement

Table 1: IP parameters for three ∼1/2 TeV c.m. NLC designs

	A-500	B-500	C-500
E_{beam} [GeV]	267.5	257.5	250.
N [10^{10}]	0.75	0.95	1.1
$\gamma\epsilon_x/\gamma\epsilon_y$ [μm-r]	4.0/0.06	4.5/0.1	5.0/0.14
β_x/β_y [mm]	10/0.1	12/0.12	13/0.2
σ_z [μm]	90.	120.	145.
σ_x/σ_y [nm]	276/3.4	327/4.9	365/7.6
$\mathcal{L}_0$ [10^{33} m^{-2}]	4.78	4.50	3.50
A_x/A_y	0.009/0.90	0.010/1.0	0.011/0.73
D_x/D_y	0.094/7.7	0.117/7.9	0.136/6.5
Υ_{eff}	0.14	0.11	0.09
$\mathcal{L}_D$ [10^{33} m^{-2}]	6.51	5.84	5.21
H_D	1.36	1.30	1.49
n_γ	1.08	1.18	1.24
δ_B	4.3%	3.9%	3.7%
Bunches/train	95	95	95
Rep. rate	120	120	120
L_D [10^{33}cm^{-2}sec^{-1}]	7.42	6.66	5.94

Table 2: IP parameters for three ∼1 TeV c.m. NLC designs

	A-1000	B-1000	C-1000
E_{beam} [GeV]	523.	504.	489.
N [10^{10}]	0.75	0.95	1.1
$\gamma\epsilon_x/\gamma\epsilon_y$ [μm-r]	4.0/0.06	4.5/0.1	5.0/0.14
β_x/β_y [mm]	10/0.125	12/0.15	13/0.2
σ_z [μm]	90.	120.	145.
σ_x/σ_y [nm]	198/2.7	234/3.9	261/5.4
$\mathcal{L}_0$ [10^{33} m^{-2}]	8.37	7.87	6.83
A_x/A_y	0.009/0.72	0.01/0.80	0.011/0.725
D_x/D_y	0.094/6.9	0.103/7.0	0.136/6.5
Υ_{eff}	0.39	0.30	0.25
$\mathcal{L}_D$ [10^{33} m^{-2}]	12.4	11.4	10.2
H_D	1.50	1.44	1.50
n_γ	1.4	1.5	1.6
δ_B	9.5%	9.2%	8.7%
Bunches/train	95	95	95
Rep. rate	120	120	120
L_D [10^{33}cm^{-2}sec^{-1}]	14.3	12.9	11.7

Table 3: IP parameters for two ∼1.5 TeV c.m. NLC designs

	A-1500	B-1500
E_{beam} [GeV]	703	739
N [10^{10}]	1.4	0.95
$\gamma\epsilon_x/\gamma\epsilon_y$ [μm-r]	4.5/0.14	4.5/0.1
β_x/β_y [mm]	15/0.2	13/0.2
σ_z [μm]	130.	150.
σ_x/σ_y [nm]	222/4.5	201/3.7
$\mathcal{L}_0$ [10^{33} m^{-2}]	15.6	9.6
A_x/A_y	0.009/0.65	0.012/0.75
D_x/D_y	0.15/7.3	0.14/7.3
Υ_{eff}	0.60	0.41
$\mathcal{L}_D$ [10^{33} m^{-2}]	25.1	14.4
H_D	1.61	1.50
n_γ	2.2	1.7
δ_B	17%	12%
Bunches/train	95	95
Rep. rate	60	90
L_D [10^{33}cm^{-2}sec^{-1}]	14.3	12.3

between analytic and simulation results is quite good (of course this does not prove that they agree with nature, but does give some degree of confidence).

In Table 7 we give the final outgoing depolarization and in Table 8 the luminosity-weighted depolarization, for the two designs shown in Table 4. These have significantly higher depolarization than the nominal designs. Since the beam-beam disruption and consequent pinching of the beam are much higher in this case, a better analytic approximation can be obtained by taking the modification of the effective transverse beam size into account according to a prescription given by Chen[6]. This beam size correction to the analytic estimate is negligible for the NLC nominal designs, but is significant for the higher luminosity designs. Including the correction brings the analytic and simulation results into good agreement for the EqBetas1 case, but there is still some discrepancy for the EqBetas2 case, which has the highest depolarization.

Since there is always some jitter in the beam position at the IP, it is also of interest to look at the depolarization as a function of the offset of the two beams. CAIN simulation results for depolarization versus horizontal and vertical offsets, for the NLC-B-1000 design, are shown in Figure 1. In this figure, plots for horizontal offsets are on the left and vertical offsets on the right The two plots on the top show the outgoing depolarization, the middle

Table 4: IP parameters for two modified ∼1.0 TeV c.m. NLC designs, with equal beta functions

	EqBetas1	EqBetas2
E_{beam} [GeV]	504	504
N [10^{10}]	0.475	0.55
$\gamma\epsilon_x/\gamma\epsilon_y$ [μm-r]	4.5/0.1	4.5/0.1
β_x/β_y [mm]	1.3/1.3	1.3/1.3
σ_z [μm]	120.	120.
σ_x/σ_y [nm]	77/11.5	77/11.5
$\mathcal{L}_0$ [10^{33} m^{-2}]	2.03	2.72
A_x/A_y	0.092/0.092	0.092/0.092
D_x/D_y	0.48/3.2	0.56/3.7
Υ_{eff}	0.50	0.62
$\mathcal{L}_D$ [10^{33} m^{-2}]	4.68	6.81
H_D	2.3	2.5
n_γ	2.2	2.7
δ_B	16%	20%
Bunches/train	190	190
Rep. rate	120	120
L_D [10^{33}cm^{-2}sec^{-1}]	10.7	15.5

plots show the luminosity-weighted depolarization, and the bottom plots show the ratio of the luminosity-weighted to the outgoing depolarization. Total depolarization is shown as a solid curve and BMT-only depolarization as a dashed curve. The difference between total and BMT-only (representing ST depolarization) is shown as a dotted curve. Only the vertical offset gives a noticeable effect on the luminosity-weighted depolarization, and even here it is quite small – only 0.2% for a $\Delta y = 2\sigma_y$ offset.

The depolarization as function of beamstrahlung-induced energy spread is illustrated by Figure 2, which shows the correlation between energy and depolarization of the macroparticles in an NLC-B-1000 simulation. Figure 3 shows histograms of the average depolarization (top) and number of electron beam macroparticles (bottom), as a function of macroparticle energy. This dependence of depolarization on energy of individual beam particles is a very significant effect that would need to be taken into account in studies of processes whose cross sections peak significantly below the nominal CM energy.

Table 5: Final outgoing electron beam depolarization $< \Delta P >$, for nominal NLC designs. "anlyt" denotes analytic results, "sim" denotes CAIN simulation results.

	BMT anlyt	ST anlyt	TOTAL anlyt	BMT sim	ST sim	TOTAL sim
NLC-A-500	0.6%	0.4%	1.1%	0.4%	(0.5%)	0.9%
NLC-B-500	0.8%	0.4%	1.1%	0.5%	(0.4%)	0.9%
NLC-C-500	0.9%	0.3%	1.1%	0.5%	(0.3%)	0.9%
NLC-A-1000	0.8%	2.0%	2.8%	0.5%	(1.6%)	2.1%
NLC-B-1000	1.0%	1.4%	2.5%	0.6%	(1.3%)	2.0%
NLC-C-1000	1.2%	1.2%	2.4%	0.8%	(1.2%)	1.9%
NLC-A-1500	1.6%	3.8%	5.4%	1.1%	(3.4%)	4.5%
NLC-B-1500	1.2%	2.1%	3.2%	0.7%	(2.0%)	2.7%

Table 6: Luminosity-weighted electron beam depolarization $[\Delta P]$, for nominal NLC designs

	BMT anlyt	ST anlyt	TOTAL anlyt	BMT sim	ST sim	TOTAL sim
NLC-A-500	0.2%	0.1%	0.3%	0.1%	(0.1%)	0.2%
NLC-B-500	0.2%	0.1%	0.3%	0.1%	(0.1%)	0.2%
NLC-C-500	0.2%	0.1%	0.3%	0.1%	(0.1%)	0.2%
NLC-A-1000	0.2%	0.5%	0.8%	0.1%	(0.4%)	0.5%
NLC-B-1000	0.3%	0.4%	0.7%	0.1%	(0.3%)	0.5%
NLC-C-1000	0.3%	0.3%	0.7%	0.2%	(0.3%)	0.4%
NLC-A-1500	0.4%	1.0%	1.5%	0.2%	(0.9%)	1.1%
NLC-B-1500	0.3%	0.6%	0.9%	0.1%	(0.5%)	0.6%

I thank K. Yokoya, M. Woods, and P.Chen for helpful discussions related to this work.

References

1. K.Yokoya and P.Chen, 8th International Conference on High Energy Spin Physics, Minneapolis, 12-17 September 1988; SLAC-PUB-4692.
2. K.Yokoya, "User's Manual of CAIN", 1997.
3. K.Yokoya and P.Chen, in M.Dienes, et.al. (ed.), Frontiers of Particle Beams: Intensity Limitations (Springer-Verlag, 1988).
4. V.Baier, unpublished.
5. NLC parameters as of 1998.
6. P.Chen, Particle Accelerator Conference, Washington, DC, 17-20 May, 1993

Table 7: Final outgoing electron beam depolarization $< \Delta P >$, for two equal-beta NLC designs. Starred values are analytic estimates with reduction of transverse beam size due to disruption taken into account.

	BMT anlyt	ST anlyt	TOTAL anlyt	BMT sim	ST sim	TOTAL sim
EqBetas1	2.0%	3.1%	5.1%	1.6%	(3.7%)	5.3%
	1.6% *	3.8% *	5.4% *			
EqBetas2	3.7%	7.8%	11.5%	2.5%	(9.8%)	12.4%
	1.7% *	10.3% *	12.0% *			

Table 8: Luminosity-weighted electron beam depolarization $[\Delta P]$, for two equal-beta NLC designs. Starred values are analytic estimates with reduction of transverse beam size due to disruption taken into account.

	BMT anlyt	ST anlyt	TOTAL anlyt	BMT sim	ST sim	TOTAL sim
EqBetas1	0.6%	0.9%	1.4%	0.4%	(1.1%)	1.5%
	0.4% *	1.0% *	1.5% *			
EqBetas2	1.0%	2.1%	3.2%	0.7%	(3.4%)	4.2%
	0.5% *	2.8% *	3.3% *			

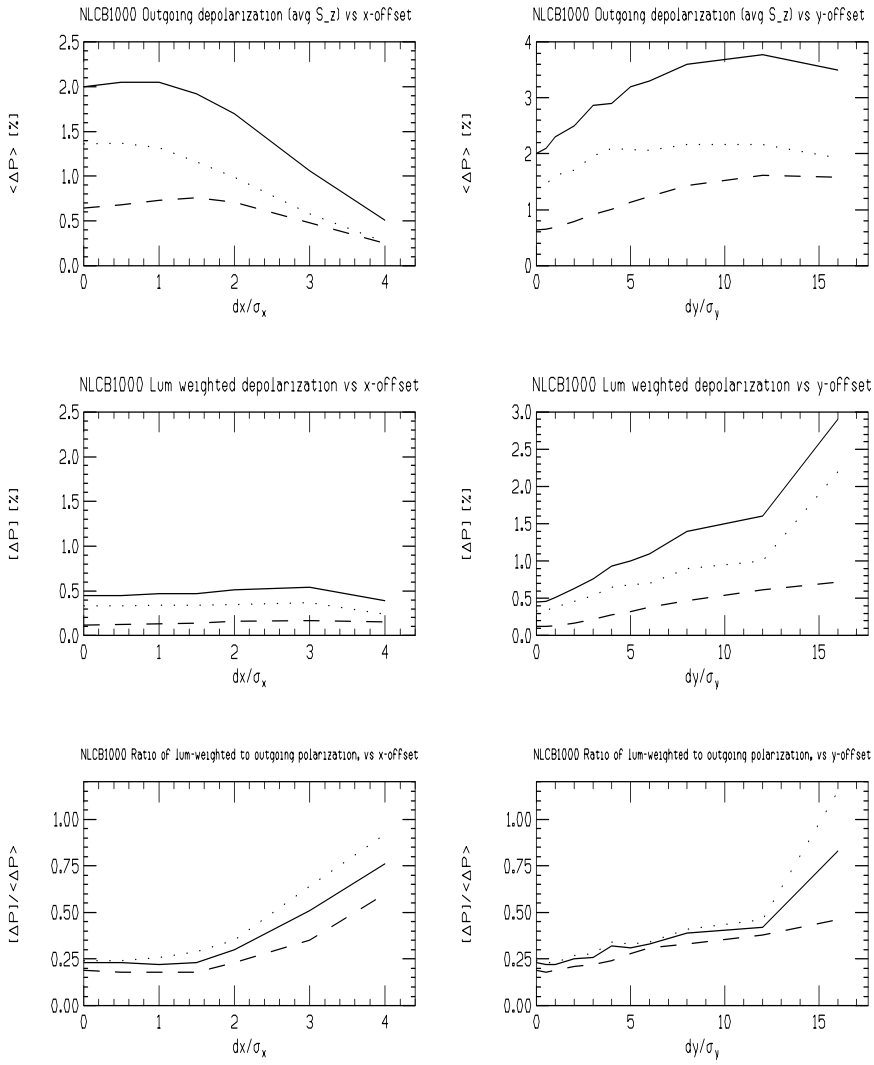

Figure 1: Top: Final outgoing polarization, Middle: Luminosity-weighted polarization, Bottom: Ratio of luminosity-weighted polarization to final outgoing polarization, as a function of horizontal (figures on left) and vertical offset (figures on right) for NLC-B-1000 design. Total depolarization (solid curve), BMT-only depolarization (dashed curve), Difference between total and BMT-only representing ST depolarization (dotted curve).

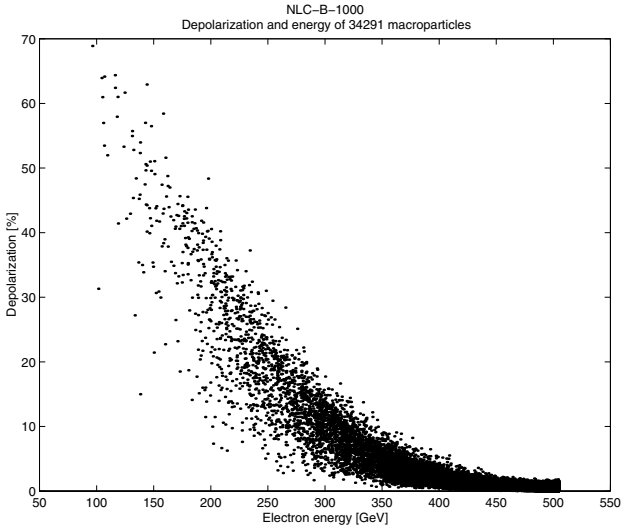

Figure 2: Depolarization and energy of 34291 electron beam macroparticles, for NLC-B-1000 design.

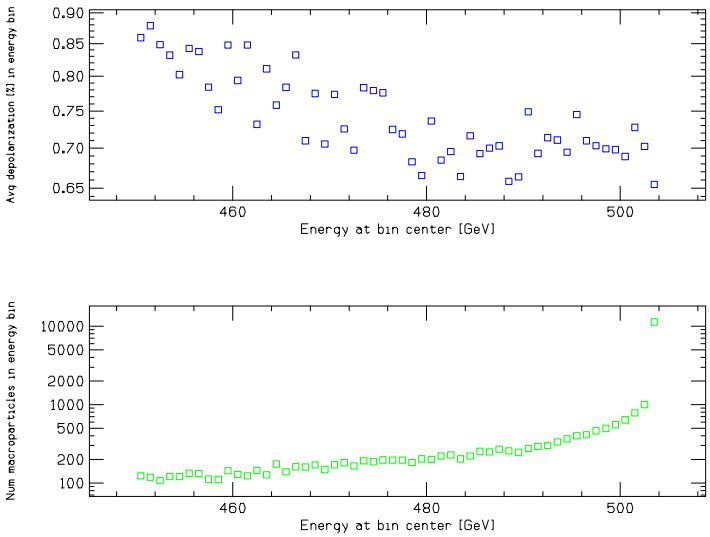

Figure 3: Histograms of average depolarization (top) and number of electron beam macroparticles (bottom), as a function of macroparticle energy, for NLC-B-1000 design.

GRAVITATIONAL ČERENKOV RADIATION AND SCALAR STARS

S. CAPOZZIELLO AND G. LAMBIASE
Dipartimento di Scienze Fisiche E.R. Caianiello, Università di Salerno, 84081 Baronissi (SA), Italy and INFN, Sez. Napoli, Italy
E-mail: capozziello, lambiase@sa.infn.it

D.F. TORRES
Instituto Argentino de Radioastronomía, C.C.5, 1894 Villa Elisa, Buenos Aires, Argentina
E-mail: dtorres@venus.fisica.unlp.edu.ar

We explore the possibility that a charged particle moving in the gravitational field generated by a scalar star could radiate energy via gravitational Čerenkov mechanism. We show that soliton stars have Čerenkov radiation for particular values of the boson mass, although diluteness of the star grows and actual observational possibility decreases for the more usually discussed boson masses.

1 Introduction

During last years, many attention has been devoted to investigate if scalar fields may be the seed of astrophysical structures and if observable phenomena could signal their existence. Objects made up of scalar massive particles were introduced in[1,2] as a new type of star model, the so-called boson star. Such objects are macroscopic quantum states that are gravitationally prevented from collapsing (in opposition to black holes) by the Heisenberg uncertainty principle, which keeps scalar particles from being localized to within their Compton wavelength.

The gravitational redshift of the radiation emitted within a boson star potential and the rotational curves of accreted particles to assess the possible detectability of these scalar stars has been studied in[3]. The conclusion is that very massive boson stars could look very similar to an active galactic nucleus with a black hole at its center, in agreement to Ref. [4]. Later, moreover, in Ref. [5] it has been explored to what extent these properties are exclusive of the boson star potential used in [3], finding that in fact they are even common to more generic Lagrangian densities.

In our own galactic center, while the existence of a single large mass has been favored as the upper bound on its size tighten and stability criteria rules out complex clusters[6], it is not established that this central mass has to be a black hole. If Sgr A* (the super-massive compact object name) is a black hole,

its luminosity should be three order of magnitude bigger than what actually is. This discrepancy is called "the blackness problem", and led to the concept of a black hole on starvation. However, observational data comes from regions 4×10^4 Schwarzschild radius away from a black hole of mass $2.6 \times 10^6 M_\odot$ (the inferred mass of the central object). Proofs of the existence of a super-massive black hole in the center of the galaxy are not conclusive by now. We have constructed a model of a boson star galactic center and studied some of its properties elsewhere [7].

With the aim to search for some new physical effect able to reveal the presence of scalar stars in the universe, other than the already considered gravitational lensing [8], we analyze the possibility that a charged particle, propagating in the gravitational field generated by such a compact object, could emit radiation via Čerenkov process.

2 Čerenkov radiation

Čerenkov radiation occurs when a charged particle moves through a medium at a constant velocity v greater than the velocity of light in that medium. Because of the superluminal motion of the particle, a shock wave is created and this yields to a loss of energy. The wavefront of the radiation propagates at a fixed angle

$$\cos\theta = \frac{v_{phase}}{v} = \frac{c/n(\nu)}{v} \tag{1}$$

where ν is the photon frequency and n is the refractive index. Obviously, $\cos\theta < 1$ can not be satisfied (and then will be no radiation) if $n < 1$ (because v always is less than c)[9]. As is well known, charged particles with acceleration a emit electromagnetic radiation according to the Larmour's relation $dE/dt \sim a^2$. A particle propagating in an external gravitational field, can emit Čerenkov radiation, as recently shown in[10], and the background gravitational field has an effective refractive index given by

$$n_\gamma^2(k_0) = |\eta^{00}| \left(1 - \frac{R^i{}_i}{|\eta^{00}| k_0^2}\right) , \tag{2}$$

where $R^i{}_i$ is understood as the sum on the spatial indices of the Ricci tensor $R^\mu{}_\nu$, i.e. $R^i{}_i = \sum_{i=1}^3 R^i{}_i$, k_0 is the frequency of the emitted photon γ, and η^{00} is the 00-component of the metric tensor in the inertial frame, $\eta_{\mu\nu} = (-1, 1, 1, 1)$. The crucial point, in order that the Čerenkov radiation be kinematically allowed, is that $R^i{}_i < 0$, so that $n_\gamma^2(k_0) > 1$. The energy

radiated by Čerenkov process by a charged particle moving in a background gravitational field is given by (for details, see [10])

$$\frac{dE}{dt} = \frac{Q^2\alpha_{em}}{4\pi p_0^2}\int_{k_{01}}^{k_{02}} dk_0 \left[p_0(p_0-k_0)-\frac{1}{2}k_0^2\right] k_0 \frac{n_\gamma^2-1}{n_\gamma^2}\,, \tag{3}$$

where Q is the charge of the fermion emitting the photon, α_{em} is the electromagnetic coupling constant, p_0 is the energy of the fermion, and k_{01}, k_{02} stands for the allowed range of frequencies where radiation can occur.

The interesting result is obtained for $n_\gamma^2 \gg 1$, since the spectrum of energy radiated by a charged particle, Eq. (3), assumes the form

$$\frac{d}{dk_0}\left(\frac{dE}{dt}\right) = \frac{Q^2\alpha_{em}}{4\pi}\left[1-\frac{k_0}{p_0}-\frac{k_0^2}{2p_0^2}\right] k_0\,, \tag{4}$$

which differs in a substantial way from thermal or synchroton emission. We show this spectrum for a monochromatic proton energy $p_0 = 10$ GeV in Fig. 1. If this result holds for boson stars, it strongly suggest the possibility to reveal their presence via their output in Čerenkov radiation, in addition to gravitational lensing effects [8]. Note that in most astrophysical situations, the dense media that could give rise to Čerenkov radiation are also optically thick to the emitted radiation, making it not easily observed.

3 A brief review of boson stars

We shall now introduce the formalism which gives rise to mini-boson, boson, and soliton stars. To do this we study the Lagrangian density of a massive complex self-gravitating scalar field, which is (taking $\hbar = c = 1$)

$$\mathcal{L} = \frac{1}{2}\sqrt{\mid g \mid}\left[\frac{m_{\rm Pl}^2}{8\pi}R + \partial_\mu\psi^*\partial^\mu\psi - U(|\psi|^2)\right]\,, \tag{5}$$

where R is the scalar of curvature, g the determinant of the metric $g_{\mu\nu}$, and ψ is a *complex* scalar field with potential U. Using this Lagrangian as the generator of the matter sector of the theory, we get the standard field equations

$$R_{\mu\nu} - \frac{1}{2}g_{\mu\nu}R = -\frac{8\pi}{m_{\rm Pl}^2}T_{\mu\nu}(\psi)\,, \tag{6}$$

$$\nabla_\mu\nabla^\mu\psi + \frac{dU}{d|\psi|^2}\psi = 0\,, \tag{7}$$

where the stress energy tensor is given by,

$$T_{\mu\nu} = (\partial_\mu\psi^*)(\partial_\nu\psi) - \frac{1}{2}g_{\mu\nu}\Big[g^{\alpha\beta}(\partial_\alpha\psi^*)(\partial_\beta\psi) - U(|\psi|^2)\Big], \tag{8}$$

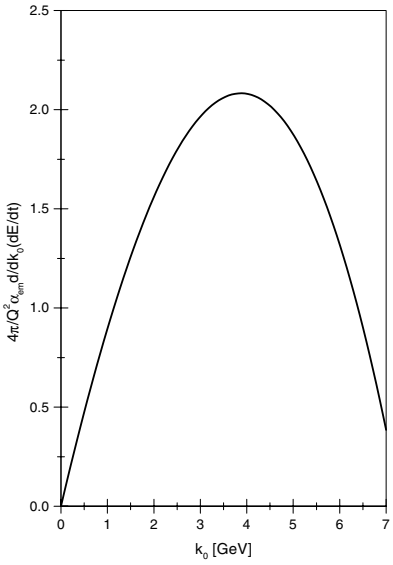

Figure 1. Typical spectrum for the radiation emitted by monochromatic charged particles with $|p| = 10$ GeV in a gravitational field with effective refractive index bigger than 1.

and $\nabla_\mu \nabla^\mu = \partial_\mu \left[\sqrt{\mid g \mid}\ g^{\mu\nu} \partial_\nu \right] / \sqrt{\mid g \mid}$ is the covariant d'Alembertian. Because of the fact that the potential is a function of the square of the modulus of the field, we obtain a global $U(1)$ symmetry. This symmetry is related with the conserved number of particles. The particular form of the potential, however, is what makes the difference between mini-boson, boson, and soliton stars. Conventionally, when the potential is given by

$$U(|\psi|^2) = m^2|\psi|^2 + \frac{\lambda}{2}|\psi|^4 \,, \tag{9}$$

where m is the scalar mass and λ a dimensionless constant measuring the self-interaction strength, mini-boson stars are those spherically symmetric equilibrium configurations with $\lambda = 0$. Boson stars, on the contrary, have a non-null value of λ. The previous potential with $\lambda \neq 0$ was introduced by Colpi et al. [11], who numerically found that the masses and radius of the configurations

were deeply enlarged in comparison to the mini-boson case, even in the case of extremely small λ.

Soliton (also called non-topological soliton) stars are different in the sense that, apart from the requirement that the Lagrangian must be invariant under a global $U(1)$ transformation, it is required that –in the absence of gravity– the theory must have non-topological solutions; i.e. solutions with a finite mass, confined to a finite region of space, and non-dispersive. An example of these kind of potentials is the one introduced in[12].

We shall now briefly explain how these boson configurations can be obtained (see [13] for details). We adopt a spherically symmetric line element

$$ds^2 = e^{\nu(r)}dt^2 - e^{\mu(r)}dr^2 - r^2(d\vartheta^2 + \sin^2\vartheta\, d\varphi^2)\ , \tag{10}$$

with a scalar field time dependence ansatz consistent with this metric:

$$\psi(r,t) = \sigma(r)e^{-i\omega t} \tag{11}$$

where ω is the (eigen-)frequency. This form of the field, when the scalar has no nodes, ensures us to be working in the configurations of minimal energy.

The non-vanishing components of the energy-momentum tensor are

$$T_0{}^0 = \rho = \frac{1}{2}[\omega^2\sigma^2(r)e^{-\nu} + \sigma'^2(r)e^{-\mu} + U]\ , \tag{12}$$

$$T_1{}^1 = p_r = \frac{1}{2}[\omega^2\sigma^2(r)e^{-\nu} + \sigma'^2(r)e^{-\mu} - U]\ , \tag{13}$$

$$T_2{}^2 = T_3{}^3 = p_\perp = -\frac{1}{2}[\omega^2\sigma^2(r)e^{-\nu} - \sigma'^2(r)e^{-\mu} - U], \tag{14}$$

where $' = d/dr$. One interesting characteristic of this system is that the pressure is anisotropic; thus, there are two equations of state $p_r = \rho - U$ and $p_\perp = \rho - U - \sigma'^2(r)e^{-\mu}$. The non-vanishing independent components of the Einstein equation are

$$\nu' + \mu' = \frac{8\pi}{m_{\rm Pl}^2}(\rho + p_r)re^{\mu}\ , \tag{15}$$

$$\mu' = \frac{8\pi}{m_{\rm Pl}^2}\rho re^{\mu} - \frac{1}{r}(e^{\mu} - 1)\ . \tag{16}$$

Finally, the scalar field equation is

$$\sigma'' + \left(\frac{\nu' - \mu'}{2} + \frac{2}{r}\right)\sigma' + e^{\mu-\nu}\omega^2\sigma - e^{\mu}\frac{dU}{d\sigma^2}\sigma = 0\ . \tag{17}$$

To do numerical computations and order of magnitude estimations, it is useful to have a new set of dimensionless variables. The usual ones are: $x = mr$ for the radial distance, $\Omega = \omega/m$ for the eigenvalue, we redefine the radial

part of the boson field as $\sigma = \sqrt{4\pi}\,\sigma/m_{\rm Pl}$, and introduce $\Lambda = \lambda m_{\rm Pl}^2/4\pi m^2$. In order to obtain solutions which are regular at the origin, we must impose the following boundary conditions $\sigma'(0) = 0$ and $\mu(0) = 0$. These solutions have two fundamental parameters: the self-interaction and the central density (represented by the value of the scalar field at the centre of the star). The mass of the scalar field fixes the scale of the problem. Boundary conditions representing asymptotic flatness must be applied upon the metric potentials, these determine -which is actually accomplished via a numerical shooting method- the initial value of $\nu = \nu(0)$. Then, having defined the value of the self interaction, or alternatively, the form of the soliton potential, the equilibrium configurations are parameterized by the central value of the boson field. As this central value increases, so does the mass and radius of the the star. This happens until a maximum value is reached in which the star looses its stability and disperses away (the binding energy being positive). Up to this value of $\sigma(0)$, catastrophe theory can be used to show that these equilibrium configurations are stable [14].

4 Čerenkov radiation and scalar stars

In this Section we calculate if Čerenkov radiation can be emitted by a charged particle which feels the gravitational field generated by a boson star. In order to allow for the emission of radiation by Čerenkov process, the sum on the spatial components of the Ricci tensor has to be negative. To calculate it, let us rewrite the Einstein equation (6) in the following form

$$R^{\mu}{}_{\nu} = -\frac{8\pi}{m_{Pl}^2}\left(T^{\mu}{}_{\nu} - \frac{1}{2}\delta^{\mu}_{\nu}T\right), \tag{18}$$

where T is the trace of the stress–energy tensor (8). The scalar curvature is then (for details see [15])

$$R = \frac{8\pi}{m_{Pl}^2}\,T = \frac{8\pi}{m_{Pl}^2}[-|\partial_\mu\psi|^2 + 2U(|\psi|^2)] \tag{19}$$

where the potential U is defined in (9). From (18) one can calculate the component $R^0{}_0$, getting

$$R^0{}_0 = \frac{8\pi}{m_{Pl}^2}[-|\partial_0\psi|^2 + \frac{1}{2}U(|\psi|^2)]\,, \tag{20}$$

so that the sum of the spatial components of the Ricci tensor are given by

$$R^i{}_i = R - R^0{}_0 = \frac{8\pi}{m_{Pl}^2}[-|\partial_i\psi|^2 + \frac{3}{2}U(|\psi|^2)]\,. \tag{21}$$

Inserting Eq. (21) into (2), one infers the effective refractive index

$$n_\gamma^2(k_0) = |\eta^{00}| \left[1 - \frac{8\pi}{|\eta^{00}| m_{Pl}^2 k_0^2}(-|\partial_i \psi|^2 + \frac{3}{2} U(|\psi|^2))\right] . \tag{22}$$

If $R^i{}_i$ in Eq. (21) is negative, then the emission of Čerenkov radiation is a kinematically allowed process. The condition $R^i{}_i < 0$ (so that $n_\gamma^2 > 1$) can be satisfied if one invokes the condition that the spatial variation of the scalar field ψ is greater than three half its potential energy, i.e.

$$|\partial_i \psi|^2 > \frac{3}{2} U(|\psi|^2) . \tag{23}$$

In order to evaluate the order of magnitude of this requirement for boson stars let us turn into dimensionless variables the expression

$$\frac{8\pi}{m_{Pl}^2 k_0^2} \left[-|\partial_i \psi|^2 + \frac{3}{2} U(|\psi|^2)\right] . \tag{24}$$

The requirement expressed by Eq. (23) depends on the form of the potential. As an example of this we study here the Lee et al.'s soliton star potential given by

$$U = m^2 |\psi|^2 \left(1 - \frac{|\psi|^2}{\chi_0^2}\right)^2 , \tag{25}$$

where χ_0 is a constant. As we already mentioned, compared with the usual boson star case, non-topological soliton stars have to fulfill two characteristics: 1. The Lagrangian must be invariant under a global $U(1)$ transformation. 2. In the absence of gravity, the theory must have non-topological solutions. In general, boson stars accomplish the requirement 1. but not 2. Invariance under $U(1)$ only requires that the potential be a function of $\psi^*\psi$, but in order to accomplish condition 2., U must contain attractive terms. This is why the coefficient of $(\psi^*\psi)^2$ of Lee's potential has a negative sign. Finally, when $|\psi| \to \infty$, U must be positive, which leads, minimally, to a sixth order function of ψ for the self-interaction.

We shall obtain the dimensionless form for expression (24), considering the soliton potential. It is given by (without multiplying factors)

$$g(x) = -\left(\frac{d\sigma}{dx}\right)^2 + \frac{3}{2}\left(\sigma(x)^2 - 2\alpha^2 \sigma(x)^4 + \alpha^4 \sigma(x)^6\right) , \tag{26}$$

where $\alpha = m_{Pl}^2 / 4\pi\chi_0^2$. Then, $n_\gamma^2 = 1 - (m^2/2k_0^2) g(x)$. Note that the parameter α does not directly depend on the mass of the boson, but just on the particular

value of the χ_0 parameter. It is usually assumed, however, that this parameter is of the order of the boson mass.

We can now think of the following situation: as σ depends on x, for values of $\sigma = 1/\alpha$, the second term is exactly zero, and then $g(x)$ will be negative if the derivative of the field is not null. This can be easily obtained starting from a central value of σ slightly higher than $1/\alpha$ (so as to pass through $\sigma = 1/\alpha$ well inside the structure of the star, where the derivative is not zero). In Fig. 3 of Ref.[**??**], different models fulfilling these constraints are shown. The result is that the higher the value of α, the more dilute the center of the star is. It is also possible to see that for bigger values of α, $|g(x)|$ takes even smaller values. Note too that a particular choice for the parameters (basically, for the central density) determine the spherical shell in which $g(x)$ is negative, and thus where Čerenkov radiation might occur. For instance, if α is very big, but $\sigma(0)$ is also very large, we could still find Čerenkov radiation in the outer *crust* of the star.

This shows, in principle, an interesting observable difference between boson and non-topological stars, which is caused by the form of the potential. The actual prospects for really observing this are to be determined particularly by the value of the boson mass involved. If m is about 30 GeV, and χ_0 is of the order of the boson mass, the parameter α is quite large, and the observational possibility diminishes, since Čerenkov radiation would happen only for extremely dilute stars (the concept of star itself looses sense in this situation). We have checked, however, that the negativeness of $g(x)$ is numerically preserved up to values of $\alpha = 10^4$. But is so small as 10^{-10}. Observing radiation generated in these conditions would be quite a different story. However, we may note that there could be a sort of fine tuning in the values of χ_0 and m for which $n_\gamma^2 = 1 - (m^2/2k_0)g(x)$ be large. If this fine tuning has any physical motivation should be decided on particle physics grounds. Additionally, we mention that for values of $m_{Pl}/m \sim 10^{17}$, it is needed a different numerical technique: basically we need to solve the equations in three separate parts, making adequate expansions (see the papers by Lee et al.'s for details [12]). In those cases, the mass and radius of the stars are enlarged up to galaxy and galaxy cluster masses within some light years of linear spread. We have not taken these cases here into account.

5 Discussion

We have analyzed the possibility that a charged particle, moving in a gravitational field generated by a scalar star, could emit radiation through the gravitational Čerenkov process recently introduced in Ref. [10]. The usual bo-

son star model, based on the potential introduced in this context by Colpi et al., is not able to generate a refractive index bigger than 1, and thus, that Čerenkov radiation can not proceed. On the contrary, we have that soliton stars could have Čerenkov radiation for particular values of the boson mass. However, diluteness of the star grows and actual observational possibility decreases for the more usually assumed boson masses and χ_0 parameters. For these cases, $(n_\gamma^2 - 1) \sim 0$ and Čerenkov process might be considered as experimentally insignificant within current observational constraints. We may think of a possibility to overcome the smallness of $(n_\gamma^2 - 1)$ if a soliton star is alligned with a strong proton source. A more, maybe unexpected form, would be to find soliton stars with the right combination of χ_0 and m, as to have a large effective refractive index.

As final comment we want report here the following preliminary result: a charged particle propagating in space-time, whose curvature is induced by *cosmological constant* Λ, will emit Čerenkov radiation according to the relation

$$\frac{dE}{dt} = \frac{Q^2 \alpha_{em}}{4\pi} \frac{8\pi G}{3} \Lambda \ln \frac{2p_0}{m} \,. \tag{27}$$

This process nowadays gives irrelevant effects due to the smallness of Λ, but it could have been relevant in early epochs when Λ was large.

References

1. D. J. Kaup, *Phys. Rev.* **172**, 1331 (1968).
2. R. Ruffini, S. Bonazzola, *Phys. Rev.* **187**, 1767 (1969).
3. F.E. Schunck, A.R. Liddle, *Phys. Lett. B* **404**, 25 (1997).
4. I. Tkachev, *Astron. Lett.* **12**, 305 (1986).
5. F.E. Schunck, D.F. Torres, *Int. J. of Mod. Phys.* D **9**, 601 (2000).
6. A. Eckart and R. Genzel, *Nature* **383**, 415 (1996); *Mon.Not.R.Astron.Soc.* **284**, 576 (1997).
7. D. F. Torres, S. Capozziello, G. Lambiase, *Phys. Rev.* D **62**, 104012 (2000)
8. M.P. Dabrowski, F.E. Schunck, astro–ph/9807207.
9. M. Longair, *High energy astrophysics, Vol I.* (Cambridge U. Press, Cambridge, 1997).
10. A. Gupta, S. Mohanty, M. Samal, *Class. Quantum Grav.* **16**, 291 (1999).
11. M. Colpi, S. L. Shapiro, I. Wasserman, *Phys. Rev. Lett.* **57**, 2485 (1986).
12. T.D. Lee, *Phys. Rev. D* **35**, 3637 (1987); R. Friedberg, T.D. Lee, Y. Pang, *Phys. Rev. D* **35** 3640, *ibid.* 3658, 3678 (1987).
13. T. D. Lee, Y. Pang, *Phys. Rep.* **221**, 251 (1992); Phys. Jetzer, *Phys.*

Rep. **220**, 163 (1992); A. R. Liddle, M. S. Madsen, *Int. J. Mod. Phys. D* **1**, 101 (1992); E. W. Mielke, F. E. Schunck, gr-qc/9801063.
14. F. V. Kusmartsev, E. W. Mielke, F. E. Schunck, *Phys. Rev. D* **43**, 3895 (1991); *Phys. Lett.* **A157**, 465 (1991).
15. S. Capozziello, G. Lambiase, D.F. Torres, *Class. Quant. Grav.* **17**, 3171 (2000).

Section 4

Quantum Methodologies in Beam Physics

SUPERSYMMETRY AND BEAM DYNAMICS[a]

J. D. Bjorken and Pisin Chen
Stanford Linear Accelerator Center
Stanford University, Stanford, California 94309

We report on our initial exploration of possible connections between supersymmetry and accelerator physics. We demonstrate that the longitudinal dynamics of proton and antiproton beams in a proton-antiproton collider storage ring exhibits the property of supersymmetry.

1 Introduction

Supersymmetry is a beautiful and seductive topic. In particle physics it is now, to large extent, a solution looking for a problem. Despite precious little experimental support, great attention is focused on supersymmetry as the key to understanding the underlying physics at the electroweak scale as well as at the Planck scale.

Here we ask the question for accelerator physics: is there any phenomenon for which the ideas of supersymmetry might be applicable? It is a stretch to think that the answer will be affirmative. But there are some hints of a connection, because supersymmetric quantum mechanics can be constructed from a procedure known as stochastic quantization[1]. Stochastic quantization in turn is related to the physics of diffusion, as expressed by Langevin and Fokker-Planck equations. These are of course commonplace tools in accelerator physics, in particular in the descriptions of beam dynamics in longitudinal phase space.

In this note we report on initial explorations of this question. In Section 2, we review simple supersymmetric Schrödinger equations. In Sections 3 and 4, we connect this to the formalism of stochastic quantization. In Section 5, we suggest that motion of particles in longitudinal phase space, in particular on a synchrotron resonance in the presence of RF noise, may be related to the above systems, and describe the physics of the supersymmetry. Section 6 discusses conclusions, such as they are, and what remains to be done to sharpen these ideas.

2 Simple Supersymmetry

A supersymmetry operation transfers bosons into fermions and vice versa. The simplest example is a harmonic oscillator ("boson") combined with a two-level

[a]Work supported by the Department of Energy, contract DE–AC03–76SF00515.

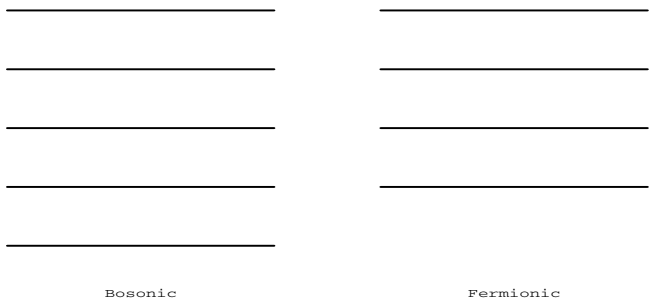

Figure 1: The bosonic and fermionic spectra of the supersymmetric Hamiltonian H.

system ("fermion"). The Hamiltonian is

$$H = a^\dagger a + b^\dagger b \tag{1}$$

where $a^\dagger$ and $b^\dagger$ are creation operators for the boson and fermion respectively. Evidently the vacuum is the state annihilated by a and b. The bosonic sector consists of those states annihilated by b (no fermion present) and the fermionic sector those states annihilated by $b^\dagger$ (one fermion present). Note that

1. The Hamiltonian can be written as the anticommutator of a "supercharge" Q and its adjoint

$$H = \{Q, Q^\dagger\} \qquad Q = a^\dagger b \; . \tag{2}$$

2. The supercharge commutes with H and changes bosons to fermions.

3. The vacuum has zero energy.

These three features are general properties of supersymmetric systems. The spectrum of H is shown in Fig. 1.

A natural question is whether there is a generalization to the case where there is unequal spacing of the bosonic levels. The answer is affirmative, and was exhibited in detail by Witten [2]. The supercharge is changed as follows:

$$Q = a^\dagger b = \frac{1}{\sqrt{2}}\,(x - ip)b \qquad \Rightarrow \qquad \frac{1}{\sqrt{2}}\,(W(x) - ip)b \tag{3}$$

with $W(x)$ the "superpotential." This leads to a "factorizable" Hamiltonian which had been noticed and studied for a long time prior to Witten's work;

e.g. by Schrödinger himself [3]:

$$H \Rightarrow \frac{1}{2}\,p^2 + \frac{1}{2}\,W(x)^2 - \frac{\left[b, b^\dagger\right]}{2}\,W'(x)\ . \tag{4}$$

There are by now books and long review articles on this subject[4], and we will not pause here for more discussion, but move on to the topic of stochastic quantization.

3 Sophisticated Stochastic Quantization

Consider a particle moving under a prescribed external influence as well as noise:

$$\frac{dx}{dt} = W(x) + D\xi(t)\ . \tag{5}$$

This is essentially the Langevin equation, when one identifies the coordinate we call x with the velocity of the particle. Here we do not yet make a commitment to the physical interpretations of the coordinate x. The quantity ξ is "white noise," a random variable acting on the particle, with no time-correlation present. It has a probability distribution normalized as follows:

$$P(\xi) = \frac{1}{\sqrt{2\pi}}\ e^{-\frac{1}{2}\xi^2}\ . \tag{6}$$

Thus the diffusion constant D measures the strength of the noise term. Now consider, as is often the convenient thing to do, expectation values of the coordinate x and its correlation functions; with ensemble averaging over the noise. Suppose that the process occurs over the time interval $(0, T)$. Then the averages are formally determined by a path integral

$$\langle x_1 \cdots x_n \rangle \equiv \int \mathcal{D}\xi(t)\, e^{-\frac{1}{2}\int_0^T dt'\,\xi^2(t')}\,(x(t_1)\cdots x(t_n))\ . \tag{7}$$

The proficient theorist will instantly "remove" the noise via a change of variables from ξ to x using the equation of motion, Eq. (5). Consequently there is a functional Jacobian (determinant) to consider. This Jacobian does not daunt our proficient theorist, because the determinant can be described in terms of integrals over Grassman variables[5]. When this is done, one finds the following expression:

$$\langle x_i \cdots x_n \rangle = C \int \mathcal{D}x\, e^{-\frac{1}{2D^2}\int_0^T dt\left[\frac{dx}{dt} - W(x)\right]^2} \det\left(\frac{d}{dt} - W'(x)\right)(x(t_1)\cdots x(t_n))$$

$$= C \int \mathcal{D}x\, \mathcal{D}b\, \mathcal{D}b^\dagger \, (x(t_1) \cdots x(t_n))$$

$$\times \exp\left\{ -\frac{1}{2} \int_0^T dt \left[\frac{1}{D^2} \left(\frac{dx}{dt} - W(x) \right)^2 - b^\dagger \left(\frac{db}{dt} - W'(x) b \right) \right] \right\} \quad (8)$$

The "action" in this expression is nothing more than the Witten supersymmetric Hamiltonian, in imaginary time. While we do not "explain" the i in the Schrödinger equation, we do end up with a "fermion" in the description, which in addition is supersymmetric!

This "derivation" has been deliberately presented here with lightning speed, just to provide a glimpse of how the formal machinery suggests the presence of a supersymmetry. But even when this "derivation" is elaborated it remains only a formal argument. It requires more careful scrutiny in order to understand what is going on. In the next section we repeat the discussion in more detail to more clearly see what is really happening.

4 Naive Stochastic Quantization

We now go back to the diffusion problem and make the mathematics better defined by choosing a discretization of the time variable. Here we might imagine the coordinate x to be some variable characterizing the motion of a charged particle in a storage ring, sampled once per revolution, and in the presence of an external force such as RF voltage, and also subject to (RF?) noise. We discretize the time variable and write for the equation of motion

$$x_i \equiv x(t_i) = K(x_{i-1}) + D\xi_i \quad (i = 1, \cdots, N) \ . \quad (9)$$

Now we may compute the expectation values as before

$$\langle O(x) \rangle = C \int d\xi_1 \cdots d\xi_n \, e^{-\frac{1}{2}\sum_{i=1}^N \xi_i^2} O(x) \ , \quad (10)$$

where C is chosen such that $\langle 1 \rangle = 1$. With the change of variables,

$$\xi_i = \frac{x_i - K(x_{i-1})}{D} \ , \quad (11)$$

we obtain an $N \times N$ Jacobian determinant:

$$\langle O(x) \rangle = C \int dx_1 \cdots dx_n \left\| \frac{\partial \xi_i}{\partial x_j} \right\| e^{-\frac{1}{2}\sum_{i=1}^N \frac{(x_i - K(x_{i-1}))^2}{D^2}} O(x) \ . \quad (12)$$

While it is tempting to express it fermionically, in the Grassmanian style, it is more safely evaluated directly

$$\Delta = D^n \left\| \frac{\partial \xi_i}{\partial x_j} \right\| = \begin{vmatrix} 1 & 0 \cdots & 0 & 0 \\ -K'(x_1) & 1 \cdots & 0 & 0 \\ & \cdots & & \\ 0 & 0 \cdots & 1 & 0 \\ 0 & 0 \cdots & -K'(x_{N-1}) & 1 \end{vmatrix} \tag{13}$$

We see that the value of the determinant is going to depend crucially upon boundary conditions. If we have a standard diffusion problem, where $x(0) \equiv x_0$ is specified, then the determinant Δ is written correctly in Eq. (13), and it is trivial, just unity.

$$\Delta \equiv \Delta_b = 1 \ . \tag{14}$$

On the other hand, suppose the boundary conditions are "acausal." This means that we compute the averages given the restriction that $x(T)$ is specified at time T rather than at time 0. Then

$$\langle O(x) \rangle = C \int dx_0 \cdots dx_{n-1} \left\| \frac{\partial \xi_i}{\partial x_j} \right\| e^{-\frac{1}{2} \sum_{i=0}^{N-1} \frac{(x_i - K(x_{i-1}))^2}{D^2}} O(x) \ , \tag{15}$$

and

$$\Delta \equiv \Delta_f = D^n \left\| \frac{\partial \xi_i}{\partial x_j} \right\| = \begin{vmatrix} -K'(x_0) & 1 & \cdots & 0 & 0 \\ 0 & -K'(x_1) & \cdots & 0 & 0 \\ & & \cdots & & \\ 0 & 0 & \cdots & -K'(x_{N-1}) & 1 \\ 0 & 0 & \cdots & 0 & -K'(x_{N-1}) \end{vmatrix}$$

$$= \prod_{i=0}^{N-1} \left[-K'(x_i) \right] \ . \tag{16}$$

Neither of these is the formal, supersymmetric answer quoted in Section 3. In order to obtain it, the boundary conditions should be *periodic*. One must specify

$$x_N = x_0 \ . \tag{17}$$

Under this circumstance, the determinant is

$$\Delta_{SUSY} = \begin{vmatrix} 1 & 0 & \cdots & 0 & -K'(x_N) \\ -K'(x_1) & 1 & \cdots & 0 & 0 \\ & & \cdots & & \\ 0 & 0 & \cdots & 1 & 0 \\ 0 & 0 & \cdots & -K'(x_{N-1}) & 1 \end{vmatrix}$$

$$= \Delta_b - \Delta_f = 1 - \prod_{i=1}^{N} [-K'(x_i)] \ . \tag{18}$$

The individual contributions to the determinant are what one obtains from the "bosonic" (causal) and "fermionic" (anticausal) sectors respectively.

Therefore the "miracle" of fermions and supersymmetry emerging out an apparently mundane classical stochastic process really occurs because of an *assumption of periodicity of the stochastic time variable*. Forward in time (clockwise?) is just "spin down" while backward in time (anticlockwise?) is "spin up". This feature is well-understood by the experts[6].

5 Application in Beam Dynamics

What, if anything, can this have to do with beam dynamics? We ourselves are not too sure. It seems to us that a particle in a storage ring, subject to noise on each revolution, might be a prototype. However, its coordinates satisfy second order differential equations, unless one casts them in Hamiltonian form. But in Hamiltonian form, there is in addition to the coordinate its conjugate momentum to consider. Therefore the simple Witten model with one degree of freedom would need generalization—something not completely straightforward to do. On the other hand, we may consider going to action-angle variables, assuming that the noise acts only on the angle variable, and considering what happens when the action J is held fixed or varies very slowly. This is an approach we favor at present.

But what about the backward propagation in time?? What does that correspond to? One possibility is to put both antiparticles and particles into the storage ring and compare the motion of the antiparticles in the presence of the common noisy system with that of the particles. If the particles moves clockwise in the phase space then the antiparticle motion is counterclockwise. So it would seem that the antiparticle sector might provide the "fermionic" complement to the standard "bosonic" component.

The longitudinal dynamics of a proton under the influence of a noise-free, ideal RF potential, $U(\phi)$, is governed by the Hamiltonian

$$H = \frac{1}{2}\delta^2 + U(\phi) \ , \tag{19}$$

with

$$U(\phi) = \Omega^2(1 - \cos\phi) \ , \tag{20}$$

where δ is the energy deviation from the synchronous value, Ω is the *synchrotron frequency*, and ϕ is the RF phase where the proton locates. One

synchrotron period is typically much longer than the proton's orbital period, i.e., $2\pi/\Omega \gg T_0$.

For our purpose, we transcribe the phase space variables, (δ, ϕ), into the action-angle variables, (J, θ), via the transformations

$$\delta = \sqrt{2J\Omega}\cos\theta \ ,$$

$$\phi = \sqrt{2J/\Omega}\sin\theta \ . \tag{21}$$

A stored proton executes bounded motion in the RF potential, with a maximum phase ϕ_m. Assume that $\phi_m \ll 1$, which means the corresponding maximum value of action J_m that we consider satisfies the condition $J_m/\Omega \ll 1$. Then the Hamiltonian can be approximated by

$$H = J\Omega\cos^2\theta + \Omega^2\Big(\frac{\phi^2}{2!} - \frac{\phi^4}{4!} + \cdots\Big)$$

$$\approx J\Omega - \frac{1}{6}J^2\sin^4\theta + \mathcal{O}(J^3/\Omega) \ . \tag{22}$$

The equations of motion are thus

$$\dot{\theta} = \frac{\partial H}{\partial J} = \Omega - \frac{1}{3}J\sin^4\theta + \cdots \ ,$$

$$\dot{J} = -\frac{\partial H}{\partial \theta} = \frac{2}{3}J^2\sin^3\theta\cos\theta + \cdots \ . \tag{23}$$

As $J/\Omega \ll 1$, we retain only the terms up to the order of J/Ω. Therefore to this accuracy we have $\dot{J} = 0$, and thus J is a constant of motion. Note that while $J = \text{const.}$ would be exact had we retained only the leading term in the Hamiltonian, i.e., $H = J\Omega$, it is still self-consistent when we further retain the second term, $-(1/6)J^2\sin^4\theta$, i.e., the leading J/Ω perturbation, as is evident from the above equations. It is therefore also true that the phase space is preserved within our approximation. Note also that the evolution of the action-angle variable θ is nonlinear in time. Figure 2 shows a schematic diagram of a generic phase-space RF "bucket" in the $\delta - \phi$-space and the corresponding $J - \theta$ variables.

It is well-known in accelerator physics that the RF potential is commonly subjected to an intrinsic Gaussian noise.[7,8] Assuming that such a noise acts only on the angle variable, the effective equation of motion for θ becomes

$$\dot{\theta} = \Omega - \frac{1}{3}J\sin^4\theta + D\xi(t) \ , \tag{24}$$

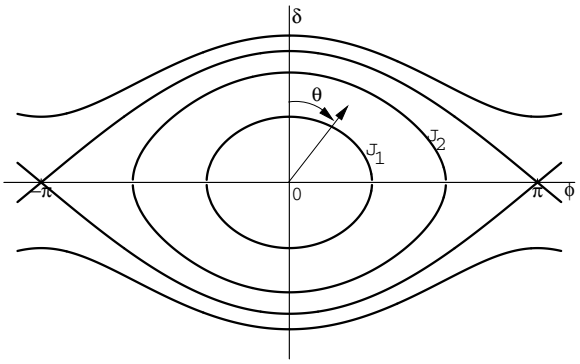

Figure 2: Phase-space diagram for the longitudinal dynamics. Each closed loop is associated with a constant action J_i.

where $\xi(t)$ is the time-dependent noise.

In the absence of noise, the phase space motion of the proton is periodic in θ, with $\theta(t=0) = \theta(t = 2\pi/\Omega)$. Imagine that one samples $\theta(t)$ once per revolution of the proton in the storage ring. We therefore in effect discretize the time with $\Delta t = T_0$. As mentioned above, typically in storage rings $2\pi/\Omega \gg T_0$. Let us assume an integer harmonic number N, i.e., $2\pi/\Omega = NT_0$, where typically $N \gg 1$. This gives the boundary condition

$$\theta_N = \theta_0 \ . \tag{25}$$

This condition corresponds to the return of the θ variable to its original location along the loop of a constant action, say J_1 in Fig. 2, after one complete synchrotron cycle.

The discretized equation of motion in θ is then described by the difference equation

$$\begin{aligned} \theta_i &= \theta_{i-1} + \Omega T_0 - \frac{1}{3} J T_0 \sin^4 \theta_{i-1} + D\xi_i \\ &\equiv K(\theta_{i-1}) + D\xi_i \quad (i = 1, \cdots, N) \ , \end{aligned} \tag{26}$$

and from which we find

$$K'(\theta_{i-1}) = 1 - \frac{4}{3} J T_0 \sin^3 \theta_{i-1} \cos \theta_{i-1} \ . \tag{27}$$

Down to this point we have explicitly established a model proton longitudinal beam dynamics where its phase space motion can be recapitulated into exactly the form of stochastic quantization described in Section 4. We are thus

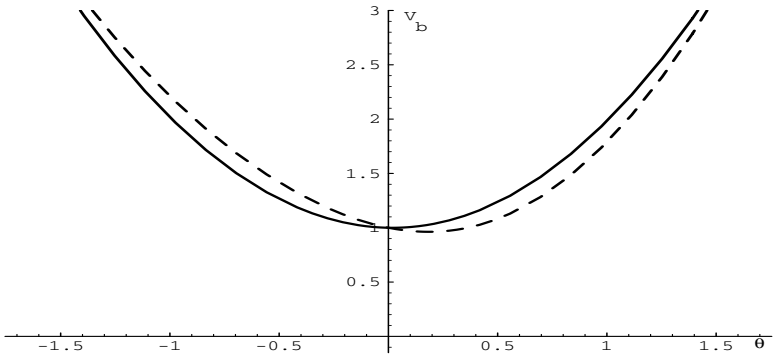

Figure 3: Bosonic potential with $\eta = 0.01$ (solid curve) and $\eta = 0.1$ (dashed curve).

ready to invoke the language of supersymmetry, with the "bosonic potential" (proton motion) and the "fermionic potential" (antiproton motion) cast as

$$V_b = K^2(\theta_i) + K'(\theta_i) \ ,$$

$$V_f = K^2(\theta_i) - K'(\theta_i) \ . \tag{28}$$

Figures 3 and 4 show the potentials at different values of $\eta = (4/3)JT_0$.

It is evident that the supersymmetric determinant in this example is indeed non-trivial, i.e.,

$$\begin{aligned} \Delta_{SUSY} &= 1 - \prod_{i=1}^{N} [-K'(x_i)] \\ &= 1 - \prod_{i=1}^{N} \left[\frac{4}{3} JT_0 \sin^3\theta_i \cos\theta_i - 1 \right] \neq 1 \ . \end{aligned} \tag{29}$$

6 Discussion

We have thus demonstrated a physical example of supersymmetry in the longitudinal beam dynamics of a proton storage ring in which the RF potential is subjected to a stochastic noise. However, the neglect of the effect of noise on phase-space growth can be legitimately questioned. Exploration of this issue is beyond the scope of this brief note.

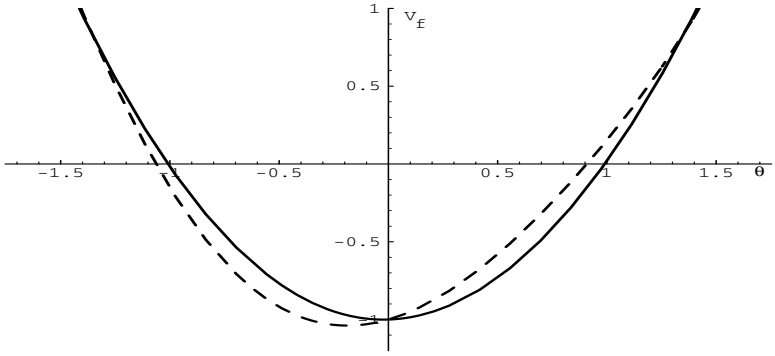

Figure 4: Fermionic potential with $\eta = 0.01$ (solid curve) and $\eta = 0.1$ (dashed curve).

7 References

1. G. Parisi and Y.-S. Wu, *Sci. Sinica* **24**, 483 (1981).
2. E. Witten, *Nucl. Phys.* **B185**, 513 (1981).
3. E. Schrödinger, *Proc. Roy. Ir. Acad.* **A46**, 9 (1940).
4. For a review, see P. H. Damgaard and H. Hüffel, *Phys. Repts.* **152**, 227 (1987).
5. A thorough discussion of path ingetration and Grassman variables can be found in M. Peskin and D. Schroeder, *An Introduction to Quantum Field Theory*, Addison-Wesley (Menlo Park, Cal.), 1995.
6. For example, see H. Nakazato, K. Okano, L. Schülke, and Y. Yamanaka, *Nulc. Phys.* **B346**, 611 (1990) and references therein.
7. G. Dôme, *Theory of RF Acceleration and RF Noise*, in Proc. CERN Accelerator School on *Antiprotons for Colliding Beam Facilities*, eds. P. Bryant and S. Newman, CERN84-15, 1984.
8. H.-J. Shih, J. A. Ellison, B. S. Newsberger and R. Cogburn, *Part. Accel.* **43**, 159 (1994).

LANDAU DAMPING IN NONLINEAR SCHRÖDINGER EQUATIONS *

R. FEDELE, S. DE NICOLA, V.G. VACCARO
Dipartimento di Scienze Fisiche, Università Federico II and INFN,
Complesso Universitario di M.S. Angelo,
Via Cintia, I-80126 Napoli, Italy

D. ANDERSON, M. LISAK
Department of Electromagnetics, Chalmers University of Technology,
S-41296 Göteborg, Sweden

By using the Wigner transform, the modulational instability analysis for a wide class of nonlinear Schrödinger equations describing different physical situations is carried out in phase space. In this framework, a kinetic-like description similar to the one based on the Vlasov equation which is used for describing the collective longitudinal dynamics of charged-particle bunches in accelerating machines is provided. In particular, the modulational instability (MI) corresponds to the usual coherent instability of the particle bunch. The main result od this analysis is the prediction of the phenomenon of Landau damping (LD) which seems to be in competition with the MI. This approach provides stability charts fully similar to the ones describing charged-particle beams in accelerating machines. Recent investigations on MI and LD in nonlinear Schrödinger equations including memory-effect terms are reviewed and new results are put forward.

1 INTRODUCTION

During the last three decades special attention has been devoted to the nonlinear propagation of wavepackets governed by a nonlinear Schrödinger equation (NLSE) in several different branches of scientific and technological applications. The typical form of a NLSE can be cast as follows (1-D):

$$i\frac{\partial \Psi}{\partial s} + P\frac{\partial^2 \Psi}{\partial x^2} + \mathcal{F}\left[|\Psi|^2\right]\Psi = 0 \quad , \tag{1}$$

where s and x are the time-like and the space-like variables, respectively; the *dispersion term* P is a real constant and $\mathcal{F}$ is an arbitrary functional of $|\Psi(x,s)|^2$. The most known NLSE is the one obtained with (cubic NLSE)

$$\mathcal{F}\left[|\Psi|^2\right] = q\left(|\Psi|^2 - |\Psi_0|^2\right) \quad , \tag{2}$$

where the *nonlinear-term coefficient* q and Ψ_0 are real and complex constants, respectively. The above applications have been mainly done in nonlinear

*PLENARY TALK PRESENTED BY R. FEDELE

optics (especially in the theory of optical fibers), in plasma physics, in mesoscopic physics and in the quantumlike theory of charged-particle beam dynamics.

1.1 Nonlinear optics

It is well known that the propagation of an electromagnetic wavepacket can be described by a Schrödinger-like equation for the (complex) electromagnetic wave amplitude, where $\hbar$ and potential energy are replaced by the inverse of the wave number $\overline{\lambda} \equiv \lambda/2\pi \equiv 1/k$ and refractive index, respectively [1]. In general, the refractive index depends on the wave amplitude, and the corresponding equation becomes the nonlinear Schrödinger equation (NLSE). Due to the interplay between nonlinearity and diffraction, a wide spectrum of effects may be produced during the nonlinear propagation of a wavepacket, such as self-compression and self-modulation of electromagnetic (e.m.) wavepackets in nonlinear media [2] (see fibre optics and transmission line theory [3]). Special attention has been devoted to the longitudinal dynamics of a wavepacket during its propagation in a nonlinear medium, e.g. modulational instability and soliton formation [2]). The typical 1-D NLSE for a complex electromagnetic field amplitude which governs this nonlinear propagation is the one obtained by Eq.s (1) and (2) with $2P = \partial^2\omega/\partial k^2$ and $q = \partial\omega/\partial|\Psi_0|^2$ (ω and k being frequency and wavenumber, respectively). Thus, (1) becomes [2]:

$$i\frac{\partial\Psi}{\partial s} + \frac{1}{2}\frac{\partial^2\omega}{\partial k^2}\,\frac{\partial^2\Psi}{\partial x^2} + \frac{\partial\omega}{\partial|\Psi_0|^2}\left(|\Psi|^2 - |\Psi_0|^2\right)\Psi = 0 \quad , \tag{3}$$

The quantity $\left(\partial\omega/\partial|\Psi_0|^2\right)\left(|\Psi|^2 - |\Psi_0|^2\right)$ plays the role of *nonlinear refractive index* of the medium. Modulational instability for small perturbation of a monochromatic wave train arises when the Lighthill criterion [4] is satisfied, i.e.

$$Pq > 0 \quad , \tag{4}$$

whilst the stability is obtained with the opposite inequality. Modulational instability evolves toward an asymptotic stage which is represented by the envelope soliton, which is a very stable structure.

1.2 Plasma physics

Nonlinear propagation of Langmuir wavepackets in plasma physics has been extensively investigated with the Zakharov equations [5] which in some limits may be reduced to appropriate NLSEs [6]. Also in this case the typical form

for the nonlinear refractive index is given by (2), whose physical origin is here due to the ponderomotive effect produced by the inhomogeneity of large amplitude waves traveling in the plasma. Self-focusing and self-modulation can be described in a way formally identical to the general case of nonlinear media [6,7]. In particular, the electro-acoustic wavepacket propagation in the plasma is governed by the following NLSE for the complex electric field amplitude [6]:

$$i\frac{\partial\Psi}{\partial s} \; + \; \frac{1}{2}\frac{v_e^2}{\omega_p}\,\frac{\partial^2\Psi}{\partial x^2} \; + \; \frac{e^2}{8\omega_p mM\left(c_s^2 - V^2\right)}\,\left(|\Psi|^2 - |\Psi_0|^2\right)\Psi \; = \; 0 \quad , \qquad (5)$$

where $2P \, = \, v_e^2/2\omega_p$, $q \, \equiv \, e^2/\left[8\omega_p mM\left(c_s^2 - V^2\right)\right]$; additionally, v_e is the electron thermal velocity, ω_p is the electron plasma frequency, m is the electron mass, M is the ion mass, c_s the ion sound velocity, and c is light speed.
The final stage of modulaltional instability of electro-acoustic envelope waves are the well-known Langmuir solitons [6].

1.3 Mesoscopic physics

Collective states in mesoscopic physics has been studied within the Ginzburg-Landau theory [8] where several nonlinear phenomena are governed by the Ginzburg-Landau equation which basically represents a wide family of nonlinear Schrödinger equations; for instance, special cases of such a family are given by the complex Ginzburg-Landau equation [9], Ginzburg-Pitaevskii equation [10], and Gross-Pitaevskii equation [11]. The n-Dimensional Complex Ginzburg-Landau equation has been recently considered for investigating the existence of new soliton solutions [12]. Again, the typical form of this equation is similar to the one given by (1) and (2) [11]:

$$i\frac{\partial\Psi}{\partial s} \; + \; \sum_{j=1}^{n}\frac{\partial}{\partial x_j}\frac{\partial}{\partial x_j}\Psi \; + \; \left(|\Psi|^2 - \mu\right)\Psi \; = \; 0 \quad , \qquad (6)$$

where Ψ is a complex function which plays the role of order parameter and μ is the diffusion coefficient.
Recently, the interest in the literature for the Gross-Pitaevskii equation increased very much in connection with the intensive research devoted to the Bose-Einstein condensation [11]. The usual form of this nonlinear equation is:

$$i\hbar\frac{\partial\Psi}{\partial s} \; + \; \frac{\hbar^2}{2m}\,\nabla^2\Psi \; + \; NU_0\left(|\Psi|^2 - V(r)\right)\Psi \; = \; 0 \quad , \qquad (7)$$

where m is the atom mass, N is the number of atoms in the condensate, U_0 accounts for the interaction between atoms, and $V(r)$ describes an effective external 3-D potential well. In particular, for very low temperatures U_0 has

the following form: $U_0 = 4\pi\hbar^2 a/m$; typically, $V(r)$ has the form of harmonic trap potential, i.e. $V(r) = m\omega_t^2 r^2/2$, where ω_t is the (isotropic) angular trap frequency.

1.4 Nonlinear collective dynamics of charged-particle beams

The nonlinear longitudinal dynamics of a relativistic particle bunch in circular accelerating machines has been recently described in terms of a NLSE of the cubic form, within the context of the *thermal wave model* [13]. For the case of purely reactive impedance, neglecting radiation damping and quantum excitation, the nonlinear interaction between the bunch and the surroundings (potential well and wake fields) is governed by the following NLSE equation fully similar to the ones quoted above [14]:

$$i\epsilon\eta\frac{\partial\Psi}{\partial s} = -\frac{\epsilon^2\eta^2}{2}\frac{\partial^2\Psi}{\partial x^2} + V_{RF}(x)\Psi - \eta\frac{q_e I}{2\pi E_0}\left(\frac{X}{n}\right)|\Psi|^2\Psi \quad , \qquad (8)$$

where ϵ is the longitudinal emittance, η is the slip factor, q_e is the particle charge, X is the total coupling purely reactive impedance (n being the harmonic number), E_0 is the synchronous particle energy, and I is the beam current. The effective potential well $V_{RF}(x)$ is due to the radio frequency (RF) cavity; usually it can be assumed harmonic, i.e. $V_{RF}(x) = Kx^2/2$, where K is the RF strength.
When the RF is *off*, the well known conditions of the coherent instability (stability) both for monochromatic coasting beams and for bunched beams have been recovered [14]. In particular, for monochromatic coasting beams the conditions for coherent instability (stability) are summarized by the following inequality

$$\eta X > 0 \quad ,$$

where $\eta > 0$ ($\eta < 0$) means below (above) the transition energy and $X > 0$ ($X < 0$) corresponds to a purely inductive (capacitive) total longitudinal coupling impedance. In the analogy with the electromagnetic case (see Eq. (3)), it corresponds to the *Lighthill criterion* (modulational instability).
Additionally, under the condition $\eta X > 0$, a soliton-like profile for the beam density is predicted as a final stage of the coherent instability [14].

1.5 The NLSE with a memory term

Recently, a new type of NLSE of integro-differential form have been considered in both nonlinear optics [15] and in the quantumlike description of charged-particle beam physics [16] for modulational instability investigations. For these

cases, the functional $\mathcal{F}(|\Psi|^2)$ has the following form:

$$\mathcal{F}\left[|\Psi|^2\right] \;=\; -\,\mathcal{X}\alpha\left[|\Psi|^2 \;-\; |\Psi_0|^2\right] \;-\; \mathcal{R}\alpha\int\left[|\Psi|^2 \;-\; |\Psi_0|^2\right]\,dx \quad , \quad (9)$$

where the coefficients α, $\mathcal{X}$, and $\mathcal{R}$ are real constant. At the right-hand side, the first term is the stardard one accounting for the cubic nonlinearity, whilst the integral one is a sort of *memory term*. Consequently, nonlinear wavepacket propagation is governed by the following integro-differential NLSE:

$$i\frac{\partial\Psi}{\partial s}+\frac{\alpha}{2}\frac{\partial^2\Psi}{\partial x^2}+\mathcal{X}\left[|\Psi|^2 \;-\; |\Psi_0|^2\right]\Psi+\mathcal{R}\,\Psi\int_0^x\left[|\Psi(x',s)|^2 \;-\; |\Psi_0|^2\right]dx' \;=\; 0 \quad . \quad (10)$$

Other kind of memory effects have been taken into account also in the pioneeristic works on four-photon parametric processes (i.e. modulational instability) in nonlinear media, such as Kerr media (see f.i. molecular orientation Kerr effect) [17].

The modulational instability analysis carried out in Ref. [16] with Eq. (10) was capable of reproducing all the results of the coherent instability theory for a coasting beam in circular accelerating machines in case of longitudinal coupling impedance with non-zero resistive part. This approach improved the one described in Ref. [14] in which only a purely reactive coupling impedance has been considered. In particular, $\mathcal{X}$ and $\mathcal{R}$ appearing in (9) are the reactance and the resistence per unity length, respectively. Furthermore, in the charged-particle beam dynamics, the physical origin of the integral-memory term is that it accounts for the resistive tension per unity length along the pipe of the machine.

It is whorth to remark that these approches to the modulational instability analysis with memory effects have been carried out with the standard techniques in configuration space. In this framework, no phenomena of the kind of Landau damping [18] was possible to predict. Only more recently, a Landau-type damping has been predicted for e.m. wavepackets whose propagation is governed by Eq. (10) [19]. The analysis has been carried out in phase space making use of the Wigner transform and the von Neumann equation. As a consequence of this result, the Landau damping phenomenon [18] is automatically predicted for all the NLSEs (3), (5), (6), and (7), quoted above, in the special case of constant or zero external potential.

In this paper, we present in a review form all the results concerning both the modulational instability analysis and the Landau damping prediction obtained with the above NLSEs.

2 FORMULATION OF THE PROBLEM

In order to include all the physical cases quoted in the sections 1.1-1.4, we carry out the approach starting from Eq (1) with an arbitrary functional $\mathcal{F}\left[|\Psi|^2\right]$.
We assume that an equilibrium state for the system exists and is represented by a wavefunction $\Psi_0(x,s)$ for which

$$\mathcal{F}\left[|\Psi_0|^2\right] \;=\; 0 \quad . \tag{11}$$

For simplicity we confine our analysis to the case of constant or zero external potential. Thus, we want to show that:

- Nonlinear wavepacket propagation can be also suitably described in phase space with a kinetic-like equation
- MI of a monochromatic wavetrain is formally identical to CI of a coasting beam
- The concept of coupling impedance for the wavepacket propagation can be naturally introduced
- A sort of Landau damping for a wavepacket is predicted

3 WIGNER PICTURE ASSOCIATED WITH NLSE

According to the last part of section 1.5, to provide for a Landau damping description within the context of the nonlinear dynamics governed by an arbitrary NLSE a transition to the phase-space framework is very helpful . Such a kind of transition can be easily performed by using the Wigner transform of the complex amplitude $\Psi(x,s)$. This allows us to write a sort of von Neumann equation for the Wigner function $\rho_w(x,p,s)$ [20], $p \equiv dx/ds$ being the conjugate momentum associated with x. First of all, we observe that Eq. (1) can be cast in the form:

$$i\alpha\frac{\partial\Psi}{\partial s} \;=\; -\,\frac{\alpha^2}{2}\frac{\partial^2\Psi}{\partial x^2} \;+\; U\Psi \quad , \tag{12}$$

where U is the following arbitrary nonlinear potential:

$$U\left[|\Psi|^2\right] \;=\; -\,\alpha\,\mathcal{F}\left[|\Psi|^2\right] \quad , \tag{13}$$

with $\alpha = 2P$ and $\mathcal{F}\left[|\Psi|^2\right]$ obeys to the condition (11), namely:

$$\mathcal{F}\left[\Psi_0\right] \;=\; 0 \quad . \tag{14}$$

Note that, in particular, the nonlinear potential with the memory term

$$U\left[|\Psi|^2\right] \;=\; -\mathcal{X}\alpha\left[|\Psi|^2 \;-\; |\Psi_0|^2\right] \;-\; \mathcal{R}\alpha\int\left[|\Psi|^2 \;-\; |\Psi_0|^2\right]\,dx \quad , \tag{15}$$

associated with (9) and (10) obeys to this condition.
We now transit from configuration space to phase space by the following Wigner-like transform [20] :

$$\rho_w(x,p,s) = \frac{1}{2\pi\alpha}\int_{-\infty}^{\infty}\Psi^*\left(x+\frac{y}{2},s\right)\;\Psi\left(x-\frac{y}{2},s\right)\;\exp\left(i\frac{py}{\alpha}\right)\;dy \quad . \tag{16}$$

The following normalization condition is also assumed:

$$\int_{-\infty}^{\infty}\,dx\,\int_{-\infty}^{\infty}\,dp\;\rho_w(x,p,s) \;=\; 1 \quad . \tag{17}$$

We observe that, if Ψ satisfies Eq.n (12), then ρ_w satisfies the following von Neumann-like equation :

$$\frac{\partial\rho_w}{\partial s} + p\frac{\partial\rho_w}{\partial x} - \sum_{n=0}^{\infty}\frac{(-1)^n}{(2n+1)!}\left(\frac{\alpha}{2}\right)^{2n}\frac{\partial^{2n+1}U}{\partial x^{2n+1}}\frac{\partial^{2n+1}\rho_w}{\partial p^{2n+1}} \;=\; 0 \quad . \tag{18}$$

On the other hand, (16) implies that

$$|\Psi|^2 \;=\; \int_{-\infty}^{\infty}\rho_w(x,p,s)\;dp \quad . \tag{19}$$

Consequently, (9) can be expressed as a functional of ρ_w:

$$U \;=\; U\left[|\Psi|^2\right] \;=\; U\left[\int_{-\infty}^{\infty}\rho_w(x,p,s)\;dp\right] \quad , \tag{20}$$

with the condition

$$U\left[\int_{-\infty}^{\infty}\rho_0(p)\;dp\right] \;=0 \quad , \tag{21}$$

where $|\Psi_0|^2 \;\equiv\; \int_{-\infty}^{\infty}\rho_0(p)\;dp$.
In particular, the nonlinear potential with the memory term (15) can be cast as:

$$U \;=\; -\mathcal{X}\alpha\int_{-\infty}^{\infty}(\rho_w \;-\; \rho_0)\;dp - \mathcal{R}\alpha\int dx\int_{-\infty}^{\infty}(\rho_w \;-\; \rho_0)\;dp = \quad , \tag{22}$$

which trivially satisfies the condition (21). Thus, (18) and (20) (or, in particular, (18) and (22)) constitute a set of coupled equations governing the nonlinear propagation of an electromagnetic wavepacket. In order to get the

linear dispersion relation of the system, we can perform the Fourier analysis, after linearizing the set of equation (18) and (20) (or, in particular (18) and (22)). The procedure is similar to the one of Vlasov-Poisson used in plasma physics [18,21]. Likewise, in the longitudinal dynamics description of charged-particle beams, travelling through the pipe of a circular accelerating machine, Vlasov equation is usually coupled with a relationship which connects the longitudinal electric voltage per turn with the beam current [22].

4 LINEARIZATION

Let us start from the equilibrium state: $\rho_w = \rho_0(p)$, $U = U_0 \equiv U[\rho_0] = 0$, and perturb the system according to:

$$\rho_w(x,p,s) = \rho_0(p) + \rho_1(x,p,s) \quad , \tag{23}$$

$$U(x,s) \;=\; U_0 \;+\; U_1(x,s) \;=\; U_1(x,s) \quad , \tag{24}$$

where $\rho_1(x,p,s)$ and $U_1(x,s)$ are first-order quantities. Consequently, (18) and (22) can be linearized as follows:

$$\frac{\partial \rho_1}{\partial s} + p\frac{\partial \rho_1}{\partial x} = \sum_{n=0}^{\infty} \frac{(-1)^n}{(2n+1)!}\left(\frac{\alpha}{2}\right)^{2n} \frac{\partial^{2n+1} U_1}{\partial x^{2n+1}} \rho_0^{(2n+1)} \quad , \tag{25}$$

where $\rho_0^{(2n+1)} \equiv d^{2n+1}\rho_0/dp^{2n+1}$. Additionally, linearization of Eq. (19) gives (with obvious meaning of symbols) that:

$$n(x,s) \;=\; |\Psi(x,s)|^2 \;=\; \int_{-\infty}^{\infty} \rho_w(x,p,s)\; dp = \;\; n_0 \;+\; n_1(x,s) \quad , \tag{26}$$

where $n_0 \equiv |\Psi_0|^2$ and $n_1(x,s) \equiv \int_{-\infty}^{\infty} \rho_1(x,p,s)\, dp$ is the density perturbation in configuration space (i.e., the perturbation of the e.m. power density in case of e.m. wavepacket).

4.1 The concept of coupling impedance

Let us introduce the Fourier transform of $U(x,s)$ and $\rho_1(x,p,s)$, i.e.:

$$U_1(x,s) = \int_{-\infty}^{\infty} dk \int_{-\infty}^{\infty} d\omega\; \widetilde{U_1}(k,\omega)\; \exp\left(ikx - i\omega s\right) \quad , \tag{27}$$

$$\rho_1(x,p,s) = \int_{-\infty}^{\infty} dk \int_{-\infty}^{\infty} d\omega\; \widetilde{\rho_1}(k,p,\omega)\; \exp\left(ikx - i\omega s\right) \quad . \tag{28}$$

Note that $\int_{-\infty}^{\infty} \widetilde{\rho_1}(k,p,\omega)\ dp$ is the Fourier transform of the density perturbation $n_1(x,s)$. Thus:

$$n_1(x,s) = \int_{-\infty}^{\infty} dk \int_{-\infty}^{\infty} d\omega\ e^{ikx-i\omega s} \int_{-\infty}^{\infty} \widetilde{\rho_1}(k,p,\omega)dp \quad . \tag{29}$$

Let us now observe that, by definition, the Fourier transform of the density $n(x,s)$ is the *characteristic function* $G(k,\omega)$. Thus, it follows that $G_1(k,\omega) \equiv \int_{-\infty}^{\infty} \widetilde{\rho_1}(k,p,\omega)\ dp$ is its first-order perturbation. We define *the wavepacket coupling impedance* Z as the following ratio:

$$Z \ = \ \frac{k}{\alpha}\ \frac{\widetilde{U_1}(k,\omega)}{iG_1(k,\omega)} \ = \ Z(k,\omega) \quad . \tag{30}$$

Consequently, $Z(k,\omega)$ plays the role of transfer function of the system; its analytical properties account for stability features. Since it is evident that Z is a complex quantity, let us put: $Z \equiv Z_R + i\ Z_I$, Z_R and Z_I being real and imaginary part, respectively.
It is easy to see that in the special case of potential with the memory term given by (22) we have:

$$\widetilde{U_1}(k,\omega) \ = \ \frac{k}{\alpha}\ (\mathcal{R} + ik\mathcal{X})\ iG_1(k,\omega) \quad , \tag{31}$$

which implies that:

$$Z_R \ = \ \mathcal{R}\ , \quad \text{and} \quad Z_I \ = \ i\ k\mathcal{X} \quad . \tag{32}$$

4.2 Linear dispersion relation

Fourier transform of (25) gives

$$\widetilde{\rho_1}(k,p,\omega) \ = \ \frac{\rho_0\ (p+\alpha k/2) \ - \ \rho_0\ (p-\alpha k/2)}{\alpha}\ \frac{\widetilde{U_1}(k,\omega)}{kp-\omega} \quad , \tag{33}$$

which combined with (30) (or in particular with (31)) allows us to get the following dispersion relation:

$$1 \ = \ i\ Z\alpha \int_{-\infty}^{\infty} \frac{\rho_0\ (p+\alpha k/2) \ - \ \rho_0\ (p-\alpha k/2)}{\alpha k}\ \frac{dp}{kp-\omega} \quad . \tag{34}$$

This relation plays a role similar to the one played by the dispersion relations obtained in the linear Vlasov theory for both plasma waves [21] and charged-particle beams [22]. In the next sections we carry out an analysis in phase space to describe the modulational instability in a new way (with respect to the standard approach given in configuration space) and predict a phenomenon fully similar to the one known as Landau damping [18].

5 MODULATIONAL INSTABILITY ANALYSIS FOR MONOCHROMATIC WAVE TRAINS

In the limiting case of monochromatic wavetrain the equilibrium distribution function is a delta-function, i.e.

$$\rho_0(p) \;=\; n_0\delta(p) \quad , \tag{35}$$

n_0 being constant.Thus, (34) reduces to:

$$1 \;=\; -\,i\;n_0\frac{Z}{k}\;\left[\frac{1}{\alpha k^2/2+\omega}+\frac{1}{\alpha k^2/2-\omega}\right] \quad , \tag{36}$$

which can be cast in the form:

$$\omega^2 \;=\; \frac{\alpha^2 k^4}{4}+i\alpha n_0 k Z \quad . \tag{37}$$

From (37) we can see that ω can be complex, namely we can write:

$$\omega \;=\; \omega_R \;+\; i\,\omega_I \quad . \tag{38}$$

By separating (37) in its real and imaginary parts, we finally get

$$Z_I \;=\; -\,\frac{\alpha k}{4n_0\omega_I^2}Z_R^2 \;+\; \frac{\omega_I^2}{\alpha n_0 k} \;+\; \frac{\alpha k^3}{4n_0} \quad . \tag{39}$$

The dispersion relation (39), for given value of ω and k, determines a connection between Z_I, Z_R, and the growth rate ω_I. In the (Z_R, Z_I)-plane we have a family of symmetric parabolas around Z_I-axis, whose concavity orientation depends on the sign of α, parametrized with respect to ω_I, with the following features. Eq. (39) fully recovers the results of the modulational instability analysis that has been recently carried out in configuration space for the NLSE with the nonlinear potential including the memory term similar to the one defined by Eq. (15) [19].

Since the condition $\omega_I \neq 0$ ($\omega_I = 0$) gives the instability (stability) of the system, (39) provides for universal charts of instability (stability) in the (Z_R, Z_I)-plane, which are very similar to the ones obtained in particle accelerators with the standard Vlasov theory for coherent instability [22]. In fact, for $\omega_I \to 0$, the parabolas collapse into a vertical straight line on Z_I-axis given by the condition: $-\infty < Z_I \leq \alpha k^3/4n_0$, for $\alpha > 0$, and $\alpha k^3/4n_0 \leq Z_I < \infty$, for $\alpha < 0$.

The above straight line represents the stability region of the system which is enclosed by all the parabolas. This means that all the points in the (Z_R, Z_I)-plane for which $Z_R \neq 0$, represent unstable states of the system.

In the case $Z_R = 0$, we are dealing with the cubic NLSE. It is easily seen from (39) that $\omega_I^2 = \left(Z_I \alpha - \alpha^2 k^3/4n_0\right) n_0 k$. Consequently, the instability condition is now $Z_I\ \alpha\ >\ \alpha^2 k^3/4n_0$. Of ourse, the opposite inequality represents the stability condition.

If $\alpha k << 1$, (39) gives the instability charts which formally coincide with the ones of coherent instability of a coasting beam, i.e

$$Z_I\ =\ -\frac{n_0 \alpha k}{4\omega_I^2} Z_R^2\ +\ \frac{\omega_I^2}{\alpha n_0 k}\quad . \tag{40}$$

This relation shows clearly that the stability region (for $Z_R = 0$) corresponds to the interval of Z_I satisfying the condition:

$$Z_I\ \alpha\ <\ 0\quad , \tag{41}$$

and, consequently, instability is obtained for

$$Z_I\ \alpha\ >\ 0\quad , \tag{42}$$

which coincides with the well known *Lighthill criterion* [14] of modulational instability associated with the cubic NLSE. Eq.s (41) and (42) formally coincide with coherent stability and instability conditions, respectively, provided that Z_I and α are formally replaced by the longitudinal coupling impedance and the slip factor of a coasting beam, respectively.

6 MODULATIONAL INSTABILITY ANALYSIS FOR NON-MONOCHROMATIC WAVE TRAINS AND LARGE PHASE VELOCITIES: PREDICTION OF WEAK LANDAU DAMPING

In this section we confine our attention to the case of non-monochromatic wavetrains which correspond to the assumption that $\rho_0(p)$ is not a della function but has a finite spread in the p-space. Additionally is assumed that each Fourier component of perturbation of the wave train has a very large phase-velocity, which corresponds to the condition $\omega/k >> 1$.

6.1 Case of $\alpha k << 1$

Since $\alpha k << 1$, we have:

$$\frac{\rho_0\ (p + \alpha k/2)\ -\ \rho_0\ (p - \alpha k/2)}{\alpha k}\ \approx d\rho_0/dp\ \equiv \rho_0^{'}\quad . \tag{43}$$

Consequently, Eq. (34) becomes:

$$1 \;=\; i\alpha Z(k,\omega) \int_{-\infty}^{\infty} \frac{\rho_0^{'}}{kp-\omega}\, dp \quad . \tag{44}$$

Eq. (44) is formally identical to the linear dispersion relation that holds for warm plasma waves [21] or for non-monochromatic charged-particle bunches in circular accelerating machines [22], the former being related to the case of a purely imaginary Z and the latter being related to a more general complex Z.

We note that the limit of small wavenumbers here considered allows us to predict a sort of weak Landau damping, as described in plasma physics as well as in charged-particle beam physics. We call this phenomenon *quantum-like Landau damping* (QLLD).

A. If we assume that $Z_R = 0$, thus $Z = iZ_I$, (44) becomes:

$$1 \;=\; -\alpha Z_I \int_{-\infty}^{\infty} \frac{\rho_0^{'}}{kp-\omega}\, dp \quad . \tag{45}$$

Provided that $\alpha\ Z_I < 0$, by replacing $-\alpha\ Z_I$ with the ratio ω_p^2/k^2 (ω_p being the electron plasma frequency), Eq. (45) becomes formally identical to the linear dispersion relation for a warm unmagnetized electron plasma, which predicts the existence of Landau damping [18,21]. Consequently, following the well known Landau method [18,21], and using the small wavenumber approximation, we easily get the following dispersion relation:

$$1 \;=\; -\alpha\ k\ \mathcal{X}\left[D(\omega,k) \;+\; i\frac{\pi}{k}\ \rho_0^{'}(\omega/k)\right] \quad , \tag{46}$$

where

$$D(\omega,k) \;\equiv\; \int_{PV} \frac{\rho_0^{'}}{kp-\omega}\, dp \tag{47}$$

is the principal value of the integral in (45).

B. In the case $Z_R \neq 0$, the analysis can be carried out as in the case of a charged-particle beam in a circular accelerating machine. Thus, following the standard treatment of accelerator physics [22], we have:

$$V_R + i\,V_I \;\equiv\; \alpha\left(\frac{Z_R}{k} \;+\; i\ \frac{Z_I}{k}\right) \;=\; -\left[i\ \int_{PV} \frac{\rho_0^{'}}{p-\beta_{ph}}\, dp \;+\; \pi\ \rho_0^{'}(\beta_{ph})\right]^{-1} , \tag{48}$$

where $V_R = \alpha Z_R/k$, $V_I = \alpha Z_I/k$, and $\beta_{ph} = \omega/k$. This equation determines a relationship between V_R, V_I, and β_{ph}. In principle, β_{ph} is a complex quantity.

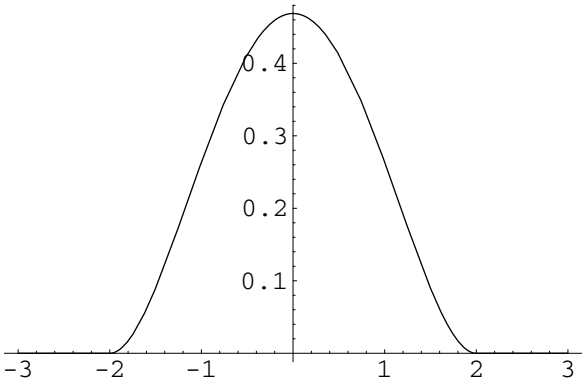

Figure 1. Plot of the equilibrium distribution $\rho_0(p) = \left(1 - p^2/4\right)^2 / 2.133$, defined in the intervall of p $(-2, 2)$.

Thus, we put: $\beta_{ph} \equiv \gamma_R + i\,\gamma_I$. Consequently, we can plot curves in the V_R-V_I plane for a given equilibrium distribution funtion $\rho_0(p)$ and for different growth rates γ_I. For instance, we assume $\rho_0(p) = \left(1 - p^2/4\right)^2 / 2.133$ which is plotted in Figure 1. Figure 2 shows these curves, for $\alpha k = .01$ and for the smooth distribution plotted in Figure 1. This picture is analogous to the one for charged-particles in circular accelerating machines in which coherent instabilities (for instance, the negative-mass instability) competes with Landau damping to produce stability diagrams [22]. We would like to stress that Figure 2 represents a sort of universal stability chart for the nonlinear wave packet propagation as described by NLSE (10). Any impedance Z leading to a (V_R, V_I) pair belonging the area surrounded by the curve with $\gamma_I = 0$ corresponds to a stable operation.

6.2 Case of arbitrary αk

When the αk assumes arbitrary values, approximation (43) is no longer valid. In this case, the instability analysis must be carried out directly with Eq. (34). To perform the integration, the residui theory can be applied as in the previous case. Figure 3 shows the instability charts in the $(V_R,\, V_I)$ plane produced by (34), for $\alpha k = .4$,and for ρ_0 plotted in Figure 1. Note that the stability region are enlarged with respect to the one corresponding to $\alpha k = .01$.

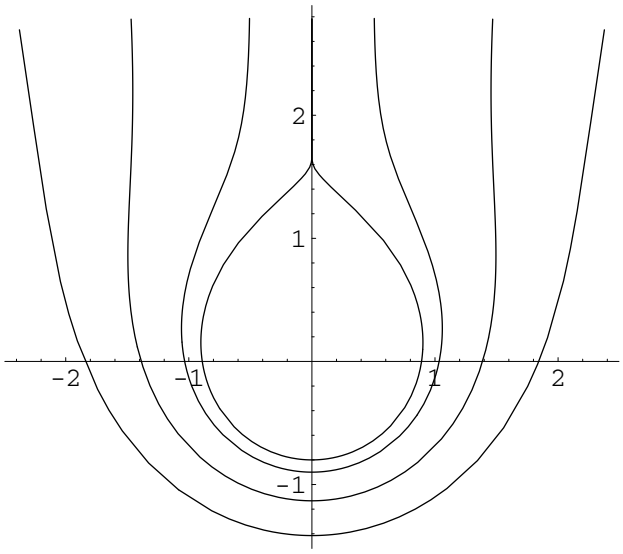

Figure 2. Instability chart for $\alpha k = .01$ and for ρ_0 plotted in Figure 1. *The area inside the curve with $\gamma_I = 0$ represents the stability region. For increasing values of γ_I ($\gamma_I = 0, .1, .3, .5$), the curves plotted cover in the instability region. They are a sort of "deformed parabolas". However, as γ_I increases more and more, their shapes become more and more similar to the parabolas described by Eq. (40) as given in the monochromatic case. We note that in the present case the stability region is larger. This effect, together with the deformation of the above parabolas, is due to the stabilizing effect of the quantum-like Landau damping of the wave packet which exists for a p-distribution with non–negligible spread. In fact, in this case, the stabilizing effect is in competition with the modulational instability.*

7 CONCLUSIONS

In this paper an analysis to describe modulational instability and predict the phenomenon of Landau damping in a wide class of nonlinear Schrödinger equations has been carried out. This has been done in phase space by using the Wigner transform to get a von Neumann equation. The main results of recent investigations of MI in NLSEs has been reviewed. In particular, a recently proposed integro-differential NLSE, containing a memory term, has been taken into account. The above phase-space framework has provided for a kinetic-like description of the nonlinear dynamics governed by NLSE which is very natural for predicting the Landau damping in a way fully similar to the one in plasma physics and in particle accelerators. Remarkably, in this

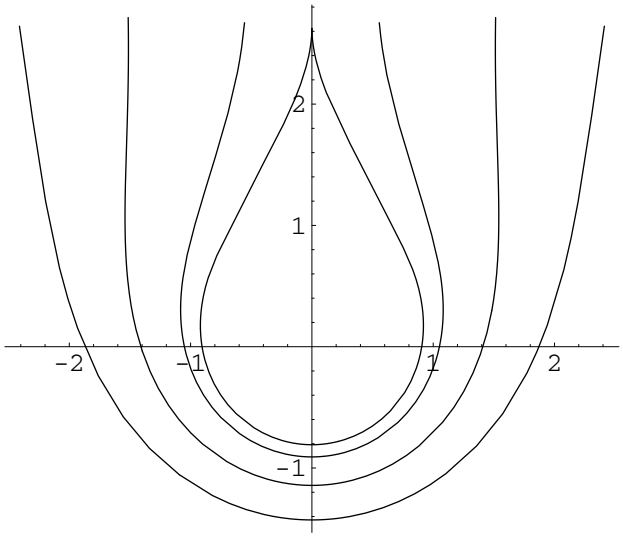

Figure 3. Instability chart for $\alpha k = .4$, ρ_0 plotted in Figure 1, and for encreasing values of γ_I ($\gamma_I = 0, .1, .3, .5$). *In this case, the area inside of the stability region ($\gamma_I = 0$) is larger than the one of $\alpha k << 1$ (compare with Figure 2). The "deformed parabolas" do not coicide with the case of Figure 2. However, as γ_I is encreasing, also in this case the deformation becomes more and more negligible and the parabolas shown is Figure 2 are exactly recovered for very large values of this parameter.*

framework the concept of coupling impedance comes out very easily. Instability charts in the normalized impedance plane, similar to the accelerator ones, have been plotted for a tipical smooth $\rho_0(p)$. The plot corresponding to the case $\alpha k << 1$ (see Figure 2 where $\alpha k = .01$) exactly reproduces the corresponding charts of particle accelerators, whilst the case corresponding to larger values of this parameter (see Figure 3 where $\alpha k = .4$), shows a larger stability region.

References

1. Y.R. Shen and S.H. Liu *The Principles of Nonlinear Optics* (Wiley-Interscience Publication, New York, 1962).
2. G.S. He and S.H. Liu *Physics of Nonlinear Optics* (World Scientific, Singapore, 1999).
3. G.P. Agrawal, *Nonlinear Fibre Optics* (Academic Press, San Diego, 1995).

4. M.J. Lighthill, *J. Inst. Math. Appl.* **1**, 269 (1965); Proc. Roy. Soc. **229**, 28 (1967).
5. V.E. Zakharov, *Sov. Phys. JETP*, **35**, 908 (1972).
6. V.I. Karpmann, *Nonlinear Waves in Dispersive Media* (Pergamon Press, Oxford, 1975).
7. G.B. Whitham, *Linear and Nonlinear Waves* (J. Wiley and Sons, New York, 1974).
8. D.R. Tilley and J.Tilley, *Superfluidity and Superconductivity* (Van Nostrand Reinhold Compamy, New York, 1974).
9. K. Stewartson and J.T. Stuart, *J. Fluid Mech.* **48**, 529 (1971).
10. V.L. Ginzburg and L.P. Pitaevskii, *Sov Phys. JETP* **7**, 858 (1958).
11. M.H. Anderson, J.R. Ensher, M.R. Matthews, C.E. Wieman, and E.A. Cornell, *Science*, **269**, 198 (1995); C.C. Bradley, C.A. Sackett, J.J. Tollett, and R.G. Hulet, *Phys. Rev. Lett.*, **75**, 1687 (1995).
12. A.H. Khater, D.K. Callebaut and A.R. Seadawy, *Phys. Sr.* **62**, 353 (2000).
13. R. Fedele and G. Miele *Nuovo Cimento* 13 D, 1527 1991.
14. R. Fedele, G. Miele, L. Palumbo, and V.G. Vaccaro, *Phys. Lett.* **A179**, 407 (1993).
15. K. Blow and D. Wood, *IEEE J. Quantum Electron.* **25**, 2665 (1989).
16. D. Anderson, R. Fedele, V.G. Vaccaro, M. Lisak, A. Berntson, and S. Johanson, *Phys. Lett. A* **258**, 244 (1999).
17. R. Y. Chiao, P. L. Kelley and E. Garmire, *Phys. Rev. Lett.* 17, 1158 (1966).
18. L.D. Landau, *J. Phys. USSR*, **10**, 25 (1946).
19. R. Fedele and D. Anderson, *J. Opt. B: Quantum Semiclass. Opt.*, **2**, 207 (2000); R. Fedele, D. Anderson and M. Lisak, *Phys. Scr.* **T84**, 27 (2000).
20. E. Wigner, *Phys. Rev.*, **40** 749 (1932).
21. P. A. Sturrock, *Plasma Physics*, (Cambridge University Press, Cambridge, 1994).
22. J. Lawson, *The Physics of Charged Particle Beams*, (Clarendon Press, Oxford, 1988); A.W. Chao *Physics of Collective Instabilities in High Energy Accelerators* (John Wiley and Sons, Somerset, USA, 1990).

SUMMARY OF WORKING GROUP D

A.J. DRAGT
Department of Physics, University of Maryland
College Park, MD 20742 USA
Email: dragt@physics.umd.edu

M. PUSTERLA
Dipartimento di Fisica Galileo Galilei Universita di Padova
Istituto Nazionale di Fisica Nucleare (INFN) Sezione di Padova
Via Marzolo 8 Padova 35131 ITALY
Email: modesto.pusterla@pd.infn.it

Summaries of the lectures presented in Working Group D, Quantum Methodology in Beam Physics, are given in alphabetical order by author.

1 N. Cufaro–Petroni (in collab. with De Martino, De Siena and Illuminati)

Collective dynamics of particle beams, in the regime of stability, are illustrated by using a suitable form of stochasticity compatible with time–reversal invariance (Nelson, Guerra).

The global motion of a macroscopic system (in this specific case a bunched beam) follows from the motion of the microscopic constituents (ex.: protons) that move coherently. The aim here is the connection between microscopic and macroscopic parameters and the derivation of the quantum–like approach from the Quantum Mechanics of a single particle.

Although quite general, the approach is described in detail for the transverse motion of beams in circular machines (storage rings, accelerators, colliders).

Significant points of the work are:

a. introduction of a unit minimal action (called α) for a single particle ($\alpha \simeq m\tilde{v}^2 \cdot \tau$);

b. a characteristic mean velocity $\tilde{v}$ and a characteristic microscopic time $\tau \simeq \frac{\overline{\tau}}{\sqrt{N}}$ where $\overline{\tau}$ is a typical (macroscopic) time necessary for a particle to go through the whole length R of the system and N is the number of particles present in the macroscopic system (in a bunch), obviously $\tilde{v} = R/\overline{\tau}$;

c. possible inclusion of external forces (external electric and magnetic fields), in order to control the stability of the system (ex.: proton bunched beam).

Research still in progress for future applications (halo, beam stability.... with non–linear lenses....etc).

Main results obtained:

a. from "HERA" parameters $\alpha \simeq h$ (Planck's const.), $\epsilon \simeq h\sqrt{N}$ and $\frac{\epsilon}{mc} \simeq \lambda_c\sqrt{N}$ with $\lambda_c = \frac{\bar{h}}{mc}$ (Compton wave length);

b. using N estimated for "HERA" bunches predicts transverse bunch length between 10^{-7} and 10^{-8} m;

c. Quantum–like approach as a global description of the beam (introduction of the Schrödinger–like beam wave function).

2 A.Dragt

The lecture treats a very general important subject: classification and decomposition of analytic vector fields under the symplectic group $S_p(2n)$ that appears as the underlying group present in both classical and Quantum Mechanics (in Hamiltonian form).

We refer to Dragt's paper for notations and details.

After defining a vector field $\mathcal{L}_f = \sum_a f_a \frac{\partial}{\partial z_a}$ where z stands for the phase-space point $(q_1, q_2 ... q_n; p_1, p_2 ... p_n)$, f_a being a function of z and t, we have

$$\dot{z}_a = f_a(z,t) = \mathcal{L}_f z_a$$

The $\mathcal{L}_f$ fields create a Lie Algebra under commutation:

$$\{\mathcal{L}_f, \mathcal{L}_g\} = \mathcal{L}_h$$

Within this context a relevant role is played by the Hamiltonian vector fields,

$$: h(z,t) := \sum_i \frac{\partial h}{\partial q_i}\frac{\partial}{\partial p_i} - \frac{\partial h}{\partial p_i}\frac{\partial}{\partial q_i} = \sum_a \frac{\partial h}{\partial z_a} : z_a :$$

They also form a Lie Algebra (∞ dimensional). Notice that [h,g] is the Poisson bracket = :h:g. We also may notice that a homogeneus polynomial

f_n of degree n satisfies the following relation: $[f_m, f_n] = f_{m+n-2}$. Hence the $f_2's$ form also a Lie Algebra.

From all these definitions and from the standard analysis of Lie Algebras and groups (Cartan, irreducible representations, root vectors, weights, Clebsch–Gordan series...) the author derives the expansion of the general vector field

$$\mathcal{L}_{g^l} = \sum_a g_a^l : z_a :$$

(ℓ= degree of homogeneous polynomial g^l)

$$\mathcal{L}_{g^l} = H^{(l+1)} + R^{(l-1)}$$

where $H^{(l+1)}$ is the Hamiltonian part of $\mathcal{L}_{g^l}$ (namely : $H_{l+1)}$:) and $R^{(l-1)}$ represents the non–Hamiltonian parts.

Two important examples:

a. Illustration of this approach: the damped harmonic oscillator.

b. A relevant application (particularly useful in electron rings) given an analytic map $M : Mz \to \bar{z}$ with

$$\bar{z}_a = k_a + \sum_b R_{ab} z_b + \sum_{b,c} T_{abc} z_b z_c + ... \tag{1}$$

we obtain for M a unique factorization

$$M = e^{G_2} \cdot e^{G_3} .... \times e^{:f2:} e^{:f3:} ....e^{:fn:} \tag{2}$$

where $\Pi_j exp G_j$ represents the non–Hamiltonian factor (non symplectic, for instance, in accelerator physics, the radiation damping) whereas $\Pi_j e^{:f_j:}$ is the sympletic part.

3 A. Fedorova, M. Zeitlin

They propose calculations in nonlinear beam dynamics both in the classical and in the quantum cases via wavelets. Two particular subjects are emphasized:

a. collective effects;

b. quasiclassical calculations.

For item *a* the wavelet approach allows the construction of exact "nonlinear eigenmode" expansions or multiscale expansions for solutions of nonlinear dynamic problems. Other positive aspects are:

i) introduction of symmetry via multiresolution at the level of function spaces;

ii) the control of convergence and better convergence compared with other methods;

iii) application to RMS envelope dynamics, Vlasov–Maxwell–Poisson, nonlinear Schrödinger–type equations, renormalization group.

For item *b* the authors show that the use of the general wavelet approach can solve problems of quantum beam dynamics, deformation quantization, multiresolution representation and the Wigner–transform.

4 P.V. Hartemann

Lecture consists of a short summary of the paper "Radiative corrections in symmetrized classical electrodynamics" (Phys. Rev. E, 62 n.6 – Dec. 2000 in collab. with J.R. Van Meter, A. K. Kareman and P. Chen).

Main goal: derive from symmetrized (between electric and magnetic charges) classical electrodynamics the equation of motion of a dyon (point particle with charge q and magnetic charge g) and obtain its self force (radiation reaction).

One starts from Dirac's approach and assumes Maxwell eqs. and Lorentz force in a covariant form with the introduction of the field tensor and its dual (double tetra potential A_μ and V^μ). The self force F^μ has the form:

$$F^\mu = Re[\bar{q}(\partial^\mu A^{\nu *} - \partial^\mu A^{\mu *})\, u_\nu]$$

where $\bar{A}_\mu = A_\mu + iV_\mu$ and $\bar{q} = q + ig$; the Maxwell eqs. become:

$$\partial_\nu \partial^\nu A_\mu = 4\pi J_\mu \text{ and } \partial_\nu \partial^\nu V_\mu = -4\pi g_\mu$$

Conclusions: the authors obtain the general self force expression which is proportional to Dirac's self force formula: they differ only by a factor involving

the electric and magnetic charge. In the point particle limit (as Dirac did) they get the equation of motion for a dyon.

5 R. Jaganathan

He reviews the Lie algebraic approach to classical beam optics based on the work of Dragt and and collaborators. He points out that the Lie methods are quite general and can be applied to classical, quantum and quantum–like approaches to beam optics. As shown by Heifets and Yan in QABP98 (Monterey), quantum corrections to classical maps can affect significantly the classical predictions for trajectories close to a separatrix. Thus quantum maps could be useful in finding the boundaries of non–linear resonances. With these remarks in mind, the author discusses the way of constructing the quantum maps for phase space and spin transport through optical elements for beams of spin 1/2 particles starting systematically from the Dirac equation.

6 S. Khan

The author gives a detailed account of the quantum maps for a beam of Dirac particles that move through a normal and a skew magnetic quadrupole. These maps include the Stern–Gerlach and Thomas–BMT effects as shown in a formal way by Conte, Jaganathan, Khan and Pusterla (Particle Accel. 56, 99-1966). [Detailed formulae in the contributed papers].

7 M.A. Man'ko

In this lecture the speaker points out the possibility of describing quantum–like processes with the use of special methods of Quantum Mechanics such as Wigner–functions (quasi–distributions) and more recently tomographic probabilities.

According to the thermal wave model one can introduce the density operator which in the phase–space representation is described by the Wigner function

$$\rho_\omega(x,p,z;\epsilon) = \frac{1}{2\pi\epsilon}\int_{-\infty}^{+\infty} \psi^*(x+\frac{y}{2},z)\varphi(x-\frac{y}{2},z)exp\{i\frac{py}{\epsilon}\}dy$$

with the normalization

$$\int \rho_\omega(x,p,z;\epsilon)dxdp = 1$$

In analogy with quantum optics and in view of the Fourier–Radon transform for the Wigner function ρ_ω of the charged particle beam (electrons), one defines the tomographic–probability distribution function of the particle beam

$$\omega(X,\mu,\nu,z;\epsilon) = \int exp\ \{ik(X-\mu x-\nu p)\}\cdot\rho_\omega(x,p,z;\epsilon)\cdot\frac{dxdkdp}{(2\pi)^2}$$

which contains all the information of ρ_ω. Both in Quantum Mechanics and quantum–like systems the advantage of using the tomographic probabilities resides in the fact that they are conventional probability distributions and therefore positive.

Signal theory is an example where the quantum notion is used to visualize better signal properties in presence of a small ratio between signal and noise.

8 M.Pusterla

The author tests the Schrödinger–like approach of beam dynamics on actual projects of accelerators (LHC– CERN/AC/95–05) or systems of storage rings and linear accelerators (HIDIF – GSI –98–06). Indeed the Quantum–like approach in classical macroscopic systems allows the use of the whole apparatus of Q.M. with a different interpretation of the fundamental parameters; particularly one can make use of the propagator method (Feynman).

Small betatron and synchrotron oscillations suggest to consider the propagator of the harmonic oscillator (obviously with a proper re–interpretation of the basic parameters).

Complicated physical processes that cannot be treated in detail in the bunched beam (intrabeam scattering, space–charge etc...) require the introduction of at least one (or more) phenomenological parameter. This may be identified with the aperture of a "diffraction slit" (-b, +b).

The convolution property of the Feynman path integral, together with the diffraction parameter, generates a propagator expression in an analytic closed form that provides us with information on the beam losses and the modified transverse beam profile after each revolution in the ring.

More specifically one starts from the equation

$$i\epsilon\partial_t\psi = -\frac{\epsilon^2}{2m}\partial_x^2\psi + U(x,t)\psi$$

[$\psi \equiv$ beam wave function]. In the nonlinear case $U(x,t)$ is also a functional of $|\psi|^2$; ϵ is the normalized emittance $\equiv$ (in phase space) $\oint pdq = m_0 c\gamma\tilde{\epsilon}$; $\tilde{\epsilon} \equiv$ usual emittance. The propagator satisfies the multiple–integral representation

$$K(x+x_0, T+\tau|X', 0) = \int_{-b}^{+b} dy_1 dy_2 ... dy_n K(x+x_0, T+\tau|x_0+y_n, T+(u-1)\tau) \cdot$$

$$K(x_0+y_n, T+(n-1)\tau'|.....)....K(x_0+y_1, T|X', 0)$$

where $n\tau' \equiv \tau \equiv$ total time spent by the beam in the ring; $T \equiv$ time necessary to inject the bunch; $(-b,+b)$ interval defining the phenomenological slit.

Results (on LHC and HIDIF):

a. beam losses in both projects are such that that the power loss, after $\sim 10^9$ revolutions, is smaller than 1 Watt/m (despite the creation of a halo) and therefore under control;

b. in HIDIF the probability of losing particles is higher $\sim 10^3$ times than in LHC (related with higher intensity);

c. regarding the longitudinal motion, the interpretation of the slit is less clear; calculations are very preliminary and seem to predict a scenario of coasting beam (undesirable), but need further investigation.

9 M. Venturini

The author's paper, "Single particle quantum dynamics in a magnetic lattice", illustrates how it is possible to derive from a relativistic spin–less quantum equation (Klein–Gordon) an approximate Schrödinger equation and then compute exactly the single particle wave–function. The main goal consists of working out the expression for the wave function of a charged particle in a transport channel or in a storage ring.

Several motivations for this research:

a. calculation of transition rates for processes involving charged particles;

b. radiation emission and absorption;

c. discover Q.M. limitations to minimum achievable transverse spot–size of the beam.

The reduced K.G. equation for ψ (slow z variation) is:

$$i\hbar\partial_z\psi = (-\frac{\hbar^2}{2p_0}\frac{\partial^2}{\partial x^2} - \frac{\hbar^2}{2p_0}\frac{\partial^2}{\partial y^2} + p_0\frac{k(z)}{2}(x^2 - y^2))\psi$$

[same form as a Schrödinger equation with z as the independent time-like variable].

Conclusions

a. For a charged spinless particle confined in a transport line or storage ring it is possible to write down the wave function explicity.

b. The lattice (betatron, dispersion) functions are built into the classical orbit of a particle as well as into its quantum wave function.

c. An explicit expression of the wave function may be useful as a basis for studying the quantum dynamics of ultracold beams.

d. Coherent (or "quasi classical") states can also be explicitly constructed. They represent those states for which the wave-like effects associated with quantum particle behavior are minimal.

e. Inclusion of spin effects in this framework should be possible by using perturbation theory.

CONTROLLED STOCHASTIC COLLECTIVE DYNAMICS OF PARTICLE BEAMS

N. CUFARO PETRONI
Dipartimento Interateneo di Fisica dell'Università e del Politecnico di Bari;
INFN Sezione di Bari and INFM Unità di Bari;
Via G. Amendola 173, 70126 Bari, Italy;
Email: cufaro@ba.infn.it

S. DE MARTINO, S. DE SIENA, F. ILLUMINATI
Dipartimento di Fisica dell'Università di Salerno;
INFM Unità di Salerno and INFN Sezione di Napoli, Gruppo collegato di Salerno;
Via S. Allende, I–84081 Baronissi (SA), Italy;
Email: demartino@sa.infn.it, desiena@sa.infn.it, illuminati@sa.infn.it

Introducing a description of the collective transverse dynamics of charged (proton) beams in the stability regime by suitable classical stochastic fluctuations, we show that the transition probabilities associated to Nelson processes can be exploited to model evolutions suitable to control the transverse beam dynamics. In particular we show how to control, in the quadrupole approximation to the beam–field interaction, both the focusing and the transverse oscillations of the beam, either together or independently.

1 Introduction

In this paper we study the intermediate, but physically relevant, regime of beam dynamics in which a balance is realized, on the average, between the energy dissipation and the external RF energy pumping [1]. We thus describe the beam dynamics exploiting the theory of *classical* stochastic dynamical systems with time–reversal invariance, which has been introduced and extensively studied in the context of Nelson stochastic mechanics [2]. The study of these dynamical systems is based on an extension of the variational principles of classical mechanics to include the case of a diffusive kinematics replacing the deterministic one [3]. This is remarkable since variational principles are a very powerful tool in the description of physical systems. Here the stochastic variational principle yields two coupled hydrodynamic equations, respectively for the density and for the forward drift, which provide an effective description of the transverse oscillations of the beam profile in the regime of stability.

On the other hand, it is also interesting to remark that the two real, nonlinearly coupled hydrodynamic equations of the stochastic mechanics are equivalent to one complex, linear equation of the form of a Schrödinger equation, with the Planck action constant replaced by the diffusion coefficient of

the random kinematics. This fact connects our stochastic approach, which is developed in full detail elsewhere [4], to the recently developed quantum–like approaches to beam dynamics [5]. Moreover, since this description involves not only a Fokker–Planck equation but also a dynamical prescription, i.e. the specification of the external potential, it allows to implement the powerful techniques of active control [6] also to beam dynamics. This is at variance with the case of a purely dissipative Fokker–Planck dynamics which only describes a passive, irreversible evolution of the state [7].

In fact, once we obtain the description of the collective dynamics of the beam in terms of the hydrodynamic equations of Nelson stochastic mechanics with the proper diffusion coefficient, we can implement techniques of control already developed in the general context of stochastic dynamical systems [6]. These techniques exploit the transition probabilities, a fundamental object in the theory of diffusion processes, in order to drive the beam toward a specified and controlled evolution. In particular, we construct time–dependent potentials which drive the system from an initial state with a certain degree of collimation towards a final state characterized by a better focusing. At the same time, and independently, also the transverse betatron oscillations can be controlled and varied.

2 Stochastic collective dynamics in the stability regime

In this section we model the spatial fluctuations through the random kinematics performed by a representative particle that oscillates, in a reference frame comoving with the bunch, around the closed ideal orbit. This representative particle is identified with the collective degree of freedom by letting the associated probability density coincide with the real density of particles in the bunch. This last step is achieved by rescaling the normalization of the total number of particles. Before proceeding, we establish the notations that will be used in the following, according to the standard conventions.

We denote by $\mathbf{r} \equiv (x, y)$ a point in the transverse section orthogonal to the beam direction. We then measure the time in units of length through the arc length s along the design orbit (curvilinear coordinate). We now consider the (two–dimensional) diffusion process $\mathbf{q}(s)$ which describes the transverse motion of the representative particle and whose probability density coincides with the particle density of the bunch in the transverse direction. The evolution in the "time" s of the process $\mathbf{q}$ is described by the Itô stochastic differential equation

$$d\mathbf{q}(s) = \mathbf{v}_{(+)}(\mathbf{q}(s), s)ds + \sqrt{\mathcal{E}}d\mathbf{w}(s)\,, \tag{1}$$

where $\mathbf{v}_{(+)}$ is the (forward) drift, and $d\mathbf{w}(s) \equiv \mathbf{w}(s + ds) - \mathbf{w}(s)$ is the δ–correlated time increment of the standard white noise, and where we have

fixed the diffusion coefficient to be the characteristic transverse emittance. Equation (1) defines the random kinematics performed by the collective degree of freedom.

In the stability regime the energy lost by photonic emissions is regained in the RF cavities, and on average the dynamics is time–reversal invariant. We are thus in a situation in which there are both a random kinematics and time reversal invariance. Therefore the dynamics must be independently added to the kinematics (at variance with the purely dissipative Fokker–Planck or Langevin case) by introducing a stochastic generalization of the least action principle [3]. The latter is obtained as a generalization of the variational principle of classical mechanics, by replacing the classical deterministic kinematics, $d\mathbf{q}_c(s) = \mathbf{v}_c(s)ds$, with the random diffusive kinematics of equation (1). The equations of motion thus obtained take the form of two coupled hydrodynamic equations describing the evolution in time of the beam density and of the velocity field of the beam profile.

As a first consequence of the stochastic variational principle [3] we find that the current velocity has a gradient form:

$$m\mathbf{v}(\mathbf{r},s) = \nabla S(\mathbf{r},s)\,. \tag{2}$$

The two (nonlinearly coupled) Lagrange equations of motion for the density ρ and for the current velocity $\mathbf{v}$, of the form (2) are: the continuity equation

$$\partial_s \rho = -\nabla\cdot(\rho\mathbf{v})\,, \tag{3}$$

and a dynamical equation

$$\partial_s S + \frac{m}{2}\mathbf{v}^2 - 2m\mathcal{E}^2\frac{\nabla^2\sqrt{\rho}}{\sqrt{\rho}} + V(\mathbf{r},s) = 0\,. \tag{4}$$

This dynamical equation is typical for time–reversal invariant diffusion processes (Nelson processes). It has the same form of the Hamilton–Jacobi–Madelung (HJM) equation, originally introduced in the hydrodynamic description of quantum mechanics by Madelung [8]. It can also be shown that (3) it is equivalent to the standard Fokker–Planck equation

$$\partial_s \rho = -\nabla\cdot[\mathbf{v}_{(+)}\rho] + \mathcal{E}\,\nabla^2\rho\,. \tag{5}$$

The time–reversal invariance is assured by the fact that the forward drift velocity $\mathbf{v}_{(+)}(\mathbf{r},s)$ is not a field given *a priori*, as usual for diffusion processes of the Langevin type. On the contrary, given a certain initial condition, it is dynamically determined at any instant of time by the HJM evolution equation (4).

The equations (3) and (4) describe the collective behaviour of the beam at each instant of time through the evolution of both the beam profile and the velocity field of the beam.

It is finally worth noticing that, introducing the trivial representation [8]

$$\psi(\mathbf{r}, s) = \sqrt{\rho(\mathbf{r}, s)}\, \mathrm{e}^{iS(\mathbf{r},s)/2m\mathcal{E}}\,, \tag{6}$$

the coupled equations (3) and (4) are equivalent to a single linear equation of the form of the Schrödinger equation in the function ψ, with the Planck action constant replaced by the emittance $\mathcal{E}$:

$$i2m\mathcal{E}\partial_s\psi = -2m\mathcal{E}^2\nabla^2\psi + V\psi\,. \tag{7}$$

In this formulation the "wave function" ψ carries the information on both the dynamics of the bunch density ρ, and of the velocity field of the bunch, where the velocity field is determined through equation (2) by the phase function $S(\mathbf{r}, s)$. This shows, as previously claimed, that our procedure, starting from a different point of view, leads to a description formally analogous to that of the quantum–like approaches to beam dynamics [5].

3 Controlled beam dynamics in the quadrupole approximation

We now move on to construct explicit examples of controlled beam dynamics. In considering an accelerating machine we assume, as usual, that the longitudinal and the transverse dynamics can be deemed independent with a high degree of approximation. We will work in the framework of the quadrupole approximation, with the further simplification of considering decoupled evolutions along the radial direction x and the vertical direction y in the local reference frame.

Under these conditions, we can separate the original, two–dimensional diffusion process into two independent, one–dimensional processes respectively along x and y, each ruled by a harmonic potential. The configurational variable ξ of the previous section can here indifferently be either x or y depending on the considered transverse direction. The potential in each transverse direction has, in units of mass, the general form:

$$V(\xi, s) = \frac{1}{2}m\omega^2(s)\xi^2 - mf(s)\xi + mU(s)\,. \tag{8}$$

We have considered here a time–dependent frequency (parametric oscillator) in order to describe also the effects due to strong focusing [1]. Our aim is now to exploit the hydrodynamic equations (3) and (4) as control equations for the

beam dynamics. In particular, we will show how to compute a controlling, time–dependent potential which allows to drive a bunch prepared in a state with a certain degree of collimation towards a final state with better focusing.

We consider a Gaussian shape for the initial density profile of a bunch in each transverse direction, with constant dispersion, and with the centre of the profile which performs a classical harmonic motion with the same frequency associated to the initial potential (8). The motion of the centre models the betatron oscillations of the bunch. In our quantum–like approach, the state of the bunch is thus formally represented by a coherent state. As anticipated at the end of the previous section, we will now consider an instance of controlled evolution that does not require an extra smoothing procedure for the driving velocity field, i.e. the transition between pairs of Gaussian densities. In particular we will describe transitions from a coherent oscillating packet to another Gaussian state with a better collimation (smaller dispersion). It is worth noticing that we can also implement a procedure that allows to vary independently the dispersion (collimation) of the bunch density and the motion of the centre of the density profile (characteristics of the betatron oscillations).

To this end we will recall that if the velocity field of a Fokker-Planck equation (5) with constant diffusion coefficient $\mathcal{E}$ (the transverse emittance) has the linear form $v_{(+)}(\xi, s) = A(s) + B(s)\xi$, with $A(s)$ and $B(s)$ continuous functions of s, then there are always Gaussian solutions $\mathcal{N}\big(\mu(s), \nu(s)\big)$, where $\mu(s)$ is the displacement of the centre of the Gaussian distribution and $\nu(s)$ is the variance of the Gaussian distribution.

As previously stated, all along the time evolution our states keep a Gaussian shape for the density, and the centre of the density profile performs an arbitrarily assigned motion. Then, if we adopt the concise quantum–like representation of the bunch state (6) it is straightforward to show that the general form for the wave packet will be:

$$\psi(\xi, s) = (2\pi\nu)^{-1/4} \exp\left[-\frac{(\xi-\mu)^2}{4\nu} + \frac{i}{2m\mathcal{E}}\left(m\mu'\xi + m\frac{\nu'}{4\nu}(\xi-\mu)^2 + \theta\right)\right], \tag{9}$$

while the forward velocity field reads

$$v_{(+)}(\xi, s) = \mu' + \frac{\nu' - 2\mathcal{E}}{2\nu}(\xi - \mu). \tag{10}$$

Here the s-dependent functions $\mu(s)$ and $\nu(s)$ describe respectively the motion of the centre of the density profile and the spreading of the bunch density in the chosen transverse direction; on the other hand $\theta(s)$ plays the role of an arbitrary integration constant. Of course a suitable potential must also be

tailored in order to keep the evolution of the wave function (9) on the right track: we will show that in fact this control potential has the form suggested in (8).

The equation (9) represents the most general Gaussian packet, with a given generic motion $\mu(s)$ of its centre and with a given dispersion $\nu(s)$, associated to a linear form of the forward velocity in the Fokker–Planck equation (5). This also allows us to keep independent the initial and the final motion of the centre of the packet from the dispersions. As a first example let us now consider the transitions between two states of the form (9) with constant dispersion and with a harmonic motion of the centre of the profile. If initially (namely for $s \ll \tau$, where from now on τ is the transition instant) we start with $\nu(s) = \nu_1$ and $\mu(s) = a_1 \cos(\omega_1 s)$, we will have an initial Gaussian density profile with spreading ν_1 and with harmonic betatron oscillation of frequency $\omega_1 = \mathcal{E}/\nu_1$. We now want to drive the system towards a final (for $s \gg \tau$) state of the form (9), but with a spreading $\nu_2 < \nu_1$ (better collimation) and a new betatron oscillation $\mu_2(s)$. To this end we only need to put in the solution $\mathcal{N}(\mu(s), \nu(s))$ two functions $\mu(s), \nu(s)$ which interpolate between the corresponding initial and final functions of the motion of the centre, and of the spreading respectively. Moreover, with a suitable choice of the ξ–independent part of the phase function in (9), the forward velocity field will also smoothly interpolate between the initial and the final velocity fields [6]. The control potential which drives the solution toward the required end is finally obtained with $\tilde{\rho}$ given by the interpolating solution $\mathcal{N}(\mu(s), \nu(s))$, and with $v_{(+)}$ given by the associated forward velocity. Of course there is a large number of possible choices for the interpolating functions $\mu(s), \nu(s)$: this will allow us to single out the forms that better realize specific requirements. For example, it is possible to choose a characteristic transition time (the time needed to go from the initial to the final state) by inserting exponential relaxation terms in the interpolating functions.

We will now present a few explicit examples of transitions. Our initial ($s \ll \tau$) Gaussian, coherent, oscillating wave function has the form

$$\psi_1(\xi, s) = (2\pi\nu_1)^{-1/4} \exp\left[\frac{-(\xi - a_1 \cos\omega_1 s)^2}{4\nu_1}\right] \times \tag{11}$$

$$-i \ \exp\left[\frac{4a_1\xi \sin\omega_1 s - a_1^2 \sin 2\omega_1 s + 4\nu_1\omega_1 s}{8\nu_1}\right],$$

where we must also remember that

$$\omega_1 = \frac{\mathcal{E}}{\nu_1}. \tag{12}$$

The relation (12) means that our initial potential is purely harmonic with frequency ω_1. From the wave function (11) we have

$$\mu(s) = a_1 \cos\omega_1 s = a_1 \cos\left(\frac{\mathcal{E}s}{\nu_1}\right) , \qquad \nu(s) = \nu_1 , \qquad (s \ll \tau) . \tag{13}$$

As for the initial phase function, by inspection of equations (11) and (6), and by taking (12) into account, we immediately get

$$S(\xi, s) = m\omega_1 \left(\frac{a_1^2}{4}\sin 2\omega_1 s - \mathcal{E}s - a_1\xi \sin\omega_1 s\right) , \qquad (s \ll \tau) . \tag{14}$$

First of all we want to describe the (smooth) transition of our initial wave function to a final one of the same form but characterized by a new set of parameters:

$$a_1 \to a_2 , \qquad \nu_1 \to \nu_2 , \qquad \omega_1 = \frac{\mathcal{E}}{\nu_1} \to \omega_2 = \frac{\mathcal{E}}{\nu_2} . \tag{15}$$

The choice (15) also means that the final potential is still purely harmonic with a new frequency ω_2. In order to achieve that we consider for example the function

$$\Gamma(s) = \frac{1}{1 + \mathrm{e}^{-(s-\tau)/\gamma}} \tag{16}$$

which smoothly goes from 0 (for $s \ll \tau$) to 1 (for $s \gg \tau$) with a flex point in $s = \tau$ and a transition velocity equal to $1/\gamma$. Of course here τ and γ are completely free parameters: a suitable choice of them will allow to fine tune the timing and the velocity of the transition. Now the required transition is implemented by choosing $\mu(s) = a_1 \cos(\mathcal{E}s/\nu_1)(1 - \Gamma(s)) + a_2 \cos(\mathcal{E}s/\nu_2)\Gamma(s)$, and $\nu(s) = \nu_1(1 - \Gamma(s)) + \nu_2\Gamma(s)$, which clearly interpolates between the two initial and final Gaussian, coherent, oscillating states.
The phase function can now be calculated from (9) and we have

$$S(\xi, s) = m\left[\alpha(s)\xi^2 + \beta(s)\xi + H(s) + \theta(s)\right] \tag{17}$$

$$\alpha(s) = \frac{\nu'}{4\nu} , \qquad \beta(s) = \mu' - \frac{\mu\nu'}{2\nu} , \qquad H(s) = \frac{\nu'\mu^2}{4\nu} . \tag{18}$$

Since α, β and H are now fixed by the chosen interpolating $\mu(s)$ and $\nu(s)$, a comparison between (17) and (14), and in particular between the asymptotic ($s \to \pm\infty$) expressions of the ξ–independent term of the phase, will suggest the following form for the arbitrary $\tilde{\theta}(s)$ function (where $\tilde{\theta}(s) \equiv \theta(s) + H(s)$):

$$\theta(s) = \left[\frac{\mathcal{E}a_1^2}{4\nu_1}\sin\left(\frac{2\mathcal{E}s}{\nu_1}\right) - \frac{\mathcal{E}^2 s}{\nu_1}\right](1 - \Gamma(s)) + \left[\frac{\mathcal{E}a_2^2}{4\nu_2}\sin\left(\frac{2\mathcal{E}s}{\nu_2}\right) - \frac{\mathcal{E}^2 s}{\nu_2}\right]\Gamma(s). \tag{19}$$

Finally the potential will have the form

$$V_c(\xi,s) = m\left[\frac{1}{2}G(s)\xi^2 - F(s)\xi + W(s)\right]\ ,\ G(s) = \frac{\mathcal{E}^2}{\nu^2} - \frac{\nu''}{2\nu} + \frac{\nu'^2}{4\nu^2}, \quad (20)$$

$$F(s) = \mu'' + \mu G\ ,\ W(s) = \frac{G\mu^2}{2} - \frac{\mu'^2}{2} - \frac{\mathcal{E}^2}{\nu} - \theta'(s)\,, \quad (21)$$

where now all the terms are given by the previous relations.
As already remarked this potential has exactly the form (8). The functions $\alpha(s)$, $\beta(s)$, $G(s)$, $F(s)$ and $W(s)$, which determine the potential, can now be explicitly calculated. However their analytic expressions are by far too long (albeit elementary), and we do not report them here. They are plotted in [4].

The potential V_c has the required time behaviour since it is a simple harmonic potential for $s \ll \tau$ and $s \gg \tau$ (albeit with two different frequencies), and shows some extra terms only in a limited interval around the transition. Of course this does not constitute the only potential we can obtain in this way. For example the function $\mu(s)$, instead, could be chosen in such a way that the oscillation of the centre of the profile be slower than the initial one, despite the fact that the better collimation requires a final potential associated to a frequency $\omega_2 = \mathcal{E}/\nu_2$ larger than the initial one and then to a stronger betatron oscillation. This can be achieved by keeping a suitable forcing part $F(s)$ different from zero also for $s \gg \tau$: namely in this case the final potential does not reduces itself to a simple harmonic one. It is easy to show that if the final oscillation has the generalized form

$$\mu(s) = a\,\cos(\omega s) + \frac{b}{m}\,\sin(\omega s), \quad (22)$$

with ω not coincident with $\mathcal{E}/\nu$, the forcing function $F(s)$ calculated from (20) will correspondingly be

$$F(s) = m\left(\omega^2 - \frac{\mathcal{E}^2}{\nu^2}\right)\left(a\,\cos\omega s + \frac{b}{m}\,\sin\omega s\right). \quad (23)$$

In this case the potentials are more complicated but can still be suitably explored by means of our method. As an example we consider the case where the final state is characterized by two independent parameters: ω_2 for the frequency and ν_2 for the packet spreading. Now a relation similar to (12) will be no longer satisfied. As a consequence the original choice of interpolating $\mu(s)$ and $\nu(s)$ will be changed in $\mu(s) = a_1\cos\left(\frac{\mathcal{E}s}{\nu_1}\right)(1-\Gamma(s)) + a_2\cos(\omega_2 s)\,\Gamma(s)$ and $\nu(s) = \nu_1(1-\Gamma(s)) + \nu_2\Gamma(s)$, while we get a new determination for the

arbitrary $\tilde{\theta}(s)$ function:

$$\tilde{\theta}(s) = \left[\frac{\mathcal{E}a_1^2}{4\nu_1}\sin\left(\frac{2\mathcal{E}s}{\nu_1}\right) - \frac{\mathcal{E}^2 s}{\nu_1}\right](1-\Gamma(s)) + \left[\frac{\omega_2 a_2^2}{4}\sin(2\omega_2 s) - \mathcal{E}\omega_2 s\right]\Gamma(s). \tag{24}$$

The functions defining the time evolution of both the phase and the potential can now be calculated once more and we find that, the functions $\alpha(s)$, $\beta(s)$ keep a form very similar to the previous one. Instead the new $G(s)$ displays an opposite behaviour, since the final frequency ω_2 is smaller than the initial frequency ω_1, and thus the betatron oscillations are suppressed. Regarding the functions $F(s)$ and $W(s)$, they do not disappear any more for $s \gg \tau$, so that asymptotically we do not have a purely harmonic potential since now in (8) both the term linear and that constant in ξ will be present for every $s > \tau$. However it is clear that other choices are always possible: for example the arbitrary function $\theta(s)$ could be defined so that in (20) the ξ-independent term $W(s)$ of the potential V_c be identically zero. Of course there would be a price to pay for that: in fact now in the phase function S the ξ-independent term will no more follow an asymptotic behaviour of the type (14) since the relation (24) will no more be satisfied.
In the most general case of transitions between states with non constant dispersion (strong focusing) it is clear that the procedure can also be suitably extended. In fact it is sufficient to exploit for instance the expressions for the interpolating dispersion, but with time dependent initial and final dispersions $\nu_1(s)$ and $\nu_2(s)$. The general form (20) of the controlling potential is thus calculated, but with a new expression for $\nu(t)$. Finally, also the initial and final laws of motion of the profile centre, $\mu_1(s)$ and $\mu_2(s)$, can always be chosen as in the previously discussed example. However, in this case, a forcing part $F(s)$ is needed to retain the oscillatory motion (22) for $s \gg \tau$.

In future work we will study the extension of these control techniques beyond the quadrupole approximation and address in detail problems related to dynamical instabilities and halo formation. This latter problem has recently been addressed in the framework of a quantum–like approach[9].

1. M. Conte and W. W. MacKay, *An Introduction to the Physics of Particle Accelerators* (World Scientific, Singapore, 1991);
   D. A. Edwards and M. J. Syphers, *An Introduction to the Physics of High Energy Accelerators* (Wiley, N. Y., 1993);
   H. Wiedemann, *Particle accelerator physics* (Springer, Berlin, 1998).
2. E. Nelson, *Quantum Fluctuations* (Princeton University Press, Princeton N. J., 1985);
   F. Guerra, Phys.Rep. **77**, 263 (1981).

3. F. Guerra and L. M. Morato, Phys. Rev. **D 27**, 1774 (1983).
4. N. Cufaro Petroni, S. De Martino, S. De Siena and F. Illuminati, Phys. Rev. **E 63** (2001), in press.
5. R. Fedele, G. Miele and L. Palumbo, Phys. Lett. **A 194**, 113 (1994), and references therein;
   S.I.Tzenov, Phys.Lett. **A 232**, 260 (1997).
6. N. Cufaro Petroni, S. De Martino, S. De Siena, and F. Illuminati, J. Phys. A: Math. Gen. **32**, 7489 (1999).
7. S. Chattopadhyay, AIP Conf. Proc. **127**, 444 (1983);
   F. Ruggiero, Ann. Phys. (N.Y.) **153**, 122 (1984);
   J. F. Schonfeld, Ann. Phys. (N.Y.) **160**, 149 (1985);
   F. Ruggiero, E. Picasso and L. A. Radicati, Ann. Phys. (N. Y.) **197**, 396 (1990).
8. E. Madelung, Z. Physik **40**, 332 (1926);
   D. Bohm, Phys. Rev. **85**, 166, 180 (1952).
9. S.A.Khan and M.Pusterla, Eur.Phys.J. **A 7**, 583 (2000).

QUANTUM MECHANICAL FORMALISM OF PARTICLE BEAM OPTICS

S. A. KHAN
Dipartimento di Fisica Galileo Galilei Università di Padova
Istituto Nazionale di Fisica Nucleare (INFN) Sezione di Padova
Via Marzolo 8 Padova 35131 ITALY
E-mail: khan@pd.infn.it, http://www.pd.infn.it/∼khan/

A general procedure for construction of the formalism of quantum beam optics for any particle is reviewed. The quantum formalism of spin-$\frac{1}{2}$ particle beam optics is presented starting *ab initio* with the Dirac equation. As an example of application the case of normal magnetic quadrupole lens is discussed. In the classical limit the quantum formalism leads to the well-known Lie algebraic formalism of classical particle beam optics.

1 Introduction

Whenever the possibility of a quantum formalism of particle beam optics is mentioned the immediate response, invariably, in the accelerator physics community is to ask what is the need to use quantum mechanics when classical mechanics has been so successful in the design and operation of numerous accelerators? Of course, this is a natural question and, though the system is quantum mechanical at the fundamental level, in most situations classical mechanics is quite adequate [1] since *the de Broglie wavelength of the* (*high energy*) *beam particle is very small compared to the typical apertures of the cavities in accelerators* as has been pointed out clearly by Chen. [2] But, the recent attention to the sensitivity of tracking of particle trajectories to quantum granularities in the stochastic regions of phase space [3] and the limits placed by quantum mechanics on the achievable beam spot sizes in accelerators [4] clearly indicates the need for a formalism of quantum beam optics relevant to such issues. [5] Besides this, with ever increasing demand for higher energies and luminosity and lower emittance beams, and the need for polarized beams, the interest in the studies on the various quantum aspects of beam physics is growing. [6] So, it is time that a quantum formalism of particle beam dynamics is developed in which all aspects (optical, spin, radiation, ..., etc.) are considered in a unified framework.

The grand success of the classical theories accounts for the very few quantum approaches to the charged-particle beam optics in the past. Notable among these are:

- 1930 Glaser: Quantum theory of image formation in electron microscopy - Semiclassical theory based on the nonrelativistic Schrödinger equation. [7]

- 1934 Rubinovicz; 1953 Durand; 1953 Phan-Van-Loc: Studies on electron diffraction based on the Dirac equation. [7]

- 1986 Ferwerda *et al.*: Justified the use of scalar (Klein-Gordon) equation for image formation in practical electron microscopes operating even at relativistic energies. [7]

- 1989-90 Jagannathan *et al.*: The first derivation of the focusing theory of electron lenses using the Dirac equation. [8] 1995: Quantum theory of aberrations to all orders using the Klein-Gordon theory and the Dirac Theory. [9] 1996: Spin dynamics of the Dirac particle beam. [10]

The formalism of *quantum theory of charged-particle beam optics* developed by Jagannathan *et al.*, based on the Klein-Gordan and Dirac equations, provides a recipe to work out the quantum maps for any particle optical system up to any desired order. [8−11]. The classical limit (de Broglie wavelength $\longrightarrow 0$) of this quantum formalism reproduces the well-known Lie algebraic approach of Dragt *et al.* [12] for handling the classical beam optics. Spin evolution, independent of orbital motion, can also be treated classically using the Lie algebraic approach. [13] This brief note is to present the essential features of the quantum formalism of spin-$\frac{1}{2}$ particle beam optics based on the Dirac equation.

2 The general formalism of quantum beam optics

In many accelerator optical elements the electromagnetic fields are static or can be reasonably assumed to be static. In such devices one can further ignore the times of flights which may be negligible, or of no direct relevance, as the emphasis is more on the profiles of the trajectories. The idea is to analyze the evolution of the beam parameters of the various individual charged-particle beam optical elements (quadrupoles, bending magnets, $\cdots$) along the optic axis of the system. Let us consider a charged-particle at the point $(\boldsymbol{r}_\perp, s_{\rm in})$ where $\boldsymbol{r}_\perp$ is the transverse coordinate and s refers to the coordinate along the optic axis. After passing through the system this particle arrives at the point $(\boldsymbol{r}_\perp, s_{\rm out})$. Note that $(\boldsymbol{r}_\perp, s)$ constitute a curvilinear coordinate system, adapted to the geometry of the system. Given the initial quantities at an $s_{\rm in}$, the problem is to determine the final quantities at an $s_{\rm out}$, and to design an optical device in such a way that the relations between the initial and final

quantities have the desired properties. Since we want to know the evolution of the beam parameters along the optic axis of the system the starting equation of the quantum formalism should be desirably of the form

$$i\hbar\frac{\partial}{\partial s}\psi(\boldsymbol{r}_\perp; s) = \hat{\mathcal{H}}\psi(\boldsymbol{r}_\perp; s), \tag{1}$$

linear in $\partial/\partial s$, irrespective of the basic time-dependent equation (Schrödinger, Klein-Gordon, Dirac, $\cdots$) governing the system. So the step - I of building the quantum formalism is to cast the basic equation of quantum mechanics, relevant for the system under study, in the form (1). Once this is done the step - II would be to obtain the relationship for the quantities at any point s to the quantities at the point $s_{\rm in}$. This in the language of the quantum formalism would require to obtain the relationship for an observable $\{\langle O\rangle(s)\}$ at the transverse plane at s to the observable $\{\langle O\rangle(s_{\rm in})\}$ at the transverse plane at $s_{\rm in}$. This can be achieved by integrating (1). Formally,

$$\psi(\boldsymbol{r}_\perp; s) = \hat{U}(s, s_{\rm in})\,\psi(\boldsymbol{r}_\perp; s_{\rm in}) , \tag{2}$$

which leads to the required transfer maps

$$\langle O\rangle(s_{\rm in}) \longrightarrow \langle O\rangle(s) = \langle\psi(s)|O|\psi(s)\rangle = \left\langle \psi(s_{\rm in}) \left| \hat{U}^\dagger O \hat{U} \right| \psi(s_{\rm in}) \right\rangle . \tag{3}$$

Equation (1) is the basic equation of the quantum formalism of charged-particle beam optics and we call it as the *beam optical equation*, $\hat{\mathcal{H}}$ as the *beam optical Hamiltonian* and ψ as the *beam optical wavefunction*.

To summarize, we have a two-step algorithm to build a quantum formalism of charged-particle beam optics. On may question the applicability of the two-step algorithm: Does it always work? From experience we know that it works for the Schrödinger, Klein-Gordon and Dirac equations. The above description gives an oversimplified picture of the formalism than, it actually is. There are several crucial points to be noted to understand the success of the two-step algorithm. The first step in the algorithm to obtain the beam optical equation is much more than a mere mathematical transformation which eliminates 't' in preference to a variable 's' along the optic axis. There has to be a clever set of transformations ensuring that the resultant s-dependent equation has a very close physical and mathematical analogy with the original t-dependent equation of the standard quantum mechanics. Without this guiding requirement it would not be possible to execute the second step of the algorithm which ensures that we can use all the rich machinery of the quantum mechanics to compute the transfer maps characterizing the optical system. This summarizes the recipe of obtaining the quantum prescriptions for the optical transfer maps. Rest is mostly a computational affair which

is inbuilt in the powerful algebraic machinery of the algorithm. As in any computation, there are some reasonable assumptions and some possible approximations coming from physical considerations. It is important to note that in the case of the Schrödinger, Klein-Gordon and Dirac equations the beam optical forms obtained are exact. Approximations necessarily enter only in the step - II of the algorithm, *i.e.,* while integrating the beam optical equation and computing the transfer maps for the quantum averages of the beam observables. As in the classical theory, the approximations arise due to the fact that only the first few terms are retained in the infinite series expansion of the beam optical Hamiltonian. The beam optical Hamiltonian is obtained as a power series in $|\hat{\boldsymbol{\pi}}_\perp/p_0|$ where p_0 is the design (or average) momentum of the beam particles moving predominantly along the optic axis of the system and $\hat{\boldsymbol{\pi}}_\perp$ is the small transverse kinetic momentum. The leading order contribution gives rise to the *paraxial* or the ideal behavior and higher order contributions give rise to the nonlinear or *aberrating* behavior. Both the paraxial and the aberrating behaviors deviate from their classical nature by quantum contributions which are in powers of the de Broglie wavelength of the beam particle ($\lambda_0 = 2\pi\hbar/p_0$). The classical formalism is obtained from the quantum formalism by taking the limit $\lambda_0 \longrightarrow 0$.

3 Formalism of the Dirac particle beam optics

Now we shall see how the above algorithm works for the Dirac particle. Let us consider a monoenergetic beam of Dirac particles particles of mass m, charge q and anomalous magnetic moment μ_a, transported through a magnetic optical element with a straight optic axis characterized by the static potentials $(\phi(\boldsymbol{r}), \boldsymbol{A}(\boldsymbol{r}))$. The beam propagation is governed by the stationary Dirac equation

$$\hat{\mathrm{H}}_D \, |\psi_D\rangle = E \, |\psi_D\rangle \ , \tag{4}$$

where $|\psi_D\rangle$ is the time-independent 4-component Dirac spinor, E is the total energy of the beam particle and the Hamiltonian $\hat{\mathrm{H}}_D$, including the Pauli term, is given by

$$\hat{\mathrm{H}}_D = \beta mc^2 + c\boldsymbol{\alpha} \cdot (-i\hbar\boldsymbol{\nabla} - q\boldsymbol{A}) - \mu_a \beta \boldsymbol{\Sigma} \ \cdot \boldsymbol{B} \, , \tag{5}$$

where the symbols have their usual meanings. [14] To cast (4) in the required beam optical form (1) we multiply $\hat{\mathrm{H}}_D$ (on the left) by α_z/c and rearrange the terms to get

$$i\hbar \frac{\partial}{\partial z} \, |\psi_D\rangle = \hat{\mathcal{H}}_D \, |\psi_D\rangle \ ,$$

$$\hat{\mathcal{H}}_D = -p_0\beta\chi\alpha_z - qA_zI + \alpha_z\boldsymbol{\alpha}_\perp\cdot\hat{\boldsymbol{\pi}}_\perp + (\mu_a/c)\beta\alpha_z\boldsymbol{\Sigma}\cdot\boldsymbol{B}\,, \qquad (6)$$

where χ is a diagonal matrix with elements $(\xi,\xi,-1/\xi,-1/\xi)$ and $\xi = \sqrt{(E+mc^2)/(E-mc^2)}$. Equation (6) is still not in a completely desirable form. So we resort to a further transformation:

$$|\psi_D\rangle \longrightarrow |\psi'\rangle = M\,|\psi_D\rangle\,, \qquad M = \frac{1}{\sqrt{2}}(I+\chi\alpha_z)\,. \qquad (7)$$

Then we obtain

$$i\hbar\frac{\partial}{\partial z}\,|\psi'\rangle = \hat{\mathcal{H}}'\,|\psi'\rangle\,, \quad \hat{\mathcal{H}}' = M\hat{\mathcal{H}}_D M^{-1} = -p_0\beta + \hat{\mathcal{E}} + \hat{\mathcal{O}}\,, \qquad (8)$$

where the nonvanishing matrix elements of the even term $\hat{\mathcal{E}}$ and the odd term $\hat{\mathcal{O}}$ are given by

$$\begin{aligned}
\hat{\mathcal{E}}_{11} &= -qA_z\mathbb{1} - (\mu_a/2c)\left\{\left(\xi+\xi^{-1}\right)\boldsymbol{\sigma}_\perp\cdot\boldsymbol{B}_\perp + \left(\xi-\xi^{-1}\right)\sigma_z B_z\right\}\,,\\
\hat{\mathcal{E}}_{22} &= -qA_z\mathbb{1} - (\mu_a/2c)\left\{\left(\xi+\xi^{-1}\right)\boldsymbol{\sigma}_\perp\cdot\boldsymbol{B}_\perp - \left(\xi-\xi^{-1}\right)\sigma_z B_z\right\}\,,\\
\hat{\mathcal{O}}_{12} &= \xi\left[\boldsymbol{\sigma}_\perp\cdot\hat{\boldsymbol{\pi}}_\perp - (\mu_a/2c)\left\{i\left(\xi-\xi^{-1}\right)\left(B_x\sigma_y - B_y\sigma_x\right)\right.\right.\\
&\qquad\qquad\left.\left. - \left(\xi+\xi^{-1}\right)B_z\mathbb{1}\right\}\right]\,,\\
\hat{\mathcal{O}}_{21} &= -\xi^{-1}\left[\boldsymbol{\sigma}_\perp\cdot\hat{\boldsymbol{\pi}}_\perp + (\mu_a/2c)\left\{i\left(\xi-\xi^{-1}\right)\left(B_x\sigma_y - B_y\sigma_x\right)\right.\right.\\
&\qquad\qquad\left.\left. + \left(\xi+\xi^{-1}\right)B_z\mathbb{1}\right\}\right]\,. \qquad (9)
\end{aligned}$$

The effect of the transformation (7) is to make the lower components of a Dirac spinor corresponding to a quasiparaxial beam moving in the positive z-direction negligible compared to the upper components and thus effectively making the 4-component spinor as a 2-component spinor. Now one may observe the close analogy:

Standard Dirac equation	*Beam optical form*
$mc^2\beta + \hat{\mathcal{E}}_D + \hat{\mathcal{O}}_D$	$-p_0\beta + \hat{\mathcal{E}} + \hat{\mathcal{O}}$
Positive energy	Forward propagation
Nonrelativistic, $c\,\lvert\boldsymbol{\pi}\rvert \ll mc^2$	Paraxial beam, $\lvert\boldsymbol{\pi}_\perp\rvert \ll p_0$
mc^2: Note $i\hbar\frac{\partial\psi}{\partial t} \approx mc^2\psi$	$-p_0$: Note $i\hbar\frac{\partial\psi}{\partial z} \approx -p_0\psi$
Nonrelativistic motion	Paraxial behavior
+ Relativistic corrections	+ Aberration corrections

This completes the step - I of the algorithm. To execute the step - II we proceed as follows.

The above analogy suggests that, as the most systematic way to understand the Dirac Hamiltonian as a nonrelativistic part plus relativistic correction terms is to use the Foldy-Wouthuysen (FW) transformation technique, [14]

we should adopt a similar FW-like approach in the beam optical case to understand the beam optical Hamiltonian as a paraxial part plus nonparaxial correction terms. This leads to a procedure to obtain the paraxial behavior accompanied by a systematic method to compute the aberrations to *all* orders in powers of the expansion parameter $1/p_0$. To leading order, the first FW-like transformation is

$$\left|\psi^{(1)}\right\rangle = \exp\left(-\beta\hat{\mathcal{O}}/2p_0\right)|\psi'\rangle \ . \tag{10}$$

Then

$$i\hbar\frac{\partial}{\partial z}\left|\psi^{(1)}\right\rangle = \hat{\mathcal{H}}^{(1)}\left|\psi^{(1)}\right\rangle \ , \qquad \hat{\mathcal{H}}^{(1)} = -p_0\beta + \hat{\mathcal{E}}^{(1)} + \hat{\mathcal{O}}^{(1)} \ ,$$
$$\hat{\mathcal{E}}^{(1)} = \hat{\mathcal{E}} - \frac{1}{2p_0}\beta\hat{\mathcal{O}}^2 + \cdots, \quad \hat{\mathcal{O}}^{(1)} = -\frac{1}{2p_0}\beta\left\{\left[\hat{\mathcal{O}},\hat{\mathcal{E}}\right] + i\hbar\frac{\partial}{\partial z}\hat{\mathcal{O}}\right\} + \cdots \tag{11}$$

It is to be noted that the transformation (10) keeps the upper components of the beam optical wavefunction large compared to its lower components. One can proceed with further FW-like transformations and stop at any desired stage. Let us denote the 2-component spinor comprising the upper components of the final 4-component spinor obtained in the above process as $|\tilde{\psi}\rangle$.

Up to now, all the observables, the field components, time etc., have been defined in the laboratory frame. The covariant description of the spin of the Dirac particle has the simplest operator representation in the rest frame of the particle. Thus, in accelerator physics the spin is defined in the rest frame of the particle. So we make a further transformation which takes us from the beam optical form to the *accelerator optical form*

$$\left|\psi^{(A)}\right\rangle = \exp\left\{-\frac{i}{2p_0}\left(\hat{\pi}_x\sigma_y - \hat{\pi}_y\sigma_x\right)\right\}\left|\tilde{\psi}\right\rangle \ . \tag{12}$$

Thus, up to the paraxial approximation the accelerator optical Hamiltonian [10,11] is

$$i\hbar\frac{\partial}{\partial z}\left|\psi^{(A)}\right\rangle = \hat{H}^{(A)}\left|\psi^{(A)}\right\rangle \ ,$$
$$\hat{H}^{(A)} \approx \left(-p_0 - qA_z + \frac{1}{2p_0}\hat{\pi}_\perp^2\right) + \frac{\gamma m}{p_0}\underline{\boldsymbol{\Omega}}_s\cdot\boldsymbol{S} \, , \tag{13}$$

where $\underline{\boldsymbol{\Omega}}_s = -\frac{1}{\gamma m}\left\{q\boldsymbol{B} + \epsilon\left(\boldsymbol{B}_\parallel + \gamma\boldsymbol{B}_\perp\right)\right\}$, $\gamma = E/mc^2$ and $\epsilon = 2m\mu_a/\hbar$.

4 An example of application: Magnetic quadrupole lens

Let an ideal normal magnetic quadrupole of length ℓ, characterized by the field $\boldsymbol{B} = (-Gy, -Gx, 0)$, be situated between the transverse planes at $z = z_{\rm in}$

and $z = z_{\rm out} = z_{\rm in} + \ell$. The associated vector potential can be taken to be $\boldsymbol{A} = \left(0, 0, \frac{1}{2}G\left(x^2 - y^2\right)\right)$ with G as constant inside the lens and zero outside. The accelerator optical Hamiltonian [10] is

$$\hat{H}(z) = \begin{cases} \hat{H}_F = -p_0 + \frac{1}{2p_0}\hat{p}_\perp^2\,, \quad \text{for} \;\; z < z_{\rm in} \;\; \text{and} \;\; z > z_{\rm out}\,, \\ \hat{H}_L(z) = -p_0 + \frac{1}{2p_0}\hat{p}_\perp^2 - \frac{1}{2}qG\left(x^2 - y^2\right) + \frac{\eta p_0}{\ell}\left(y\sigma_x + x\sigma_y\right)\,, \\ \qquad\qquad \text{for} \;\; z_{\rm in} \le z \le z_{\rm out}\,, \quad \text{with} \;\; \eta = (q + \gamma\epsilon)G\ell\hbar/2p_0^2\,. \end{cases} \tag{14}$$

The subscripts F and L indicate the field-free and the lens regions respectively.

Best way to compute the z-evolution operator $\hat{U}$ is *via* the interaction picture, used in the Lie algebraic formulation [12] of classical beam optics. Using the transfer operator thus derived [10] we get the transfer maps for the averages of the transverse phase-space components: with the subscripts *in* and *out* standing for $(z_{\rm in})$ and $(z_{\rm out})$, respectively,

$$\begin{pmatrix} \langle x\rangle \\ \langle\hat{p}_x\rangle/p_0 \\ \langle y\rangle \\ \langle\hat{p}_y\rangle/p_0 \end{pmatrix}_{\rm out} \approx T_Q \left(\begin{pmatrix} \langle x\rangle \\ \langle\hat{p}_x\rangle/p_0 \\ \langle y\rangle \\ \langle\hat{p}_y\rangle/p_0 \end{pmatrix} + \eta \begin{pmatrix} \left(\frac{\cosh\left(\sqrt{K}\,\ell\right)-1}{K\ell}\right)\langle\sigma_y\rangle \\ -\left(\frac{\sinh\left(\sqrt{K}\,\ell\right)}{\sqrt{K}\,\ell}\right)\langle\sigma_y\rangle \\ -\left(\frac{\cos\left(\sqrt{K}\,\ell\right)-1}{K\ell}\right)\langle\sigma_x\rangle \\ -\left(\frac{\sin\left(\sqrt{K}\,\ell\right)}{\sqrt{K}\,\ell}\right)\langle\sigma_x\rangle \end{pmatrix} \right)_{\rm in} ,$$

$$T_Q = M_> M_Q M_<\,, \qquad M_{\substack{<\\>}} = \begin{pmatrix} 1 & \Delta z_{\substack{<\\>}} & 0 & 0 \\ 0 & 1 & 0 & 0 \\ 0 & 0 & 1 & \Delta z_{\substack{<\\>}} \\ 0 & 0 & 0 & 1 \end{pmatrix}\,, \tag{15}$$

$$M_Q = \begin{pmatrix} \cosh(\sqrt{K}\ell) & \frac{1}{\sqrt{K}}\sinh(\sqrt{K}\ell) & 0 & 0 \\ \sqrt{K}\sinh(\sqrt{K}\ell) & \cosh(\sqrt{K}\ell) & 0 & 0 \\ 0 & 0 & \cos(\sqrt{K}\ell) & \frac{1}{\sqrt{K}}\sin(\sqrt{K}\ell) \\ 0 & 0 & -\sqrt{K}\sin(\sqrt{K}\ell) & \cos(\sqrt{K}\ell) \end{pmatrix}\,.$$

Thus we have got a fully quantum mechanical derivation of the combined effect of the focusing action of the quadrupole lens (note the traditional transfer matrices) and the Stern-Gerlach force. It may be noted that the quantum formalism of spinor beam optics supports, *in principle*, the idea of a Stern-Gerlach spin-splitter device to produce polarized beams. [15] The transfer map across the quadrupole lens for the spin components computed using the above accelerator optical Hamiltonian describes the well known Thomas-Bargmann-Michel-Telegdi spin evolution. [10]

5 Concluding remarks

In fine, we have seen how one can obtain the formalism of quantum beam optics for any particle, starting *ab initio* from the relevant basic quantum equation, at the single-particle level. A two-step algorithm for this purpose has been suggested. Using the general principle, the construction of a spinor theory of accelerator optics, starting from the Dirac equation and taking into account the anomalous magnetic moment, has been demonstrated. As an example of application of the resulting formalism the normal magnetic quadrupole lens has been discussed. In the classical limit the quantum formalism leads to the Lie algebraic formalism of charged-particle beam optics.

To get a formalism taking into account the multiparticle effects, particularly for the intense beams, it should be worthwhile to be guided by the quantum-*like* approaches to the particle beam transport: Thermal Wave Model [16] and Stochastic Collective Dynamical Model [17]. Recently the quantum-*like* approach has been applied to construct a *Diffraction Model* for the beam halo. [18] This model provides numerical estimates for the beam losses. In this context, another useful approach could be to use the Wigner phase-space distribution functions. Heinemann and Barber [19] have initiated the derivation of such a formalism for the Dirac particle beam physics starting from the original work of Derbenev and Kondratenko [20] who used the FW technique to get their Hamiltonian for radiation calculations.

The present study is confined to systems with straight optic axis. An extension to the curved optic axis systems should be done. This would involve the subtlities of quantization in curvilinear coordinates. Then there are the well known questions related to the position operator in the relativistic quantum theory. Also, there are doubts about the exact form of the Stern-Gerlach force for a relativistic particle. [21] To address such questions from the point of view of experiments using particle beams the right platform would be the formalism of quantum beam optics.

Acknowledgments

I am very grateful to Prof. R. Jagannathan, for all my training in the exciting field of *quantum theory of charged-particle beam optics*. I am thankful Prof. M. Pusterla for kind encouragement. It is a pleasure to thank the Organizing Committee of QABP2K and Università di Salerno, for providing full financial support for my travel and stay to participate in QABP2K.

References

1. See, *e.g.*, the following and references therein: *Handbook of Accelerator Physics and Engineering*, eds. A. W. Chao and M. Tigner (World Scientific, Singapore, 1999) (Hereafter referred to as *HAPE*); *Quantum Aspects of Beam Physics*, ed. P. Chen (World Scientific, Singapore, 1999) (Hereafter referred to as *QABP-I*); *Proceedings of this Workshop* (Hereafter referred to as *QABP-II*).
2. P. Chen, *ICFA Beam Dynamics Newsletter* **12**, 46 (1996); P. Chen, in *QABP-I*.
3. S. Heifets and Y. T. Yan, in *QABP-I*
4. C. T. Hill, *e-print*: hep-ph/0002230, and in *QABP-II*.
5. See also M. Venturini, in *QABP-II*.
6. See *QABP-I* and *QABP-II*.
7. For detailed references see the third volume of the three-volume encyclopaedic text book: P. W. Hawkes and E. Kasper, *Principles of Electron Optics* Vol. 3: *Wave Optics* (Academic Press, San Diego, 1994).
8. R. Jagannathan, R. Simon, E. C. G. Sudarshan and N. Mukunda, *Phys. Lett. A* **134**, 457 (1989); R. Jagannathan, *Phys. Rev. A* **42**, 6674 (1990).
9. S. A. Khan and R. Jagannathan, *Phys. Rev. E* **51**, 2510 (1995); R. Jagannathan and S. A. Khan, *Advances in Imaging and Electron Physics*, **97**, ed. P. W. Hawkes (Academic Press, San Diego) 257 (1996); S. A. Khan, *Quantum Theory of Charged-Particle Beam Optics*, Ph.D. Thesis, University of Madras, (1997).
10. M. Conte, R. Jagannathan, S. A. Khan and M. Pusterla, *Part. Accel.* **56**, 99 (1996).
11. R. Jagannathan and S. A. Khan *ICFA Beam Dynamics Newsletter* **13**, 21 (1997); M. Pusterla, in *QABP-I*; R. Jagannathan, in *QABP-I*; R. Jaganathan, in *QABP-II*. S. A. Khan, in *QABP-I*.
12. See, *e.g.*, the following and references therein: A. J. Dragt, in *QABP-II*; A. J. Dragt, *Lie Methods for Nonlinear Dynamics with Applications to Accelerator Physics*, University of Maryland Physics Department Report (2000); A. J. Dragt, *Lie Algebraic Methods for Ray and Wave optics*, University of Maryland Physics Department Report (1998); E. Forest, *Beam Dynamics: A New Attitude and Framework* (Harwood Academic, 1998); A. J. Dragt, F. Neri, G. Rangarajan, D. R. Douglas, L. M. Healy, and R. D. Ryne, *Ann. Rev. Nucl. Part. Sci.* **38**, 455 (1988); E. Forest and K. Hirata, *A Contemporary Guide to Beam Dynamics*, Technical Report No. 92-12, KEK; Articles of J. Irwin and A. J. Dragt, A. J. Dragt, M. Berz, H. Yoshida, and Y. T. Yan in *HAPE*.

13. K. Yokoya in *HAPE*; Yu. I. Eidelman and V. Ye. Yakimenko, *Part. Accel.* **45**, 17 (1994), **50**, 261 (1995);
14. See, *e.g.*, J. D. Bjorken and S. D. Drell, *Relativistic Quantum Mechanics* (McGraw-Hill, 1964).
15. M. Conte and M. Pusterla, *Il Nuovo Cimento A*, **103**, 1087 (1990); M. Conte, Y. Onel, A. Penzo, A. Pisent, M. Pusterla and R. Rossmanith, *The spin-splitter concept*, Internal Report : INFN/TC-93/04; M. Conte, A. Penzo and M. Pusterla, *Il Nuovo Cimento A* **108**, 127 (1995); M. Pusterla, in *QABP-I*, and references therein.
16. See R. Fedele and G. Miele, *Il Nuovo Cimento* D **13**, 1527 (1991); R. Fedele, F. Gallucio, V. I. Man'ko and G. Miele, *Phys. Lett.* A **209**, 263 (1995); eds. R. Fedele and P. K. Shukla *Quantum-Like Models and Coherent Effects*, Proc. of the 27th Workshop of the INFN Eloisatron Project, Erice, Italy (World Scientific, Singapore, 1995); R. Fedele and V. I. Man'ko, in *QABP-I*; R. Fedele, in *QABP-II*; M. A. Man'ko, in *QABP-II*.
17. See the following and references therein: N. Cufaro Petroni, S. De Martino, S. De Siena, and F. Illuminati, in *QABP-I*; N. Cufaro Petroni, S. De Martino, S. De Siena, and F. Illuminati, *Stochastic collective dynamics of charged-particle beams in the stability regime* (to appear in *Phys. Rev. E*); N. Cufaro Petroni, S. De Martino, S. De Siena, and F. Illuminati in *QABP-II*.
18. S. A. Khan and M. Pusterla, *Euro. Phys. J. A* **7**, 583 (2000); M. Pusterla, in *QABP-II*.
19. K. Heinemann and D. P. Barber, in *QABP-I*.
20. Ya. S. Derbenev and A. M. Kondratenko, *Sov. Phys. JETP* **37**, 968 (1973).
21. K. Heinemann, *e-print*: physics/9611001; J. Anandan, *Nature* **387**, 558 (1997); M. Chaichian, R. G. Felipe and D. L. Martinez, *Phys. Lett.* A **236**, 188 (1997); J. P. Costella and B. H. J. McKellar, *Int. J. Mod. Phys.* A **9**, 461 (1994); S. A. Khan and M. Pusterla, *e-print*: physics/9910034; and references therein.

LOCALIZED COHERENT STRUCTURES AND PATTERNS FORMATION IN COLLECTIVE MODELS OF BEAM MOTION

A. FEDOROVA, M. ZEITLIN
IPME, RAS, St. Petersburg, V.O. Bolshoj pr., 61, 199178, Russia
e-mail: zeitlin@math.ipme.ru
http://www.ipme.ru/zeitlin.html; http://www.ipme.nw.ru/zeitlin.html

We present applications of variational – wavelet approach to three different models of nonlinear beam motions with underlying collective behaviour: Vlasov-Maxwell-Poisson systems, envelope dynamics, beam-beam model. We have the representation for dynamical variables as a multiresolution (multiscales) expansion via high-localized nonlinear eigenmodes in the base of compactly supported wavelet bases. Numerical modelling demonstrates formation of coherent structures and stable patterns.

1 Introduction

In this paper we consider the applications of a new numerical-analytical technique which is based on the methods of local nonlinear harmonic analysis or wavelet analysis to three nonlinear beam/accelerator physics problems which can be characterized by collective type behaviour: some forms of Vlasov-Maxwell-Poisson equations[1], RMS envelope dynamics[2], the model of beam-beam interactions[3]. Such approach may be useful in all models in which it is possible and reasonable to reduce all complicated problems related with statistical distributions to the problems described by systems of nonlinear ordinary/partial differential equations with or without some (functional)constraints. Wavelet analysis is a relatively novel set of mathematical methods, which gives us the possibility to work with well-localized bases in functional spaces and gives the maximum sparse forms for the general type of operators (differential, integral, pseudodifferential) in such bases. Our approach is based on the variational-wavelet approach from [4]-[14], which allows us to consider polynomial and rational type of nonlinearities. The solution has the following multiscale/multiresolution decomposition via nonlinear high-localized eigenmodes

$$u(t,x) = \sum_{(i,j)\in Z^2} U^i(x)V^j(t), \tag{1}$$

$$V^k(t) = V_N^{k,slow}(t) + \sum_{i\geq N} V_i^k(\omega_i^1 t), \quad \omega_i^1 \sim 2^i \tag{2}$$

$$U^k(x) = U_M^{k,slow}(x) + \sum_{j \geq M} U_j^k(\omega_j^2 x), \quad \omega_j^2 \sim 2^j, \tag{3}$$

which corresponds to the full multiresolution expansion in all underlying time/space scales (x are the generalized space coordinates or phase space coordinates, t is time coordinate). Formula (1) gives us expansion into the slow part $u_{N,M}^{slow}$ and fast oscillating parts for arbitrary N, M. So, we may move from coarse scales of resolution to the finest one for obtaining more detailed information about our dynamical process. The first terms in the RHS of formulae (1)-(3) correspond on the global level of function space decomposition to resolution space and the second ones to detail space. In this way we give contribution to our full solution from each scale of resolution or each time/space scale or from each nonlinear eigenmode (Fig.1). The same is correct for the contribution to power spectral density (energy spectrum): we can take into account contributions from each level/scale of resolution. In all these models numerical modelling demonstrates the appearence of coherent high-localized structures and stable patterns formation. Starting in part 2 from Vlasov-Maxwell-Poisson equations, root-mean-square (RMS) envelope dynamics and beam-beam interaction model we consider in part 3 the approach based on variational-wavelet formulation. We give explicit representation for all dynamical variables in the base of compactly supported wavelets or nonlinear eigenmodes. Our solutions are parametrized by solutions of a number of reduced algebraical problems one from which is nonlinear with the same degree of nonlinearity and the rest are the linear problems which correspond to particular method of calculation of scalar products of functions from wavelet bases and their derivatives. In part 4 we consider numerical modelling based on our analytical approach.

2 Collective models

2.1 Vlasov-Maxwell-Poisson Equations

Analysis based on the non-linear Vlasov-Maxwell-Poisson equations leads to more clear understanding of the collective effects and nonlinear beam dynamics of high intensity beam propagation in periodic-focusing and uniform-focusing transport systems. We consider the following form of equations ([1],[2] for setup and designation):

$$\Big\{ \frac{\partial}{\partial s} + p_x \frac{\partial}{\partial x} + p_y \frac{\partial}{\partial y} - \Big[k_x(s)x + \frac{\partial \psi}{\partial x} \Big] \frac{\partial}{\partial p_x} - \Big[k_y(s)y + \frac{\partial \psi}{\partial y} \Big] \frac{\partial}{\partial p_y} \Big\} f_b(x, y, p_x, p_y, s) = 0, \tag{4}$$

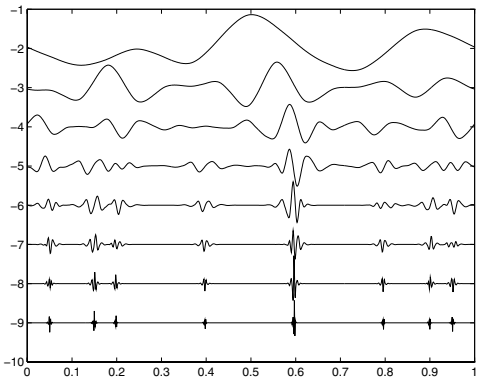

Figure 1. Multiscale/eigenmode decomposition.

$$\Big(\frac{\partial^2}{\partial x^2}+\frac{\partial^2}{\partial y^2}\Big)\psi = -\frac{2\pi K_b}{N_b}\int \mathrm{d}p_x \mathrm{d}p_y f_b, \tag{5}$$

$$\int \mathrm{d}x\mathrm{d}y\mathrm{d}p_x\mathrm{d}p_y f_b = N_b \tag{6}$$

The corresponding Hamiltonian for transverse single-particle motion is given by

$$H(x,y,p_x,p_y,s) = \frac{1}{2}(p_x^2+p_y^2)+\frac{1}{2}[k_x(s)x^2 \tag{7}$$
$$+k_y(s)y^2] + H_1(x,y,p_x,p_y,s)+\psi(x,y,s),$$

where H_1 is nonlinear (polynomial/rational) part of the full Hamiltonian. In case of Vlasov-Maxwell-Poisson system we may transform (4) into invariant form

$$\frac{\partial f_b}{\partial s}+[f,H]=0. \tag{8}$$

2.2 RMS Equations

We consider an approach based on the second moments of the distribution functions for the calculation of evolution of RMS envelope of a beam. The RMS envelope equations are the most useful for analysis of the beam self–forces (space–charge) effects and also allow to consider both transverse and longitudinal dynamics of space-charge-dominated relativistic high–brightness

axisymmetric/asymmetric beams, which under short laser pulse–driven radio-frequency photoinjectors have fast transition from nonrelativistic to relativistic regime [2]. Analysis of halo growth in beams, appeared as result of bunch oscillations in the particle-core model, also are based on three-dimensional envelope equations [2]. We can consider the different forms of RMS envelope equations, which are not more than nonlinear differential equations with rational nonlinearities and variable coefficients from the formal point of view. Let $f(x_1, x_2)$ be the distribution function which gives full information about noninteracting ensemble of beam particles regarding to trace space or transverse phase coordinates (x_1, x_2). Then we may extract the first nontrivial effects of collective dynamics from the second moments

$$\sigma^2_{x_i x_j} = < x_i x_j >= \int\int x_i x_j f(x_i, x_j) \mathrm{d}x_i \mathrm{d}x_j \tag{9}$$

RMS emittance ellipse is given by $\varepsilon^2_{x,rms} =< x_i^2 >< x_j^2 > - < x_i x_j >^2$ $(i \neq j)$. Expressions for twiss parameters are also based on the second moments. We will consider the following particular cases of RMS envelope equations, which describe evolution of the moments (9) ([2] for full designation): for asymmetric beams we have the system of two envelope equations of the second order for σ_{x_1} and σ_{x_2}:

$$\sigma^{''}_{x_1} + \sigma^{'}_{x_1}\frac{\gamma'}{\gamma} + \Omega^2_{x_1}\left(\frac{\gamma'}{\gamma}\right)^2 \sigma_{x_1} = I/(I_0(\sigma_{x_1} + \sigma_{x_2})\gamma^3) + \varepsilon^2_{nx_1}/\sigma^3_{x_1}\gamma^2, \tag{10}$$

$$\sigma^{''}_{x_2} + \sigma^{'}_{x_2}\frac{\gamma'}{\gamma} + \Omega^2_{x_2}\left(\frac{\gamma'}{\gamma}\right)^2 \sigma_{x_2} = I/(I_0(\sigma_{x_1} + \sigma_{x_2})\gamma^3) + \varepsilon^2_{nx_2}/\sigma^3_{x_2}\gamma^2$$

The envelope equation for an axisymmetric beam is a particular case of preceding equations. Also we have related Lawson's equation for evolution of the rms envelope in the paraxial limit, which governs evolution of cylindrical symmetric envelope under external linear focusing channel of strenght K_r:

$$\sigma^{''} + \sigma^{'}\left(\frac{\gamma'}{\beta^2\gamma}\right) + K_r\sigma = \frac{k_s}{\sigma\beta^3\gamma^3} + \frac{\varepsilon_n^2}{\sigma^3\beta^2\gamma^2}, \tag{11}$$

where $K_r \equiv -F_r/r\beta^2\gamma mc^2, \quad \beta \equiv \nu_b/c = \sqrt{1-\gamma^{-2}}$. According [2] we have the following form for envelope equations in the model of halo formation by bunch oscillations:

$$\begin{aligned} \ddot{X} + k_x^2(s)X - \frac{3K}{8}\frac{\xi_x}{YZ} - \frac{\varepsilon_x^2}{X^3} = 0, \\ \ddot{Y} + k_y^2(s)Y - \frac{3K}{8}\frac{\xi_y}{XZ} - \frac{\varepsilon_y^2}{Y^3} = 0, \end{aligned} \tag{12}$$

$$\ddot{Z} + k_z^2(s)Z - \gamma^2 \frac{3K}{8} \frac{\xi_z}{XY} - \frac{\varepsilon_z^2}{Z^3} = 0,$$

where X(s), Y(s), Z(s) are bunch envelopes, $\xi_x, \xi_y, \xi_z = F(X, Y, Z)$.

After transformations to Cauchy form we can see that all these equations from the formal point of view are not more than ordinary differential equations with rational nonlinearities and variable coefficients Also, we may consider regimes in which γ, γ' are not fixed functions/constants but satisfy some additional differential constraints/equations, but this case does not change our general approach of the next part.

2.3 Beam-beam modelling

In A. Chao e.a. model [3] for simulation of beam-beam interaction the initial collective description by some sort of equation for distribution function $f(s, x, p)$

$$\frac{\partial f}{\partial s} + p\frac{\partial f}{\partial x} - (k(s)x - F(x, s))\frac{\partial f}{\partial p} = 0 \tag{13}$$

is reduced to Fockker-Planck (FP) equation on the first stage and to very nontrivial dynamical system with complex behaviour,

$$\begin{aligned} &\frac{\mathrm{d}^2\sigma_k}{\mathrm{d}s^2} + \Gamma_k \frac{\mathrm{d}\sigma_k}{\mathrm{d}s} + F_k\sigma_k = \frac{1}{\beta_k^2 a_k^2 \sigma_k^3} \\ &\frac{\mathrm{d}a_n}{\mathrm{d}s} = \Gamma_k a_k (1 - a_k^2\sigma_k^2), \end{aligned} \tag{14}$$

which solution gives the parameters of enveloping gaussian anzatz for solution of FP equation, on the second stage. From the formal point of view equations (14) are particular case of system (12).

3 Rational Dynamics

After some anzatzes [15] our problems may be formulated as the systems of ordinary differential equations (cases 2.2 and 2.3 (system (14)) above)

$$\begin{aligned} &Q_i(x)\frac{\mathrm{d}x_i}{\mathrm{d}t} = P_i(x, t), \quad x = (x_1, ..., x_n), \\ &i = 1, ..., n, \quad \max_i deg\ P_i = p, \quad \max_i deg\ Q_i = q \end{aligned} \tag{15}$$

or a set of such systems (cases 2.1, 2.3 (full equation (13)) above) corresponding to each independent coordinate in phase space. They have the fixed

initial(or boundary) conditions $x_i(0)$, where P_i, Q_i are not more than polynomial functions of dynamical variables x_j and have arbitrary dependence of time. Because of time dilation we can consider only next time interval: $0 \leq t \leq 1$. Let us consider a set of functions

$$\Phi_i(t) = x_i \frac{\mathrm{d}}{\mathrm{d}t}(Q_i y_i) + P_i y_i \tag{16}$$

and a set of functionals

$$F_i(x) = \int_0^1 \Phi_i(t)dt - Q_i x_i y_i \mid_0^1, \tag{17}$$

where $y_i(t)$ $(y_i(0) = 0)$ are dual (variational) variables. It is obvious that the initial system and the system

$$F_i(x) = 0 \tag{18}$$

are equivalent. Of course, we consider such $Q_i(x)$ which do not lead to the singular problem with $Q_i(x)$, when $t = 0$ or $t = 1$, i.e. $Q_i(x(0)), Q_i(x(1)) \neq \infty$.

Now we consider formal expansions for x_i, y_i:

$$x_i(t) = x_i(0) + \sum_k \lambda_i^k \varphi_k(t) \quad y_j(t) = \sum_r \eta_j^r \varphi_r(t), \tag{19}$$

where $\varphi_k(t)$ are useful basis functions of some functional space (L^2, L^p, Sobolev, etc) corresponding to concrete problem and because of initial conditions we need only $\varphi_k(0) = 0$, $r = 1, ..., N, \quad i = 1, ..., n$,

$$\lambda = \{\lambda_i\} = \{\lambda_i^r\} = (\lambda_i^1, \lambda_i^2, ..., \lambda_i^N), \tag{20}$$

where the lower index i corresponds to expansion of dynamical variable with index i, i.e. x_i and the upper index r corresponds to the numbers of terms in the expansion of dynamical variables in the formal series. Then we put (19) into the functional equations (18) and as result we have the following reduced algebraical system of equations on the set of unknown coefficients λ_i^k of expansions (19):

$$L(Q_{ij}, \lambda, \alpha_I) = M(P_{ij}, \lambda, \beta_J), \tag{21}$$

where operators L and M are algebraization of RHS and LHS of initial problem (15), where λ (20) are unknowns of reduced system of algebraical equations (RSAE)(21).

Q_{ij} are coefficients (with possible time dependence) of LHS of initial system of differential equations (15) and as consequence are coefficients of RSAE.

P_{ij} are coefficients (with possible time dependence) of RHS of initial system of differential equations (15) and as consequence are coefficients of RSAE. $I = (i_1, ..., i_{q+2})$, $J = (j_1, ..., j_{p+1})$ are multiindexes, by which are labelled α_I and β_I are other coefficients of RSAE (21):

$$\beta_J = \{\beta_{j_1 \dots j_{p+1}}\} = \int \prod_{1 \le j_k \le p+1} \varphi_{j_k}, \tag{22}$$

where p is the degree of polinomial operator P (15)

$$\alpha_I = \{\alpha_{i_1} \dots \alpha_{i_{q+2}}\} = \sum_{i_1, \dots, i_{q+2}} \int \varphi_{i_1} \dots \dot{\varphi_{i_s}} \dots \varphi_{i_{q+2}}, \tag{23}$$

where q is the degree of polynomial operator Q (15), $i_\ell = (1, ..., q+2)$, $\dot{\varphi_{i_s}} = \mathrm{d}\varphi_{i_s}/\mathrm{d}t$.

Now, when we solve RSAE (21) and determine unknown coefficients from formal expansion (19) we therefore obtain the solution of our initial problem. It should be noted if we consider only truncated expansion (19) with N terms then we have from (21) the system of $N \times n$ algebraical equations with degree $\ell = max\{p, q\}$ and the degree of this algebraical system coincides with degree of initial differential system. So, we have the solution of the initial nonlinear (rational) problem in the form

$$x_i(t) = x_i(0) + \sum_{k=1}^{N} \lambda_i^k X_k(t), \tag{24}$$

where coefficients λ_i^k are roots of the corresponding reduced algebraical (polynomial) problem RSAE (21). Consequently, we have a parametrization of solution of initial problem by solution of reduced algebraical problem (21). The first main problem is a problem of computations of coefficients α_I (23), β_J (22) of reduced algebraical system. These problems may be explicitly solved in wavelet approach [4]-[6]. The obtained solutions are given in the form (24), where $X_k(t)$ are basis functions and λ_k^i are roots of reduced system of equations. In our case $X_k(t)$ are obtained via multiresolution expansions and represented by compactly supported wavelets and λ_k^i are the roots of corresponding general polynomial system (21). Because affine group of translation and dilations is inside the approach, this method resembles the action of a microscope. We have contribution to final result from each scale of resolution from the whole infinite scale of spaces. More exactly, the closed subspace $V_j (j \in \mathbf{Z})$ corresponds to level j of resolution, or to scale j. We consider a multiresolution analysis of $L^2(\mathbf{R}^n)$ (of course, we may consider any different

functional space) which is a sequence of increasing closed subspaces V_j:

$$...V_{-2} \subset V_{-1} \subset V_0 \subset V_1 \subset V_2 \subset ...$$

satisfying the following properties: let W_j be the orthonormal complement of V_j with respect to $V_{j+1} : V_{j+1} = V_j \bigoplus W_j$, then

$$L^2(\mathbf{R}) = \overline{V_0 \bigoplus_{j=0}^{\infty} W_j}, \tag{25}$$

This functional space decomposition corresponds to exact nonlinear (eigen)mode decompositions (2),(3). It should be noted that such representations give the best possible localization properties in the corresponding (phase)space/time coordinates. In contrast with different approaches formulae (1)-(3) do not use perturbation technique or linearization procedures and represent dynamics via generalized nonlinear localized eigenmodes expansion. So, by using wavelet bases with their good (phase)space/time localization properties we can construct high-localized coherent structures in spatially-extended stochastic systems with collective behaviour.

4 Modelling

Resulting multiresolution/multiscale representations for solutions of equations from part 2 in the high-localized bases/eigenmodes are demonstrated on Fig. 2–Fig. 7. This modelling demonstrates the appearence of stable patterns formation from high-localized coherent structures. On Fig. 2, Fig. 3 we present contribution to the full expansion (1)-(3) from level 1 and level 4 of decomposition (25). Figures 4, 5 show the representations for full solutions, constructed from the first 6 eigenmodes (6 levels in formula (25)). Figures 6, 7 show stable patterns formation based on high-localized coherent structures.

5 Acknowledgments

We would like to thank Professor Pisin Chen, Dr. Stefania Petracca and her team for nice hospitality, help and support during Capri ICFA Workshop.

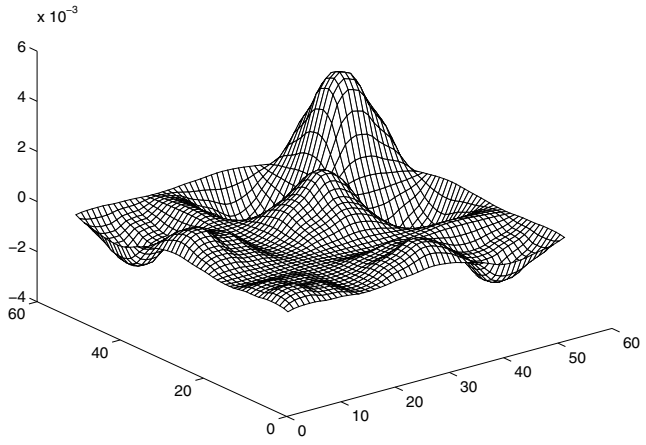

Figure 2. Eigenmode of level 1

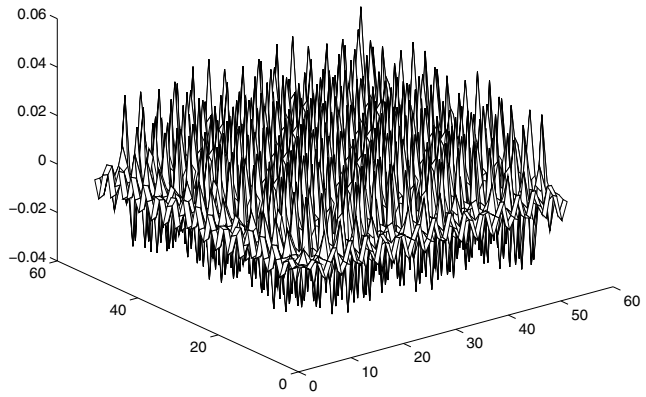

Figure 3. Eigenmode of level 3

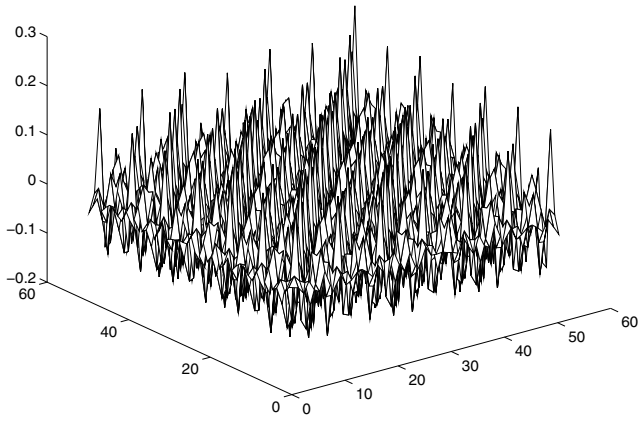

Figure 4. Appearence of coherent structure

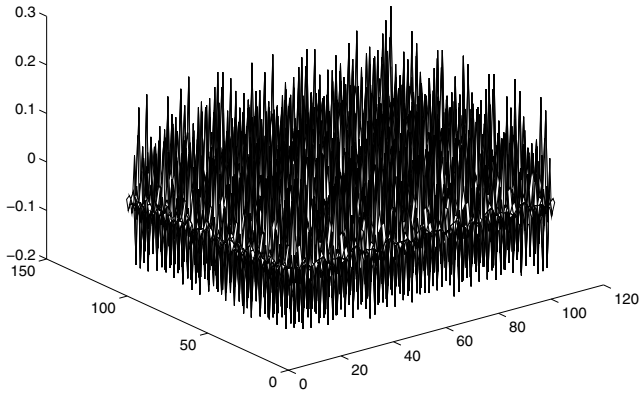

Figure 5. Six-eigenmodes decomposition

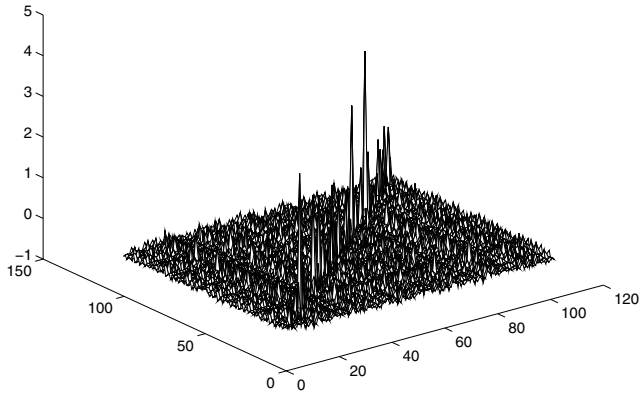

Figure 6. Stable pattern 1

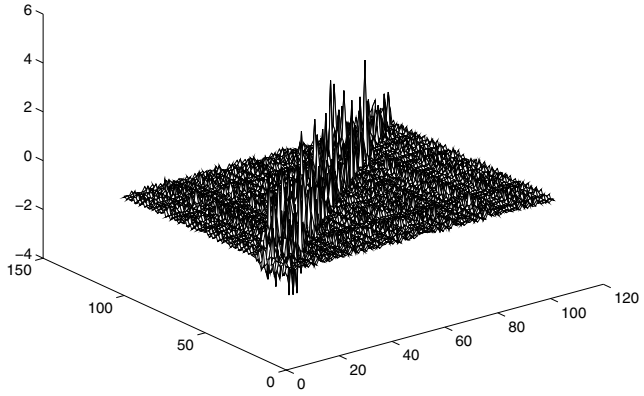

Figure 7. Stable pattern 2

References

1. R. Davidson, H. Qin, P. Channel, PRSTAB, 2, 074401, 1999
2. J.B. Rosenzweig, Fundamentals of Beam Physics, e-version: http://www.physics.ucla.edu/class/99F/250Rosenzweig/notes/ L. Serafini and J.B. Rosenzweig, *Phys. Rev. E* **55**, 7565, 1997. C. Allen, T. Wangler, papers in UCLA ICFA Proc., World Sci., 2000.
3. A. Chao, e.a., Los Alamos preprint, physics/0010055
4. A.N. Fedorova and M.G. Zeitlin, *Math. and Comp. in Simulation*, **46**, 527 (1998).
5. A.N. Fedorova and M.G. Zeitlin, 'Wavelet Approach to Mechanical Problems. Symplectic Group, Symplectic Topology and Symplectic Scales', *New Applications of Nonlinear and Chaotic Dynamics in Mechanics*, 31, 101 (Kluwer, 1998).
6. A.N. Fedorova and M.G. Zeitlin, **CP405**, 87 (American Institute of Physics, 1997). Los Alamos preprint, physics/9710035.
7. A.N. Fedorova, M.G. Zeitlin and Z. Parsa, Proc. PAC97 **2**, 1502, 1505, 1508 (IEEE, 1998).
8. A.N. Fedorova, M.G. Zeitlin and Z. Parsa, Proc. EPAC98, 930, 933 (Institute of Physics, 1998).
9. A.N. Fedorova, M.G. Zeitlin and Z. Parsa, **CP468**, 48 (American Institute of Physics, 1999). Los Alamos preprint, physics/990262.
10. A.N. Fedorova, M.G. Zeitlin and Z. Parsa, **CP468**, 69 (American Institute of Physics, 1999). Los Alamos preprint, physics/990263.
11. A.N. Fedorova and M.G. Zeitlin, Proc. PAC99, 1614, 1617, 1620, 2900, 2903, 2906, 2909, 2912 (IEEE/APS, New York, 1999).
    Los Alamos preprints: physics/9904039, 9904040, 9904041, 9904042, 9904043, 9904045, 9904046, 9904047.
12. A.N. Fedorova and M.G. Zeitlin, Proc. UCLA ICFA Workshop, in press, Los Alamos preprint: physics/0003095.
13. A.N. Fedorova and M.G. Zeitlin, Proc. EPAC00, 415, 872, 1101, 1190, 1339, 2325.
    Los Alamos preprints: physics/0008045, 0008046, 0008047, 0008048, 0008049, 0008050
14. A.N. Fedorova, M.G. Zeitlin, Proc. LINAC00, 2 papers in press, Los Alamos preprints: physics/0008043, 0008200
15. A.N. Fedorova, M.G. Zeitlin, this Volume and in press.

QUASICLASSICAL CALCULATIONS FOR WIGNER FUNCTIONS VIA MULTIRESOLUTION

A. FEDOROVA, M. ZEITLIN

IPME, RAS, V.O. Bolshoj pr., 61, 199178, St. Petersburg, Russia
E-mail: zeitlin@math.ipme.ru
http://www.ipme.ru/zeitlin.html; http://www.ipme.nw.ru/zeitlin.html

We present application of variational–wavelet analysis to numerical/analytical calculations of Wigner functions in (nonlinear) quasiclassical beam dynamics problems. (Naive) deformation quantization and multiresolution representations are the key points..

1 Introduction

In this paper we consider some starting points in the applications of a new numerical-analytical technique which is based on local nonlinear harmonic analysis (wavelet analysis, generalized coherent states analysis) to the quantum/quasiclassical (nonlinear) beam/accelerator physics calculations. The reason for this treatment is that recently a number of problems appeared in which one needs take into account quantum properties of particles/beams. Our starting point is the general point of view of deformation quantization approach at least on naive Moyal/Weyl/Wigner level (part 2). The main point is that the algebras of quantum obsevables are the deformations of commutative algebras of classical observables (functions)[1]. So, if we have the Poisson manifold M (symplectic manifolds, Lie coalgebras, etc) as a model for classical dynamics then for quantum calculations we need to find an associative (but non-commutative) product $*$ on the space of formal power series in $\hbar$ with coefficients in the space of smooth functions on M such that

$$f * g = fg + \hbar\{f, g\} + \sum_{n\geq 2} \hbar^n B_n(f, g), \tag{1}$$

where $\{f, g\}$ is the Poisson brackets, B_n are bidifferential operators $C^\infty(X) \otimes C^\infty(X) \to C^\infty(X)$. There is also an infinite-dimensional gauge group on the set of star-products

$$f \mapsto f + \sum_{n\geq 2} \hbar^n D_n(f), \tag{2}$$

where D_n are differential operators. Kontsevich gave the solution to this deformation problem in terms of formal power series via sum over graphs[1]. He

also proved that for every Poisson manifold M there is a canonically defined gauge equivalence class of star-products on M.Also there is the nonperturbative corrections to power series representation for $*$ [1]. In naive calculations we may use simple formal rules:

$$* \equiv \exp\left(\frac{i\hbar}{2}(\overleftarrow{\partial}_x \overrightarrow{\partial}_p - \overleftarrow{\partial}_p \overrightarrow{\partial}_x)\right) \tag{3}$$

$$f(x,p) * g(x,p) = f(x, p - \frac{i\hbar}{2}\overrightarrow{\partial}_x) \cdot g(x, p + \frac{i\hbar}{2}\overleftarrow{\partial}_x) \tag{4}$$

$$= f(x + \frac{i\hbar}{2}\overrightarrow{\partial}_p, p - \frac{i\hbar}{2}\overrightarrow{\partial}_x) g(x,p) \tag{5}$$

In this paper we consider calculations of Wigner functions (WF) as the solution of Wigner equations [2] (part 3):

$$i\hbar\frac{\partial}{\partial t}W(x,p,t) = H * f(x,p,t) - f(x,p,t) * H \tag{6}$$

and especially stationary Wigner equations:

$$H * W = W * H = Ef \tag{7}$$

Our approach is based on extension of our variational–wavelet approach [3]–[14]. Wavelet analysis is some set of mathematical methods, which gives us the possibility to work with well-localized bases (Fig.1) in functional spaces and gives maximum sparse forms for the general type of operators (differential, integral, pseudodifferential) in such bases. These bases are natural generalization of standard coherent, squeezed, thermal squeezed states [2], which correspond to quadratical systems (pure linear dynamics) with Gaussian Wigner functions. So, we try to calculate quantum corrections to classical dynamics described by polynomial nonlinear Hamiltonians such as orbital motion in storage rings, orbital dynamics in general multipolar fields etc. from papers [3]-[13]. The common point for classical/quantum calcultions is that any solution which comes from full multiresolution expansion in all space/time (or phase space) scales represents expansion into a slow part and fast oscillating parts (part 4). So, we may move from the coarse scales of resolution to the finest one for obtaining more detailed information about our dynamical classical/quantum process. In this way we give contribution to our full solution from each scale of resolution. The same is correct for the contribution to power spectral density (energy spectrum): we can take into account contributions from each level/scale of resolution. Because affine group of translations

and dilations (or more general group, which acts on the space of solutions) is inside the approach, this method resembles the action of a microscope. We have contribution to final result from each scale of resolution from the whole underlying infinite scale of spaces. In part 5 we consider numerical modelling of Wigner functions which explicitly demonstrates quantum interference of generalized coherent states.

2 Quasiclassical Evolution

Let us consider classical and quantum dynamics in phase space $\Omega = R^{2m}$ with coordinates (x, ξ) and generated by Hamiltonian $\mathcal{H}(x, \xi) \in C^{\infty}(\Omega; R)$. If $\Phi_t^{\mathcal{H}} : \Omega \longrightarrow \Omega$ is (classical) flow then time evolution of any bounded classical observable or symbol $b(x, \xi) \in C^{\infty}(\Omega, R)$ is given by $b_t(x, \xi) = b(\Phi_t^{\mathcal{H}}(x, \xi))$. Let $H = Op^W(\mathcal{H})$ and $B = Op^W(b)$ are the self-adjoint operators or quantum observables in $L^2(R^n)$, representing the Weyl quantization of the symbols $\mathcal{H}, b$ [1]:

$$(Bu)(x) = \frac{1}{(2\pi\hbar)^n} \int_{R^{2n}} b\left(\frac{x+y}{2}, \xi\right) \cdot e^{i<(x-y),\xi>/\hbar} u(y) \mathrm{d}y \mathrm{d}\xi, \tag{8}$$

where $u \in S(R^n)$ and $B_t = e^{iHt/\hbar} B e^{-iHt/\hbar}$ be the Heisenberg observable or quantum evolution of the observable B under unitary group generated by H. B_t solves the Heisenberg equation of motion $\dot{B}_t = (i/\hbar)[H, B_t]$. Let $b_t(x, \xi; \hbar)$ is a symbol of B_t then we have the following equation for it

$$\dot{b}_t = \{\mathcal{H}, b_t\}_M, \tag{9}$$

with the initial condition $b_0(x, \xi, \hbar) = b(x, \xi)$. Here $\{f, g\}_M(x, \xi)$ is the Moyal brackets of the observables $f, g \in C^{\infty}(R^{2n})$, $\{f, g\}_M(x, \xi) = f\sharp g - g\sharp f$, where $f\sharp g$ is the symbol of the operator product and is presented by the composition of the symbols f, g

$$\begin{aligned}(f\sharp g)(x, \xi) = \frac{1}{(2\pi\hbar)^{n/2}} \int_{R^{4n}} e^{-i<r,\rho>/\hbar + i<\omega,\tau>/\hbar} \\ \cdot f(x + \omega, \rho + \xi) \cdot g(x + r, \tau + \xi) \mathrm{d}\rho \mathrm{d}\tau \mathrm{d}r \mathrm{d}\omega\end{aligned} \tag{10}$$

For our problems it is useful that $\{f, g\}_M$ admits the formal expansion in powers of $\hbar$:

$$\{f, g\}_M(x, \xi) \sim \{f, g\} + 2^{-j} \sum_{|\alpha+\beta|=j\geq 1} (-1)^{|\beta|} \cdot (\partial_{\xi}^{\alpha} f D_x^{\beta} g) \cdot (\partial_{\xi}^{\beta} g D_x^{\alpha} f), \tag{11}$$

where $\alpha = (\alpha_1, \ldots, \alpha_n)$ is a multi-index, $|\alpha| = \alpha_1 + \ldots + \alpha_n$, $D_x = -i\hbar\partial_x$. So, evolution (1) for symbol $b_t(x, \xi; \hbar)$ is

$$\dot{b}_t = \{\mathcal{H}, b_t\} + \frac{1}{2^j} \sum_{|\alpha|+\beta|=j\geq 1} (-1)^{|\beta|} \cdot \hbar^j (\partial_\xi^\alpha \mathcal{H} D_x^\beta b_t) \cdot (\partial_\xi^\beta b_t D_x^\alpha \mathcal{H}). \qquad (12)$$

At $\hbar = 0$ this equation transforms to classical Liouville equation. Equation (12) plays a key role in many quantum (semiclassical) problem. We consider its particular case–Wigner equation–in the next section.

3 Wigner Equations

According to Weyl transform quantum state (wave function or density operator) corresponds to Wigner function, which is analog of classical phase-space distribution [2]. We consider the following form of differential equations for time-dependent WF

$$\partial_t W(p, q, t) = \frac{2}{\hbar} \sin\Big[\frac{\hbar}{2}\big(\partial_q^H \partial_p^W - \partial_p^H \partial_q^W\big)\Big] \cdot H(p, q) W(p, q, t) \qquad (13)$$

Let

$$\hat{\rho} = |\Psi_\epsilon >< \Psi_\epsilon| \qquad (14)$$

be the density operator or projection operator corresponding to the energy eigenstate $|\Psi_\epsilon >$ with energy eigenvalue ϵ. Then time-indepedent Schroedinger equation corresponding to Hamiltonian

$$\hat{H}(\hat{p}, \hat{q}) = \frac{\hat{p}^2}{2m} + U(\hat{q}) \qquad (15)$$

where $U(\hat{q})$ is arbitrary polynomial function (related beam dynamics models considered in [3]-[13]) on $\hat{q}$ is [2]

$$\hat{H}\hat{\rho} = \epsilon\hat{\rho} \qquad (16)$$

After Weyl-Wigner mapping we arrive at the following equation on WF in c-numbers:

$$H\Big(p + \frac{\hbar}{2i}\frac{\partial}{\partial q},\ q - \frac{\hbar}{2i}\frac{\partial}{\partial p}\Big) W(p, q) = \epsilon W(p, q) \qquad (17)$$

or

$$\Big(\frac{p^2}{2m} + \frac{\hbar}{2i}\frac{p}{m}\frac{\partial}{\partial q} - \frac{\hbar^2}{8m}\frac{\partial^2}{\partial q^2}\Big) W(p, q) + U\Big(q - \frac{\hbar}{2i}\frac{\partial}{\partial p}\Big) W(p, q) = \epsilon W(p, q)$$

After expanding the potential U into the Taylor series we have two real partial differential equations

$$\Big(-\frac{p}{m}\frac{\partial}{\partial q} + \sum_{m=0}^{\infty} \frac{1}{(2m+1)!}\Big(\frac{i\hbar}{2}\Big)^{2m} \frac{\mathrm{d}^{2m+1}U}{\mathrm{d}q^{2m+1}} \frac{\partial^{2m+1}}{\partial p^{2m+1}}\Big) W(p,q) = 0 \quad (18)$$

$$\Big(\frac{p^2}{2m} + U(q) - \frac{\hbar^2}{8m}\frac{\partial^2}{\partial q^2} + \sum_{n=1}^{\infty} \frac{1}{(2n)!}\Big(\frac{i\hbar}{2}\Big)^{2n} \frac{\mathrm{d}^{2n}U}{\mathrm{d}q^{2n}} \frac{\partial^{2n}}{\partial p^{2n}}\Big) W(p,q) = \epsilon W(p,q) \quad (19)$$

In the next section we consider variation–wavelet approach for the solution of these equations for the case of arbitrary polynomial $U(q)$, which corresponds to a finite number of terms in equations (18), (19), up to any order of $\hbar$.

4 Variational Multiscale Representation

Let L be arbitrary (non)linear differential operator with matrix dimension d, which acts on some set of functions $\Psi \equiv \Psi(x,y) = \big(\Psi^1(x,y), ..., \Psi^d(x,y)\big)$, $x, y \in \Omega \subset \mathcal{R}^2$ from $L^2(\Omega)$:

$$L\Psi \equiv L(Q,x,y)\Psi(x,y) = 0, \quad (20)$$

where

$$Q \equiv Q_{d_1,d_2,d_3,d_4}(x,y,\partial/\partial x, \partial/\partial y) = \sum_{i,j,k,\ell=1}^{d_1,d_2,d_3,d_4} a_{ijk\ell} x^i y^j \Big(\frac{\partial}{\partial x}\Big)^k \Big(\frac{\partial}{\partial y}\Big)^\ell \quad (21)$$

Let us consider now the N mode approximation for solution as the following ansatz (in the same way we may consider different ansatzes):

$$\Psi^N(x,y) = \sum_{r,s=1}^{N} a_{rs} \Psi_r(x) \Phi_s(y) \quad (22)$$

We shall determine coefficients of expansion from the following Galerkin conditions (different related variational approaches considered in [3]-[13]):

$$\ell^N_{k\ell} \equiv \int (L\Psi^N)\Psi_k(x)\Phi_\ell(y)\mathrm{d}x\mathrm{d}y = 0 \quad (23)$$

So, we have exactly dN^2 algebraical equations for dN^2 unknowns a_{rs}.

But in the case of equations for WF (18), (19) we have overdetermined system of equations: $2N^2$ equations for N^2 unknowns a_{rs} (in this case $d = 1$). In this paper we consider non-standard method for resolving this problem,

which is based on biorthogonal wavelet expansion. So, instead of expansion (22) we consider the following one:

$$\Psi^N(x,y) = \sum_{r,s=1}^{N} a_{rs}\Psi_r(x)\Phi_s(y) + \sum_{i,j=1}^{N} \tilde{a}_{ij}\tilde{\Psi}_i(x)\tilde{\Phi}_j(y), \qquad (24)$$

where $\tilde{\Psi}_i(x)$, $\tilde{\Phi}_j(y)$ are the bases dual to initial ones. Because wavelet functions are the generalization of coherent states we consider an expansion on this overcomplete set of bases wavelet functions as a generalization of standard coherent states expansion.

So, variational/Galerkin approach reduced the initial problem (20) to the problem of solution of functional equations at the first stage and some algebraical problems at the second stage. We'll consider now the multiresolution expansion as the second main part of our construction. Because affine group of translation and dilations is inside the approach, this method resembles the action of a microscope. We have contribution to final result from each scale of resolution from the whole infinite scale of increasing closed subspaces V_j: $...V_{-2} \subset V_{-1} \subset V_0 \subset V_1 \subset V_2 \subset ....$ The solution is parameterized by solutions of two reduced algebraical problems, one is linear or nonlinear (23) (depends on the structure of operator L) and the second one are some linear problems related to computation of coefficients of algebraic equations (23). This coefficients can be found by the method of Connection Coefficients (CC)[15] or related method [16]. We use compactly supported wavelet basis functions for expansions (22), (24). We may consider different types of wavelets including general wavelet packets (section 5 below). This coefficients depend on the wavelet - Galerkin integrals. In general we need to find ($d_i \geq 0$)

$$\Lambda^{d_1 d_2 ... d_n}_{\ell_1 \ell_2 ... \ell_n} = \int_{-\infty}^{\infty} \prod \varphi^{d_i}_{\ell_i}(x) dx \qquad (25)$$

According to CC method [15] we use the next construction for quadratic case. When N in scaling equation is a finite even positive integer the function $\varphi(x)$ has compact support contained in $[0, N-1]$. For a fixed triple (d_1, d_2, d_3) only some $\Lambda^{d_1 d_2 d_3}_{\ell m}$ are nonzero: $2 - N \leq \ell \leq N - 2$, $2 - N \leq m \leq N - 2$, $|\ell - m| \leq N - 2$. There are $M = 3N^2 - 9N + 7$ such pairs (ℓ, m). Let $\Lambda^{d_1 d_2 d_3}$ be an M-vector, whose components are numbers $\Lambda^{d_1 d_2 d_3}_{\ell m}$. Then we have the first reduced algebraical system : Λ satisfy the system of equations ($d = d_1 + d_2 + d_3$)

$$A\Lambda^{d_1 d_2 d_3} = 2^{1-d}\Lambda^{d_1 d_2 d_3}, \quad A_{\ell,m;q,r} = \sum_p a_p a_{q-2\ell+p} a_{r-2m+p} \qquad (26)$$

By moment equations we have created a system of $M + d + 1$ equations in M unknowns. It has rank M and we can obtain unique solution by combination of LU decomposition and QR algorithm. For nonquadratic case we have analogously additional linear problems for objects (25). Solving these linear problems we obtain the coefficients of reduced main linear/nonlinear algebraical system (23) and after its solution we obtain the coefficients of wavelet expansions (22), (24). As a result we obtained the explicit solution of our problem in the base of compactly supported wavelets (22).

Also in our case we need to consider the extension of this approach to the case of any type of variable coefficients (periodic, regular or singular). We can produce such extension if we add additional refinement equation encoded all information about variable coefficients to our construction [16]. So, we need to compute only additional integrals of the form

$$\int_D b_{ij}(t)(\varphi_1)^{d_1}(2^m t - k_1)(\varphi_2)^{d_2}(2^m t - k_2)\mathrm{d}x, \tag{27}$$

where $b_{ij}(t)$ are arbitrary functions and wavelet functions φ_1, φ_2 satisfy the refinement equations:

$$\varphi_i(t) = \sum_{k \in \mathbf{Z}} a_{ik}\varphi_i(2t - k) \tag{28}$$

If we consider all computations in the class of compactly supported wavelets then only a finite number of coefficients do not vanish. To approximate the non-constant coefficients, we need choose a different refinable function φ_3 along with some local approximation scheme

$$(B_\ell f)(x) := \sum_{\alpha \in \mathbf{Z}} F_{\ell,k}(f)\varphi_3(2^\ell t - k), \tag{29}$$

where $F_{\ell,k}$ are suitable functionals supported in a small neighborhood of $2^{-\ell}k$ and then replace b_{ij} in (27) by $B_\ell b_{ij}(t)$. To guarantee sufficient accuracy of the resulting approximation to (27) it is important to have the flexibility of choosing φ_3 different from φ_1, φ_2. So, if we take $\varphi_4 = \chi_D$, where χ_D is characteristic function of D, which is again a refinable function, then the problem of computation of (27) is reduced to the problem of calculation of integral

$$H(k_1, k_2, k_3, k_4) = H(k) = \int_{\mathbf{R}^s} \varphi_4(2^j t - k_1) \cdot \varphi_3(2^\ell t - k_2)\varphi_1^{d_1}(2^r t - k_3)\varphi_2^{d_2}(2^s t - k_4)\mathrm{d}x \tag{30}$$

The key point is that these integrals also satisfy some sort of algebraical equation [16]:

$$2^{-|\mu|}H(k) = \sum_{\ell \in \mathbf{Z}} b_{2k-\ell} H(\ell), \qquad \mu = d_1 + d_2. \tag{31}$$

This equation can be interpreted as the problem of computing an eigenvector. Thus, the problem of extension to the case of variable coefficients is reduced to the same standard algebraical problem as in the case of constant coefficients. So, the general scheme is the same one and we have only one more additional linear algebraic problem. After solution of these linear problems we can again compute coefficients of wavelet expansions (22), (24).

Now we concentrate on the last additional problem which come from overdeterminity of equations (18), (19), which demands to consider expansion (24) instead of expansion (22). It leads to equal number of equations and unknowns in reduced algebraical system of equations (23). For this reason we consider biorthogonal wavelet analysis. We started with two hierarchical sequences of approximations spaces [16]: $\dots V_{-2} \subset V_{-1} \subset V_0 \subset V_1 \subset V_2 \dots$, $\dots \widetilde{V}_{-2} \subset \widetilde{V}_{-1} \subset \widetilde{V}_0 \subset \widetilde{V}_1 \subset \widetilde{V}_2 \dots$, and as usually, W_0 is complement to V_0 in V_1, but now not necessarily orthogonal complement. New orthogonality conditions have now the following form: $\widetilde{W}_0 \perp V_0, \quad W_0 \perp \widetilde{V}_0, \quad V_j \perp \widetilde{W}_j, \quad \widetilde{V}_j \perp W_j$ translates of ψ span W_0, translates of $\tilde{\psi}$ span $\widetilde{W}_0$. Biorthogonality conditions are $< \psi_{jk}, \tilde{\psi}_{j'k'} >= \int_{-\infty}^{\infty} \psi_{jk}(x)\tilde{\psi}_{j'k'}(x)\mathrm{d}x = \delta_{kk'}\delta_{jj'}$, where $\psi_{jk}(x) = 2^{j/2}\psi(2^j x - k)$. Functions $\varphi(x), \tilde{\varphi}(x-k)$ form dual pair: $< \varphi(x-k), \tilde{\varphi}(x-\ell) >= \delta_{kl}, \quad < \varphi(x-k), \tilde{\psi}(x-\ell) >= 0 \quad \text{for} \quad \forall k, \forall \ell$. Functions $\varphi, \tilde{\varphi}$ generate a multiresolution analysis. $\varphi(x-k)$, $\psi(x-k)$ are synthesis functions, $\tilde{\varphi}(x-\ell)$, $\tilde{\psi}(x-\ell)$ are analysis functions. Synthesis functions are biorthogonal to analysis functions. Scaling spaces are orthogonal to dual wavelet spaces. Two multiresolutions are intertwining $V_j + W_j = V_{j+1}, \quad \widetilde{V}_j + \widetilde{W}_j = \widetilde{V}_{j+1}$. These are direct sums but not orthogonal sums. So, our representation for solution has now the form $f(t) = \sum_{j,k} \tilde{b}_{jk}\psi_{jk}(t)$, where synthesis wavelets are used to synthesize the function. But $\tilde{b}_{jk}$ come from inner products with analysis wavelets. Biorthogonal point of view is more flexible and stable under the action of large class of operators while orthogonal (one scale for multiresolution) is fragile, all computations are much more simpler and we accelerate the rate of convergence of our expansions (24). By analogous ansatsez and approaches we may construct also the multiscale/multiresolution representations for solution of time dependent Wigner equation (13) [14].

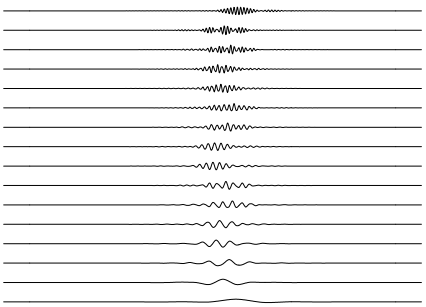

Figure 1. Localized contributions to beam motion.

5 Numerical Modelling

So, our constructions give us the following N-mode representation for solution of Wigner equations (18)-(19):

$$W^N(p,q) = \sum_{r,s=1}^{N} a_{rs}\Psi_r(p)\Phi_s(q) \tag{32}$$

where $\Psi_r(p)$, $\Phi_s(q)$ may be represented by some family of (nonlinear) eigenmodes with corresponding multiresolution/multiscale representation in the high-localized wavelet bases (Fig.1):

$$\Psi_k(p) = \Psi^{M_1}_{k,slow}(p) + \sum_{i\geq M_1} \Psi^i_k(\omega^1_i p), \quad \omega^1_i \sim 2^i \tag{33}$$

$$\Phi_k(q) = \Phi^{M_2}_{k,slow}(q) + \sum_{j\geq M_2} \Phi^j_k(\omega^2_j q), \quad \omega^2_j \sim 2^j \tag{34}$$

Our (nonlinear) eigenmodes are more realistic for the modelling of nonlinear classical/quantum dynamical processes than the corresponding linear gaussian-like coherent states. Here we mention only the best convergence properties of expansions based on wavelet packets, which realize the so called minimal Shannon entropy property (Fig. 1). On Fig. 2 we present numerical modelling [17] of Wigner function for a simple model of beam motion, which explicitly demonstrates quantum interference property. On Fig. 3 we present the multiscale/multiresolution representation (32)-(34) for solution of Wigner equation.

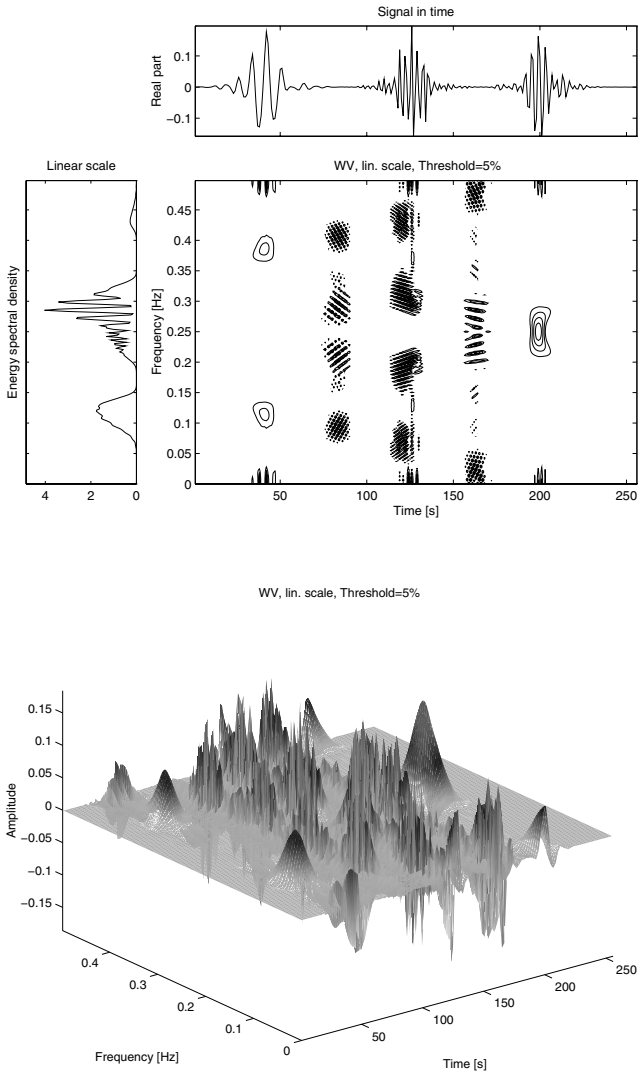

Figure 2. Wigner function for 3 wavelet packets.

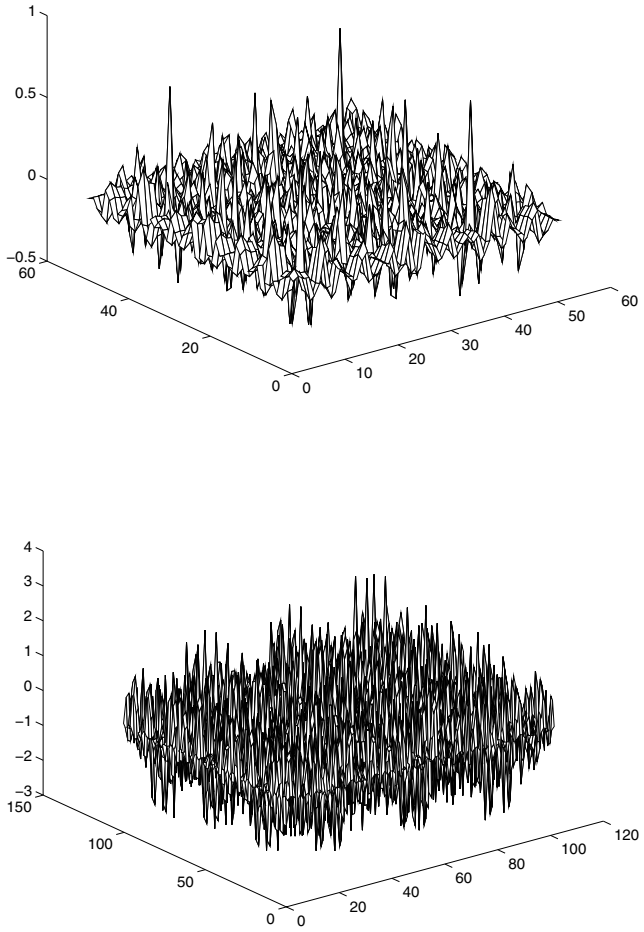

Figure 3. Multiresolution/multiscale representations for Wigner functions.

We would like to thank Professor Pisin Chen, Dr. Stefania Petracca and her team for nice hospitality, help and support during Capri ICFA Workshop.

References

1. D. Sternheimer, Los Alamos preprint: math.QA/9809056, M. Kontsevich, q-alg/9709040, V.Periwal, hep-th/0006001.
2. T. Curtright, T. Uematsu, C. Zachos, hep-th/0011137, M.Huq, e.a., *Phys. Rev.*, **A 57**, 3188 (1998).
3. A.N. Fedorova and M.G. Zeitlin, *Math. and Comp. in Simulation*, **46**, 527 (1998).
4. A.N. Fedorova and M.G. Zeitlin, 'Wavelet Approach to Mechanical Problems. Symplectic Group, Symplectic Topology and Symplectic Scales', *New Applications of Nonlinear and Chaotic Dynamics in Mechanics*, 31, 101 (Kluwer, 1998).
5. A.N. Fedorova and M.G. Zeitlin, **CP405**, 87 (American Institute of Physics, 1997). Los Alamos preprint, physics/9710035.
6. A.N. Fedorova, M.G. Zeitlin and Z. Parsa, Proc. PAC97 **2**, 1502, 1505, 1508 (IEEE, 1998).
7. A.N. Fedorova, M.G. Zeitlin and Z. Parsa, Proc. EPAC98, 930, 933 (Institute of Physics, 1998).
8. A.N. Fedorova, M.G. Zeitlin and Z. Parsa, **CP468**, 48 (American Institute of Physics, 1999). Los Alamos preprint, physics/990262.
9. A.N. Fedorova, M.G. Zeitlin and Z. Parsa, **CP468**, 69 (American Institute of Physics, 1999). Los Alamos preprint, physics/990263.
10. A.N. Fedorova and M.G. Zeitlin, Proc. PAC99, 1614, 1617, 1620, 2900, 2903, 2906, 2909, 2912 (IEEE/APS, New York, 1999).
    Los Alamos preprints: physics/9904039, 9904040, 9904041, 9904042, 9904043, 9904045, 9904046, 9904047.
11. A.N. Fedorova and M.G. Zeitlin, Proc. UCLA ICFA Workshop, in press, Los Alamos preprint: physics/0003095.
12. A.N. Fedorova and M.G. Zeitlin, Proc. EPAC00, 415, 872, 1101, 1190, 1339, 2325.
    Los Alamos preprints: physics/0008045, 0008046, 0008047, 0008048, 0008049, 0008050
13. A.N. Fedorova, M.G. Zeitlin, Proc. LINAC00, 2 papers in press, Los Alamos preprints: physics/0008043, 0008200
14. A.N. Fedorova, M.G. Zeitlin, in press
15. A.Latto, e.a. Aware Technical Report AD910708,1991
16. W.Dahmen, C.Micchelli, *SIAM J. Numer. Anal.*, **30**, 507 (1993)
17. F. Auger, e.a., Time-frequency Toolbox, CNRS/Rice Univ., 1996

SINGLE-PARTICLE QUANTUM DYNAMICS IN A MAGNETIC LATTICE

M. VENTURINI AND R. D. RUTH
SLAC, Stanford University, Stanford CA 94309, USA.
E-mail: venturin@slac.stanford.edu

We study the quantum dynamics of a spinless charged-particle propagating through a magnetic lattice in a transport line or storage ring. Starting from the Klein-Gordon equation and by applying the paraxial approximation, we derive a Schrödinger-like equation for the betatron motion. A suitable unitary transformation reduces the problem to that of a simple harmonic oscillator. As a result we are able to find an explicit expression for the particle wavefunction.

1 Introduction

Continuing progress in beam cooling techniques could lead in the future to regimes in which quantum effects will start to become important. At that point a fully quantum mechanical description of the beam dynamics will be required[1]. As a contribution to that description, in this paper we lay out a framework to compute the wavefunction for a single charged particle confined in a magnetic lattice transport line or storage ring. The expression we find may be useful as a basis to calculate transition rates in processes like synchrotron radiation emission[2] or intrabeam scattering as well as to assess the limitations to a machine performance caused by diffraction phenomena[3].

In our analysis we neglect spin effects so that the particle wavefunction is properly described by the Klein-Gordon (KG) equation. The KG equation can be solved in the paraxial approximation by exploiting the fact that in an accelerator the particle momentum is mostly longitudinal. The problem amounts to studying a non-relativistic quantum harmonic oscillator with a time-dependent restoring force – 'time' in this context is the location of the particle along the lattice. The solution can be found in the literature[4] and has already been applied in the field of quantum optics and ion traps. Here we present a method of solving the problem that involves a language more familiar to the accelerator physicist and emphasizes the correspondence with the classical motion. Previous work in this area using different methods includes that of Jagannathan and Kahn[5]. The methods employed here are more similar to those introduced by Fedele et al.[6] in their 'quantum-like' beam models.

In Sec. 2,3,4 we treat a particle dynamics in a straight channel. In Sec. 5, we discuss the coherent-state solutions and finally in Sec. 6,7 we extend the

results to circular machines.

2 The Reduced Klein-Gordon Equation for a Particle in a Straight Transport Line

Neglecting spin effects a relativistic quantum particle can be described using a wavefunction that satisfies the KG equation. In general, if the charged particle is coupled to an external static magnetic field $\boldsymbol{B} = \nabla \times \boldsymbol{A}$ the KG equation reads

$$[\hat{E}^2/c^2 - m^2c^2 - (\hat{\boldsymbol{p}} - e\boldsymbol{A})^2]\psi(t, \boldsymbol{x}) = 0, \tag{1}$$

with the operators $\hat{E}$ and $\hat{\boldsymbol{p}}$ defined as usual as $\hat{E} = i\hbar\partial_t$ and $\hat{\boldsymbol{p}} = -i\hbar\nabla$.

In a straight transport line consisting of quads and drifts with the particle traveling along z one can choose a gauge for which the vector potential has the form $A_x = A_y = 0$ and $A_z = -(p_0/e)k(z)(x^2 - y^2)/2$ with p_0 being the design particle momentum and $k(z)$ the focusing function. Such a vector potential is consistent with Maxwell's equations through second order terms. In the absence of external focusing a solution of (1) representing a particle propagating along the $z-$axis with the design energy E_0 and momentum p_0 is given by the wavefunction

$$\psi = \psi_0 e^{i(p_0 z - E_0 t)/\hbar}, \tag{2}$$

where ψ_0 is a normalization constant. As the interaction with the confining magnetic field is turned on it is natural to look for solutions of (1) in the form

$$\psi = \tilde{\psi}(x, y, z)e^{i(p_0 z - E_0 t)/\hbar}. \tag{3}$$

We can expect that the $z-$dependence in $\tilde{\psi}(x, y, z)$ results in variations taking place over distances of the order of the betatron wavelength λ_β. This defines the long-length scale of our problem, which should be compared with the short-length scale given by the De Broglie wavelength $\lambda_p = h/p_0$. After substituting (3) into (1), we use the fact $\lambda_\beta \gg \lambda_p$ to neglect $\partial_z^2\tilde{\psi}$ compared to $\partial_z\tilde{\psi}/\lambda_p$ and $(x^2 - y^2)\partial_z\tilde{\psi}$ compared to $(x^2 - y^2)\tilde{\psi}/\lambda_p$. Moreover, we can neglect the term containing $\partial_z k(z)$ because the distance over which $k(z)$ varies substantially – the magnet fringe field region – is also much longer than the De Broglie wavelength. Finally, we disregard terms more than quadratic in x and y because we are only interested in the linear approximation of the transverse dynamics. As a result we obtain the following Schrödinger-like equation for the amplitude $\tilde{\psi}(x, y, z)$:

$$i\hbar\frac{\partial\tilde{\psi}}{\partial z} = \left(-\frac{\hbar^2}{2p_0}\frac{\partial^2}{\partial x^2} - \frac{\hbar^2}{2p_0}\frac{\partial^2}{\partial y^2} + p_0\frac{k(z)}{2}(x^2 - y^2)\right)\tilde{\psi}, \tag{4}$$

where z is now interpreted as the independent 'time-like' variable. From Eq. (4) we can write off the effective Hamiltonian $\hat{\mathcal{H}}$ for the system

$$\hat{\mathcal{H}} = \frac{\hat{p}_x^2}{2p_0} + \frac{\hat{p}_y^2}{2p_0} + p_0 \frac{k(z)}{2}(x^2 - y^2). \tag{5}$$

3 The Classical Motion

The classical Hamiltonian $\mathcal{H}$ corresponding to (5) leads to the Hill equations $x'' + k(z)x = 0$, and $y'' - k(z)y = 0$, [a] the solutions of which, *i.e.* $x = \sqrt{\epsilon_x \beta_x(z)}\cos[\varphi_x(z) + \varphi_{xo}]$ and $y = \sqrt{\epsilon_y \beta_y(z)}\cos[\varphi_y(z) + \varphi_{yo}]$, can be written in terms of the Courant-Snyder betatron functions $\beta_{x,y}(z)$ and phase functions $\varphi_{x,y}(z)$ defined by $\varphi'_{x,y} = 1/\beta_{x,y}$. In turn, the betatron functions $\beta_{x,y}$ are solutions of

$$\beta''_{x,y} - \frac{\beta'^2_{x,y}}{2\beta_{x,y}} \pm 2k(z)\beta_{x,y} - \frac{2}{\beta_{x,y}} = 0, \tag{6}$$

where the + sign in front of the focusing function applies to β_x and the − sign to β_y. The solutions are determined upon specification of the appropriate initial or boundary conditions. We know from the accelerator theory literature [7] that the betatron functions can be used to define canonical transformations that cast the original Hamiltonian into a simpler form. We also know that canonical transformations correspond in quantum mechanics to unitary transformations [8]. Therefore, we can use such a correspondence to build a suitable unitary operator that turns the quantum Hamiltonian into a simpler form as well. We desire a Hamiltonian that has the $z-$dependence fully factored in order to simplify the solution of the corresponding KG equation.

Consider the classical case first. For simplicity we will focus only on the horizontal motion; extension to the vertical plane is trivial. The canonical transformation[7] that produces the desired Hamiltonian can be decomposed into a linear momentum kick that leaves x unchanged followed by a scaling. In particular the first transformation $(x, p_x) \to (x_1, p_{x1})$ is given by $x_1 = x$, and $p_{x1} = p_x - p_0 x\beta'_x(z)/2\beta_x(z)$, and has generating function $F_2(x, p_{x1}, z) = xp_{x1} + p_0 x^2 \beta'_x(z)/4\beta_x(z)$. The transformed Hamiltonian $\mathcal{H}_1$ in the new variables is

$$\mathcal{H}_1 = \mathcal{H} + \frac{\partial F_2}{\partial z} = \frac{p^2{}_{x1}}{2p_0} + \frac{\beta'_x}{2\beta_x} p_{x1}x_1 + \frac{p_0}{2\beta_x^2} x_1^2. \tag{7}$$

[a] The prime $'$ means differentiation with respect to z.

The scaling $x_2 = x_1/\sqrt{\beta_x}$ and $p_{x2} = p_{x1}\sqrt{\beta_x}$, then removes the cross term and factors out the $z-$dependence in the Hamiltonian at same time. Such a transformation has generating function $F_2(x_1, p_{x2}) = x_1 p_{x2}/\sqrt{\beta_x}$. The resulting Hamiltonian reads

$$\mathcal{H}_2 = \mathcal{H}_1 + \frac{\partial F_2}{\partial z} = \frac{1}{\beta_x(z)}\left(\frac{p_{x2}^2}{2p_0} + \frac{p_0}{2}x_2^2\right). \tag{8}$$

4 The Quantum Motion

First, let us recall how the quantum Hamiltonian transforms under unitary transformations. If the abstract vector $|\psi\rangle$ satisfies the Schrödinger equation $i\hbar\partial_z|\psi\rangle = \mathcal{H}|\psi\rangle$ the ket $|\psi'\rangle = U^{-1}|\psi\rangle$ transformed under unitary operator U^{-1} satisfies the Schrödinger equation $i\hbar\partial_z|\psi'\rangle = \mathcal{H}'|\psi'\rangle$, with the Hamiltonian $\mathcal{H}'$ given by

$$\mathcal{H}' = U^{-1}\mathcal{H}U - i\hbar U^{-1}\frac{\partial U}{\partial z}. \tag{9}$$

We are now ready to write the quantum equivalent of the canonical transformation introduced in the previous Section. The unitary operator U_1 generating the momentum kick is defined by $U_1^{-1}\hat{x}U_1 = \hat{x}$ and $U_1^{-1}\hat{p}_x U_1 = \hat{p}_x + p_0\beta_x'\hat{x}/(2\beta_x)$, where we have used $\hat{}$ to denote the quantum observables. Provided that $\beta_x(z)$ obeys Eq. (6), as in the classical case, it can be easily verified that

$$U_1 = \exp\left(i\frac{p_0}{\hbar}\frac{\beta_x'}{4\beta_x}\hat{x}^2\right), \tag{10}$$

leads to the intermediate Hamiltonian

$$\hat{\mathcal{H}}_1 = \frac{\hat{p}_x^2}{2p_0} + \frac{\beta_x'}{4\beta_x}(\hat{p}_x\hat{x} + \hat{x}\hat{p}_x) + \frac{p_0}{2\beta_x^2}\hat{x}^2. \tag{11}$$

In turn, the scaling $U_2^{-1}\hat{x}U_2 = \hat{x}\sqrt{\beta_x}$ and $U_2^{-1}\hat{p}_x U_2 = \hat{p}_x/\sqrt{\beta_x}$ defines the unitary operator

$$U_2 = \exp\left(-\frac{i}{4\hbar}\log(\beta_x)(\hat{x}\hat{p}_x + \hat{p}_x\hat{x})\right). \tag{12}$$

The transformed Hamiltonian $\hat{\mathcal{H}}_2$ is the quantum correspondent of $\mathcal{H}_2$:

$$\hat{\mathcal{H}}_2 = \frac{1}{\beta_x(z)}\left(\frac{\hat{p}_x^2}{2p_0} + \frac{p_0}{2}\hat{x}^2\right). \tag{13}$$

$\hat{\mathcal{H}}_2$ has the form of a Hamiltonian for a simple oscillator times a pure function of z. If we denote with

$$\phi_n(x) = \left(\frac{p_0}{\pi\hbar}\right)^{\frac{1}{4}} \frac{1}{\sqrt{2^n n!}} H_n\left(x\sqrt{\frac{p_0}{\hbar}}\right) e^{-p_0 x^2/2\hbar} \tag{14}$$

the eigenfunctions of the harmonic oscillator part we can easily verify that we can write the solutions of the Schrödinger equation $i\hbar\partial_z|\tilde{\psi}^{(2)}\rangle = \hat{\mathcal{H}}_2|\tilde{\psi}^{(2)}\rangle$ corresponding to the $n-$excited level of the betatron oscillations, as

$$\tilde{\psi}_n^{(2)}(x,z) = \phi_n(x) e^{-i(n+1/2)\varphi_x(z)}. \tag{15}$$

We recall that $\varphi_x(z) = \int dz/\beta_x(z)$.

By applying in sequence the transformations U_2 and U_1, we then recover the wavefunctions relative to the intermediate Hamiltonian $\hat{\mathcal{H}}_1$ and original Hamiltonian $\hat{\mathcal{H}}$. In particular, we have $|\psi_n^{(1)}\rangle = U_2|\psi_n^{(2)}\rangle$ or:

$$\tilde{\psi}_n^{(1)}(x,z) = \beta_x^{-\frac{1}{4}} \psi_n^{(2)}(x/\sqrt{\beta_x}, z), \tag{16}$$

i.e.

$$\begin{aligned}\tilde{\psi}_n^{(1)}(x,z) = & \left(\frac{p_0}{\pi\hbar\beta_x(z)}\right)^{\frac{1}{4}} \frac{1}{\sqrt{2^n n!}} H_n\left(x\sqrt{\frac{p_0}{\hbar\beta_x(z)}}\right) \times \\ & \exp\left(-p_0 x^2/[2\hbar\beta_x(z)]\right) \exp\left(-i(n+1/2)\varphi_x(z)\right).\end{aligned} \tag{17}$$

Finally, the solutions of the original Schrödinger equation (4) are ($|\psi_n\rangle = U_2|\psi_n^{(1)}\rangle$)

$$\tilde{\psi}_n(x,z) = \exp\left(i\frac{p_0}{\hbar}\frac{\beta_x'(z)}{4\beta_x(z)}x^2\right)\tilde{\psi}_n^{(1)}(x,z). \tag{18}$$

One can verify that indeed this is a solution of (4) by direct substitution.

5 Coherent-States

The wavefunctions (18) can be combined linearly to obtain localized wavepackets both longitudinally and transversally. For simplicity we will focus only on localization in the transverse plane, *i.e.* we consider only eigenstates of p_0. Of particular interest are those linear superpositions leading to coherent states. One way to introduce coherent states for a simple harmonic oscillator is to define them as eigenfunctions of the creation operator.[8] Here we can proceed in a similar way by using the creation operator a defined in terms of the observables $\hat{x}$ and $\hat{p}_x$ relative to Hamiltonian $\hat{\mathcal{H}}_2$:

$$a = \frac{1}{\sqrt{2}}\left(\sqrt{\frac{p_0}{\hbar}}\hat{x} + i\frac{1}{\sqrt{p_0\hbar}}\hat{p}_x\right). \tag{19}$$

The coherent states for the original system $\hat{\mathcal{H}}$ are then recovered by applying the unitary operators U_1 and U_2 introduced in Sec. 4. Equivalently, one can introduce coherent states by means of the displacement operator

$$D(\alpha) = e^{-i\varphi_x(z)/2} e^{\alpha a^\dagger - \alpha^* a}. \tag{20}$$

where α is the function $\alpha(z) = \alpha_0 \exp[-i\varphi_x(z)]$, with α_0 being a complex constant number. One can show that the coherent states $|\alpha_0\rangle$ result from applying $D(\alpha)$ to the harmonic oscillator ground state $|\alpha_0\rangle = D(\alpha)|\phi_0\rangle$. Use of the displacement operator allows one to quickly obtain the wavefunction representation $\psi^{(2)}_{\alpha_0}(x,z) = \langle x|\alpha_0\rangle$:

$$\psi^{(2)}_{\alpha_0}(x) = e^{-i\varphi_x(z)/2} e^{(\alpha^{*2}-\alpha^2)/4} e^{\sqrt{p_0/2\hbar}(\alpha-\alpha^*)x} \phi_0\left(x - \sqrt{\frac{\hbar}{2p_0}}(\alpha+\alpha^*)\right), \tag{21}$$

where $\phi_0(x) = \langle x|\phi_0\rangle = (p_0/\pi\hbar)^{\frac{1}{4}} \exp(-p_0 x^2/2\hbar)$ is the wavefunction of the harmonic oscillator ground state. If we then act with U_2 and U_1 on $\psi^{(2)}_{\alpha_0}(x)$ we find the coherent states in the original variables

$$\psi_{\alpha_0}(x) = \exp\left(i\frac{p_0}{\hbar}\frac{\beta_x'(z)}{4\beta_x(z)}x^2\right) \beta_x^{-\frac{1}{4}} \psi^{(2)}_{\alpha_0}(x/\sqrt{\beta_x}, z). \tag{22}$$

The function α is related to the expectation values $\overline{x} = \langle\hat{x}\rangle_{\alpha_0}$ and $\overline{p}_x = \langle\hat{p}_x\rangle_{\alpha_0}$ for the coherent state:

$$\sqrt{\frac{\hbar}{2p_0}}(\alpha+\alpha^*) = \frac{\overline{x}}{\sqrt{\beta_x}}, \tag{23}$$

$$\sqrt{\frac{\hbar p_0}{2}}(\alpha-\alpha^*) = i\sqrt{\beta_x}\overline{p}_x - ip_0\frac{\beta_x'}{2\sqrt{\beta_x}}\overline{x}. \tag{24}$$

It can be shown that two above equations indicate that $\overline{x}$ and $\overline{p}_x$ evolve according to the classical trajectory, as expected from Ehrenfest's Theorem [8].

For a simple harmonic oscillator the coherent states have the property that the wavepacket spread in both position and momentum is constant and has the minimum value consistent with the Heisenberg uncertainty principle. This is not true in our case because of the dependence of the betatron function on z and only where $\beta_x'(z) = 0$ the wavepacket spread is minimum. In particular, we have [with $(\Delta x)^2 \equiv \langle(\hat{x}-\overline{x})^2\rangle_{\alpha_0}$, etc.], $(\Delta x)^2 = \hbar\beta_x(z)/2p_0$ and $(\Delta p_x)^2 = [\hbar p_0/2\beta_x(z)](1+\beta_x'^2/4)$ and therefore $\Delta x\Delta p_x = (\hbar/2)\sqrt{1+\beta_x'^2/4}$. On the other hand the quantum quantity corresponding to the unnormalized rms

emittance evaluated on these states has the constant value

$$\varepsilon_x \equiv \left[(\Delta x)^2\frac{(\Delta p_x)^2}{p_0^2} - \frac{1}{4}\langle\frac{(\hat{p}_x-\overline{p}_x)}{p_0}(\hat{x}-\overline{x}) + (\hat{x}-\overline{x})\frac{(\hat{p}_x-\overline{p}_x)}{p_0}\rangle_{\alpha_0}^2\right]^{\frac{1}{2}} = \frac{\pi\lambda_c}{\gamma}, \tag{25}$$

where $\lambda_c = h/mc$ is the Compton wavelength and γ the relativistic factor.

6 Charged particle in uniform bending and periodic focusing

The calculation carried out in the previous Sections can be extended to include the dynamics of a charged particle in a storage ring. We assume a simplified model of storage ring for which in addition to a periodic focusing we now impose a bending provided by a uniform magnetic field of strength B_0. We assume that the magnetic field is pointing in the $y-$direction so that the classical equilibrium orbit for a charged particle is a circle of radius ρ_0 in the $x-z$ plane. We select the (classical) reference orbit to be centered at $x = z = 0$. In cylindrical coordinates[b] a vector potential $\boldsymbol{A} = (A_\rho, A_\phi, A_y)$ associated with the magnetic field that provides the desired confinement and focusing is given, through second order in terms of the deviations from the equilibrium orbit, by $A_\rho = A_y = 0$ and

$$A_\phi = \frac{B_0}{2}\rho + b_2(\phi)\frac{\rho_0}{2\rho}[(\rho-\rho_0)^2 - y^2]. \tag{26}$$

Our starting point is the KG equation, which now is expressed best in terms of cylindrical coordinates. Because the energy E of a particle does not depend on time we can still write the solution of the KG equation as

$$\Psi = e^{-iEt/\hbar}\hat{\Psi}(\rho,\phi,y) \tag{27}$$

as in Sec. 1 . To avoid possible confusion from now on we will use the capitalized letter Ψ to denote the quantum wavefunction for the system with bending. With this ansatz the KG equation becomes

$$\left[-\hbar^2\frac{1}{\rho}\frac{\partial}{\partial\rho}\rho\frac{\partial}{\partial\rho} + \left(\frac{\hbar}{i\rho}\frac{\partial}{\partial\phi} - eA_\phi\right)^2 - \hbar^2\frac{\partial^2}{\partial y^2}\right]\hat{\Psi} = p^2\hat{\Psi}, \tag{28}$$

where p is the particle mechanical momentum. We alert the reader that we will allow the possibility for the particle energy and momentum to be different from the design values E_0 and p_0. In analogy with Eq. (3) we make the following ansatz

$$\hat{\Psi} = e^{i\ell\phi}\tilde{\Psi}(\rho,\phi,y), \tag{29}$$

[b] defined by $x = \rho\cos\phi, z = \rho\sin\phi, y$.

which spells out a decomposition of the wavefunction into fast (first term on the RHS) and slow (second term on the RHS) ϕ-varying component. That is, we are assuming $\ell \gg 1$ and $\partial_\phi \tilde{\Psi} \ll \ell \tilde{\Psi}$. On the basis of the exact solution of the problem (28) for the case with vanishing focusing ($b_2 = 0$), we expect that the particle mechanical momentum to be related to the quantum number ℓ by[8] $p^2 = 2\hbar|e|B_0(\ell + 1/2) \simeq 2\hbar|e|B_0\ell$.

We can now proceed as in Sec. 1 and neglect the second order derivatives $\partial_\phi^2 \tilde{\Psi}$ compared to $\ell \partial_\phi \tilde{\Psi}$ and the term $\partial_\phi A_\phi$ compared to ℓA_ϕ. As a result the KG equation then reads

$$i\hbar \left(\frac{\hbar\ell}{\rho} - eA_\phi \right) \frac{2}{\rho} \frac{\partial \tilde{\Psi}}{\partial \phi} = \left(-\hbar^2 \frac{\partial^2}{\partial \rho^2} - \hbar^2 \frac{\partial^2}{\partial y^2} + V(\rho, y) - p^2 \right) \tilde{\Psi}, \tag{30}$$

where $V(\rho, y)$ is an effective potential that has the form

$$V(\rho, y) = -\frac{\hbar^2}{4\rho^2} + \frac{1}{\rho^2}(\hbar\ell - eA_\phi\rho)^2 \simeq \frac{1}{\rho^2}(\hbar\ell - eA_\phi\rho)^2. \tag{31}$$

The last equality holds because we are assuming $\ell \gg 1$. At this point we expand the effective potential V around its point of minimum, $\rho = \rho_{\min} = \sqrt{2\hbar\ell/|e|B_0}$. By requiring $\rho_{\min} = \rho_0$ (*i.e.* we want the expansion of V to be centered on the classical reference orbit) the equation above identifies $\ell_0 = [\rho_0^2|e|B_0/2\hbar]^{\frac{1}{2}} = p_0\rho_0/2\hbar$, as the quantum number relative to the state of an on-momentum particle. We write $\rho = \rho_0 + \xi$ and in the expansion for V we keep only terms quadratic in the variables ξ, y, and $\delta = (\ell - \ell_0)/2\ell_0 = \Delta p/p_0$. After some algebra we then obtain the reduced KG equation in the form of the following Schrödinger-like equation

$$\begin{aligned} i\hbar \frac{\partial \tilde{\Psi}}{\partial s} = \Bigg[& -\frac{\hbar^2}{2p_0}\frac{\partial^2}{\partial x^2} - \frac{\hbar^2}{2p_0}\frac{\partial^2}{\partial y^2} + \frac{p_0}{2}\left(\frac{1}{\rho_0^2} + k(s) \right) x^2 \\ & - \frac{p_0}{2}k(s)y^2 - p_0\frac{\delta}{\rho_0}x + \frac{p_0}{2}\delta^2 \Bigg] \tilde{\Psi}. \end{aligned} \tag{32}$$

In writing (32) we have rescaled the independent variable ϕ according to $\phi = s/\rho_0$, written the focusing function as $k(s) = eb_2(s/\rho_0)/p_0$, and finally re-christen ξ as x. In conclusion, the desired solution of the KG equation (28) around the reference orbit is

$$\hat{\Psi} = e^{i\ell s/\rho_0} \tilde{\Psi}(\xi, y, s)/\sqrt{\rho_0 + \xi} \simeq e^{i\ell s/\rho_0} \tilde{\Psi}(\xi, y, s)/\sqrt{\rho_0}. \tag{33}$$

with $\tilde{\Psi}$ given by the solution of (32).

7 Treatment of Dispersion

The Schrödinger equation (32) differs from (4) because of the coupling term δx. A way to solve Eq. (32) is to first introduce a suitable unitary transformation that remove the coupling. In complete analogy with the classical case[7] such a transformation consists of one translation in position and one in momentum. The first, $U_1^{-1}\hat{x}U_1 = \hat{x} + \delta D$ and $U_1^{-1}\hat{p}_x U_1 = \hat{p}_x$ is generated by $U_1 = \exp\left(-i\delta\hat{p}_x D(s)/\hbar\right)$. The second transformation is generated by $U_2 = \exp\left(i\delta\hat{x}p_0 D'(s)/\hbar\right)$, yielding $U_2^{-1}\hat{x}U_2 = \hat{x}$ and $U_2^{-1}\hat{p}_x U_2 = \hat{p}_x + p_0\delta D'(z)$. In both cases $D(s)$ is the dispersion function defined as a solution of the inhomogeneous equation

$$D'' + k_x(s)D = \frac{1}{\rho_0}. \tag{34}$$

By virtue of (34) the transformed states $|\tilde{\Psi}_n^{(2)}\rangle = U_2U_1|\tilde{\Psi}_n\rangle$ obey the Schrödinger equation $i\hbar\partial_z|\tilde{\Psi}_n^{(2)}\rangle = \hat{H}_2|\tilde{\Psi}_n^{(2)}\rangle$ with

$$\hat{H}_2 = \frac{1}{2p_0}\hat{p}_x^2 + \frac{1}{2}p_0k_x(s)\hat{x}^2 + \frac{p_0\delta^2}{2}\left(k_xD^2 - D'^2 - \frac{2D}{\rho_0}\right). \tag{35}$$

This Hamiltonian has the same form as Hamiltonian (5) apart from the last purely $s-$dependent term on the RHS. Therefore, a solution of the resulting Schrödinger equation is given by

$$\tilde{\Psi}_n^{(2)}(x,s) = \tilde{\psi}_n(x,s)\exp\left[-\frac{i}{\hbar}\frac{p_0\delta^2}{2}\int_0^s[1 + k_x(t)D^2(t) - D'^2(t) - \frac{2D(t)}{\rho_0}]dt\right] \tag{36}$$

where $\tilde{\psi}_n(x,s)$ is the same as in Eq. (18) with s replacing z. By undoing the transformations U_1 and U_2 we can finally obtain the solutions $|\tilde{\Psi}_n\rangle = U_1U_2|\tilde{\Psi}_n^{(2)}\rangle$ of the original Schrödinger equation (32):

$$\tilde{\Psi}_n(x,s) = e^{i\delta p_0(x-\delta D)D'/\hbar}\tilde{\Psi}_{2,n}(x - \delta D, s). \tag{37}$$

Next we combine Eq.'s (33) and (37) and upon including the vertical degree of freedom we finally recognize that the wavefunction corresponding to the n_x and n_y transverse levels of excitation reads

$$\Psi(x,y,s) = \frac{C}{\sqrt{\rho_0}}e^{i\ell s/\rho_0}\tilde{\Psi}_{n_x}(x,s)\tilde{\psi}_{n_y}(y,s), \tag{38}$$

with $\tilde{\Psi}_{n_x}(x,s)$ given by Eq. (37) and $\tilde{\psi}_{n_y}(y,s)$ by Eq. (18); we have introduced the constant C to guarantee a proper normalization. Enforcing periodicity

upon the wavefunction $\Psi(x,y,0) = \Psi(x,y,2\pi\rho_0)$ yields the following quantization condition on the particle momentum (through first order in $\Delta p = p_0\delta$)

$$\Delta p = \frac{\hbar}{\rho_0}\left[(m-\ell_0) + \left(n_x + \frac{1}{2}\right)\nu_x + \left(n_y + \frac{1}{2}\right)\nu_y\right], \tag{39}$$

where ν_x and ν_y are the tunes and m, n_x, n_y are integers.

In conclusion, we have succeeded in deriving an explicit expression for the wavefunction of a quantum particle confined in a storage ring or transport line. We have stressed the correspondence between classical and quantum motion by showing that they can both be described in terms of the functions $\beta_{x,y}(z)$ and $D(z)$, which obey the same equations in both cases. With the appropriate choice of the boundary conditions these can be identified as the lattice functions one is familiar with from accelerator theory.

We would like to acknowledge C. Hill, S. De Martino, F. Illuminati for useful discussions during the Workshop and in particular R. Fedele for pointing out a mistake in one of our equations. We have also benefited from many discussions with A. Kabel. Work supported by the US Dept. of Energy.

References

1. A. Kabel, Quantum Ground State and Minimum Emittance of Fermionic Particle Beam in a Circular Accelerator, these Proceedings.
2. Z. Huang, P. Chen, and R. D. Ruth, *Phys. Rev. Lett.* **74** 1759 (1995); Z. Huang and R .D. Ruth *Phys. Rev. Lett.* **80** 2318 (1998).
3. C. Hill, The Diffractive Quantum Limits of Particle Colliders, these Proceedings.
4. H. R. Lewis and W. B. Risenfield, *J. Math. Phys.* **10**, 1458 (1969); I. A. Malkin, V. I. Man'ko, and D. A.Trifonov, *Phys. Rev D*, **2** 8, p. 1371 (1970); L. S. Brown, *Phys. Rev. Lett.* **66**, 5, 527 (1991).
5. R. Jagannathan, *Phys. Rev.* A 42 6674-6689 (1990); see also the papers by R. Jagannathan and S.A. Khan in these Proceedings.
6. R. Fedele and G. Miele, *Phys. Rev.* A46, 6634 (1992); R. Fedele, G. Miele and L. Palumbo, *Phys. Lett.* A194 113-118 (1994).
7. R. D. Ruth, Single-Particle Dynamics and Nonlinear Resonances in Circular Accelerators, in *Lecture Notes in Physics* 247, (Springer-Verlag, New York 1986); Z. Huang, Radiative Cooling of Relativistic Electron Beams, Ph. D. Thesis, SLAC-R-527.
8. E. Merzbacher, *Quantum Mechanics* (J.Wiley & Sons, New York, 1970); C. Cohen-Tannoudji, et al., *Quantum Mechanics*, (J.Wiley & Sons, New York, 1977).

QUANTUM–LIKE APPROACH TO BEAM DYNAMICS - APPLICATION TO THE LHC AND HIDIF PROJECTS.

M. PUSTERLA
Dipartimento di Fisica and INFN – Padova (Italy)
E-mail: pusterla@pd.infn.it

The propagator formalism of Q.M. is here applied, within the quantum-like theory, to estimate beam losses and HALO phenomenon in accelerators. The application to the LHC and HIDIF projects appears very interesting and promising.

1 Motivations in favour of the Quantum–like model.

Each charged particle of a bunch moves according to classical mechanics under the instantaneous resultant of all the forces (external and internal) due to the elements of the lattice and to the presence of the other particles.

The whole system of the forces can be described, in a stable regime, by an average force space–time dependent, connected with a potential field, plus fluctuations.

The latter are not predictable because they are caused by intrabeam scattering, beam–bremstrahlung radiation emission and reabsorption within the same bunch, unavoidable defects and variations of the $\bar{E}, \bar{B}$ fields of the lattice. All these effects must be treated globally as random terms: under the assumption that this stochasticity is Markovian and Brownian, one arrives at a description of the motion that coincides formally with the wave quantum mechanics (Nelson–Guerra [3,4]; see also refs. [1,2] and the lecture of Cufaro–Petroni at this conference) with a new interpretation of the physical parameters (in particular Planck's constant substituted by the normalized emittance $\epsilon_N = \oint pdq$).

2 Advantages.

The whole apparatus and the exact solutions of the non–relativistic Q.M. can be used, obviously with a different interpretation of the parameters as said above.

Within such a context we can deal with the propagator approach [5] of Q.M. after linearizing the Schrodinger–like equation in the description of the betatron and synchrotron motions for the beam wave function. Indeed the propagator method appears very adequate for the calculation of the beam losses and the HALO profile with the introduction of one parameter, namely

a diffraction slit that represents, in a phenomenological manner, the forces acting on the beam particles not considered in detail; in particular we refer to the non linearities. The slit aperture may be taken either as a segment $(-b, +b)$ or in a Gaussian form, ($e^{-\frac{x^2}{2b^2}}$, more suitable for calculations).

3 Formalism for the transversal oscillation.

The Schrödinger–like equation is:

$$i\epsilon\partial_t\psi = -\frac{\epsilon^2}{2m}\partial_x^2\psi + U(x,t)\psi \tag{1}$$

where U is the potential field that is a functional of $|\psi|^2$ in the non–linear case; ϵ is the normalized emittance that is simply connected with the usual (natural) emittence $\tilde{\epsilon}$ as follows: $\epsilon = m_0 c\gamma\beta\tilde{\epsilon}$ (γ, β, are the usual relativistic function of v).

The covolution property of the path integral formula for the propagator $K(x_f, t_f|x_i, t_i)$ [5] allows us its computation as a function of the slit aperture:

$$K(x+x_0, T+\tau|x', 0) = \int_{-b}^{+b} dy K(x+x_0, T+\tau|x_0+y, T)\cdot K(x_0+y, T|x', 0) \tag{2}$$

where T coincides in our case, with the time spent to inject the bunch, τ, is the total time spent by the beam in the accelerator (total time of revolutions in a ring). We may approximate the betatronic oscillations in two ways: a) free particle motion within the apertures; b) harmonic oscillator.

If we substitute the rigid slit $(-b, +b)$ with the Gaussian one ($e^{-x^2/2b^2}$) the integration becomes elementary. In both cases a) and b) we consider an initial Gaussian profile for the beam (transversal) with the wave function $f(x) = \left[\frac{\alpha}{\pi}\right]^{1/4}$ exp $\{-\frac{\alpha}{2}x^2\}$, and after assuming $x_0 = 0$ as an initial central point, we obtain for the final beam wave function $\phi(x)$:

$$\phi(x) = \int_{-\infty}^{+\infty} dx' [\frac{\alpha}{\pi}]^{1/4} \cdot e^{-\frac{\alpha}{2}x'^2} \cdot K(x, T+\tau|x', 0) = B \exp\{Cx^2\} \tag{3}$$

<u>case a)</u>:

$$B = \left[\frac{m}{2\pi i\epsilon}\right]^{1/2} \cdot [T + \tau + T\tau\frac{i\epsilon}{mb^2}]^{-1/2} \cdot [\frac{\alpha}{\pi}]^{1/4}.$$

$$\cdot \left[\frac{\pi}{\frac{\alpha}{2} - \frac{im}{2\epsilon T} - \frac{m^2/2\epsilon^2 T^2}{\frac{im}{T}(\frac{1}{T}+\frac{1}{\tau}) - \frac{1}{b^2}}} \right]^{1/2}$$

$$C = \frac{im}{2\epsilon\tau} + \frac{m^2/2\epsilon^2 T^2}{\frac{im}{\epsilon}(\frac{1}{T}+\frac{1}{\tau}) - \frac{1}{b^2}} + \frac{\frac{\tau^2}{T^2}\left[\frac{m^2/2\epsilon^2 T^2}{\frac{im}{\epsilon}(\frac{1}{T}+\frac{1}{\tau}) - \frac{1}{b^2}}\right]}{\frac{\alpha}{2} - \frac{im}{2\epsilon T} - \frac{m^2/2\epsilon^2 T^2}{\frac{im}{\epsilon}(\frac{1}{T}+\frac{1}{\tau}) - \frac{1}{b^2}}}$$

case b): [N.B. Index ω is inserted in the parameters B and C of eq. 3 where referred to the case b)].

$$B_\omega = [\frac{\alpha}{\pi}]^{1/4} \left[\frac{\tilde{C}}{\alpha - 2\tilde{B}}\right]^{1/2} \qquad C_\omega = \tilde{A} + \frac{\tilde{C}^2}{2(\alpha - 2\tilde{B})}$$

where

$$\tilde{A} = \frac{im\omega}{\epsilon} \cdot \frac{\cos(\omega\tau)}{\sin(\omega\tau)} - \left(\frac{m\omega}{2\epsilon}\right)^2 \frac{1}{\sin^2(\omega r)} \frac{1}{D}$$

$$\tilde{B} = i\frac{m\omega}{2\epsilon} \frac{\cos(\omega T)}{\sin(\omega T)} - (\frac{m\omega}{2\epsilon})^2 \frac{1}{\sin^2(\omega T)} \frac{1}{D}$$

$$\tilde{C} = -\left(\frac{m\omega}{2\epsilon}\right)^2 \frac{2}{\sin(\omega r) \cdot \sin(\omega T)} \frac{1}{D}$$

$$D = \frac{1}{2b^2} - \frac{im\omega}{2\epsilon} \left(\frac{\cos(\omega\tau)}{\sin(\omega\tau)} + \frac{\cos(\omega T)}{\sin(\omega T)}\right)$$

For the case a) the distribution is $\rho(x) = |\phi(x)|^2 = |B|^2 = |B|^2 \exp\{-\tilde{\alpha}x^2\}$ with $\tilde{\alpha} = -(C + C^*)$ and the total probability of losing a particle $P = \int_{-\infty}^{+\infty} \rho(x)dx = |B|^2\sqrt{\frac{\pi}{\tilde{\alpha}}}$.
For the case b) the distribution is $\rho_\omega(x) = |\phi_\omega(x)|^2 = |B_\omega|^2 \exp\{-\tilde{\alpha}_\omega x^2\} =$ with

$$\tilde{\alpha} = -(C_\omega + C_\omega^*)$$

whereas the total probability of losing one particle

$$P_\omega = \int_{-\infty}^{+\infty} \rho_\omega(x)dx = |B_\omega|^2 \sqrt{\frac{\pi}{C_\omega + C_\omega^*}} \tag{4}$$

If we use these formulas and consider the LHC (CERN/AC/95–05) and the HIDIF (GSI–98–06) parameters we end up with the following table [6,7];

Table 1. Circular machine: tranverse case

Parameters	LHC (at injection	HIDIF (storage ring)
Normalized Transverse Emittance	3.75 mm mrad	13.5 mm mrad
Total Energy, E	450 GeV	5 GeV
$\frac{1}{\sqrt{\sigma}}$	1.2 mm	1.0 mm
T	25 nano sec.	100 nano sec.
τ	88 sec.	4.66 sec.
b	1.2 mm	1.0 mm
$\frac{1}{\sqrt{\bar{\alpha}}}$	1.41×10^9 m	1.96×10^7 m
P	3.39×10^{-5}	2.37×10^{-3}
ω	4.44×10^6 Hertz	1.15×10^7 Hertz
$\frac{1}{\sqrt{\alpha_\omega}}$	1.03×10^2 m	2.07×10^{-1} m
P_ω	3.40×10^{-5}	3.00×10^{-3}

4 Longitudinal motion

.

The Quantum–like approach in the propagator version must be able to treat the longitudinal synchrotron motion also. In this case however the physical interpretation of the slit parameter appears less simple (see conclusive remarks).

The non–linear equation for the beam wave function ψ:

$$i\epsilon_N \partial_t \psi = -\frac{\epsilon_N^2}{2\gamma^3 m_0}\partial_z^2 \psi + \frac{1}{2} m_0 \omega^2 z^2 \psi + \wedge |\psi|^2 \tag{5}$$

$\omega \equiv$ synchrotron frequency,
$\wedge \equiv$ non–linear coupling
$z \equiv$ longitudinal displacement related the sinchronous particle.

Preliminary results are summarized in tables 2 and 3.

Table 2. Circular machine: longitudinal case

Parameters	LHC (at injection)
Normalized Transverse Emittance	1.00 eV sec.
Total Energy, E	450 GeV
$\frac{1}{\sqrt{\alpha}}$	7.7 cm
T	25 nano sec.
τ	88 sec.
b	7.7 m
ω	4.23×10^2 Hz
$\frac{1}{\sqrt{\alpha}}$	1.14×10^6 m
P_ω	0.575

Table 3. RF main linac of HIDIF

Parameters	
Normalized Transverse Emittance	0.7 keV nano sec.
Total Energy, E	5 GeV
$\frac{1}{\sqrt{\alpha}}$	15 cm
T	75 micro sec.
τ	4.9×10^{-4} sec.
b	15 m
ω	4.13×10^5 Hz
$\frac{1}{\sqrt{\alpha}}$	6.72×10^{-2} m
P_ω	0.707

5 Conclusive comments on transversal motion

The Quantum-like method, in particular its propagator version, with the addition of phenomenological parameters appears a simple powerful tool for the study of the evolution of the transversal bunch profile in linear, circular accelerators colliders and storage rings. Indeed very few parameters (in our case the slit "b") allow us to calculate how the bunches evolve owing to the forces (linear and non–linear) acting on the particles. In this context the mechanism

of the diffraction appears an adequate phenomenological approach: the probability, local and total, for a particle leaving its position gives us the desired information on the creation of a halo around the main flux. The parameter "b" represents several physical processes that cannot be described in detail such as space–charge, intrabeam scattering, beamstrahlung etc.. and in other non–linear effects.

We finally remark the following points:
a) the total probabilities, per particle, calculated from the free particle propagator (P) and from the harmonic oscillator (P_ω) appear very close to each other for both LHC and HIDIF rings; however the local distributions between these two cases look quite different;
b) the HIDIF scenario, as expected because of the higher intensity, shows a loss of particles (and beam power) at least 10^3 times superior in comparison with LHC.

Both scenarios are however under control: losses of the beam power much smaller than the acceptable 1 Watt/m.

Comments on the longitudinal motion.

Here the calculations are still very preliminary. The probability of making the particle stay within the segment $(-b, +b)$ is almost 1 ($P_\omega \simeq 0.7$ for HIDIF and ~ 0.57 for LHC) but b tends to be very large (order of 10 m).

This fact might be interpreted as bunches tending to create a coasting beam (undesirable). However the meaning of the parameters is still under analysis and unclear.

References

1. See R. Fedele and G. Miele, *Il Nuovo Cimento* D **13**, 1527 (1991); R.Fedele, F. Galluccio, V.I. Man'ko and G. Miele *Phys. Lett.* A **209**, 263 (1995); Ed. R. Fedele and P.K. Shuka *Quantum–Like Models and Coherent Effects* Proc. of the 27^{th} Workshop of the INFN Eloisatron Project Erice, Italy 13–20 June 1994 (World Scientific, 1995); R. Fedele, "Quantum–like aspects of particle beam dynamics", in:*Proceedings of the 15^{th} Advanced ICFA Beam Dynamics Workshop on Quantum Aspects of beam Physics, Ed.* P. Chen, (World Scientific, Singapore, 1999); R. Fedele and V.G. Vaccaro, Physica Scripta **T52** 36–39 (1994). See also: N.C. Petroni, S. De Martino, S. De Siena, and F. Illuminati, A. stochas-

tic model for the semiclassical collective dynamics of charged beams in particle accelerators, in: *Proceedings of the 15th Advanced ICFA Beam Dynamics Workshop on Quantum Aspects of beam Physics, Ed.* P.Chen, (World Scientific, Singapore, 1999).

2. Sameen A. Khan and Modesto Pusterla, **Quantum mechanical aspects of the halo puzzle**, in Proceedings of the *1999 Particle Accelerator Conference* **PAC99** (29 March – 02 Aprile 1999, New York City, NY) *Editors* A. Luccio and W. MacKay, (IEEE Catalogue Number: 99CH36366) pp. 3280–3281.
   Sameen A. Khan and Modesto Pusterla, **Quantum–like approaches to the beam halo problem,** *To appear in*: Proceedings of the *6th International Conference on Squeezed States and Uncertainty Relations* **ICSSUR'99**, (24–29 May 1999, Napoli, Italy) (NASA Conference Pubblication Series)
3. E. Nelson, Phys. Rev. **50** 1079 (1966); Dynamical theories of Brownian motion (Princeton University Press, Princeton 1967)
4. Francesco Guerra, Phys. Rep. **77** 263–312 (1981)
5. Formular (3-33) in R.P. Feynman and A.R. Hibbs, Quantum Mechanics and Path Integrals, (McGraw–Hill, New York)
6. Ed. P. Lefevre and T. Pettersson, Large Hadron Collider (LHC) Conceptual Design CERN/AC/95–05(LHC) (October 1995).
7. Ed. I. Hofmann and G. Plass, Heavy Ion Driven Inertial Fusion (HIDIF) Study GSI–98–06 Report (August 1998)

QUANTUM MECHANICS OF DIRAC PARTICLE BEAM OPTICS: SINGLE-PARTICLE THEORY

R. JAGANATHAN
The Institute of Mathematical Sciences
4th Cross Road, Central Institutes of Technology Campus
Tharamani, Chennai - 600113, Tamilnadu, INDIA
E-mail: jagan@imsc.ernet.in - URL: http://www.imsc.ernet.in/~jagan

It has been found that quantum corrections can substantially affect the classical results of tracking for trajectories close to the separatrix. Hence the development of a basic formalism for obtaining the quantum maps for any particle beam optical system is called for. To this end, it is observed that several aspects of quantum maps for the beam optics of spin-$\frac{1}{2}$ particles can be studied, at the level of single particle dynamics, using the proper formalism based on the Dirac equation.

1 Introduction

The theory of particle beam optics, currently used in the design and operation of various beam devices, from electron microscopes to accelerators, is largely based on classical mechanics and classical electrodynamics. Such a treatment has indeed been very successful in practice. Of course, whenever it is essential, quantum mechanics is used in accelerator physics to understand those quantum effects which are prominent perturbations to the leading classical beam dynamics. [1] The well-known examples are quantum excitations induced by synchrotron radiation in storage rings, the Sokolov-Ternov effect of spin polarization induced by synchrotron radiation, etc. Recently, attention has been drawn by Hill [2] to the limits placed by quantum mechanics on achievable beam spot sizes in particle accelerators, and the need for the formulation of quantum beam optics relevant to such issues. [3] In the context of electron microscopy scalar wave mechanics is the main tool to understand the image formation and its characteristics, and the spin aspects are not generally essential. [4]

In the context of accelerator physics it should be certainly desirable to have a unified framework based entirely on quantum mechanics to treat the orbital, spin, radiation, and every aspect of beam dynamics, since the constituents of the beams concerned are quantum particles. First, this should help us understand better the classical theory of beam dynamics. Secondly, there is already an indication that this is necessary too: it has been found [5] that quantum corrections can substantially affect the classical results of tracking

for trajectories close to the separatrix, leading to the suggestion that quantum maps can be useful in finding quickly the boundaries of nonlinear resonances. Thus, a systematic formalism for obtaining the relevant quantum maps is required. This problem is addressed here for the case of spin-$\frac{1}{2}$ particle beams, at the level of single particle dynamics as the first step towards a more comprehensive theory.

2 Quantization of the classical particle beam optics

If the spin is ignored, one may consider obtaining the relevant quantum maps for any beam optical system by quantizing the corresponding classical treatment directly. The best way to do this is to use the Lie approach to classical beam dynamics, thoroughly developed by Dragt *et al.*, [6] particularly in the context of accelerator physics. Ignoring the effect of spin on the orbital motion, the spin motion has also been treated classically, independent of the orbital motion, using Lie methods. [7]

Let the single particle optical Hamiltonian corresponding to a classical beam optical system be $\mathcal{H}(\underline{r}_\perp, \underline{p}_\perp; z)$, where z is the coordinate along the optic axis of the system, and $\underline{r}_\perp = (x, y)$ and $\underline{p}_\perp = (p_x, p_y)$ represent the coordinates and conjugate momenta, respectively, in the transverse (x, y)-plane. We shall assume the beam to be moving in the positive z-direction. Then for any observable of the system, $\mathcal{O}(\underline{r}_\perp, \underline{p}_\perp)$, not explicitly dependent on z, the z-evolution equation, or the beam optical equation of motion, is

$$\frac{d\mathcal{O}}{dz} =: -\mathcal{H} : \mathcal{O}\,, \tag{1}$$

where the Lie operator $: f :$ associated with any function of the transverse phase-space variables, $f(\underline{r}_\perp, \underline{p}_\perp)$, is defined through the Poisson bracket,

$$: f : g = \{f, g\} = \left(\frac{\partial f}{\partial x}\frac{\partial g}{\partial p_x} - \frac{\partial f}{\partial p_x}\frac{\partial g}{\partial x}\right) + \left(\frac{\partial f}{\partial y}\frac{\partial g}{\partial p_y} - \frac{\partial f}{\partial p_y}\frac{\partial g}{\partial y}\right)\,. \tag{2}$$

When the Hamiltonian $\mathcal{H}$ is z-independent the solution of Eq. (1) can be written down as

$$\begin{aligned}
\mathcal{O}\left(z_f\right) &= \exp(\ell : -\mathcal{H} :)\mathcal{O}\left(z_i\right) \\
&= \mathcal{O}\left(z_i\right) + \ell(: -\mathcal{H} : \mathcal{O})\left(z_i\right) + \left(\ell^2/2!\right)\left(: -\mathcal{H} :^2 \mathcal{O}\right)\left(z_i\right) \\
&\qquad + \left(\ell^3/3!\right)\left(: -\mathcal{H} :^3 \mathcal{O}\right)\left(z_i\right) + \ldots \\
&= \mathcal{O}\left(z_i\right) + \ell\left(\{-\mathcal{H}, \mathcal{O}\}\right)\left(z_i\right) + \left(\ell^2/2!\right)\left(\{-\mathcal{H}, \{-\mathcal{H}, \mathcal{O}\}\}\right)\left(z_i\right) \\
&\qquad + \left(\ell^3/3!\right)\left(\{-\mathcal{H}, \{-\mathcal{H}, \{-\mathcal{H}, \mathcal{O}\}\}\}\right)\left(z_i\right) + \ldots\,,
\end{aligned} \tag{3}$$

relating $\mathcal{O}(z_i)$, the value of $\mathcal{O}$ at an initial z_i, with $\mathcal{O}(z_f)$, its value at a final z_f, where $z_f > z_i$ and $\ell = (z_f - z_i)$. When the Hamiltonian depends on z we would have

$$\mathcal{O}(z_f) = \left(\wp \left[\exp\left(\int_{z_i}^{z_f} dz : -\mathcal{H} : \right) \right] \mathcal{O} \right)(z_i) = \left(\mathcal{M}(z_f, z_i)\, \mathcal{O} \right)(z_i) \ , \qquad (4)$$

where the transfer map, $\mathcal{M}(z_f, z_i)$, a Lie transformation, is now an z-ordered exponential.

To obtain the quantum mechanical formalism for the above system we can follow the canonical quantization rule $\{\ ,\ \} \longrightarrow \frac{1}{i\hbar}[\ ,\ ]$ where $[\ ,\ ]$ represents the commutator bracket between the corresponding quantum operators. This turns Eq. (1) into the Heisenberg equation of motion

$$\frac{d\hat{\mathcal{O}}}{dz} = \frac{i}{\hbar} \left[\hat{\mathcal{H}}, \hat{\mathcal{O}} \right] \ , \qquad (5)$$

where the quantum Hamiltonian operator $\hat{\mathcal{H}}$, and $\hat{\mathcal{O}}$ for any observable, are obtained from their respective classical counterparts by the replacement

$$\underline{r}_\perp \longrightarrow \hat{\underline{r}}_\perp = \underline{r}_\perp = (x, y) \, , \qquad \underline{p}_\perp \longrightarrow \hat{\underline{p}}_\perp = -i\hbar \underline{\nabla}_\perp = \left(-i\hbar \frac{\partial}{\partial x}, -i\hbar \frac{\partial}{\partial y} \right) \ , \qquad (6)$$

followed by a symmetrization to ensure that the quantum operators are hermitian.

From the Heisenberg picture of Eq. (5) let us go to the Schrödinger picture in which a wavefunction $\psi(\underline{r}_\perp; z)$ is associated with the transverse plane at z. The z-evolution of $|\psi(z)\rangle$ is governed by the beam optical Schrödinger equation

$$i\hbar \frac{\partial}{\partial z} |\psi(z)\rangle = \hat{\mathcal{H}} |\psi(z)\rangle \, . \qquad (7)$$

Since $|\psi(\underline{r}_\perp; z)|^2$ will represent the probability density in the transverse plane at z the average of any $\hat{\mathcal{O}}$ at z will be

$$\langle \hat{\mathcal{O}} \rangle (z) = \int \int dx dy \psi^*(z) \hat{\mathcal{O}} \psi(z) = \langle \psi(z) | \hat{\mathcal{O}} | \psi(z) \rangle \, , \qquad (8)$$

with $\psi(\underline{r}_\perp; z)$ normalized as $\langle \psi(z) | \psi(z) \rangle = 1$.

The formal solution of Eq. (7) is, with $|\psi_i\rangle = |\psi(z_i)\rangle$ and $|\psi_f\rangle = |\psi(z_f)\rangle$,

$$|\psi_f\rangle = \hat{U}(z_f, z_i) |\psi_i\rangle = \hat{U}_{fi} |\psi_i\rangle \, , \qquad \hat{U}_{fi} = \wp \left[\exp\left(-\frac{i}{\hbar} \int_{z_i}^{z_f} dz \hat{\mathcal{H}} \right) \right] \ . \qquad (9)$$

Thus, we get

$$\langle\hat{\mathcal{O}}\rangle_f = \langle\hat{\mathcal{O}}\rangle(z_f) = \langle\psi_f|\hat{\mathcal{O}}|\psi_f\rangle = \langle\psi_i|\hat{U}_{fi}^\dagger\hat{\mathcal{O}}\hat{U}_{fi}|\psi_i\rangle = \langle\hat{U}_{fi}^\dagger\hat{\mathcal{O}}\hat{U}_{fi}\rangle_i\,. \qquad (10)$$

From the correspondence between Eq. (1) and Eq. (5) it follows immediately that

$$\hat{U}_{fi}^\dagger\hat{\mathcal{O}}\hat{U}_{fi} = \left(\wp\left[\exp\left(\int_{z_i}^{z_f} dz : \frac{i}{\hbar}\hat{\mathcal{H}} :\right)\right]\right)\hat{\mathcal{O}} = \hat{\mathcal{M}}\,(z_f, z_i)\,\hat{\mathcal{O}}\,, \qquad (11)$$

with the definition : $\frac{i}{\hbar}\hat{\mathcal{H}}$: $\hat{\mathcal{O}} = \frac{i}{\hbar}\left[\hat{\mathcal{H}}, \hat{\mathcal{O}}\right]$. Note that in the classical limit, when : $\frac{i}{\hbar}\hat{\mathcal{H}}$: $\hat{\mathcal{O}} \longrightarrow$: $-\mathcal{H}$: $\mathcal{O}$, the quantum Lie transformation $\hat{\mathcal{M}}\,(z_f, z_i)$ becomes the classical Lie transformation $\mathcal{M}\,(z_f, z_i)$. This shows that if a system corresponds classically to a map

$$(\underline{r}_{\perp i}, \underline{p}_{\perp i}) \longrightarrow (\underline{r}_{\perp f}, \underline{p}_{\perp f}) = (\underline{R}_\perp(\underline{r}_{\perp i}, \underline{p}_{\perp i}), \underline{P}_\perp(\underline{r}_{\perp i}, \underline{p}_{\perp i}))\,, \qquad (12)$$

then it will correspond to a map of quantum averages as given by

$$\langle\hat{\underline{r}}_\perp\rangle_i \longrightarrow \langle\hat{\underline{r}}_\perp\rangle_f = \langle\hat{\underline{R}}_\perp(\hat{\underline{r}}_\perp, \hat{\underline{p}}_\perp)\rangle_i\,, \quad \langle\hat{\underline{p}}_\perp\rangle_i \longrightarrow \langle\hat{\underline{p}}_\perp\rangle_f = \langle\hat{\underline{P}}_\perp(\hat{\underline{r}}_\perp, \hat{\underline{p}}_\perp)\rangle_i\,. \qquad (13)$$

To see what Eq. (13) implies let us consider, for example, a classical Lie transformation $\exp\left(: \frac{a}{3}x^3 :\right)$ corresponding to a kick in the xz-plane by a thin sextupole. This leads to the classical phase-space map

$$x_f = x_i\,, \qquad p_f = p_i + ax_i^2\,, \qquad (14)$$

as follows from Eq. (4). This would correspond to the quantum Lie transformation $\exp(: \frac{a}{3}\hat{x}^3 :)$ which leads, as seen from Eq. (13), to the following map for the quantum averages:

$$\langle\hat{x}\rangle_f = \langle\hat{x}\rangle_i\,, \quad \langle\hat{p}\rangle_f = \langle\hat{p}\rangle_i + a\langle\hat{x}^2\rangle_i = \langle\hat{p}\rangle_i + a\langle\hat{x}\rangle_i^2 + a\langle(\hat{x} - \langle\hat{x}\rangle)^2\rangle_i\,. \qquad (15)$$

Now, we can consider the expectation values, such as $\langle\hat{x}\rangle$ and $\langle\hat{p}\rangle$, as corresponding to their classical values *à la* Ehrenfest. Then, as the above simple example shows, generally, the leading quantum effects on the classical beam optics can be expected to be due to the uncertainties in the initial conditions like the term $a\langle(\hat{x} - \langle\hat{x}\rangle)^2\rangle_i$ in Eq. (15). As pointed out by Heifets and Yan, [5] such leading quantum corrections involve the Planck constant $\hbar$ not explicitly but only through the uncertainty principle which controls the minimum limits for the initial conditions. This has been realized earlier also, [8,9,10] particularly in the context of electron microscopy. [8,9] In a detailed study [5] of a simple example it has been found that trajectories close to the separatrix are strongly perturbed in spite of very small initial rms (10^{-15}) and small (1500) number of turns.

As is clear from the above, a quantum formalism derived from the classical beam optics can be expected to give all the leading quantum corrections to the classical maps. The question that arises is how to go beyond and obtain the quantum maps more completely starting *ab initio* with the quantum mechanics of the concerned system since such a process should lead to other quantum corrections not derivable simply from the quantization of the classical optical Hamiltonian. Essentially, one should obtain the quantum beam optical Hamiltonian $\hat{\mathcal{H}}$ of Eq. (7) directly from the original time-dependent Schrödinger equation of the system. Once $\hat{\mathcal{H}}$ is obtained Lie methods [6,7] can be used to construct the quantum z-evolution operator $\hat{U}_{fi}$ and study the consequent quantum maps. Derivations of $\hat{\mathcal{H}}$ for the Klein-Gordon and Dirac particle beams will be discussed in the following sections.

A more complete theory, even at the level of optics, must take into account multiparticle effects. To this end, it might be profitable to be guided by the models developed by Fedele *et al.* [11,12] (thermal wave model - TWM) and Cufaro Petroni *et al.* [13] (stochastic collective dynamical model - SCDM) for treating the beam phenomenologically as a quasiclassical many-body system. Though the details of approach and interpretation are different, both these models suggest phenomenological Schrödinger-like wavefunction descriptions for the collective motion of the beam. In TWM the beam emittance plays the role of $\hbar$. In SCDM it is argued that $\hbar$ is to be replaced by an effective unit of beam emittance given in terms of the Compton wavelength of the beam particle and the number of particles in the beam. It may be noted that Lie algebraic tools can be used to handle any Schrödinger-like equation.

3 Using the Klein-Gordon equation ignoring the spin

One may consider getting a theory of quantum maps for spin-$\frac{1}{2}$ particle beam optical system based on the Klein-Gordon equation ignoring the spin. For this, one has to transform the equation

$$\left(i\hbar\frac{\partial}{\partial t} - q\hat{\phi}\right)^2 \Psi\left(\underline{r}_\perp, z; t\right) = \left\{c^2\left[\hat{\underline{\pi}}_\perp^2 + \left(-i\hbar\frac{\partial}{\partial z} - q\hat{A}_z\right)^2\right] + m^2c^4\right\}\Psi\left(\underline{r}_\perp, z; t\right) , \quad (16)$$

into the beam optical form in Eq. (7); in Eq.(16) q is the charge of the particle, $\hat{\pi}_\perp = (\hat{\pi}_x, \hat{\pi}_y) = (\hat{p}_x - q\hat{A}_x, \hat{p}_y - q\hat{A}_y)$, $\hat{\underline{\pi}}_\perp^2 = \hat{\pi}_x^2 + \hat{\pi}_y^2$, and ϕ and $\underline{A} = (A_x, A_y, A_z)$ are, respectively, the scalar and vector potentials of the electric and magnetic fields of the optical system ($\underline{E} = -\underline{\nabla}\phi$, $\underline{B} = \underline{\nabla} \times \underline{A}$).

In the standard relativistic quantum theory, [14] Feshbach-Villars and Foldy-Wouthuysen techniques are used for reducing the Klein-Gordon equation to its nonrelativistic approximation plus the relativistic corrections. Applying analogous techniques in the special case of a quasiparaxial ($|\underline{p}_\perp| \ll p_z$) monoenergetic beam propagating through a system with time-independent fields one can reduce Eq. (16) to the beam optical form of Eq. (7) with $\hat{\mathcal{H}}$ containing a leading paraxial part followed by nonparaxial parts. [8,9,15] In this case the wavefunction in Eq. (16) can be assumed to be of the form

$$\Psi(\underline{r}_\perp, z; t) = \psi(\underline{r}_\perp; z) \exp\left[\frac{i}{\hbar}\left(p_0 z - Et\right)\right] , \tag{17}$$

where p_0 is the design momentum of the beam and $E = +\sqrt{c^2 p_0^2 + m^2 c^4}$. Then the resulting time-independent equation for $\psi(\underline{r}_\perp; z)$ can be regarded as describing the scattering of the beam particle by the system and transformed into an equation of the type in Eq. (7). [8,9,15]

For example, for a normal magnetic quadrupole lens with $\underline{A} = (0, 0, \frac{1}{2}K(x^2 - y^2))$, where K is nonzero inside the lens region and zero outside,

$$\hat{\mathcal{H}} \approx \frac{1}{2p_0}\left(\hat{p}_x^2 + \hat{p}_y^2\right) - \frac{1}{2}qK\left(\hat{x}^2 - \hat{y}^2\right) + \frac{1}{8p_0^3}\left(\hat{p}_x^2 + \hat{p}_y^2\right)^2 + \frac{qK\hbar^2}{4p_0^4}\left(\hat{p}_x^2 - \hat{p}_y^2\right) . \tag{18}$$

It must be noted that while the first three terms of $\hat{\mathcal{H}}$ in Eq. (18) are exactly the terms derivable by direct quantization of the classical beam optical Hamiltonian the last, $\hbar$-dependent, term is a quantum correction not derivable from the classical theory. Though such $\hbar$-dependent terms may seem to be too small, particularly for high energy beams, they may become effective when there are large fluctuations in the initial conditions since they essentially modify the coefficients in the classical maps.

4 The proper theory using the Dirac equation

For a spin-$\frac{1}{2}$ particle beam the proper theory should be based on the Dirac equation if one wants to treat all the aspects of beam optics including spin evolution and spin-orbit interaction. In such a case the Schrödinger equation to start with is

$$i\hbar\frac{d}{dt}\Psi\left(\underline{r}_\perp, z; t\right) = \hat{H}\Psi\left(\underline{r}_\perp, z; t\right) , \tag{19}$$

where Ψ is now a 4-component spinor and $\hat{H}$ is the Dirac Hamiltonian

$$\hat{H} = \beta mc^2 + q\hat{\phi} + c\underline{\alpha}_\perp \cdot \hat{\underline{\pi}}_\perp + c\alpha_z\left(-i\hbar\frac{\partial}{\partial z} - q\hat{A}_z\right) - \mu_a \beta \underline{\Sigma} \cdot \underline{B} , \tag{20}$$

including the Pauli term to take into account the anomalous magnetic moment μ_a. In Eq. (20) all the symbols have the usual meanings as in the standard Dirac theory. [14] Considering the special case of a quasiparaxial monoenergetic beam we can take $\Psi(\underline{r}_\perp, z; t)$ to be of the form in Eq. (17). Then the 4-component $\psi(\underline{r}_\perp; z)$ satisfies the time-independent Dirac equation

$$\left[\beta mc^2 + q\hat{\phi} + c\underline{\alpha}_\perp \cdot \hat{\underline{\pi}}_\perp + c\alpha_z \left(-i\hbar\frac{\partial}{\partial z} - q\hat{A}_z\right) - \mu_a \beta \underline{\Sigma} \cdot \underline{B}\right] \psi(\underline{r}_\perp; z) = E\psi(\underline{r}_\perp; z) \ . \quad (21)$$

describing the scattering of the beam particle by the system.

Actually Eq. (21) has the ideal structure for our purpose since it is already linear in $\frac{\partial}{\partial z}$. So one can readily rearrange the terms in it to get the desired form of Eq. (7). However, it is difficult to work directly with such an equation since there are problems associated with the interpretation of the results using the traditional Schrödinger position operator. [16] In the standard theory the Foldy-Wouthuysen (FW) transformation technique is used to reduce the Dirac Hamiltonian to a form suitable for direct interpretation in terms of the nonrelativistic part and a series of relativistic corrections. Derbenev and Kondratenko (DK) [17] used the FW technique to get their Hamiltonian for radiation calculations. Heinemann and Barber [18] have reviewed the derivation of the DK Hamiltonian and have used it to suggest a quantum formulation of Dirac particle beam physics, particularly for polarized beams, in terms of machine coordinates, observables, and the Wigner function.

In an independent and different approach an FW-like technique has been used to develop a systematic formalism of Dirac particle beam optics in which the aim has been to expand the Dirac Hamiltonian as a series of paraxial and nonparaxial approximations [8,9,10,19,20]. This leads to the reduction of the original 4-component Dirac spinor to an effective 2-component $\psi(\underline{r}_\perp; z)$ which satisfies the accelerator optical Schrödinger equation [20]

$$i\hbar\frac{\partial}{\partial z}\psi(\underline{r}_\perp; z) = \hat{\mathcal{H}}\psi(\underline{r}_\perp; z) \ , \qquad \psi(\underline{r}_\perp; z) = \begin{pmatrix} \psi_1(\underline{r}_\perp; z) \\ \psi_2(\underline{r}_\perp; z) \end{pmatrix} \ , \quad (22)$$

where $\hat{\mathcal{H}}$ is a 2×2 matrix operator incorporating the Stern-Gerlach (SG) spin-orbit effect and the Thomas-Bargmann-Michel-Telegdi (TBMT) spin evolution. As is usual in accelerator theory the spin operator $\underline{S} = \frac{1}{2}\hbar\underline{\sigma}$ entering the accelerator optical Hamiltonian $\hat{\mathcal{H}}$ refers to the rest frame of the moving particle. Further, $(\hat{x}, \hat{y})$ and $(\hat{p}_x, \hat{p}_y)$ in $\hat{\mathcal{H}}$ correspond to the observed particle position and momentum components in the transverse plane. It should be noted that the 2-component $\psi(\underline{r}_\perp; z)$ of Eq. (22) is an accelerator optical ap-

proximation of the original 4-component Dirac spinor, valid for any value of the design momentum p_0 from nonrelativistic to extreme relativistic region.

For the normal magnetic quadrupole lens the accelerator optical Hamiltonian reads

$$\hat{\mathcal{H}} \approx \frac{1}{2p_0}\left(\hat{p}_x^2+\hat{p}_y^2\right) - \frac{1}{2}qK\left(\hat{x}^2-\hat{y}^2\right) + \frac{1}{8p_0^3}\left(\hat{p}_x^2+\hat{p}_y^2\right)^2 + \frac{q^2K^2\hbar^2}{8p_0^3}\left(\hat{x}^2+\hat{y}^2\right) + \frac{(q+\gamma\epsilon)K}{p_0}\left(\hat{x}S_y+\hat{y}S_x\right) , \tag{23}$$

where $\gamma = E/mc^2$ and $\epsilon = 2m\mu_a/\hbar$. The last spin-dependent term accounts for the SG kicks in the transverse phase-space and the TBMT spin evolution. As in the Klein-Gordon case of Eq. (18), $\hat{\mathcal{H}}$ of Eq. (23) also contains all the terms derivable from the classical theory plus the quantum correction terms. But, it must be noted that the scalar quantum correction term in Eq. (23)) (4th term) is not the same as the 4th term in Eq. (18). Thus, besides in the $\hbar$-dependent effects of spin on the orbital quantum map (*e.g.*, the last term in Eq. (23)), even in the $\hbar$-dependent scalar quantum corrections the Dirac particle has its own signature different from that of the Klein-Gordon particle.

5 Conclusion

The problem of obtaining the quantum maps for phase-space transfer across particle beam optical systems has been reviewed. The leading quantum corrections to the classical maps are mainly due to the initial uncertainties and involve the Planck constant $\hbar$ not explicitly but only through the minimum limits set by the uncertainty principle. These corrections can be obtained by direct quantization of the Lie algebraic formalism of classical particle beam optics. The Klein-Gordon and Dirac theories add further subtle, $\hbar$-dependent, corrections which may become effective when there are large fluctuations in the initial uncertainties. Contrary to the common expectation the scalar approximation of the Dirac theory is not completely equivalent to the Klein-Gordon theory. All aspects of quantum maps for spin-$\frac{1}{2}$ particle beams, including spin evolution and spin-orbit effects, can be studied, at the level of single particle dynamics, using the proper formalism based on the Dirac equation.

Acknowledgements

I am grateful to M. Pusterla and R. Fedele who made it possible for me to participate in the QABP2K Workshop through financial support, by INFN-

Napoli and INFN-Padova, for international travel, and accommodation expenses at Napoli and Capri. My special thanks are due to R. Fedele for the kind hospitality and stimulating discussions during my visit to the INFN-Napoli. I am thankful to S. De Siena, S. De Martino, and F. Illuminati for the warm hospitality and useful discussions during my visit to the Department of Physics, University of Salerno, during the week of the Mini Workshop on Quantum Methodologies in Beam Physics.

References

1. See, *e.g.*, the following and references therein: *Handbook of Accelerator Physics and Engineering*, eds. A. W. Chao and M. Tigner (World Scientific, Singapore, 1999) (Hereafter referred to as *HAPE*); *Quantum Aspects of Beam Physics*, ed. P. Chen (World Scientific, Singapore, 1999) (Hereafter referred to as *QABP-I*); *Proceedings of this Workshop* (Hereafter referred to as *QABP-II*).
2. C. T. Hill, *arXiv:hep-ph/0002230*, and in *QABP-II*.
3. See also M. Venturini, in *QABP-II*.
4. For an excellent survey of electron wave optics see P. W. Hawkes and E. Kasper, *Principles of Electron Optics - 3: Wave Optics* (Academic Press, San Diego, 1994).
5. S. Heifets and Y. T. Yan in *QABP-I*.
6. See, *e.g.*, the following and references therein: A. J. Dragt, in *QABP-II*; A. J. Dragt, *Lie Methods for Nonlinear Dynamics with Applications to Accelerator Physics*, University of Maryland Physics Department Report (2000); A. J. Dragt, *Lie Algebraic Methods for Ray and Wave optics*, University of Maryland Physics Department Report (1998); E. Forest, *Beam Dynamics: A New Attitude and Framework* (Harwood Academic, 1998); M. Venturini, *Exact Map Computation, and the Problem of Dispersion in Space Charge Dominated Beams*, Ph.D. Thesis, University of Maryland, 1998; A. J. Dragt, F. Neri, G. Rangarajan, D. R. Douglas, L. M. Healy, and R. D. Ryne, *Ann. Rev. Nucl. Part. Sci.* **38**, 455 (1988); E. Forest and K. Hirata, *A Contemporary Guide to Beam Dynamics*, Technical Report No. 92-12, KEK; Articles of J. Irwin and A. J. Dragt, A. J. Dragt, M. Berz, H. Yoshida, and Y. T. Yan in *HAPE*.
7. K. Yokoya in *HAPE*.
8. R. Jagannathan and S. A. Khan, in *Advances in Imaging and Electron Physics*, Vol. 97, ed. P. W. Hawkes (Academic Press, San Diego, 1996).
9. S. A. Khan, *Quantum Theory of Charged Particle Beam Optics*, Ph.D. Thesis, University of Madras, 1997.

10. R. Jagannathan and S. A. Khan, *ICFA Beam Dynamics Newsletter* No. 13, 21 (1997).
11. See the following and references therein: R. Fedele and G. Miele, *Il Nuovo Cimento D***13**, 1527 (1991); R. Fedele, G. Miele, and L. Palumbo, *Phys. Lett. A***194**, 113 (1994); *Quantum-like Models and Coherent Effects*, eds. R. Fedele and P. K. Shukla (World Scientific, Singapore, 1995); *New Perspectives in the Physics of Mesoscopic Systems: Quantum-like Descriptions and Macroscopic Coherence Phenomena*, eds. S. De Martino, S. De Nicola, S. De Siena, R. Fedele, and G. Miele (World Scientific, Singapore, 1997); D. Anderson, R. Fedele, V. Vaccaro, M. Lisak, A. Berntson, and S. Johansson, *Phys. Lett. A***258**, 244 (1999); R. Fedele, M. A. Man'ko, and V. I. Man'ko, *J. Opt. Soc. Am. A***17**, No. 12 (2000); R. Fedele and V. I. Man'ko, in *QABP-I*; R. Fedele, in *QABP-II*; M. A. Man'ko, in *QABP-II*.
12. S. A. Khan and M. Pusterla, in *Proceedings of the Particle Accelerator Conference PAC'99*, eds. A. Luccio and W. MacKay (IEEE, New York, 1999); S. A. Khan and M. Pusterla, *Eur. Phys. J. A***7**, 583 (2000); M. Pusterla, in *QABP-II*.
13. See the following and references therein: N. Cufaro Petroni, S. De Martino, S. De Siena, and F. Illuminati, in *QABP-I*; N. Cufaro Petroni, S. De Martino, S. De Siena, and F. Illuminati, *Stochastic collective dynamics of charged-particle beams in the stability regime* (to appear in *Phys. Rev. E*); N. Cufaro Petroni, S. De Martino, S. De Siena, and F. Illuminati in *QABP-II*.
14. See, *e.g.*, J. D. Bjorken and S. D. Drell, *Relativistic Quantum Mechanics* (McGraw Hill, New York, 1964).
15. S. A. Khan and R. Jagannathan, *Phys. Rev. E* **51**, 2510 (1995).
16. See, *e.g.*, I. M. Ternov, *Sov. Phys. JETP* **71**, 654 (1990).
17. Ya. S. Derbenev and A. M. Kondratenko, *Sov. Phys. JETP* **37**, 968 (1973).
18. K. Heinemann and D. P. Barber, in *QABP-I* and references therein.
19. R. Jagannathan, R. Simon, E. C. G. Sudarshan, and N. Mukunda, *Phys. Lett. A***134**, 457 (1989); R. Jagannathan, in *Dirac and Feynman: Pioneers in Quantum Mechanics*, ed. R. Dutt and A. K. Ray (Wiley Eastern, New Delhi, 1993); R. Jagannathan, *Phys. Rev. A***42**, 6674 (1990).
20. M. Conte, R. Jagannathan, S. A. Khan, and M. Pusterla, *Part. Accel.* **56**, 99 (1996); Articles of R. Jagannathan, M. Pusterla, and S. A. Khan in *QABP-I*; S. A. Khan, in *QABP-II*.

QUANTUMLIKE MODELS IN BEAM PHYSICS AND SIGNAL ANALYSIS

M. A. MAN'KO
P. N. Lebedev Physical Institute, Leninskii Prospect 53, Moscow 117924 Russia
E-mail: mmanko@sci.lebedev.ru

The application of tomographic map introduced recently in quantum mechanics is discussed in connection with classical problems which are described by equations formally coinciding with the equations of quantum theory. Examples of the classical problems such as the charged-particle-beam transport and analytic-signal analysis are reviewed.

1 Introduction

The aim of this contribution is to discuss some quantumlike aspects of the classical charged-particle-beam transport and to point out that there exists the quantumlike formalism in another classical domain — signal analysis. The consideration presented is based on new results obtained recently in quantum mechanics and related to the so-called tomographic method of measuring quantum states of photons in quantum optics and trapped ions in atomic physics. Recent progress in these quantum domains gave the possibility of theoretical progress in the description of quantum states in terms of tomographic probabilities (which are conventional positive probability distributions) instead or alternatively to the description in terms of wave functions or density matrices.

The well-known quantumlike phenomenon is the classical propagation of beams of electromagnetic radiation in optical fibers and in the other types of optical waveguides. The propagation of these beams (which are paraxial) is described in the Fock–Leontovich approximation[1,2] by the Schrödinger-like equation, where the Planck's constant is replaced by the wavelength. Recently in the charged-particle-beam transport the thermal wave model was suggested,[3] which also corresponds to the quantumlike description of the classical phenomenon. The last quantumlike example which will be discussed is classical signal analysis, where the main object of investigation is analytic signal. It is known that analytic signal is described by a complex function of time mathematically identical to the wave function of quantum mechanics.

Thus, we will discuss the classical but quantumlike phenomena of beam physics making accent on a more detailed review of the thermal wave model of the charged-particle-beam transport. Also a new approach of noncommutative tomography[4] of analytic signal will be discussed as an example of the application of new results obtained in quantum mechanics to signal analysis.

The quantumlike description of states of the charged-particle beam was also considered within the framework of tomographic probability,[5,6] used in the tomographic representation of quantum states, where the standard probability stands instead of the wave function.[7,8] Noncommutative tomography of analytic signal introduced by Mendes and Man'ko[4] was used for the description of analytic signal depending both on time and the spatial variable.[9]

The paper is organized as follows. The wave function and Schödinger equation of quantum mechanics are reviewed and the thermal wave model for charged-particle beams is discussed in Sec. 2. Properties of the Fock–Leontovich approximation for paraxial beams of electromagnetic radiation are studied in Sec. 3. The density matrix and Wigner function in quantum mechanics are considered in Sec. 4. In Sec. 5 the Moyal-like equation for the Wigner function is derived. Tomographic probability for the charged-particle-beam transport is presented in Sec. 6. Quantumlike integrals of motion for the charged-particle-beam transport are introduced in Sec. 7 and the charged-particle-beam propagators in different representations are studied in Sec. 8. Noncommutative tomography of analytic signal is reviewed in Sec. 9. Conclusions, remarks, and perspectives are presented in Sec. 10.

2 Wave Function and Thermal Wave Model

The state of a quantum particle is described by a complex wave function $\Psi(x,t)$ which obeys the Schrödinger evolution equation

$$i\hbar\,\frac{\partial\Psi(x,t)}{\partial t} = -\frac{\hbar^2}{2m}\,\frac{\partial^2\Psi(x,t)}{\partial x^2} + U(x,t)\,\Psi(x,t)\,, \tag{1}$$

where x and m are the particle's position and mass, respectively, t is time, $\hbar$ is the Planck's constant, and $U(x,t)$ is the particle's potential energy which can vary with time.

The thermal wave model was suggested to describe the charged-particle-beam transport in the pioneer work by Fedele and Miele.[3] A year later the similar model was considered by Datolli et al.[10] The thermal wave model was developed in series of publications (see, for example,[11,12]). Within the framework of thermal wave model, the electron beam is described by a beam wave function $\psi(x,z)$ where x and z are transversal and longitudinal coordinates, respectively, (we consider the planar situation). The complex beam wave function obeys the Schrödinger-like equation (for a particle with mass $m=1$)

$$i\epsilon\,\frac{\partial\psi(x,z)}{\partial z} = -\frac{\epsilon^2}{2}\,\frac{\partial^2\psi(x,z)}{\partial x^2} + U(x,z)\,\psi(x,z)\,, \tag{2}$$

where the parameter ϵ is the beam emittance $\epsilon = 2\left[\langle x^2\rangle\langle p^2\rangle - \langle xp\rangle^2\right]^{1/2}$, with $\langle x^2\rangle$ and $\langle p^2\rangle$ being the dispersion of coordinate and momentum, respectively, and the momentum being $p = dx/dz$ (a dimensionless variable). Thus, emittance plays a role of the beam size in the phase space, which describes the thermal spreading of electronic rays. It is small for small temperatures being scaled as $\sqrt{T}$. In view of the physical meaning of the beam wave function, $|\psi(x,z)|^2\, dx = P(x,z)\, dx$ is the number of charged particles at the longitudinal coordinate z in the interval dx around the transversal coordinate x in the beam's cross-section.

3 Fock–Leontovich Approximation for Paraxial Beams of Electromagnetic Radiation

There exist examples of classical processes such as electromagnetic paraxial beams propagating in media, which can be described using the formalism of quantum-mechanics equations, as it was shown by Fock and Leontovich in their study of the propagation of electromagnetic waves along the Earth's surface.[1,2] Another example was considered in our group in Lebedev while studying the electromagnetic-field propagation in the so-called active waveguides (active region of diode lasers based on the heterostructures in compound semiconductors) and passive waveguides (fiber optics).[13,14]

Fock and Leontovich have shown that the wave equation for paraxial beams of the electromagnetic field radiation can be reduced to a Schrödinger-like equation (the so-called parabolic approximation), where the Planck's constant is replaced by the inverse of the wave number and time is replaced by the longitudinal coordinate z:

$$i\lambda\,\frac{\partial\psi(x,z)}{\partial z} = -\frac{\lambda^2}{2n_0(z)}\,\frac{\partial^2\psi(x,z)}{\partial x^2} + U(x,z)\,\psi(x,z) \tag{3}$$

(again we cosider the planar configuration). In Eq. (3), $\lambda = 2\pi/k$ is the wavelength in vacuum and $U(x,z)$ is an effective potential related to the refractive index of medium $n(x,z)$ as $U(x,z) = \left[2\,n_0(z)\right]^{-1}\left[n_0^2(z) - n^2(x,z)\right]$, with $n_0(z)$ being the refractive index of medium at the beam axis. The complex function $\psi(x,z)$ is slowly varying amplitude of the electric field

$$E(x,z) = \left[n_0(z)\right]^{-1/2}\,\psi(x,z)\,\exp\left[ik\int_0^z n_0(\xi)\,d\xi\right]. \tag{4}$$

Thus, one can see that the thermal wave model for the charged-particle-beam transport plays the same role as the Fock–Leontovich approximation does in the theory of electromagnetic-wave propagation in media.

4 Density Matrix and Wigner Function in Quantum Mechanics

Another motivation for the possibility to use the thermal wave model is clear from the arguments, which we adopted from a review paper[12] and present below. First of all, one needs to remind the notion of density matrix[15] and Wigner function[16] in quantum mechanics. The density matrix of a pure quantum state $\rho_\Psi\,(x,x',t)$ is related to the wave function $\Psi\,(x,t)$ as

$$\rho_\Psi\,(x,x',t) = \Psi\,(x,t)\;\Psi^*\,(x',t)\;. \tag{5}$$

The Wigner function $W\,(x,p)$ is related to the wave function $\Psi\,(x,t)$ as

$$W\,(x,p) = \int \Psi\,(x+u/2\,,t)\;\Psi^*\,(x-u/2\,,t)\;e^{-ipu/\hbar}\;du/\hbar\,, \tag{6}$$

and it obeys the equation found by Moyal[17]

$$\frac{\partial W}{\partial t} + p\,\frac{\partial W}{\partial x} + \frac{i}{\hbar}\left[U\left(x + i\,\frac{\hbar}{2}\,\frac{\partial}{\partial p}\right) - U\left(x - i\,\frac{\hbar}{2}\,\frac{\partial}{\partial p}\right)\right] W = 0\,, \tag{7}$$

where U is potential energy and the argument of this potential energy is replaced by the differential operators.

5 Moyal-like Equation for Charged-Particle Beam

Now we duscuss the possibility to associate the quantumlike equation to the classical kinetic equation.[5,6,12] We consider the classical Boltzman equation for the classical distribution function $\rho\,(x,p,z)$ with a coordinate z instead of time

$$\frac{\partial \rho}{\partial z} + p\,\frac{\partial \rho}{\partial x} - \left(\frac{\partial U}{\partial x}\right)\frac{\partial \rho}{\partial p} = 0\,; \tag{8}$$

this equation describes the phase-space evolution of electronic rays.

The key ansatz if the following. The derivative of the potential can be replaced by the difference term

$$\frac{\partial U}{\partial x} \approx \frac{U\,(x+\epsilon/2) - U\,(x-\epsilon/2)}{\epsilon}\,, \tag{9}$$

where a parameter ϵ (called emittance) describes a size of beam spreading inside which the electronic rays are indistinguishable due to thermal fluctuations. Since for small ϵ,

$$\frac{U\left(x+\frac{i\,\epsilon}{2}\right) - U\left(x-\frac{i\,\epsilon}{2}\right)}{i\,\epsilon}\,i\,\frac{\partial \rho}{\partial p} \approx \frac{U\left(x+\frac{i\,\epsilon}{2}\,\frac{\partial}{\partial p}\right) - U\left(x-\frac{i\,\epsilon}{2}\,\frac{\partial}{\partial p}\right)}{i\,\epsilon}\,\rho\,, \tag{10}$$

which is the other important step, one obtains the equation

$$\frac{\partial \rho}{\partial z} + p\,\frac{\partial \rho}{\partial x} + \frac{i}{\epsilon}\left[U\left(x + \frac{i\,\epsilon}{2}\,\frac{\partial}{\partial p}\right) - U\left(x - \frac{i\,\epsilon}{2}\,\frac{\partial}{\partial p}\right)\right]\rho = 0\,. \qquad (11)$$

In fact, the presented procedure is a logic jump, but it is compatible with the approximate formulas discussed. Nevertheless, this logic jump provides the clear picture how the quantumlike equation can "naturally" emerges from the classical equation.

6 Tomographic Probability for Charged-Particle-Beam Transport

The beam wave function can be mapped on the probability density (tomographic probability) $w\,(X, \mu, \nu)$ in the form

$$w\,(X, \mu, \nu) = \frac{1}{2\,\pi|\nu|}\left|\int \psi(y)\,\exp\left(\frac{i\mu}{2\,\nu}\,y^2 - \frac{ix}{\nu}\,y\right)\,dy\right|^2. \qquad (12)$$

The physical meaning of the real variable X and real parameters μ and ν is the following. The beam wave function is an analog of the wave function in quantum mechanics which is a function of the particle's position. If one measures the particle's position X in scaled and rotated reference frame in the particle's phase space, the relationship arises

$$X = \mu q + \nu p\,, \qquad \mu = e^{\lambda}\cos\theta\,, \qquad \nu = e^{-\lambda}\sin\theta\,, \qquad (13)$$

where θ is a rotation angle of the reference frame and λ is a scaling parameter. Thus, for the charged-particle beam, the random variable X and parameters μ and ν are quantumlike analogs of the quantum particle's position measured in the reference frame in the phase space labeled by two real parameters — rotation and scaling. One can invert the map (up to a constant phase factor):

$$\psi(y)\,\psi^*\,(y') = \frac{1}{2\,\pi}\int w\,(X, \mu, y - y')\,\exp\left[i\left(X - \mu\,\frac{y + y'}{2}\right)\right]\,d\mu\,dX\,. \qquad (14)$$

Transform

$\psi(y) \Rightarrow w\,(X, \mu, \nu)$ is related to the fractional Fourier transform.[9]

For the normalized states, the tomographic probability is also normalized and it can be used to reconstruct the beam Wigner function as well.[12]

7 Quantumlike Integrals of Motion for the Charged-Particle-Beam Transport

Within the framework of quantumlike thermal wave model, one can describe the integrals of motion of charged-particle beam, which are operators $\widehat{I}(z)$ with the property

$$\frac{d}{dz}\langle\widehat{I}(z)\rangle = \frac{d}{dz}\int \psi^*(x,z)\,\widehat{I}(z)\,\psi(x,z)\;dx = 0\,. \tag{15}$$

Equation (15) means that the average value of the quantumlike observable $\widehat{I}(z)$ does not change along the longitudinal coordinates z.

For example, for z-dependent quadrupole lens with the potential

$$U(x,z) = k_1(z)\,x^2/2, \tag{16}$$

one has two linear in position $\widehat{x}$ and momentum $\widehat{p}$ integrals of motion:

$$\widehat{A}(z) = \frac{i}{\sqrt{2}}\left[\xi(z)\left(-i\frac{\partial}{\partial x}\right) - \dot{\xi}(z)x\right]; \tag{17}$$

$$\widehat{A}^\dagger(z) = -\frac{i}{\sqrt{2}}\left[\xi^*(z)\left(-i\frac{\partial}{\partial x}\right) - \dot{\xi}^*(z)x\right], \tag{18}$$

with (18) being the Hermitian conjugate operator of (17).

In Eqs. (17) and (18) the function $\xi(z)$ satisfies the differential equation

$$\ddot{\xi}(z) + k_1(z)\,\xi(z) = 0\,, \tag{19}$$

where we take units with $k_1(0) = 1$, $\epsilon = 1$. The initial conditions for the solution of Eq. (19) $\xi(0) = 1$, $\dot{\xi}(0) = i$ provide the commutation relations of the oscillator's creation and annihilation operators to the integrals of motion (17) and (18). The integrals of motion $\widehat{A}(z)$ and $\widehat{A}^\dagger(z)$ are related to the initial position and momentum operators:

$$\widehat{x}_0(z) = \frac{\widehat{A}(z) + \widehat{A}^\dagger(z)}{\sqrt{2}}\,; \qquad \widehat{p}_0(z) = \frac{\widehat{A}(z) - \widehat{A}^\dagger(z)}{i\sqrt{2}}\,. \tag{20}$$

There exist other integrals of motion for the electronic beam, which are arbitrary functions either of the initial position and momentum operators $\widehat{x}_0(z)$ and $\widehat{p}_0(z)$ or of the operators $\widehat{A}(z)$ and $\widehat{A}^\dagger(z)$.

8 Charged-Particle-Beam Propagator

In quantum mechanics, there exists the notion of quantum propagator (or the Green function of the Schrödinger evolution equation). Also there exists a propagator for the Wigner function (the Green function of the Moyal evolution equation). The quantumlike propagator $G\,(x,x',z)$ describes the evolution of the beam wave function $\psi(x,z)=\int G\,(x,x',z)\,\psi(x',0)\;dx'$.

The propagator is connected with the integrals of motion

$$\widehat{x}_0(z)\,G\,(x,x',z)=x'G\,(x,x',z)\,; \tag{21}$$

$$\widehat{p}_0(z)\,G\,(x,x',z)=i\epsilon\,\frac{\partial}{\partial x'}\,G\,(x,x',z)\,. \tag{22}$$

There exist two other propagators:

(i) $\Pi\,(x,p,x',p',z)$ for the Wigner function of the quantum particle

$$W\,(x,p,z)=\int\Pi\,(x,p,x',p',z)\;W\,(x',p',0)\;\;dx'\;dp'; \tag{23}$$

(ii) $\Pi\,(X,\mu,\nu,X',\mu',\nu',z)$ for the tomographic probability of the charged-particle beam

$$w\,(X,\mu,\nu,z)=\int\Pi\,(X,\mu,\nu,X',\mu',\nu',z)\;w\,(X',\mu',\nu',0)\;\;dX'\;d\mu'\;d\nu'\,. \tag{24}$$

The influence of the aberration potential $V(x',z')$ can be described by means of perturbation theory analogously to the case of quantum mechanics. Thus, the influence of aberration for the beam wave function $\psi(x,z)$ in a first approximation is given by the relationship:

$$\psi(x,z)=\psi_0(x,z)+\frac{1}{i}\int_0^z dz'\int G_0\,(x,x',z,z')\;V\,(x',z')\,\psi_0(x',z')\;\;dx'\,, \tag{25}$$

where $\psi_0(x,z)$ and $G_0\,(x,x',z,z')$ are the beam wave function and the beam propagator without aberration, respectively.

The same procedure for the influence of aberration potential can be developed for the Wigner function and tomographic probability. The result of the consideration[6] follows

(i) for the Wigner-like function:

$$\rho_\omega\,(x,p,z)=\rho_\omega^{(0)}(x,p,z)-i\int_0^z dz'\int\Pi_0(x,p,x',p',z,z')$$
$$\times\left[V\left(x'+\frac{i}{2}\,\frac{\partial}{\partial p'}\,,z'\right)-V\left(x'-\frac{i}{2}\,\frac{\partial}{\partial p'}\,,z'\right)\right]\rho_\omega^{(0)}\,(x',p',z')\,, \tag{26}$$

where $\rho_\omega^{(0)}$ is the solution of the Moyal-like equation for unperturbed Hamiltonian H_0 and Π_0 corresponds to unperturbed Hamiltonian H_0;

(ii) for the tomographic probability:

$$w(X,\mu,\nu,z) = w_0(X,\mu,\nu,z) + \int_0^z dz' \int \widetilde{\Pi}_0(X,\mu,\nu,X',\mu',\nu',z,z')$$
$$\times i\left[V\left(-\frac{1}{\partial/\partial X'}\,\frac{\partial}{\partial\mu'} - \frac{i\nu'}{2}\,\frac{\partial}{\partial X'}, z'\right) - V\left(-\frac{1}{\partial/\partial X'}\,\frac{\partial}{\partial\mu'} + \frac{i\nu'}{2}\,\frac{\partial}{\partial X'}, z'\right)\right]$$
$$\times w_0(X',\mu',\nu',z')\; dX'\, d\mu'\, d\nu'\,, \tag{27}$$

where the propagator $\widetilde{\Pi}_0$ corresponds to the evolution of unperturbed tomographic probability

$$w_0(X,\mu,\nu,z) = \int \widetilde{\Pi}_0(X,\mu,\nu,X',\mu',\nu',z,z')\; w_0(X',\mu',\nu',z')\, dX'\, d\mu'\, d\nu'\,.$$

The function $w_0(X,\mu,\nu,z)$ is the solution of the Fokker–Planck-like equation with unperturbed Hamiltonian H_0.[12] The formulas obtained correspond to a first Born approximation of the perturbation series.

9 Noncommutative Tomography of Analytic Signal

In information processing, the main object to investigate is analytic signal which is described by a normalized complex function of time $f(t)$. Ville introduced a map of the analytic signal onto the quasidistribution function of two variables — time t and frequency ω[18]

$$W(t,\omega) = \int f\,(t+u/2)\; f^*\,(t-u/2)\; e^{-i\omega u}\; du\,, \tag{28}$$

which has the inverse (up to a constant phase factor)

$$f(t)\, f^*\,(t') = (2\,\pi)^{-1} \int W\,(t+t'/2\,,\omega)\; e^{i\omega\,(t-t')}\; d\omega\,. \tag{29}$$

The notion of analytic signal in information processing mathematically is analogous to the notion of wave function in quantum mechanics, and the Ville quasidistribution corresponds to Wigner function of quantum mechanics.[16]

In view of the analogy of quantum mechanics and analytic signal theory, the tomographic approach was introduced into signal analysis by using the probability distribution density

$$w\,(X,\mu,\nu) = \frac{1}{2\,\pi|\nu|}\left|\int f(t)\,\exp\left(\frac{i\mu}{2\,\nu}\,t^2 - \frac{iX}{\nu}\,t\right)\; dt\right|^2\,, \tag{30}$$

which is a simple replacement $y \to t$, $\Psi \to f$ in the corresponding formula of quantum mechanics.[4]

Thus, one has relationships between the Ville–Wigner function $W(t,\omega)$ and the tomographic probability density $w(X,\mu,\nu)$ in signal analysis:

$$W(t,\omega) = \frac{1}{2\,\pi}\int w(X,\mu,\nu)\; e^{-i(X-\mu t-\nu\omega)}\; dX\; d\mu\; d\nu\,; \tag{31}$$

$$w(X,\mu,\nu) = \int W(t,\omega)\,\delta(X-\mu t-\nu\omega)\;\frac{dt\;d\omega}{2\,\pi}\,, \tag{32}$$

which are mathematically identical to the formulas of quantum mechanics.

10 Conclusions and Perspectives

We have demonstrated that there exists a possibility to describe quantumlike processes (classical in their nature) using notions of quantum mechanics such as well-known quasidistributions (like Wigner function) and recently introduced tomographic probabilities. The analytic signal theory is an example where the quantum notion can be used to visualize better the signals' properties. Tomograms of analytic signal can be used to detect noisy signals with small signal-to-noise ratio.[4]

There exists the important perspective to use quantumlike processes to imitate many aspects of purely quantum phenomenon, which are relevant in quantum computing. As we have shown, the electromagnetic radiation in optical fibers obeys to the Schrödinger-like equation due to the Fock–Leontovich approximation. This means that the purely classical signal in optical fibers can be used to code the information analogously to coding the information in quantum computing by the wave function. Several optical fibers imitate then the quantum system with many degrees of freedom. The superposition of electromagnetic fields in optical fiber imitates the phenomenon of entanglement. Tomographic detection of the electromagnetic field in optical fibers is analogous to tomographic measuring the quantum states in quantum computers and quantum communication lines.

Not only optical fibers can be used as imitators of elements of quantum computer. The charged-particle-beam transport within the framework of thermal wave model can be also discussed as an object, which is appropriate to imitate some quantum phenomena. The study of these perspectives needs deeper understanding of the applicability of the quantumlike superposition principle within the framework of thermal wave model.

Acknowledgments

The author thanks the Organizers for kind hospitality, the Russian Foundation for Basic Research for the partial support of this study under Projects Nos. 00-02-16516 and 99-02-17553, and the RF Ministry for Science and Technology for the partial support within the framework of the Programs "Optics. Laser Physics" and "Fundamental Nuclear Physics."

1. M.A. Leontovich, *Izv. Akad. Nauk SSSR, Ser. Fiz.* **8**, 16 (1944).
2. V.A. Fock and M.A. Leontovich, *Zh. Éksp. Teor. Fiz.* **16**, 557 (1946).
3. R. Fedele and G. Miele, *Nuovo Cim.* D **13**, 1527 (1991).
4. V.I. Man'ko and R.V. Mendes, *Phys. Lett.* A **263**, 53 (1999).
5. R. Fedele, M.A. Man'ko, and V.I. Man'ko, *J. Russ. Laser Res.* (Kluwer Academic/Plenum Publishers) **21**, 1 (2000).
6. R. Fedele, M.A. Man'ko, and V.I. Man'ko, *J. Opt. Soc. Am.* A (December 2000, to appear).
7. S. Mancini, V.I. Man'ko, and P. Tombesi, *Phys. Lett.* A **213**, 1 (1996).
8. S. Mancini, V.I. Man'ko, and P. Tombesi, *Found. Phys.* **27**, 801 (1997).
9. M.A. Man'ko, *J. Russ. Laser Res.* (Kluwer Academic/Plenum Publishers) **20**, 226 (1999); **21**, 411 (2000).
10. G. Dattoli, L. Gianessi, C. Mari, M. Rihetta, and A. Torre, *Opt. Commun.* **87**, 175 (1992).
11. R. Fedele and G. Miele, *Phys. Rev.* A **46**, 6634 (1992).
12. R. Fedele and V.I. Man'ko, *Phys. Rev.* E **58**, 992 (1998).
13. M.A. Man'ko and G.T. Mikaelyan, *Sov. J. Quantum Electron.*, **416**, 895 (1986); "Modes and mode conversions in active semiconductor waveguides,"
    in *The Nonlinear Optics of Semiconductor Lasers*,
    Proceedings of the P.N. Lebedev Physical Institute (Nauka, Moscow, 1986), Vol. 166, p. 126 [(Nova Science, Commack,
    New York, 1987), Vol. 166, p. 170].
14. M.A. Man'ko, "Some aspects of nonlinear optics of semiconductor lasers," in *ECOOSA-90 Quantum Optics*, ed. M. Bertolotti (IOP Publishing House, Bristol, 1991), p. 247.
15. J. von Neumann, *Mathematische Grundlagen der Quantenmechanik* (Springer, Berlin, 1932).
16. E. Wigner, *Phys. Rev.* **40**, 749 (1932).
17. J.E. Moyal, *Proc. Cambridge Phylos. Soc.* **45**, 99 (1949).
18. J. Ville, *Cables et Transmission* **2**, 61 (1948).

RADIATIVE CORRECTIONS IN SYMMETRIZED CLASSICAL ELECTRODYNAMICS

J. R. VAN METER[1,2], A. L. TROHA[1,2], D. J. GIBSON[1,2], A. K. KERMAN[3], P. CHEN[4], AND F. V. HARTEMANN[1]

[1]*Institute for Laser Science and Applications, Lawrence Livermore National Laboratory, Livermore, CA 94550*

[2]*Physics Department, University of California, Davis, CA 95616*

[3]*Center for Theoretical Physics and Physics Department,Massachusetts Institute of Technology, Cambridge, MA 02139*

[4]*Stanford Linear Accelerator Center, Stanford, CA 94305*

Abstract The physics of radiation reaction for a point charge is discussed within the context of classical electrodynamics. The fundamental equations of classical electrodynamics are first symmetrized to include magnetic charges: a double 4-potential formalism is introduced, in terms of which the field tensor and its dual are employed to symmetrize Maxwell's equations and the Lorentz force equation in covariant form. Within this framework, the symmetrized Dirac-Lorentz equation is derived, including radiation reaction (self-force) for a particle possessing both electric and magnetic charge. The connection with electromagnetic duality is outlined, and an in-depth discussion of nonlocal 4-momentum conservation for the wave-particle system is given.

1 Introduction

Recently, close attention has been paid to the concept of duality in quantum field theories, as summarized by Witten [1]. In particular, recent work in superstring theory has resulted in the convergence of four main themes: electromagnetic duality in four dimensions, the symmetries of supergravity, dualities in superstring theory, and gauge theory dynamics in four dimensions. Occurrence

The concept of duality in electrodynamics results from the symmetry between the electric and magnetic components of the field tensor: the source-free equations of the Maxwell set are symmetrical in vacuum under the transformation $E \to B$ and $B \to -E$ in addition, the symmetry can be maintained in the presence of 4-currents, provided that both electric and magnetic monopoles are introduced, thus suggesting a deeper hidden symmetry. Since Dirac's brilliant insight on charge quantization [2-4], the role and importance of magnetic monopoles and duality in electrodynamics have taken on a much more profound significance. Feynman and Wheeler first demonstrated the

deep connection between time reversal and charge conjugation [5], while Schwinger proposed to associate the electric and magnetic charge in a single electrically charged monopole, referred to as a dyon [6]. Such a particle should exhibit the full symmetries of the electromagnetic interaction.

Although magnetic monopoles have never been observed, it can be argued that the apparent quantization of electric charge might represent indirect evidence for the existence of magnetic charge. The argument, originally put forth by Dirac [2,3] and later simplified by Saha [7], can be summarized as follows: if a magnetic field with non-zero divergence is added to an electric field with the same property, the total field has non-zero angular momentum, even in the static case. The field angular momentum turns out to be proportional to the product of the charges of the electric and magnetic sources involved, and independent of distance. Since angular momentum is quantized, and assuming that the amount of magnetic charge in the universe is finite, it follows that electric charge must be quantized. Although other explanations have been proposed for the observed quantization of charge, Dirac's argument remains the most elegant. In addition, in 1977, Montonen and Olive showed that in a limiting case of electroweak interaction theory, a particle of electric charge q and magnetic charge g, acquires a mass $m = \langle \psi \rangle \sqrt{q^2 + g^2}$ under spontaneous symmetry breaking, where $\langle \psi \rangle$ is a constant measuring the gauge symmetry breaking [8].

Within this theoretical context, there exists a beautiful and compelling case for studying fully symmetrized versions of classical and quantum electrodynamics (CED and QED); in addition, these theories might also provide the correct approach to demonstrating that CED indeed represents the classical limit of QED, a problem that is still unresolved. This is because the duality of fully symmetrized QED implies that if the electric fine structure constant, $\alpha = \frac{e^2}{2\varepsilon_0 hc} \cong \frac{1}{137.036}$, and its magnetic counterpart, $\frac{1}{\alpha}$. are exchanged, electric and magnetic phenomena will appear to be switched, for a classical observer. This, in turn can be related to the notion of running coupling constants, used in gauge theory dynamics, where two important limiting cases might shed some light on the exact relation between QED and CED: the case where $\alpha \to \infty$, and quantum effects disappear, and the case where the full symmetry between electricity and magnetism is restored, with $\alpha = 1$.

Thus, the main thrust of this paper is to present a classical derivation of radiation reaction for electric and magnetic monopoles, as well as dyons. The approach used here includes a generalization of Dirac's derivation of classical radiation reaction for a point charge from general principles, including gauge invariance and Lorentz covariance [9], where the double 4-potential introduced by Cabbibo and Ferrari [10] is further extended by introducing a complex electromagnetic tensor unifying the conventional

electromagnetic tensor and its dual. In addition, the electric and magnetic 4-currents are unified into a single complex 4-vector, and the connection with electromagnetic duality is now completely explicit: electric and magnetic charges can be rotated into one another, while preserving the global invariance of the symmetrized form of Maxwell's equations. One advantage of the complex 4-potential formalism over Dirac's well-known model of magnetic monopoles is the absence of string-like singularities; in addition, within this framework, one can readily derive a Hamiltonian for dyon-dyon interactions. Finally, our complex notation proves extremely compact, allowing for an elegant derivation of the symmetrized Dirac-Lorentz equation.

This paper is organized as follows: in Section 2, we develop the aforementioned complex double 4-potential formalism; the symmetrized form of the Dirac-Lorentz equation, which describes the dynamics of a dyon with radiation reaction, is derived in Section 3, while the conceptual difficulties associated with this classical model for a point charge are briefly reviewed in Section 4, including electromagnetic mass renormalization, runaways, and acausal effects; finally, conclusions are drawn in Section 5, where the implications of electromagnetic duality for QED are also outlined. In addition, a few technical points and a physical interpretation of the Schott term in terms of nonlocal 4-momentum conservation are presented in Appendices.

2 Symmetrized Electrodynamics

Here, and throughout the remainder of this paper, we use electron units, where length is measured in units of the classical electron radius, $r_0 = e^2 / 4\pi\varepsilon_0 m_0 c^2$, while time is measured in units of r_0/c, mass is measured in units of m_0, electric charge is measured in units of e, and magnetic charge in units of $\hbar / e$. In these units, $\varepsilon_0 = 1/4\pi$, $\mu_0 = 4\pi$, and for a particle of mass m_0, the 4-momentum is equal to the 4-velocity: $p_\mu = u_\mu = d_\tau x_\mu$, where $x_\mu(\tau)$ is the world-line of the particle, and τ is its proper time.

We now focus on the problem of a dyon, having both electric and magnetic charges q and g, respectively [6]. If magnetic sources are allowed, Maxwell's equations become symmetrized as follows:

$$\partial_\nu F^{\mu\nu} = 4\pi j^\mu, \qquad \partial_\nu \tilde{F}^{\mu\nu} = 4\pi g^\mu, \tag{1}$$

where j^{μ} and g^{μ} correspond to the electric and magnetic 4-current densities, and where $\tilde{F}^{\mu\nu}$ is the dual electromagnetic tensor. Here, the 4-gradient operator [11,12] is defined as $\partial_{\mu} \equiv (-\partial_{t}, \boldsymbol{\nabla})$.

Now introducing the electric 4-potential $A_{\mu} = (\phi, \boldsymbol{A})$, and its magnetic counterpart, $V^{\mu} = (\varphi, \boldsymbol{V})$, the field tensor and its dual may be written as

$$F^{\mu\nu} = \partial^{\mu} A^{\nu} - \partial^{\nu} A^{\mu} - \varepsilon^{\mu\nu\alpha\beta} \partial_{\alpha} V_{\beta} \tag{2}$$

and

$$\tilde{F}^{\mu\nu} = \varepsilon^{\mu\nu\alpha\beta} \partial_{\alpha} A_{\beta} + \partial^{\mu} V^{\nu} - \partial^{\nu} V^{\mu}, \tag{3}$$

where $\varepsilon^{\mu\nu\alpha\beta}$ is the completely antisymmetrical Levi-Civita tensor [13]. Applying the Lorentz gauge condition to the 4-potentials, we have $\partial_{\mu} A^{\mu} = 0$ and $\partial_{\mu} V^{\mu} = 0$; and the symmetrized version of Maxwell's equations become

$$\partial_{\nu} \partial^{\nu} A_{\mu} = -4\pi j_{\mu} \tag{4}$$

and

$$\partial_{\nu} \partial^{\nu} V_{\mu} = -4\pi g_{\mu}. \tag{5}$$

At this point, we note that Eqs. (4) and (5) are invariant under the dual transformation

$$A'_{\mu} = A_{\mu} \cos\theta + V_{\mu} \sin\theta, \qquad V'_{\mu} = V_{\mu} \cos\theta - A_{\mu} \sin\theta \tag{6}$$

provided that the charges and 4-currents are also transformed:

$$j'_{\mu} = j_{\mu} \cos\theta + g_{\mu} \sin\theta, \qquad g'_{\mu} = g_{\mu} \cos\theta - j_{\mu} \sin\theta. \tag{7}$$

By analogy with the idea that Lorentz invariance becomes manifest in covariant notation, dual-invariance can be clearly expressed in complex notation: since the dual transformation is essentially a rotation in the complex charge plane, this suggests the notation $\overline{q} = q + ig$, which yields the complex 4-current density $\overline{j}_{\mu} = j_{\mu} + ig_{\mu}$; similarly, the complex 4-potential is defined as $\overline{A}_{\mu} = A_{\mu} + iV_{\mu}$, from which the complex electromagnetic field tensor is derived as:

$$\overline{F}_{\mu\nu} = F_{\mu\nu} + i\tilde{F}_{\mu\nu} = \partial_\mu A_\nu - \partial_\nu A_\mu + i\varepsilon_{\mu\nu\alpha\beta}\partial^\alpha A^\beta . \tag{8}$$

Within this context, the dual transform reduces to

$$\overline{F}'_{\mu\nu} = \overline{F}_{\mu\nu} e^{-i\theta}, \qquad \overline{j}'_\mu = \overline{j}_\mu e^{-i\theta} . \tag{9}$$

This notation also proves extremely compact: the symmetrized form of Maxwell's equations takes the form

$$\partial_\mu \overline{F}^{\mu\nu} = -\partial_\nu \partial^\nu \overline{A}^\mu = 4\pi \overline{j}^\mu , \tag{10}$$

and it is now obvious that Eqs. (8) and (10) are dual-invariant. Within this context, the dual-invariant Lorentz force equation takes the form

$$F_\mu = (qF_{\mu\nu} + g\tilde{F}_{\mu\nu})u^\nu = \mathscr{R}\left(\overline{q}\,\overline{F}^*_{\mu\nu}u^\nu\right). \tag{11}$$

Note that whenever a product between any two complex electromagnetic quantities defined previously is taken, one of the quantities must be complex-conjugated so that its magnetic component changes sign. This operation is analogous to raising and lowering an index in covariant notation, when contracting tensors, so that the sign of the time-like component is reversed: in both cases, the sign reversal ensures the invariance of the product under the respective transform. The duality and Lorentz transforms are both rotations, in 2 and 4-dimensional spaces, respectively.

3 Symmetrized Dirac-Lorentz Equation

To derive the radiation force, two different approaches can be used. First, one can follow Dirac's treatment [9,14] and derive the radiation reaction from general principles including gauge invariance and Lorentz covariance; this is the focus of the present section. The second type of derivation relies on a careful study of the conservation of the 4-momentum of the electromagnetic field [15-18] during the interaction.

In the case of a classical point dyon [6], which possesses both an electric charge q, and a magnetic charge g, the complex 4-current is given by

$$\overline{j}_\mu(x_\nu) = \overline{q}\int_{-\infty}^{+\infty} u_\mu(x'_\nu)\,\delta_4(x_\nu - x'_\nu)\,d\tau', \tag{12}$$

where the integral over proper time allows the use of the invariant 4-dimensional Dirac delta-function, as discussed in Appendix 1.

Now assuming, as Dirac did, that a particle acts on itself through the Lorentz force [9], but using the symmetrized expression thereof, the self-force is

$$F_s^\mu = \mathscr{R}\left[\overline{q}\left(\partial^\mu \overline{A}_s^\nu - \partial^\mu \overline{A}_s^\nu + i\varepsilon^{\mu\nu\alpha\beta}\partial_\alpha \overline{A}_\beta^s\right)^* u_\nu\right], \tag{13}$$

where the complex self-potential satisfies the driven wave equation

$$\partial_\nu \partial^\nu \overline{A}_\mu^s = -4\pi\overline{q}\int_{-\infty}^{+\infty} u(x'_\nu)\,\delta_4(x_\nu - x'_\nu)\,d\tau'. \tag{14}$$

Equation (13) can be written as

$$F_s^\mu = \mathscr{R}\left[\overline{q}\left(\partial^\mu \overline{A}_s^{\nu *} - \partial^\nu \overline{A}_s^{\mu *}\right)u_\nu - i\overline{q}\,\varepsilon^{\mu\nu\alpha\beta}\partial_\alpha \overline{A}_\beta^{s*} u_\nu\right], \tag{15}$$

while the driven wave equation (14) can be solved in terms of Green functions:

$$\overline{A}_\mu^s(x_\lambda) = -4\pi\overline{q}\int_{-\infty}^{+\infty} u_\mu(x'_\lambda)\,G(x_\lambda - x'_\lambda)\,d\tau', \tag{16}$$

where G is the Green function formally defined as $G(x_\lambda - x'_\lambda) \equiv -\left[\partial_\nu\partial^\nu\right]^{-1}\delta_4(x_\lambda - x'_\lambda)$. Using this Green function solution in Eq. (15), it becomes clear that the last term in the square brackets is pure imaginary: $-i\overline{q}\,\varepsilon^{\mu\nu\alpha\beta}\partial_\alpha \overline{A}_\beta^{s*} u_\nu \propto i\overline{q}\,\overline{q}^* = i\left|\overline{q}\right|^2$; thus, the self-force reduces to

$$F_s^\mu = \mathscr{R}\left[\overline{q}\left(\partial^\mu \overline{A}_s^{\nu *} - \partial^\nu \overline{A}_s^{\mu *}\right)u_\nu\right]. \tag{17}$$

Lest this manipulation appears as slight of hand, we depart momentarily from our elegant shorthand to elucidate the reason for the vanishing of the last term in Eq. (15): in terms of real quantities, the self-force reads

$$F_s^\mu = q\left(\partial^\mu A_s^\nu - \partial^\nu A_s^\mu - \varepsilon^{\mu\nu\alpha\beta}\partial_\alpha V_\beta^s\right)u + g\left(\varepsilon^{\mu\nu\alpha\beta}\partial_\alpha A_\beta^s + \partial^\mu V_s^\nu - \partial^\nu V_s^\mu\right)u_\nu; \tag{18}$$

where the electric and magnetic self-potentials are driven by the dyon electric and magnetic 4-currents, with

$$\begin{bmatrix} A \\ V \end{bmatrix}^{s}_{\mu}(x_\lambda) = -4\pi \begin{bmatrix} q \\ g \end{bmatrix} \int_{-\infty}^{+\infty} u_\mu(x'_\lambda)\, G(x_\lambda - x'_\lambda)\, d\tau' , \tag{19}$$

which implies that $V^s_\mu = (g/q) A^s_\mu$. This last relation allows some cancellation in Eq. (18), yielding the simpler expression

$$F^s_\mu = q\left(\partial^\mu A^\nu_s - \partial^\nu A^\mu_s\right) u_\nu + g\left(\partial^\mu V^\nu_s - \partial^\nu V^\mu_s\right) u_\nu \tag{20}$$

in agreement with Eq. (17).

Physically, the disappearance of the cross-terms involving the action of the magnetic self-potential on the electric charge, and that of the electric self-potential on the magnetic charge, is due to the fact that the corresponding ponderomotive self-forces exactly cancel out. This decoupling of the radiation reaction forces is to be expected because the polarization of the radiation generated by the dyon's electric charge is always orthogonal to that radiated by the magnetic charge; thus, there is no interference between the electric and magnetic components of the dyon self-electromagnetic field. Using the explicit form of the Green function in the force equation, we have

$$F^s_\mu(x_\lambda) = -4\pi \left|\overline{q}\right|^2 \int_{-\infty}^{+\infty} u^\nu \left[u'_\nu \partial_\mu - u'_\mu \partial_\nu\right] G(x_\lambda - x'_\lambda)\, d\tau' , \tag{21}$$

where we have used the notation $u'_\mu = u_\mu(x'_\lambda)$.

We now apply Dirac's procedure for finding the self-force in the point limit. The Green function in Eq. (21) depends on the space-time interval $s^2 = (x - x')_\mu (x - x')^\mu$; using s^2 as the independent variable, the 4-gradient operator reads $\partial_\mu \equiv 2(x_\mu - x'_\mu)\partial_{s^2}$, and the self-force is

$$F^s_\mu = -8\pi \left|\overline{q}\right|^2 \int_{-\infty}^{+\infty} d\tau' u^\nu \left[u'_\nu (x_\mu - x'_\mu) - u'_\mu (x_\nu - x'_\nu)\right] \partial_{s^2} G . \tag{22}$$

At this point, we introduce the new variable $\tau'' = \tau - \tau'$, so that the range of integration explicitly includes the electron (singular point at $\tau'' = 0$). To evaluate the integral in Eq. (22), we can now use Taylor-McLaurin expansions in powers of τ'': we first have

$$x_\mu - x'_\mu = x_\mu(\tau) - x_\mu(\tau - \tau'') = \tau'' u_\mu - \tfrac{1}{2}\tau''^2 a_\mu + \tfrac{1}{6}\tau''^3 d_\tau a_\mu + \dots , \qquad (23)$$

where we have used the 4-velocity and 4-acceleration. For the 4-velocity, we have

$$u'_\mu = u_\mu(\tau - \tau') = u_\mu - \tau'' a_\mu + \tfrac{1}{2}\tau''^2 d_\tau a_\mu + \dots . \qquad (24)$$

Using expansions (23) and (24), and factoring, we have

$$\begin{aligned} \frac{u^\nu}{\tau''}\left[u'_\nu(x_\mu - x'_\mu) - u'_\nu(x_\nu - x'_\nu)\right] &= (u^\nu u_\nu)\left(u_\mu - \tfrac{1}{2}\tau'' a_\mu + \tfrac{1}{6}\tau''^2 d_\tau a_\mu\right) \\ &+ \tfrac{1}{2}\tau''^2\left(u^\nu d_\tau a_\nu\right)u_\mu - \left(u_\mu - \tau'' a_\mu + \tfrac{1}{2}\tau''^2 d_\tau a_\mu\right)(u^\nu u_\nu) \\ &- \tfrac{1}{6}\tau''^2\left(u^\nu d_\tau a_\nu\right)u_\mu + \mathcal{O}\left(\tau''^3\right). \end{aligned} \qquad (25)$$

We now use the Lorentz invariant $u^\mu u_\mu = -1$. Differentiating this equation with respect to the proper time τ, we first find that $u_\mu d_\tau u^\mu = 0 = u_\mu a^\mu$; this result corresponds to the fact that the derivative of a vector with fixed length is orthogonal to the original vector: the 4-acceleration is always perpendicular to the 4-velocity. Differentiating a second time with respect to τ, we also have $a_\mu a^\mu = -u_\mu d_\tau a^\mu$ [11,14,17]. Grouping terms, we finally obtain the important result

$$u^\nu\left[u'_\nu(x_\mu - x'_\mu) - u'_\mu(x_\nu - x'_\nu)\right] = \tau''^2\left\{-\tfrac{1}{2}a_\mu + \tfrac{1}{3}\tau''\left[d_\tau a_\mu - u_\mu(a_\nu a^\nu)\right]\right\} + \mathcal{O}\left(\tau''^4\right). \qquad (26)$$

The relation between the space-time interval s^2 and the proper time difference τ'' can be expanded as well: $s^2 = \tau''^2(u_\mu u^\mu) - \tfrac{1}{2}\tau''^3(u_\mu a^\mu + a_\mu u^\mu) + \mathcal{O}\left(\tau''^4\right)$; using the orthogonality of the 4-velocity and 4-acceleration, this reduces to $s^2 = -\tau''^2 + \mathcal{O}\left(\tau''^4\right)$, and we have $\partial_{s^2} G = \left[-(1/2\tau'') + \mathcal{O}(\tau'')\right]\partial_{\tau''} G$.

With this, the expression for the self-force reads

$$F_\mu^s = 4\pi|\overline{q}|^2 \int_{-\infty}^{+\infty} d\tau'' \left\{ -\tfrac{1}{2}\tau'' a_\mu + \tfrac{1}{3}\tau''^2 \left[d_\tau a_\mu - u_\mu (a_\nu a^\nu) \right] + \mathcal{O}\left(\tau''^3\right) \right\} \partial_{\tau''} G \,. \qquad (27)$$

We can integrate Eq. (27) by parts, according to $\int d\tau'' f(\tau'') \partial_{\tau''} G = -\int d\tau'' \left(\partial_{\tau''} f\right) G(\tau'')$, and obtain

$$F_\mu^s = -4\pi|\overline{q}|^2 \int_{-\infty}^{+\infty} d\tau'' \left\{ -\tfrac{1}{2} a_\mu + \tfrac{2}{3}\tau'' \left[d_\tau a_\mu - u_\mu (a_\nu a^\nu) \right] + \mathcal{O}\left(\tau''^2\right) \right\} G(\tau'') \,. \qquad (28)$$

We now use the retarded (causal) Green function [9,14]; Eq. (28) reads

$$\begin{aligned} F_\mu^s = |\overline{q}|^2 \int_{-\infty}^{+\infty} d\tau'' \left\{ -\tfrac{1}{2} a_\mu + \tfrac{2}{3}\tau'' \left[d_\tau a_\mu - u_\mu (a_\nu a^\nu) \right] + O\left(\tau''^2\right) \right\} \\ \times \left(\delta(\tau'')/|\tau''|\right)\left[1 + \left(\tau''/|\tau''|\right)\right], \end{aligned} \qquad (29)$$

where we have used $(x_0 - x_0')/|x_0 - x_0'| = \tau''/|\tau''|$, and $\delta\left(s^2\right) = \delta\left(-\tau''^2\right) = \delta(\tau'')/|\tau''|$. This last identity has to be defined mathematically with care, as discussed in Appendix 2.

We now proceed with the integration of Eq. (29) to obtain

$$F_\mu^s = -\tfrac{1}{2}|\overline{q}|^2 \left[\int_{-\infty}^{+\infty} \left(\delta(\tau'')/|\tau''|\right) d\tau'' \right] a_\mu + \tfrac{2}{3}|\overline{q}|^2 \left[d_\tau a_\mu - u_\mu (a_\nu a^\nu) \right], \qquad (30)$$

which is the sought-after expression for the self-force. Note that we have dropped the antisymmetrical terms in $\left(\tau''/|\tau''|\right)\delta(\tau'')$ and $\left(1/|\tau''|\right)\delta(\tau'')$, and that this expression is exact because all the higher-order terms in the expansion integrate out; this fact is rarely appreciated in the literature. The momentum transfer equation, including the radiation reaction, now reads

$$\left[m + \tfrac{1}{2}|\overline{q}|^2 \int_{-\infty}^{+\infty} \left(\delta(\tau'')/|\tau''|\right) d\tau'' \right] a_\mu = \mathcal{R}\left(\overline{q}\,\overline{F}^*_{\mu\nu} u^\nu\right) + \tfrac{2}{3}|\overline{q}|^2 \left[d_\tau a_\mu - u_\mu (a_\nu a^\nu) \right]. \qquad (31)$$

Equation (31) clearly exhibits the infinite electromagnetic mass, in the form of the divergent integral multiplying the 4-acceleration.

4 Conceptual Difficulties: Electromagnetic Mass Renormalization, Runaways, Acausal Effects

In this section, the main conceptual problems associated with the classical Dirac-Lorentz electron model are reviewed and discussed. The Dirac-Rohrlich asymptotic condition [9,16] is then introduced to determine the physical solutions of the Dirac-Lorentz equation.

As shown in Eq. (31), the mass term contains an infinite contribution from the self-electromagnetic fields of the point dyon. There are two different ways to circumvent this difficulty. First, we can consider that the infinite potential energy associated with a point charge model must be balanced by an infinite binding energy -*W*, such as that produced by the Poincaré stress tensor [16,19,20], so that the finite observed rest mass of the dyon is given in units of m_0 by $m = \frac{1}{2}|\overline{q}|^2 \int \left(\delta(\tau'') / |\tau''| \right) d\tau'' - W$. This procedure is essentially equivalent to mass renormalization in QED. The divergent electromagnetic mass, which is produced by the singular part of the Green function can also be removed by considering the time-symmetrical Green function $G = \frac{1}{2}(G^- - G^+)$, as first proposed by Dirac [9]; here $G^{\pm}$ represent the retarded and advanced Green functions. There is little doubt that the removal of the infinite self-energy of the (non-radiative) Coulomb field is deeply connected to the charge conjugation and time reversal properties of electrodynamics, as exemplified by the Wheeler-Feynman electrodynamics [21,22]; however, the connection is not entirely clear.

Using either approach to renormalize the electromagnetic mass, we finally obtain the complete equation of motion for a particle with arbitrary electric and magnetic charge:

$$m a_\mu = \mathscr{R}\left(\overline{q}\, \overline{F}^*_{\mu\nu} u^\nu \right) + \tfrac{2}{3}|\overline{q}|^2 \left[d_\tau a_\mu - u_\mu (a_\nu a^\nu) \right], \tag{32}$$

where *m* is the renormalized dyon mass. It is manifest that Eq. (32), like the generalized form of Maxwell's equations, is invariant under a duality transform. In the case of an electron, $\overline{q} = -1$, which yields the well-known Dirac-Lorentz equation:

$$a_\mu = -F_{\mu\nu} u^\nu + \tau_0 \left[d_\tau a_\mu - u_\mu (a_\nu a^\nu) \right], \tag{33}$$

where $\tau_0 = \frac{2}{3}$ is the Compton time-scale, expressed in the units of r_0 / c used here. In MKSA units, $\tau_0 = \mu_0 e^2 / 6\pi m_0 c = 0.626 \times 10^{-23}$ s. The first term on the right-hand side is the Lorentz force, while the radiation reaction contain the Schott term [9-12,14-20,23] and the radiation damping force [11,17-19,24].

A very important property of the Dirac-Lorentz equation is the fact that it satisfies energy-momentum conservation, as is easily seen by contracting Eq. (33) with the 4-velocity; we then have

$$u^\mu a_\mu = 0 = -u^\mu F_{\mu\nu} u^\nu + \tfrac{2}{3}\left[u^\mu d_\tau a_\mu - (u^\mu u_\mu)(a_\nu a^\nu) \right], \qquad (34)$$

which is satisfied by virtue of the antisymmetry of the electromagnetic field tensor $F_{\mu\nu}$ and the orthogonality of u_μ and a_μ.

We now briefly review some of the conceptual difficulties associated with the Dirac-Lorentz equation itself. First, it is easily seen that, in the absence of an external field, Eq. (33) can be contracted with a^μ to obtain $a^\mu a_\mu = \frac{1}{2}\tau_0 \, d_\tau (a^\mu a_\mu)$, which admits the so-called "runaway" solution $\left[a^\mu a_\mu \right](\tau) = \left[a^\mu a_\mu \right]_{\tau=0} \exp\left(2\tau / \tau_0 \right)$. Note that this self-excited motion implies that $\left[a^\mu a_\mu \right]_{\tau=0} \neq 0$, and can be eliminated through the use of the appropriate asymptotic conditions, $\lim_{\tau \to \pm\infty} a_\mu(\tau) = 0$, as suggested by Dirac [9] and Rohrlich [16]. This type of boundary condition on the electron motion also satisfies the law of inertia: the electron velocity remains constant when no external force is applied. A detailed analysis of Eq. (33) [16,20] also reveals the existence of acausal, or "pre-acceleration" solutions. This is directly connected to the implicit electromagnetic mass renormalization underlying the Dirac-Lorentz equation: the self-force can be explicitly derived by using the time-symmetrical Green function $G = \frac{1}{2}(G^- - G^+)$ [14], as first noted by Dirac [9]. As a result, although the electron is modeled as a point charge, it can interact electromagnetically with external fields localized within its classical radius: to show the implicit acausality of the Dirac-Rohrlich solution, we recast the Dirac-Lorentz equation in the form [16,20]

$$a_\mu - \tau_0 \, d_\tau a_\mu = K_\mu, \qquad K_\mu = -F_{\mu\nu} u^\nu - \tau_0 u_\mu (a_\nu a^\nu). \qquad (35)$$

Multiplication by the integrating factor $e^{-\tau/\tau_0}$ yields

$$d_\tau\left[a_\mu(\tau)e^{-\tau/\tau_0}\right] = -\left(1/\tau_0\right)e^{-\tau/\tau_0}K_\mu(\tau)\,. \tag{36}$$

Equation (36) can now be formally integrated to obtain

$$a_\mu(\tau) = \exp\left(\tau/\tau_0\right)\int_{-\infty}^{\tau}\exp\left(-\tau'/\tau_0\right)\left[\left(1/\tau_0\right)u^\nu F_{\mu\nu} + u_\mu(a_\nu a^\nu)\right](\tau')\,d\tau'\,. \tag{37}$$

The structure of this formal solution, which implicitly satisfies the Dirac-Rohrlich asymptotic condition, clearly exhibits the acausal convolution integral operator $\int_{-\infty}^{\tau}d\tau'\exp\left(-\tau'/\tau_0\right)$ which "weighs" the externally applied electromagnetic field exponentially within a characteristic space-time interval equal to the classical electron radius. This type of solution does not run away because the pre-acceleration of the electron over the Compton time-scale "launches" it on a stable trajectory. In other words, the preacceleration exactly compensates the runaway instability, and when the external field is applied, the electron executes a motion which conserves the total 4-momentum, including the pump and scattered fields, and asymptotically satisfies the law of inertia.

5 Discussion

At this point, the connection between duality and the fully symmetrized version of electrodynamics can be discussed within the context of a dynamical gauge theory, where the fine structure constant is now a running coupling constant. We start from the Dirac-Schwinger charge quantization condition [6] for electric and magnetic monopoles:

$$\boldsymbol{q}_1\times\boldsymbol{q}_2 = \mathscr{I}\left(\overline{q}_1\overline{q}_2^{\,*}\right)\hat{z} = n\alpha^{-1}\hat{z}, \qquad n\in\mathrm{N} \tag{38}$$

In Eq. (38) the $\hat{z}$-axis corresponds to angular momentum; this is schematically illustrated on Fig. 1 (top) where two different charge state vectors are shown in the complex charge plane for a positron, with $\boldsymbol{q}_1 = \left[\hat{x}\mathscr{R}(\overline{q}_1) + \hat{y}\mathscr{I}(\overline{q}_1)\right] = \hat{x}$, along the electric axis, and a magnetic monopole, $\boldsymbol{q}_2 = \left[\hat{x}\mathscr{R}(\overline{q}_2) + \hat{y}\mathscr{I}(\overline{q}_2)\right] = \hat{y}$, along the magnetic axis. The $\pi/2$ angle between both charge states corresponds to the

orthogonality of the electric and magnetic axes. The total angular momentum of the system is now represented by the cross product of $\boldsymbol{q}_1$ and $\boldsymbol{q}_2$, and is quantized according to Eq. (38). It is clear that a duality transform simply rotates the electric and magnetic axes, as shown in Fig. 1 (top); however, the cross product remains unchanged, as the relative angle between the monopole charge states and their length are preserved by this rotation. Therefore, to fully symmetrize electrodynamics, one needs to take $\alpha = 1$, as first observed by Dirac [2,3], in which case the distinction between electric and magnetic charges disappears. In this case, radiation reaction are equal for an electric or a magnetic point charge interacting with external fields, and the full symmetry of electrodynamics is realized, as illustrated in Fig. 1 (bottom). One of the deepest questions associated with this theory is the exact connection with spin and the Dirac equation of QED [25].

In conclusion, the basic electrodynamic equations for a dyon was presented within the context of a covariant formalism in the complex charge plane. A double-potential formalism has been introduced which aids in the symmetrization of the calculations. An expression for the general self-force of a dyon was derived, and it was found that this expression is proportional to Dirac's expression for the self-force on an electron, differing only by a factor involving the electric and magnetic charge. Dirac's procedure for taking the point limit of the self-force was applied, and the complete electrodynamic equation of motion for a dyon was obtained. Finally, the connection with electromagnetic duality was outlined.

6 Acknowledgments

This work was supported under the auspices of the US DoE by LLNL under contract No. W-7405-ENG-48 through the Institute for Laser Science and Applications. We would like to acknowledge useful discussions with M. Zolotorev; one of us (FVH) would also like to personally acknowledge very stimulating conversations with D.T. Santa Maria.

References

[1] E. Witten, Phys. Today **50**, No. 5, 28 (1997).
[2] P.A.M. Dirac, Proc. R. Soc. London Ser. **A133**, 60 (1931).
[3] P.A.M. Dirac, Phys. Rev. **74**, 817 (1948).
[4] R.P. Feynman, "The reason for antiparticles", in *Elementary Particles and the Laws of Physics* (Cambridge University Press, Cambridge, 1987).

[5] R.P. Feynman, Phys. Rev. **74**, 939 (1948).
[6] J. Schwinger, Phys. Rev. **D12**, 3105 (1975).
[7] M.N. Saha, Phys. Rev. **75**, 1968 (1949).
[8] C. Montonen and D. Olive, Phys. Lett. **B72**, 117 (1977).
[9] P.A.M. Dirac, Proc. R. Soc. London Ser. **A167**, 148 (1938).
[10] N. Cabbibo and E. Ferrari, Nuovo Cimento **23**, 1147 (1962).
[11] W. Pauli, *Theory of Relativity* (Dover, New York, NY, 1958), Secs. 31, 32, 63, 64, 65.
[12] R.P. Feynman, R.B. Leighton and M. Sands, *The Feynman Lectures on Physics* (Addison-Wesley, Reading, MA, 1964), Vol. 2, Chaps. 25-28.
[13] T. Levi-Civita, *The Absolute Differential Calculus* (Dover, New York, 1977).
[14] A.A. Sokolov and I.M. Ternov, *Radiation from Relativistic Electrons* (American Institute of Physics, New York, NY, 1986), Part 1, Part 2, Chap. 11, Part 3.
[15] A. Sommerfeld, *Electrodynamics* (Academic Press, New York, NY, 1964), Vol. 3, Secs. 19, 33, 36, 37.
[16] F. Rohrlich, *Classical Charged Particles* (Addison-Wesley, Reading, MA, 1965), Chaps. 6 and 9.
[17] R. Becker, *Electromagnetic Fields and Interactions* (Blaisdell Publishing Co., New York, NY, 1964), Vol. 1. Chaps. 80,84,85, and Vol. 2, Chap. 4.
[18] F.V. Hartemann and N.C. Luhmann, Jr., Phys. Rev. Lett. **74**, 1107 (1995).
[19] J.D. Jackson, *Classical Electrodynamics* (2nd edition, John Wiley and Sons, New York, NY, 1975), Chaps. 14 and 17.
[20] *Electromagnetism, Paths to Research,* edited by D. Teplitz (Plenum Press, New York and London, 1982), Chaps. 6, by S. Coleman and 7, by P. Pearle.
[21] J.A. Wheeler and R.P. Feynman, Rev. Mod. Phys. **17**, 157 (1945).
[22] J.A. Wheeler and R.P. Feynman, Rev. Mod. Phys. **21**, 425 (1949).
[23] A.O. Barut and N. Zanghi, Phys. Rev. Lett. **52**, 2009 (1984).
[24] H.A. Lorentz, *The Theory of Electrons* (Dover, New York, NY, 1952), 2nd ed., Secs. 26-37, 178-183.
[25] B. Thaller, *The Dirac Equation* (Springer-Verlag, New York, NY, 1992).
[26] R. Courant and D. Hilbert, *Methods of Mathematical Physics* (Interscience Publishers, John Wiley and Sons, New York, NY, 1962), Vol. 2, Chapter 6.
[27] E. Butkov, *Mathematical Physics* (Addison-Wesley, Reading, MA, 1968).
[28] H.A. Haus, Am. J. Phys. **54**, 1126 (1986).
[29] A.O. Barut and N. Unal, Phys. Rev. **A40**, 5404 (1989).
[30] F.V. Hartemann and Z. Toffano, Phys. Rev. **A41**, 5066 (1990).
[31] A.D. Yaghjian, *Relativistic Dynamics of a Charged Sphere* (Springer-Verlag, New York, NY, 1992).
[32] F.V. Hartemann *et al.*, Phys. Rev. **E51**, 4833 (1995).

[33] F.V. Hartemann and A.K. Kerman, Phys. Rev. Lett. **76**, 624 (1996).
[34] W. Pauli, *Pauli Lectures on Physics* (MIT Press, Cambridge, MA, 1973), Vol. 6.
[35] P. Penfield, Jr. and H.A. Haus, *Electrodynamics of Moving Media* (MIT Press, Cambridge, MA, 1967).
[36] P. Poincelot, *Principes et Applications Usuelles de la Relativité* (Editions de la Revue D'Optique Théorique et Instrumentale, Paris, France, 1968), Chap. 14.
[37] L.D. Landau and E.M. Lifshitz, *The Classical theory of Fields* (Pergamon, Oxford and Addison-Wesley, Reading, MA, 1971), 3rd revised English ed., Sec. 9.9.
[38] W. Pauli, *Pauli Lectures on Physics* (MIT Press, Cambridge, MA, 1973), Vol. 1, Secs. 18, 26, 28-30.
[39] C. Teitelboim, Phys. Rev. **D1**, 1572 (1970).
[40] G.C. Dente, Phys. Rev. **D12**, 1733 (1975).
[41] C. Bula *et al*., Phys. Rev. Lett. **76**, 3116 (1996).
[42] D.L. Burke *et al*., Phys. Rev. Lett. **79**, 1626 (1997)

Figure Captions

Figure 1. Illustration of the Dirac-Schwinger quantization condition and the duality transform.
Figure 2. Top: dipole radiation pattern, as observed in the instantaneous rest frame of the accelerated electron. Bottom: the same pattern, as observed in a frame where $\gamma = 1.01$.
Figure 3. Scattering of a laser pulse by an electron initially at rest.

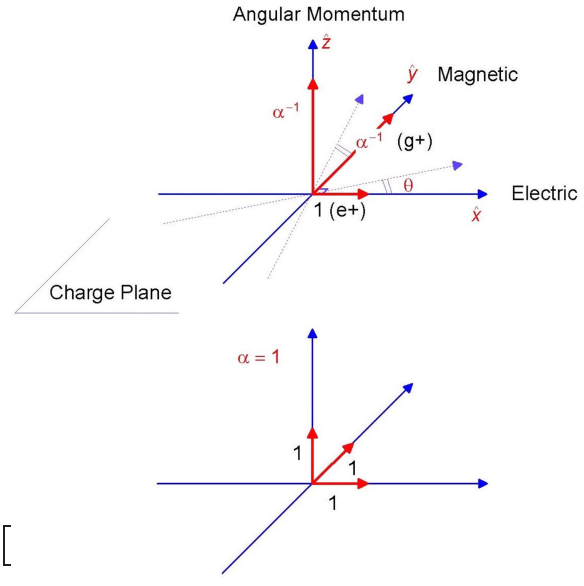

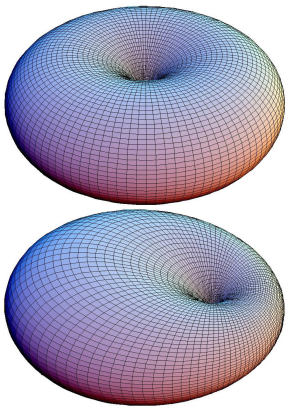

Figure 1 **Figure 2**

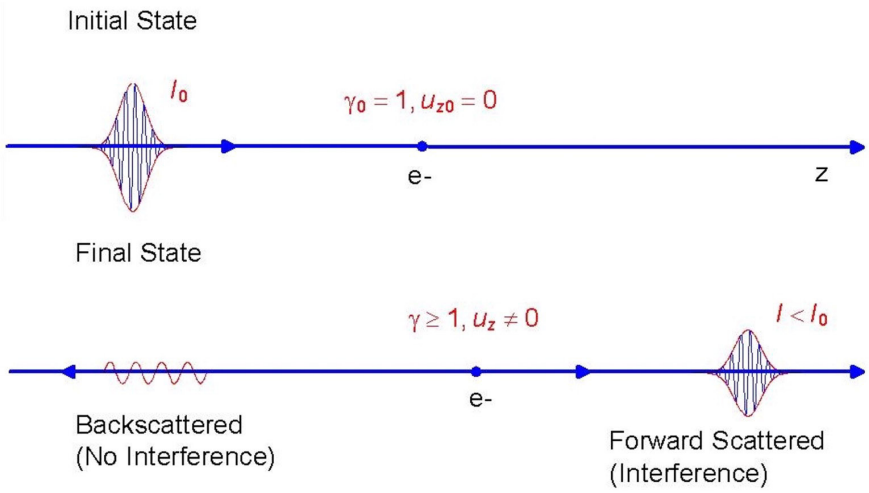

Figure 3

Appendix 1: Dyon 4-Current

In Section 2, the dyon 4-current is modeled by the integral over the dyon proper time of a 4-dimensional delta function; here, we show how to go from a 3-dimensional point charge model to an invariant delta function. In general, the 4-current density can be expressed in terms of 4-velocity and charge density as

$$j_\mu(x_\lambda) = \left[u_\mu(x_\lambda) / \gamma(x_\lambda)\right]\rho(x_\lambda)\,, \tag{A1}$$

which can be formally expressed as an integral over all times if we use the properties of the Dirac δ-distribution:

$$j_\mu(x_\lambda) = \int_{-\infty}^{+\infty} u(x'_\lambda)\rho(x'_\lambda)\left(\delta(t-t')/\gamma'\right)dt'\,. \tag{A2}$$

Here, $x'_\lambda = x_\lambda(t') \equiv [t', \boldsymbol{x}(t')]$, and is measured in units of r_0. The charge density of the dyon is now modeled by a three-dimensional δ-distribution, and we have

$$j^s_\mu(x_\lambda) = \overline{q}\int_{-\infty}^{+\infty} u(x'_\lambda)\,\delta_3(\boldsymbol{x}-\boldsymbol{x}')\,\delta(t-t')\,d\tau', \tag{A3}$$

where we have introduced the dyon proper time, defined by $dt' = \gamma'\,d\tau'$. The invariant 4-dimensional δ-distribution can now be introduced, to yield

$$j^s_\mu(x_\lambda) = \overline{q}\int_{-\infty}^{+\infty} u(x'_\lambda)\,\delta_4(x_\lambda - x'_\lambda)\,d\tau'. \tag{A4}$$

Appendix 2

In Section 3, we have used the identity:

$$\delta\left(s^2\right) = \delta\left(-\tau''^2\right) = \left(\delta(\tau'')/|\tau''|\right). \tag{A5}$$

The identity given by Eq. (A5) has to be defined mathematically with care. We need to show that, for a certain class of suitably defined functions, we have

$$\int f(x)\,\delta\left(x^2\right)dx = \int f(x)\left(\delta(x)/|x|\right)dx. \tag{A6}$$

Starting from the well-known identity [14,19,26,27]

$$\delta\left(x^2-a^2\right) \equiv [\delta(x-a)+\delta(x+a)]/(2|a|), \tag{A7}$$

and defining $g(x) = \left(f(x)/|x|\right)$, we first have

$$\begin{aligned}\int f(x)\,\delta\left(x^2-a^2\right)dx &= \int |x|\,g(x)\,\delta\left(x^2-a^2\right)dx \\ &= |a|[g(a)+g(-a)]/(2|a|) = \tfrac{1}{2}[g(a)+g(-a)].\end{aligned} \tag{A8}$$

Applying this result to a function $f(x)$ such that $\lim_{x\to 0}\left(f(x)/|x|\right) = g(0)$ exists, we can now write

$$\lim_{a\to 0}\left[\int f(x)\,\delta\left(x^2-a^2\right)dx\right]=\lim_{a\to 0}\tfrac{1}{2}\left[g(a)+g(-a)\right]$$
$$=g(0)=\int f(x)\,\delta\left(x^2\right)dx\,, \tag{A9}$$

which is identical to

$$\int f(x)\left(\delta(x)/|x|\right)dx=\int g(x)\,\delta(x)\,dx=g(0)\,. \tag{A10}$$

In this sense, the identity (A5) is properly defined.

Appendix 3: Schott term

Here, we consider the exchange of 4-momentum between the electron, the external field and the scattered field. An elementary treatment of this problem can be given in the instantaneous rest frame of the particle, as discussed by Jackson [19], where one can balance to zero the time-averaged work produced by the radiation force on the particle with the time-averaged radiated electromagnetic energy [19], to obtain the Schott term of the Abraham-Lorentz force [9,28-34]. The Schott term depends on the second time derivative of the particle velocity. However, it should be noted here that, strictly speaking, in the instantaneous rest frame $(\boldsymbol{\beta}=\mathbf{0})$ where, by definition, both the particle velocity and kinetic energy are equal to zero, the infinitesimal variation of the work of the damping force, $dW=\boldsymbol{F}\cdot\boldsymbol{\beta}\,d\tau$, must also be zero. In fact, it will be shown that in that frame, the dipole radiation pattern of the scattered field is symmetrical, and that there is no momentum exchanged between the charge and the radiated wave [17,18]. The method of derivation used here consists of evaluating the instantaneous variation of the energy-momentum of the radiated field first [11,17,18]. This can be done either by integrating the Poynting vector flux and the radiation pressure of the scattered field on a sphere of finite radius, then taking the limit where the radius tends to zero, assuming no internal particle structure [18], or by generalizing results obtained in the instantaneous rest frame in a covariant way [11,20].

For a point charge moving along a world line $x_\mu(\tau)$ with 3-velocity $\boldsymbol{\beta}=d_t\boldsymbol{x}$ and 3-acceleration $\dot{\boldsymbol{\beta}}=d_t\boldsymbol{\beta}$, the radiative electric field at r_μ is obtained by deriving the Liénard-Wiechert 4-potential. In electron units, we have for the radiative field [11,12,15-17,19,24,35-39]

$$\boldsymbol{E}(r_\mu) = -\left\{ \left[\boldsymbol{n} \times (\boldsymbol{n} - \boldsymbol{\beta}) \times \dot{\boldsymbol{\beta}} \right] / \left[(1 - \boldsymbol{\beta} \cdot \boldsymbol{n})^3 R \right] \right\}^- , \qquad \text{(A11)}$$

where the quantities in the bracket are evaluated at the retarded time t^- such that $t - t^- = R(t^-) = \left| \boldsymbol{r} - \boldsymbol{x}(t^-) \right|$, and where $\boldsymbol{n}$ is the unit vector in the direction of observation.

The instantaneous electromagnetic momentum flux is given in terms of the Maxwell stress tensor [11,12,15-17,19,24,35-39], defined as

$$T_{ij} = \tfrac{1}{4\pi} \left[E_i E_j + B_i B_j - \tfrac{1}{2} \left(\boldsymbol{E}^2 + \boldsymbol{B}^2 \right) \delta_{ij} \right]. \qquad \text{(A12)}$$

The total radiation pressure force applied to a sphere of radius *R*, corresponding to the momentum recoil of the photons emitted by the particle at t^- is given by $\iint T_{ij} n_j R^2 d\Omega$, where n_j is the *j*-th component of $\boldsymbol{n}$. From Reference [18], the instantaneous variation of the momentum of the scattered field can be written as

$$d_t \boldsymbol{G} = -\lim_{R \to 0} \left[\iint (\boldsymbol{n} \circ \boldsymbol{T}) R^2 d\Omega \right], \qquad \text{(A13)}$$

where $\circ$ denotes tensorial contraction. The details of the derivation are given in Appendix 4; the covariant form of the instantaneous variation of the scattered wave 4-momentum is found to be

$$d_t G_\mu = \tfrac{2}{3} (a_\nu a^\nu) u_\mu . \qquad \text{(A14)}$$

The corresponding radiation damping force acting on the charge is essentially a relativistic effect. Indeed, if we first consider the instantaneous rest frame of the particle, we see that this force vanishes, as indicated by Eq. (A14). This is due to the symmetry of the dipole radiation pattern in this particular frame, as shown in Fig. 2 (top): although electromagnetic energy is radiated by the particle, there is no net recoil force because for each photon radiated in a given direction of space there is a photon with the same momentum radiated in the opposite direction. In any other frame, as shown in Fig. 2 (bottom), the relativistic Doppler effect breaks this symmetry: the photons radiated in the forward direction are blue-shifted and carry more momentum than their backscattered counterparts, resulting in a net radiation force opposite to the direction of motion. In the instantaneous rest frame, the electron merely mediates the transfer of

energy from the external field to the radiated wave by scattering the incident photons. This physical picture is in agreement with the fact that in that frame the electron has no free energy to yield, and that the work of any force acting on the electron must be zero; it also clearly indicates that in that frame, energy is directly exchanged between the external field and the scattered wave. With this in mind, we now need to carefully investigate the conservation of the energy-momentum of the three interacting bodies.

The covariant energy-momentum transfer equation between the charge and the electromagnetic field now takes the form $a_\mu = d_\tau p_\mu = -F_{\mu\nu}u^\nu - d_\tau G_\mu - d_\tau H_\mu$, where the first term is the usual Lorentz force expressed in terms of the electromagnetic tensor, while the second term corresponds to the 4-momentum radiated away by the scattered wave as derived above, and where we have introduced a third term corresponding to the instantaneous variation of the energy-momentum of the external field resulting from the interaction. Within this context, the radiation force is defined as $F_\mu^s = -d_\tau(G_\mu + H_\mu)$; here, we have also used the principle of action and reaction which holds as long as we consider the instantaneous interaction of a point particle: in that case, both the space-like and time-like intervals are zero and there is no propagation delay to consider.

We now use the relations between the 4-velocity and its successive derivatives [11,14,17]; using Eq. (A14), and contracting the 4-momentum transfer equation with the 4-velocity, we first have

$$u^\mu a_\mu = 0 = -u^\mu F_{\mu\nu}u^\nu + \tfrac{2}{3}(u_\nu\, d_\tau a^\nu)(u^\mu u_\mu) - u^\mu\, d_\tau H_\mu . \qquad \text{(A15)}$$

The first term on the right-hand side is equal to zero, since the electromagnetic tensor is antisymmetrical; in the second term, we use $u^\mu u_\mu = -1$ to obtain $\tfrac{2}{3}u_\nu\, d_\tau a^\nu = -u^\mu\, d_\tau H_\mu$. As noted by Pauli [11], the general solution is $d_\tau H_\mu = -\tfrac{2}{3}u_\mu\, d_\tau a_\mu + \kappa u^\nu K_{\mu\nu}$, where we have introduced the antisymmetrical tensor $K_{\mu\nu} = \tfrac{2}{3}\left(u_\mu\, d_\tau a_\nu - u_\nu\, d_\tau a_\mu\right)$, and where κ is an arbitrary constant.

It is clear that $\kappa = 0$ yields the Dirac-Lorentz equation; in that case, we can identify the variation of the 4-momentum in the external field with the Schott term: $d_\tau H_\mu = -\tfrac{2}{3}\, d_\tau a_\mu$. With this, the manifestly covariant expression for the radiation reaction becomes

$$F_\mu = \tfrac{2}{3}\left[\, d_\tau a_\mu - u_\mu (a_\nu a^\nu)\,\right], \qquad \text{(A16)}$$

and it is easily seen that $F_\mu = u^\nu K_{\mu\nu}$. In addition, the antisymmetrical character of the tensor $K_{\mu\nu}$ guarantees that $u^\mu F_\mu = 0$. For completeness, we give the corresponding expression of the radiation reaction force in vector form, as expressed in electron units where the force is normalized to $m_0 c^2 / r_0$:

$$\boldsymbol{F} = \tau_0 \gamma^2 \left\{ \ddot{\boldsymbol{\beta}} + 3\gamma^2 \dot{\boldsymbol{\beta}} \left(\boldsymbol{\beta} \cdot \dot{\boldsymbol{\beta}} \right) + \gamma^2 \boldsymbol{\beta} \left[\boldsymbol{\beta} \cdot \ddot{\boldsymbol{\beta}} + 3\gamma^2 \left(\boldsymbol{\beta} \cdot \dot{\boldsymbol{\beta}} \right)^2 \right] \right\}. \qquad \text{(A17)}$$

It is easily verified that the variation of the electron energy due to the radiative effects (time-like component of the radiation force) satisfies the equation

$$d_t \gamma = \tau_0 \gamma^4 \left[\boldsymbol{\beta} \cdot \ddot{\boldsymbol{\beta}} + 3\gamma^2 \left(\boldsymbol{\beta} \cdot \dot{\boldsymbol{\beta}} \right)^2 \right] = \boldsymbol{\beta} \cdot \boldsymbol{F} \ . \qquad \text{(A18)}$$

Eq. (A16) corresponds exactly to the covariant expression of the Abraham-Lorentz force. The self-interaction nature of the radiation force is evident, as the expression derived scales with the square of the particle charge: $\tau_0 = \mu_0 e^2 / 6\pi m_0 c$. In the first term of Eq. (A16), we recover the Schott term which depends on the second time derivative of the particle velocity, and which is identified here with the depletion of energy-momentum from the pump (accelerating) field, while we recover the quadratic scaling with acceleration for the second term corresponding to the radiation damping force. As indicated by Eq. (A16), the total radiation force can be attributed to two distinct effects. On the one hand, energy-momentum is radiated away by the scattered wave, as described by Eq. (A14). The asymmetry of the Doppler-shifted dipole radiation pattern in any frame where the particle is not instantaneously at rest gives rise to this force, which dominates in the ultrarelativistic limit; it also has a non-zero value for a particle submitted to a constant acceleration, as opposed to the Schott term. On the other hand, the second term in Eq. (A16) is attributed to the energy-momentum exchanged between the scattered wave and the external field. This term allows for the local simultaneous conservation of energy and momentum during the radiation process.

The physics of the interaction can be illustrated by considering the process shown in Fig. 3. Here, we consider the total energy and momentum of the electrodynamical system initially comprising a high intensity, short wavelength incoming laser pulse (pump) and an electron at rest. In general, after the interaction, the electron has gained some energy and momentum (in the minimal case, the electron would be left precisely at rest after the scattering), and is now moving at relativistic velocity, while the scattered

wave carries energy and momentum in all spatial directions. In this case, it is clear that all the energy and momentum gained by both the electron and the scattered wave come at the expense of the external field. It is equally clear that in such a process, the radiated electromagnetic power and the variation of the electron energy cannot be equal, therefore invalidating any theoretical model based on the local conservation of 4-momentum between the electron and the radiated field only. We also note that while the backscattered radiation does not interfere with the laser pulse, the forward scattered radiation, which has the same spectral characteristics as the pump, and co-propagates in the positive z direction, does interfere destructively with the laser pulse and lowers its energy and momentum, yielding pump-field depletion.

Finally, in the case of an external electric field deriving from a static potential $\varphi(\boldsymbol{r})$, the time-like component of the Dirac-Lorentz equation, which describes energy conservation, takes the simple form

$$d_\tau \gamma = \boldsymbol{u} \cdot \boldsymbol{\nabla} \varphi + \tfrac{2}{3} d_\tau^2 \gamma - d_\tau G_0 = d_\tau \left[\varphi + \tfrac{2}{3} d_\tau \gamma - G_0 \right], \qquad \text{(A19)}$$

and can formally be integrated to yield the conservation law $\Delta\left(\gamma - \varphi + G_0\right) = \tfrac{2}{3}\left[d_\tau \gamma\right]_{-\infty}^{+\infty}$, which indicates that, provided the Dirac-Rohrlich asymptotic condition $\lim_{\tau \to \pm\infty} \left[d_\tau \gamma\right] = 0$ is satisfied, the electron potential energy is converted to kinetic energy and radiation. Within this context, the small value of the fine structure constant, which corresponds to the ratio of the classical to quantum electron scale (classical electron radius divided by the electron Compton wavelength), guarantees that the acausal effects related to the electromagnetic mass renormalization will be smeared by quantum fluctuations before the strong classical radiative correction regime is reached, thus preventing "naked acausalities". If magnetic charges are considered, however, the radiation reaction dominate over the quantum effects because the effective coupling constant is now α^{-1}, which is a large number.

Appendix 4: Maxwell Stress Tensor

The instantaneous variation of the momentum of the scattered field can be expressed in terms of the electromagnetic stress tensor as:

$$d_t \boldsymbol{G} = -\lim_{R \to 0} \left[\iint (\boldsymbol{n} \circ \boldsymbol{T}) R^2 d\Omega \right], \qquad \text{(A20)}$$

where ∘ denotes tensorial contraction. Introducing the vector $\boldsymbol{\xi}$, defined such that

$$\boldsymbol{E} = \dot{\beta}\,\boldsymbol{\xi} / \left[(1 - \boldsymbol{n}\cdot\boldsymbol{\beta})^3 R \right], \tag{A21}$$

and using the fact that $\boldsymbol{B} = \boldsymbol{n} \times \boldsymbol{E}$, Eq. (A20) reduces to

$$\begin{aligned} & d_t G_i \\ & = \tfrac{1}{4\pi} \iint n_j \left[\dot{\beta}^2 \left\{ \delta_{ij}\xi^2 - \xi_i\xi_j - \left(n_j\xi_k - n_k\xi_j\right)\left(n_k\xi_i - n_i\xi_k\right) \right\} / (1 - \boldsymbol{n}\cdot\boldsymbol{\beta})^6 \right]_{t=t^-} d\Omega . \end{aligned} \tag{A22}$$

Following Sommerfeld [15], we change variables, and express the variation of momentum as a function of the retarded time. After some straightforward vector calculations, we obtain

$$d_{t^-}\boldsymbol{G} = -\tfrac{1}{4\pi}\,\dot{\beta}^2 \iint \left\{ \left[\boldsymbol{\xi} \times (\boldsymbol{\xi} \times \boldsymbol{n}) \right] / (1 - \boldsymbol{\beta}\cdot\boldsymbol{n})^5 \right\} d\Omega , \tag{A23}$$

which can be further reduced to

$$d_{t^-}\boldsymbol{G} = \tfrac{1}{4\pi}\,\dot{\beta}^2 \iint \boldsymbol{n} \left[\left\{ \boldsymbol{n} \times \left[(\boldsymbol{n} - \boldsymbol{\beta}) \times \dot{\boldsymbol{\beta}} \right] \right\}^2 / (1 - \boldsymbol{\beta}\cdot\boldsymbol{n})^5 \right] d\Omega , \tag{A24}$$

by noting that $\boldsymbol{\xi} \times (\boldsymbol{\xi} \times \boldsymbol{n}) = (\boldsymbol{n}\cdot\boldsymbol{\xi})\boldsymbol{\xi} - \xi^2 \boldsymbol{n}$ and $\boldsymbol{n}\cdot\boldsymbol{\xi} = 0$. It is interesting to notice that Eq. (A24) can also be derived directly by using the Poynting vector $\boldsymbol{S} = \boldsymbol{E} \times \boldsymbol{H}$ in the simpler equation $\lim_{R\to 0} \left(\iint \boldsymbol{S} R^2 d\Omega \right)$, as shown in reference [18]. To evaluate the integral in Eq. (A24), we expand the numerator using spherical coordinates

$$\begin{aligned} & \left\{ \boldsymbol{n} \times \left[(\boldsymbol{n} - \boldsymbol{\beta}) \times \dot{\boldsymbol{\beta}} \right] \right\}^2 = \dot{\beta}^2 \left[\left(\sin\alpha \sin\theta \cos\phi + \cos\alpha \cos\theta \right)^2 \left(\beta^2 - 1 \right) \right. \\ & \left. + \left(1 - \beta\cos\theta \right)^2 + 2\beta\cos\alpha \left(1 - \beta\cos\theta \right) \left(\sin\alpha \sin\theta \cos\phi + \cos\alpha \cos\theta \right) \right]. \end{aligned} \tag{A25}$$

Here, we have chosen the axis of the Galilean frame *L* such that we have

$$\boldsymbol{\beta} = \hat{z}\,\beta, \qquad \dot{\boldsymbol{\beta}} = \dot{\beta} \left(\hat{z}\cos\alpha + \hat{x}\sin\alpha \right),$$

and $$\boldsymbol{n} = \hat{x} \left(\sin\theta \cos\phi \right) + \hat{y} \left(\sin\theta \sin\phi \right) + \hat{z}\cos\theta .$$

The integral over all solid angles is

$$d_{t'}\boldsymbol{G} = \tfrac{1}{4\pi}\int_0^{2\pi} d\phi \int_0^{\pi} \boldsymbol{n}\left[\left\{\boldsymbol{n}\times\left[(\boldsymbol{n}-\boldsymbol{\beta})\times\dot{\boldsymbol{\beta}}\right]\right\}^2 / (1-\boldsymbol{\beta}\cdot\boldsymbol{n})^5\right]\sin\theta\, d\theta\,, \quad \text{(A26)}$$

where the explicit dependence of the numerator on θ and ϕ is given by Eq. (A25). The integral corresponding to the *y*-component averages to zero over ϕ, and the integral corresponding to the *x*-component averages to zero over θ. We are left with

$$d_{t^-}\boldsymbol{G} = \hat{z}\ \tfrac{1}{4\pi}\dot{\beta}^2\left[\tfrac{8}{3}\pi\beta\gamma^6\left(1-\beta^2+\beta^2\cos^2\alpha\right)\right]. \quad \text{(A27)}$$

At this point it is important to note that, as the sphere radius tends to zero, the retarded time tends to the instantaneous interaction time; Eq. (A27) is easily shown to reduce to

$$d_t\boldsymbol{G} = \tfrac{2}{3}\boldsymbol{\beta}\gamma^4\left[\dot{\beta}^2+\gamma^2\left(\boldsymbol{\beta}\cdot\dot{\boldsymbol{\beta}}\right)^2\right]. \quad \text{(A28)}$$

The instantaneous variation of the energy of the scattered wave can be derived in the same way by integrating the Poynting vector flux over all solid angles, and taking the limit where *R* tends to zero, to recover the Liénard formula

$$d_t W = \tfrac{2}{3}\gamma^4\left[\dot{\beta}^2+\gamma^2\left(\boldsymbol{\beta}\cdot\dot{\boldsymbol{\beta}}\right)^2\right]. \quad \text{(A29)}$$

The velocity-dependent term in Eqs. (A28) and (A29) can be expressed in terms of the 4-acceleration as

$$\gamma^4\left[\dot{\beta}^2+\gamma\left(\boldsymbol{\beta}\cdot\dot{\boldsymbol{\beta}}\right)^2\right] = a_\mu a^\mu\,. \quad \text{(A30)}$$

The covariant generalization of Equations (A28) and (A29) then becomes quite straightforward. Following Becker [17], we combine Equations (A28) and (A29) to obtain the sought-after covariant form of the instantaneous variation of the energy-momentum of the scattered wave:

$$d_\tau G_\mu = d_\tau t\ d_t G_\mu = \gamma\, d_t G_\mu = \tfrac{2}{3}(a_\nu a^\nu)u_\mu\,. \quad \text{(A31)}$$

BEYOND UNRUH EFFECT: NONEQUILIBRIUM QUANTUM DYNAMICS OF MOVING CHARGES

B.L. HU AND PHILIP R. JOHNSON
Department of Physics, University of Maryland
College Park, Maryland 20742-4111, USA
E-mail: hub@physics.umd.edu; pj19@umail.umd.edu

We discuss some common misconceptions in Unruh effect[1] and Unruh radiation for the cases of linear and circular uniform acceleration of a charged particle or detector moving in a quantum field. We point to the need to go beyond Unruh effect and develop a new theoretical framework for treating the stochastic dynamics of particles interacting with quantum fields under more general nonequilibrium conditions. This framework has been established in recent years using the influence functional formalism[2,3,4] and applied to relativistically moving charged particles[5,6,7]. Only with nonequilibrium concepts and methodology applied to particle-field interaction can one grasp the full complexity of the problems of beam physics under more realistic conditions, from electrons and heavy ions to coherent atoms.

1 Introduction and Summary

In this talk we would like to address two sets of issues, one related to Unruh effect, the other related to moving charges in a quantum field, with the hope of clarifying some misconceptions related to these problems. Unruh effect attests that a detector (made of an oscillator, atom, electron, or particle states of a quantum field) moving with a uniform proper acceleration of magnitude a sees the vacuum state of a quantum field as a thermal bath with temperature $T_U = \hbar a/(2\pi c k_B)$. This effect may be understood purely as a kinematic aspect of ordinary quantum field theory and does not require the notion of horizon, despite the connection with the black hole Hawking effect[8]. It is important to recognize that the Unruh effect is a manifestation of thermal noise in the detector, not radiation from the detector. We explain this point below. The first set of issues of interest are:

1) *Is there radiation emitted from a uniformly accelerated detector* [9]*?* This is the title of the other talk by BLH, contained in a summary paper by Hu and Raval in this volume[10]. The simple answer is NO, when the detector has reached a steady state. There is emitted radiation in nonequilibrium conditions associated with transients or nonuniform accelerated motion (though the time for a uniformly accelerating charge to equilibrate may be quite long). One example of nonequilibrium conditions is finite time acceleration. This problem was treated with the influence functional method by Raval, Hu and

Koks[3]. The other example of nonequilibrium (though stationary) condition is the case of circular motion, to which one can ask the question:

2) *Is there a circular Unruh effect*[11]*?* The strict answer is NO, in the sense that the detector undergoing circular motion will NOT detect a thermal bath, and hence there is strictly speaking no associated Unruh temperature. Laboratory (e.g., storage ring) conditions may allow a range of parameters (radius versus angular acceleration) such that a near-equilibrium condition exists, in which case and only in such cases can one use the concept of effective temperature, such as was proposed by Unruh [12]. Under general conditions, the moving particle/detector will register a colored noise, (which turns white in linear uniform acceleration), and acquire a stochastic component in its trajectory and other degrees of freedom.

For treating these general cases, one needs to invoke statistical field theory applied to the nonequilibrium dynamics of moving charges or detectors in a quantum field. This is the subject matter of the Ph.D. theses of Alpan Raval and Philip Johnson. A partial summary of the latter work, specifically on the derivation of the Abraham-Lorentz-Dirac (ALD) equation[13] and its stochastic counterpart, the ALD-Langevin equation, is contained in our other paper in this volume. To facilitate our discussion of this class of problems, including the "circular Unruh effect", we need to develop some basic concepts such as backreaction, fluctuations, dissipation and decoherence, and understand the demarcation of quantum, stochastic and semiclassical regimes. For this we bring in the second set of issues:

3) *Are radiation reaction (RR) and vacuum fluctuations (VF) related by a fluctuation-dissipation relation (FDR)?* The answer is NO, not directly. *Is there a FDR at work?* YES. But it relates vacuum fluctuations to quantum dissipation distinguished as the quantum backreaction which is over and above the classical radiation reaction. It balances the stochastic component in the particle trajectory so that the noise-averaged mean trajectory follows a semiclassical equation of motion.

4) *Are runaway solutions and preacceleration necessary evils of ALD equation?* NO, if one adopts the correct conceptual framework and methodology. Key to the resolution of these puzzles is the concept of decoherent history and emergent classical behavior from quantum systems. Vacuum fluctuations not only bring about quantum dissipation, it is also a source for decoherence in the quantum system. Decoherence legitimatizes a classical description such as particle trajectories. We will discuss the gist of these issues in the following sections. Full details can be found in the original papers.

2 Quantum, Stochastic, Semiclassical and Classical

2.1 Quantum Open System

A closed quantum system can be partitioned into several subsystems according to the relevant physical scales. If one is interested in the details of one such subsystem, call it the distinguished *system*, and decides to ignore certain details of the other subsystems, comprising the *environment*, the distinguished *system* is thereby rendered an open-system. The overall effect of the coarse-grained environment on the open-system can be captured by the influence functional technique of Feynman and Vernon, or the closely related closed-time-path effective action method of Schwinger and Keldysh[14]. These are initial value formulations. For the model of particle-field interactions under study, this approach yields an exact, nonlocal, coarse-grained effective action (CGEA) for the particle motion[15]. The CGEA may be used to treat the nonequilibrium quantum dynamics of interacting particles. However, only when the particle trajectories become largely well-defined (with some degree of stochasticity caused by noise) as a result of decoherence due to interactions with the field can the CGEA be meaningfully transcribed into a stochastic effective action, describing stochastic particle motion. In this program of investigation we take a microscopic view, using quantum field theory as the tool to give a first-principles derivation of moving particle interacting with a quantum field from an open-systems perspective.

2.2 Fluctuation-Dissipation Relations

A consequence of coarse-graining the (quantum field) environment is the appearance of noise which is instrumental to the decoherence of the system and the emergence of a classical particle picture. At the **semiclassical** level, where a classical particle is treated self-consistently with backreaction from the quantum field, an equation of motion for the *mean* coordinates of the particle trajectory is obtained. This is identical in form to the classical equation in the case of linearly coupled theories. Backreaction of radiation emitted by the particle on the particle itself is called *radiation reaction*. (For the special case of uniform acceleration it is equal to zero, due to a balance between the acceleration field and the radiation field[16].) Radiation reaction (RR) is often regarded as balanced by *vacuum fluctuations* (VF) via a fluctuation dissipation relation (FDR). This is a misconception: RR exists already at the classical level, whereas VF is of quantum nature. There is nonetheless a FDR at work balancing quantum dissipation (the part which is over and above the classical radiation reaction) and vacuum fluctuations. But it first

appears only at the **stochastic** level, when self consistent backreaction of the *fluctuations* in the quantum field is included in our consideration. Fluctuations in the quantum field is also responsible for a stochastic component in the particle trajectory (beyond the mean). Their balance is embodied in a set of generalized fluctuation-dissipation relations.

2.3 Decoherent Histories, Preacceleration and Runaway Solutions

Not only can coarse-graining of the environment lead to dissipation in the system dynamics, it is also responsible for the decoherence and emergence of classicality in the system, such as the appearance of a classical trajectory. When the environment is a quantum field and the system decoheres, then quantum fluctuations can act effectively as a classical stochastic noise[17,18].

The view that semiclassical solutions arise as decoherent histories[19] also suggests a new way to look at the radiation-reaction problem for charged particles. The classical equations of motion with backreaction are the Abraham-Lorentz-Dirac (ALD) equations. The solutions to the ALD equations have prompted a long history of controversy due to such puzzling features as pre-accelerations, runaways, and the need for higher-derivative initial data[20]. It has long been felt that the resolution of these problems must lie in the progenitory quantum theory. But this still leaves open the question of when, if ever, the ALD equation appropriately characterizes the classical limit of particle backreaction; how the classical limit emerges; and what imprints the correlations of the quantum field environment leave. Further questions pertinent to the classical behavior arising from the quantum realm, in the context of a moving charge in a quantum field, include whether the decoherent histories are 1) solutions to the ALD equation, 2) unique and runaway free, and 3) causal (no pre-acceleration). In[7] we show how these puzzles and pathologies, both technical and conceptual, are resolved in the context of the initial value quantum open system approach, and that quantum corrected ALD equations satisfying these criteria describe the semiclassical limit.

3 Radiation Reaction and Vacuum Fluctuations

3.1 Classical Radiation and Radiation Reaction

Uniformly accelerated charges classically radiate according to the Larmor formula, but experience vanishing RR[16]. There is an existing belief that the extra work done on the charge against RR must be the direct source of radiant energy, but this static viewpoint is inappropriate. Fields are dynamical

objects and have complex interactions with particles. For example, the acceleration field has been shown to do work on charges (and visa versa) and therefore one can not expect a detailed balance between particle and radiation energy alone since that would require a "freezing" out of the near and intermediate field degrees of freedom in a way incompatible with locality and causality.

3.2 Quantum Radiation and Vacuum Fluctuations

Let us now examine the quantum properties of this system. Our result based on self-consistent backreaction says that the stochastic equations when averaged over the noise distribution (noise-average) gives the (mean-field) semiclassical form. In the uniform acceleration case with linear coupling the expectation value of the field (quantum mean) is exactly the same as the classical value where the particle/detector is treated as a "classical" source, though the mean particle trajectory must be self-consistently determined as we have emphasized. At the stochastic level, the particle detector does fluctuate in its worldline, and other degrees of freedom. How does this stochastic component affect the field? As shown by Ravel, Hu and Anglin[2] (for an alternative derivation, see[10]), fluctuations in a detector modify the near field correlations– a polarization cloud is found around the detector trajectory. The same is true for stochastic particle motion in the linearized regime. This quantum effect of modified field correlations would add on to the average classical field value (the two-point function is different from the free field value). By extrapolating the RHA results to 3+1 dimensions, one may see that these altered field correlations showing up as vacuum polarization drop off faster than $1/r^2$ and hence are not seen by observers at infinity[21]. Since the equivalence of a quantum mean to the classical value holds only under the one-loop, Gaussian approximations, when these conditions are lifted, there may be new effects as yet undiscovered.

Whether there is quantum-corrected radiation from a nonuniformly accelerated charge or detector is therefore what one should focus on here when one asks a question like "Is there emitted radiation in Unruh effect?" Our result obtained with self-consistent backreaction of quantum fluctuations shows that the (noise-averaged) of a decohered particle trajectory obeys the ALD equation, which is known to be consistent with the classical Larmor formula (if one include the nonlocal acceleration field effects, as one must). This applies to any accelerated trajectory, uniform or nonuniform, which implies that there is no additional "extra" average radiation in the semiclassical/stochastic regime beyond the usual classical quantity, even though there are fluctuations (noise)

induced in the particle (the Unruh effect in the uniform acceleration case). It has been verified that the presence of detector fluctuations is not inconsistent with the absence of additional radiation.

When quantum decoherence is incomplete, the mean-field equations of motion for both radiation and particle have quantum corrections (an example of this is Schwinger's synchrotron radiation calculation[22] which must be included to answer questions beyond the semiclassical or stochastic domain.

3.3 Nonequilibrium quantum dynamics of charges

One major improvement of our approach to the problem of moving charges in a quantum field is the consideration of full backreaction of the quantum field on the particle in the determination of its trajectory. Dynamical backreaction ensures self-consistency between the particle/detector and the quantum field. The lack thereof is where many of the problems and paradoxes arise. We also find that conceptual issues are easier to consider if we deal with such problems at four distinct levels: quantum, stochastic, semiclassical and classical, as explained earlier. Confusion will arise when one mixes physical processes of one level with another without knowing their interconnections, such as drawing the equivalence between radiation reaction with vacuum fluctuations. Before summarizing our thoughts for processes under nonequilibrium conditions, which cover most cases save a few special yet important ones, such as uniform acceleration, let us remark that these well-known cases are what we would call 'test field' or prescribed (trajectory) cases and not self-consistent or backreaction-sensitive. These cases are easier to study because they possess some special symmetry, such as is present for the uniform acceleration case (Rindler spacetime), inertial case (Minkowski), or the eternal black hole case (Killing tensor). They are legitimate only if the backreaction of the field on the particle permits such solutions. Under these special conditions, a detector feels a thermal bath (in the inertial case it is the zero-temperature vacuum).

Let us analyze the physics of nonequilibrium processes at separate levels:

Classical level- the decohered self-consistent (mean) solutions for particle and field. If the system is sufficiently coarse-grained and decohered, the particle obeys classical equations of motion, such as the ALD equation from QED[6]. There is no Unruh effect because it is quantum in nature (at the classical level the effect of quantum fluctuations are averaged out).

Semiclassical level – defined as a classical system (particles or detectors) interacting with a quantum field. Coarse-graining over quantum field for reduced particle dynamics at one-loop gives back the classical equations of motion for the mean trajectory of the particle. Higher-order quantum correc-

tions arising from nonlinearities modify the mean of the quantum equations of motion for the particle. Quantum corrections may not however show up significantly at the low energy macroscopic description because decoherence tends to suppress these higher-order (e.g., higher-loop) nonlinear quantum effects.

Stochastic level - where fluctuations of the quantum field manifest as stochastic noise in the system dynamics. Coarse-graining the field (to some but not the fullest –classical –extent), one obtains a classical stochastic equation for the system (such as the Einstein Langevin equation for semiclassical stochastic gravity[23,24] or the ALD-Langevin equation for QED[6,7]). It is possible to encode much of the quantum statistical information of the field and the state of motion of the system in the noise correlator and the two point function of the particle. Thus effects of both quantum (field environment) and kinematic (particle system) nature show up as a stochastic component in the particle trajectory which is self-consistently determined. The stochastic equations of motion have a quantum dissipation term (not classical radiation reaction!) that balances the quantum fluctuations, and is governed by a FDR. The latter is described by the noise kernel, which for general conditions is nonlocal, entailing that the noise in the detector is colored and temperature is no longer a viable concept.

4 'Circular Unruh Effect' – Misconceptions

We now apply these ideas to discuss radiation from a particle in circular motion in a quantum field and in particular we address two common sets of misconceptions related to it. (We only present the main points here, see[25] for calculations and further discussions.) These misconceptions arise from unclear distinction between a) linear uniform acceleration and circular motion, b) thermal radiance felt by the detector/charge in uniform acceleration (Unruh effect) versus emitted radiation (misconjured as Unruh 'radiation') sensed by probes afar, and c) emitted radiation of classical and quantum origin.

It has been asserted that Unruh radiation is already observed in storage rings[11]. This is the so-called circular Unruh effect. For this discussion we assume that RF fields give the particle average circular (steady state) motion by restoring the energy loss from synchrotron radiation. Questions:

4.1 Is there a circular Unruh effect?

NO. In fact, the circular case displays nonequilibrium (albeit steady state) quantum field statistics that are more general than the linear uniform (ther-

mal) Unruh case. There is a difference between linear acceleration and angular acceleration. Just from dimensional grounds, there is only one parameter in the linear case, the proper acceleration a, but two in the circular case, the angular acceleration α and the radius of the orbit R. In the linear case, as the velocity of the particle increases to the speed of light, an event horizon forms. In the circular case, the direction of velocity changes but its magnitude remains constant, there is no event horizon. (Invoking Kerr metric to describe circular motion is unnecessary and misleading, as the problem is basically about kinematics in relativistic quantum field theory.)

4.2 Is temperature a viable concept?

NO. To the extent that the existence of an event horizon is the condition for the appearance of an Unruh or Hawking temperature (this is the traditional argument based on global geometry[26], the modern one is via kinematic effect, which enables one to consider nonequilibrium conditions[8]), one can already see that there is no well-defined Unruh temperature in circular motion. For circular motion one needs to incorporate the effect of a second physical scale other than acceleration (e.g., the radius). If the system is in near-equilibrium conditions, one can introduce an 'effective (frequency dependent) temperature'[12].

4.3 Emittance and Vacuum fluctuations

A related point is the emittance (spread) of particle beams, which is commonly understood to result from quantum field- induced fluctuations. One can treat beam emittance without invoking temperature or Unruh effect. For general cases there is no need for temperature to play the intermediary between quantum field and induced beam fluctuations (on this point we concur with Jackson[27]).

Beam emittance is indeed the working of kinematic effects (particle motion) on vacuum fluctuations (quantum noise). (For viewing Hawking -Unruh effect in this light see[8]). Beams in linear uniform acceleration are expected to show thermal spread (neglecting possible sources of non-thermal noise). Beams in circular motion do not come into thermal equilibrium, though they may achieve a steady state balance between vacuum fluctuations and quantum dissipation. Our prediction is that the detector (a particle with internal degrees of freedom such as an electron with spin) will see colored noise whose correlator is related to the nonthermal electron populations in their two polarization states. This is more general than the Unruh effect as it is under nonequilibrium conditions.

4.4 Isn't synchrotron radiation Unruh radiation?

No. Synchrotron radiation occurs for classical systems (where there is no $\hbar$); or arises in the semiclassical limit of quantum systems where quantum noise has been averaged out. The Unruh *effect* is thermal radiance in the system arising from quantum fluctuations; it is seen in the stochastic and quantum limit. One argument views synchrotron radiation as the scattering of virtual vacuum fluctuations into real photons by a moving charge. But in the Unruh effect there is no radiation after the system has equilibrated, yet there are thermal fluctuations in the particle. This highlights the distinction between emitted radiation (synchrotron or Larmor) and thermal radiance felt by the particle/detector (Unruh effect). There is no direct link between the classical limit of radiation and the quantum Unruh effect; but at the stochastic level a FDR relates quantum dissipation and vacuum fluctuations[7].

4.5 Is there emitted quantum radiation from the charge?

At the stochastic level there is nonequilibrium noise in the particle/detector; these fluctuations alter field correlations around the particle trajectory as a polarization effect[2]. At the quantum level one can use the open system approach but coarse-grain the particle, and determine the quantum corrections to radiation. Take note that quantum corrections modifying both the mean-field radiation and noise-average trajectory must be found self-consistently. The result should be compared with Schwinger's[22] and/or the quasi-classical operator method because discrepancies, if any, will be of considerable interest.

Acknowledgments

We thank Pisin Chen for his invitation to this interesting workshop and Stefania Petracca for her warm hospitality. This research is supported in part by NSF grant PHY98-00967.

References

1. W. G. Unruh, Phys. Rev. **D14**, 3251 (1976).
2. A. Raval, B. L. Hu and J. Anglin, Phys. Rev. **D 53**, 7003 (1996).
3. A. Raval, B. L. Hu and D. Koks, Phys. Rev. **D 55**, 4795 (1997).
4. A. Raval, Ph. D. Thesis, University of Maryland, College Park, 1996.
5. P. R. Johnson, Ph.D. thesis, University of Maryland, College Park, 1999.
6. P. R. Johnson and B. L. Hu, "Worldline Influence Functional Derivation of Lorentz- Dirac- Langevin Equation from QED ". This volume.

7. P. R. Johnson and B. L. Hu, *Stochastic Theory of Relativistic Particles Moving in a Quantum Field: I, II, III* (Preprints 2000).
8. B. L. Hu, "Hawking-Unruh Thermal Radiance as Relativistic Exponential Scaling of Quantum Noise", Invited talk at the Fourth International Workshop on Thermal Field Theory and Applications, Dalian, China, August, 1995. Proceedings edited by Y. X. Gui and K. Khanna (World Scientific, Singapore, 1996) gr-qc/9606073.
9. Pisin Chen, "Event Horizon" This volume.
10. B. L. Hu and A. Raval, "Is there Radiation in Unruh Effect?". This Volume.
11. J. M. Lennias, "Unruh Effect in Storage Rings" This volume.
12. W. G. Unruh, in Monterey Workshop on Quantum Aspects of Beam Physics, edited by Pisin Chen (World Scientific, Singapore, 1998).
13. H. A. Lorentz, *The Theory of Electrons* (Dover Books, New York, 1952), pp. 49,253; P. A. M. Dirac, Proc. R. Soc. London **A 167**, 148 (1938).
14. R. Feynman and F. Vernon, Ann. Phys. **24**, 118 (1963); J. Schwinger, J. Math. Phys. **2** (1961) 407; L. V. Keldysh, Zh. Eksp. Teor. Fiz. **47** , 1515 (1964) [Engl. trans. Sov. Phys. JEPT **20**, 1018 (1965)].
15. B. L. Hu and Y. Zhang, "Coarse-Graining, Scaling, and Inflation" Univ. Maryland Preprint 90-186 (1990); B. L. Hu, in *Relativity and Gravitation: Classical and Quantum* Proc. SILARG VII, Cocoyoc, Mexico 1990. eds. J. C. D' Olivo et al (World Scientific, Singapore 1991).
16. J. D. Jackson, *Classical Electrodynamics* (J. Wiley, N. Y. 1983).
17. B. L. Hu and A. Matacz, Phys. Rev. D49, 6612 (1994).
18. E. Calzetta and B. L. Hu, Phys. Rev. **D49**, 6636 (1994).
19. M. Gell-Mann and J. B. Hartle, Phys. Rev. **D47**, 3345 (1993).
20. G. N. Plass, Rev. Mod. Phys. **33**, 37 (1961); F. Rohrlich, Am. J. Phys. **28**, 639 (1969).
21. M. L. Tseng, A. Raval and B. L. Hu, in preparation (2000).
22. J. Schwinger, Proc. Nat. Acad. Sci., **40**, 132 (1954); V. M. Baier and V. M. Katkov, *Zh. Eksp. Teor. Fiz.,* **53**, 1478 (1967). transl., Sov. Phys. JETP 26, 854 (1968).
23. B. L. Hu, Int. J. Theor. Phys. 38, 2987 (1999) gr-qc/9902064
24. R. Martín and E. Verdaguer, Int. J. Theor. Phys. 38, 3049 (1999) .gr-qc/9812063. Phys. Rev. **D60**, 084008 (1999). gr-qc/9904021.
25. B. L. Hu, P. R. Johnson and M-L Tseng (in progress).
26. J. B. Hartle and S. W. Hawking, Phys. Rev. D13, 2188 (1976).
27. J. D. Jackson, in Monterey Workshop on Quantum Aspects of Beam Physics, edited by Pisin Chen (World Scientific, Singapore, 1998).
28. P. Davies, T. Drey and C. Manogue, Phys. Rev. D (1998).

Appendices

COMMITTEES

International Advisory Committee

N. Cabibbo (Rome), J. Dorfan (SLAC), E. Picasso (Pisa), A. Sessler(LBL), A. Skrinsky (BINP), D. Sutter (USDOE), S. Tazzari (Rome), V. Vaccaro (Napoli), A. Wagner (DESY), T. Wilson (CERN), M. Witherell (Fermilab), A. Zichichi (Bologna), ICFA Beam Dynamics Panel Members

Program Committee

D. Barber (DESY), S. Chattopadhyay (LBL), P. Chen (SLAC) (Chairman), A. Dragt (U. Maryland), K. J. Kim (Argonne), K. McDonald (Princeton), C. Pellegrini (UCLA), M. Pusterla (Padova), F. Ruggiero (CERN), R. Ruth (SLAC), T. Tajima (LLNL/U. Texas), V. Telnov (BINP), E. Uggerhoj (Aarhus), K. Yokoya (KEK)

Organizing Committee

P. Chen (SLAC) (Chairman), S. De Martino (Salerno), S. De Nicola (Napoli), S. De Siena (Salerno), R. Fedele (Napoli), K. Hirata (Sokendai), L. Palumbo (Rome), S. Petracca (Benevento)

Secretariat (Dip. Scienze Fisiche, University of Naples)

Mrs. Camilla De Felice, Mrs. Annamaria Esposito, Mr. Michele Scarpati Mr. Dino Terranova

LIST OF PARTICIPANTS

Baier, Vladimir N.	baier@inp.nsk.su	BINP Novosibirsk, Russia
Bessonov, Eugueni	bessonov@sgi.lpi.msk.su	Lebedev Physical Inst RAS, Moscow
Capozziello, Salvatore	capozziello@sa.infn.it	Univ of Salerno and INFN, Italy
Carrigan, Richard A.	carrigan@fnal.gov	FERMILAB, Batavia
Chao, Alex	achao@slac.stanford.edu	SLAC, Stanford
Chattopadhyay, Swapan	chapon@lbl.gov	LBNL, Berkeley
Charman, Andrew	acharman@socrates.berkeley.edu	Univ of California, Berkeley
Chen, Pisin	chen@slac.stanford.edu	SLAC, Stanford
Chiao, Raymond	chiao@physics.berkeley.edu	Univ of California, Berkeley
Cufaro, Petroni Nicola	curfaro@ba.infn.it	Univ of Bari and INFN, Italy
De Martino, Salvatore	demartino@sa.infn.it	Univ of Salerno and INFN, Italy
De Nicola, Sergio	denicola@cib.cnr.na.it	Ist Cibernetica CNR Napoli, Italy
De Siena, Silvio	desiena@sa.infn.it	Univ of Salerno and INFN, Italy
Dragt, Alex	dragt@physics.umd.edu	Univ of Maryland
Ertmer, Wolfgang	ertmer@iqo.uni-hannover.de	Univ of Hannover, Germany
Fedele, Renato	fedele@na.infn.it	Univ of Napoli and INFN, Italy
Fedorova, Antonina	anton@math.ipme.ru	IPME RAS St Petersburg
Fusco, Mario	mario@sa.infn.it	Univ of Salerno
Gallardo, Juan C.	gallardo@bnl.gov	BNL, New York
Hartemann, Fred V.	hartemannl@llnl.gov	LLNL, Livermore
Heifets, Samuel	heifets@slac.stanford.edu	SLAC, Stanford
Hill, Christopher	hill@fnal.gov	FERMILAB, Batavia
Hirata, Kohji	hirata@post.kek.jp	Sokendai Hayama, Japan
Hirose, Tachishige	hirose@comp.metro-u.ac.jp	Tokyo Metropolitan Univ, Tokyo
Hu, Bei Lok	hub@physics.umd.edu	Univ of Maryland
Illuminati, Fabrizio	fabrizio@leopardi.csied.unisa.it	Univ of Salerno and INFN, Italy
Jaganathan, Ramaswamy	jagan@imsc.ernet.in	Inst of Math Sci, Chennai, India
Johnson, Philip	pj19@umail.umd.edu	Univ of Maryland
Jowett, John	jowett@cern.ch	CERN, Switzerland

Kabel, Andreas C.	kabel@slac.stanford.edu	SLAC, Stanford
Klein, Spencer R.	srklein@lbl.gov	LBNL Berkely
Khan, Sameen A.	khan@pd.infn.it	India
Kim, Kwangje	kwangje@aps.anl.gov	Argonne National Lab
Lee, Roman	lee@inp.nsk.su	BINP Novosibirsk, Russia
Leinaas, Jon Magne	j.m.leinaas@fys.uio.no	Univ of Oslo, Norway
Man'ko, Margarita A.	mmanko@sci.lebedev.ru	Lebedev Physical Inst RAS, Moscow
Mais, Helmut	mais@mail.desy.de	DESY Hamburg, Germany
Mirabel, Felix	mirabel@discovery.saclay.cea.fr	Saclay, France
Modanese, Giovanni	modanese@ect.it	Univ of Bolzano, Italy
Napolitano, Marco	napolitano@na.infn.it	Univ of Napoli and INFN, Italy
Ng, Johnny S.T.	jng@slac.stanford.edu	SLAC, Stanford
Ogata, Atsushi	ogata@sci.hiroshima-u.ac.jp	Graduate School of Adv Science of Matter,Hiroshima
Pellegrini, Claudio	pellegrini@physics.ucla.edu	Univ of California, Los Angeles
Petracca, Stefania	petracca@sa.infn.it	Univ of Sannio and INFN, Italy
Placidi, Massimo	massimo@mail.cern.ch	CERN, Switzerland
Pusterla, Modesto	pusterla@pd.infn.it	Univ. of Padova and INFN, Italy
Ruffini, Remo	ruffini@icra.it	Univ of Rome and INFN, Italy
Ruth, Ron	ruth@slac.stanford.edu	SLAC, Stanford
Scarsi, Livio	scarsi@ifcai.pa.cnr.it	Univ of Palermo and CNR, Italy
Schroeder, Carl B.	schroeder@ssrl.slac.stanford.edu	Univ of California, Los Angeles
Sessler, Andrew M.	amsessler@lbl.gov	LBL, Berkeley
Solimeno, Salvatore	solimeno@na.infn.it	Univ of Napoli and INFN, Italy
Strolin, Paolo	strolin@na.infn.it	Univ of Napoli and INFN, Italy
Suzuki, Toshio	toshio.suzuki@kek.jp	KEK Tsukuba, Japan
Takahashi, Hiroshi	takahashi@bnl.gov	BNL, New York
Telnov, Valery I	telnov@mail.desy.de	BINP Novosibirsk, Russia
Teng, Lee	teng@aps.anl.gov	Argonne National Lab
Thompson, Kathleen	kthom@slac.stanford.edu	SLAC Stanford
Torelli, Gabriele	torelli@difi.unipi.it	Univ of Pisa, Italy

Uggerhoj, Erik	ugh@ifa.au.dk	Univ of Aarhus, Denmark
Vaccaro, Vittorio	vaccaro@na.infn.it	Univ of Napoli and INFN, Italy
Venturini, Marco	venturin@slac.stanford.edu	SLAC, Stanford
Wei, Jie	weil@bnl.gov	BNL, New York
Wang, Xije	xwang@bnl.gov	BNL, New York
Warnock, Robert	warnock@slac.stanford.edu	SLAC, Stanford
Weng, Wu-Tsung	weng@bnl.gov	BNL, New York
Yashin, Aleksander	ayashin@slac.stanford.edu	SLAC, Stanford
Yokoya, Kaoru	yokoya@post.kek.jp	KEK Tsukuba, Japan
Zeitlin, Michael G.	zeitlin@math.ipme.ru	IPME RAS, St Petersburg, Russia

CONFERENCE PROGRAM

Sunday, October 15

17:00–20:00	Early Registration	
20:00–21:30	Welcome Reception (Dinner)	

Monday, October 16

07:30–08:30	Breakfast and Registration	
08:30–10:50	**PLENARY SESSION I**	L.Teng, Chair
08:30–08:35	K. Hirata	Opening Address of ICFA Beam Dynamics Pannel
08:35–08:40	P. Strolin	Opening Address on behalf of the INFN Napoli Director
08:40–08:45	P. Chen	Welcoming Address by the Conference Chair
08:45–08:50	S. Petracca	Announcements by the Organizing Committee Chair
08:50–09:30	R. Ruth	"Fundamental Aspects of Low Emittance ElectronBeams"
09:30–10:10	C. Hill	"Quantum Limit of a Linear Collider"
10:10–10:50	C. Schroeder	11Quantum Fluctuations in Free Electron Lasers"
10:50–11:15	Coffee Break	
11:15–13:15	**PLENARY SESSION II**	J. Gallardo, Chair
11:15–11:55	S. Chattopadhyay	"Femto- and Atto-Second Pulse Generation for Probing Quantum Entanglement"
11:55–12:35	W. Ertmer	"Bose-Einstein Condensate and Atom Laser"
12:35–13:15	R. Chiao	"Weakly Interacting Photon Gas in Two-Dimensions: Bose-Einstein Condensate, Superfluidity, and Vortices"
13:15–14:30	Lunch	
14:30–15:30	Free Time	
15:30–17:30	**PLENARY SESSION III**	V. Baier, Chair
15:30–16:10	J. Wei	"Crystalline Beams"
16:10–16:50	E. Uggerhoj	"Recent Results in Crystal Channeling Experiment"
16:50–17:30	S. Klein	"Nonlinear QED Effects in Heavy Ion Collisions"

17:30–17:50	Coffee Break	
17:50–19:00	**PLENARY SESSION IV**	R. Jaganathan, Chair
17:50–18:30	R. Fedele	"Landau Damping in Nonlinear Schroedinger Equation"
18:30–19:00	P. Chen	"Supersymmetry and Beam Dynamics"
19:30	Dinner	
21:00	Opening Night Concert	

Tuesday, October 17

07:00–08:30	Breakfast	
08:30–10:30	**PLENARY SESSION V**	R. Carrigan, Chair
08:30–09:10	F. Mirabel	"Microquasars"
09:10–09:50	L. Scarsi	"Gamma Ray Bursts and Ultra-High Energy Cosmic Rays"
09:50–10:30	R. Ruffini	"Black Holes and Gamma Ray Bursts"
10:30–11:00	Coffee Break	
11:00–12:40	**PLENARY SESSION VI**	V. Vaccaro, Chair
11:00–11:40	J. Leinaas	"Unruh Effect in Storage Rings"
11:40–12:10	K.-J. Kim	"Introduction to Working Group A"
12:10–12:40	V. Telnov	"Introduction to Working Group B"
12:40–13:40	Lunch	
13:40–15:00	Free Time	
15:00–16:00	**PLENARY SESSION VII**	J. Jowett, Chair
15:00–15:30	K. Yokoya/J. Ng	"Introduction to Working Group C"
15:30–16:00	A. Dragt/M. Pusterla	"Introduction to Working Group D"
16:00–19:00	**PARALLEL SESSION I**	
16:00–17:30	Working Group A	K-J. Kim and H. Mais, Co-chairs
	Working Group B	V. Telnov and F. Hartemann, Co-chairs
	Working Group C	K. Yokoya and J. Ng, Co-chairs
	Working Group D	A. Dragt and M. Pusterla, Co-chairs
17:30–18:00	Coffee Break	

18:00–19:00 Working Groups continue

19:30 Dinner

Wednesday, October 18

07:00–08:00 Breakfast
08:00–18:00 Excursion to Pompei

Thursday, October 19

07:00–08:30 Breakfast
08:30–10:30 **PARALLEL SESSION II** Working Groups
10:30–11:00 Coffee Break
11:00–13:00 **PARALLEL SESSION III** Working Groups
13:00–14:00 Lunch
14:00–16:00 Free Time
16:00–19:00 **PARALLEL SESSION IV**
16:00–17:30 Working Groups
17:30–18:00 Coffee Break
18:00–19:00 Working Groups continue
20:00 Conference Banquet
22:00 Tarantella Performance

Friday, October 20

07:30–09:00 Breakfast

09:00–10:00 **PARALLEL SESSION V** Working Groups

10:00–10:30 Coffee Break

10:30–12:00 **PARALLEL SESSION VI** Working Groups

12:00–13:00 Lunch
13:00–16:00 **PLENARY SESSION VIII** K. Hirata, Chair
13:00–13:40 H. Mais "Report on Working Group A"
13:40–14:20 F. Hartemann "Report on Working Group B"
14:20–14:40 Coffee Break
14:40–15:20 J. Ng/K. Yokoya Report on Working Group C"
15:20-16:00 M. Pusterla/A. Dragt "Report on Working Group D"
16:00 Conference Ends P. Chen